THE UNIVERSITY
of EDINBURGH

Endothelin-1 antagonism in glomerulonephritis

Elizabeth Louise Owen

BSc. (Hons), MSc.

A thesis submitted towards the degree of PhD

The University of Edinburgh

2016

Declaration

I declare that the work presented in this thesis is my own and has not previously been published or presented towards another higher degree except where clearly acknowledged as such in the text.

…… ……..

Elizabeth Louise Owen **Date**

Acknowledgements

I would like to express my gratitude to my supervisor David Kluth for his support, guidance and efforts during my PhD; Bean, thankyou for your patience and input. Thankyou also to Jeremy Hughes and Simon Brown for your advice and input for the various aspects of labwork, presentations and general how to's. Jason King, thanks for all your help in the lab, you were always my 'go-to-guy' for all things technical….and for your many cool pairs of trainers. The rest of the PIG lab- Katie Mylonas, Jillian Rennie, Katherine Miles, Davis Vass, Matt Beesley and Madeline Vernon, a sincere thankyou for all the lab nights out and help and support. A big thankyou to Matt Bailey and Spike Clay, and John and Willie for all their hard work with the animals and in *ex vivo.* Also to Shonna Johnston and Fiona for their hard work and support in the flow lab. To Catherine and Madhavi- thankyou and well done for being hardworking diligent students.

Certain other friends and family also deserve a special mention; Yvonne Nelson- years spent together in the QMRI, many long crazy days and nights navigating youth together, the occasional youtube ABBA video and drunken nights proved for the forging of a lifelong friendship. Madina, Jonathan and Dave.. those papers never did read themselves, but we muddled through!! Ekin Bolukbassi- without you and Demis Roussos I'm not sure I would have made it through! James Catterson- alreet pal…thanks for being good friends….the lunchbreak chats and nights out will remain forever in my heart and mind. Andy and Greig Mackie, thankyou for dealing with me through all our life dramas.

Thankyou to my oldest friend Charlotte… We've had many years of life to contend with together and apart. Sometimes we break up, but we always make up. No matter how much time passes without seeing you, when we come back together its like we've never been apart. Thankyou for being a true friend who is a part of my past and present and will undoubtedly be an integral part of my future. To Dr Gandy… the time has come to break out the popping candy and sloe gin. Thankyou for showing me the light at the end of the tunnel!

Finally, my family- my siblings and parents who have always done the best they can through difficult times, thankyou for all your support over the years.

I would also like to express my gratitude to Kidney Research UK for funding this work.

Table of Contents

Endothelin-1 antagonism in glomerulonephritis **1**

Declaration **2**

Acknowledgements **3**

Table of Contents **4**

Figures and Tables **9**

Abbreviations **12**

Abstract **17**

Lay Summary **19**

Chapter 1 ..... **20**

1.1 The burden of chronic kidney disease **21**
1.1.1 Definition of chronic kidney disease 21
1.1.2 Hypertension 24
1.1.3 Epidemiology and aetiology of CKD 25
1.1.4 Progression of CKD to ESRD 26
1.1.5 Proteinuria in CKD 27
1.1.6 Preventing the progression of CKD 28
1.2 Glomerular diseases **30**
1.2.1 Normal glomerular filtration 30
1.2.2 Glomerular disease classification 33
1.2.3 Clinical presentation of glomerulopathies 34
1.2.4 Aetiology of glomerulonephritis 39
1.2.5 Pathogenesis of glomerulonephritis 39
1.2.6 Podocyte structure and function 49
1.3 Therapeutic intervention **55**
1.3.1 Protecting the glomerulus from podocyte loss and effacement 56
1.3.2 The Endothelin System 61
1.3.3 Endothelins in the Kidney 62
1.3.4 Therapeutic intervention by ET receptor blockade 63
1.4 Overview **69**
1.5 Hypothesis and Aims **70**

Chapter 2 ..... **71**

2.1 *In vitro* studies **72**
2.1.1 Cell Culture 72
2.1.2 ET-1 stimulation assay 73
2.1.3 ET-1 stability assay 74
2.1.4 ET-1 quantification 74
2.1.5 Enzyme-linked immunosorbent assay (ELISA) 74
2.1.6 ET receptor antagonist assays 75
2.1.7 Immunofluorescence (IF) studies 76
2.1.8 Cellular protein extraction 77
2.1.9 Total protein quantification 77
2.1.10 SDS-PAGE and Western blot 77
2.1.11 RNA extraction and RT-PCR 78
2.1.12 Mϕ migration assay 80
2.1.13 Mϕ phagocytosis assay 80
2.1.14 Mϕ Endocytosis assays 81
2.1.15 Mϕ protease inhibitor assay 81
2.2 *In vivo* studies **82**
2.2.1 Rat nephrotoxic nephritis (NTN) 82
2.2.2 Murine Mϕ depletion in CD11b-DTR mice 88
2.2.3 Statistical analyses 100

Chapter 3 ..... **101**

3.1 Introduction **102**
3.1.1 Experimental hypothesis and aims 102
3.2 Experimental protocol **103**
3.3 Preliminary studies with NTN model **105**
3.3.1 NTS treated animals develop progressive glomerulonephritis 105
3.3.2 Sitaxsentan improves renal function and glomerular inflammation 105
3.4 Selective ET_AR antagonism in nephrotoxic nephritis studies **109**
3.4.1 NTS treated animals develop progressive GN 109
3.4.2 STX treatment reduces hypertension 109
3.5 Selective ET_A receptor antagonism in severe NTN **113**
3.5.1 NTS treated animals develop progressive proteinuria 113
3.5.2 STX improves proteinuria and blood pressure 113
3.6 Summary **117**
3.7 Discussion **118**
3.7.1 ET_AR antagonism in experimental NTN 118
3.7.2 NTS induces progressive GN 119
3.7.3 Sitaxsentan reduces hypertension and macrophage infiltration in experimental nephrotoxic nephritis 119
3.7.4 Podocyte cell structure and function remain un-assessed 119
3.7.5 Glomerular inflammation is reduced in STX treated NTN animals 120
3.7.6 Further Work 120

Chapter 4 ..... **123**

4.1 Introduction **124**
4.1.1 Experimental hypothesis and aims 125
4.2 Experimental Protocol **127**
4.3 Human monocyte/macrophage (Mϕ) cell culture **130**
4.4 Mϕ express ET_A and ET_B receptors **130**
4.5 ET-1 effects on Mϕ activation **133**
4.5.1 ET-1 does not classically activate human Mϕ 133
4.6 ET-1 effects on Mϕ ET-1 production **135**
4.6.1 Mϕ eliminate ET-1 from culture media 135
4.7 ET-1 effects on Mϕ migration **137**
4.7.1 ET-1 is chemokinetic for Mϕ 137
4.8 Effects of ET-1 on Mϕ phagocytosis **140**
4.8.1 ET-1 induces increased phagocytosis in human Mϕ 140
4.9 Mechanisms of Mϕ ET-1 handling **144**
4.9.1 Chloroquine does not prevent ET-1 loss 144
4.9.2 ET-1 degradation is prevented by protease inhibition 146
4.9.3 Quiescent Mϕ do not release proteases responsible for degrading ET-1 146
4.9.4 Selective ET_BR Blockade partially prevents ET-1 loss 149
4.9.5 Inhibition of microtubule formation prevents ET-1 loss 151
4.9.6 ET-1 induced Mϕ chemokinesis is ETBR mediated 153
4.10 Summary **158**
4.11 Discussion **159**
4.11.1 Human Mϕ possess ET receptors, but are not classically activated by ET stimulation 159
4.11.2 ET-1 is cleared by Mϕ and induces migration in an ET_BR dependant manner 160
4.11.3 Further investigations 162

Chapter 5 ..... **165**

5.1 Introduction **166**
5.1.1 Experimental hypothesis and aims 166
5.2 Experimental Protocol **167**
5.3 Effects of diptheria toxin administration on monocyte/ macrophage ablation **168**
5.3.1 Monocytes are depleted by diphtheria toxin 168
5.3.2 Resident renal macrophages are depleted by DT 168
5.4 Effects of Mϕ depletion on physiological responses to ET-1 ..... **173**
5.4.1 Monocyte/ Mϕ ablation exacerbates the pressor response to ET-1 173
5.5 Summary **175**
5.5.1 Mϕ regulation of the pressor effects of ET-1 176
5.5.2 Future studies 177

Chapter 6 ..... **179**

6.1 Introduction **180**
6.1.1 Experimental hypothesis and aims 181
6.2 Experimental Protocol **182**
6.3 Podocytes propagate under growth permissive conditions and differentiate under non-permissive conditions **183**
6.4 Podocyte specific structural and functional proteins are expressed by the immortalised human podocyte cell line. **185**
6.4.1 Podocytes express functional proteins nephrin and podocin 185
6.4.2 Podocytes express structural proteins synaptopodin and filamentous actin. 188
6.5 Podocytes express ET_A and ET_B receptors **190**
6.6 Exogenous ET-1 induces podocyte ET-1 production **193**
6.6.1 Podocytes produce ET-1 over time, preceded by cellular ET-1 uptake 193
6.6.2 ET-1 induces ET-1 production in a dose dependant manner 194
6.7 Exogenous ET-1 induces podocyte cytokine production **197**
6.7.1 ET-1 induces podocyte IL-6 and IL-8 production 197
6.8 ET-1 induces podocyte de-differentiation **199**
6.8.1 ZO-1 staining was not sufficient to show abberations in tight junctions 199
6.8.2 In response to ET-1 stimulation, podocytes undergo cytoskeletal re-arrangements 200
6.8.3 ET-1 reduces synaptopodin expression 202
6.8.4 ET-1 treatment reduces SD protein nephrin expression 205
6.9 ET receptor antagonism influences podocyte ET-1 induced ET-1 production **208**
6.9.1 Selective ET_AR antagonism reduces ET-1 induced ET-1 production 208
6.9.2 Selective ET_BR antagonism prevents clearance of ET-1 208
6.10 ET receptor antagonism affects ET-1 induced cytokine production **210**
6.10.1 Selective ET_AR antagonism reduces ET-1 induced IL-6 and IL-8 production 210
6.10.2 Selective ET_BR antagonism does not affect IL-6 or IL-8 production 210
6.11 ET receptor antagonism influences ET-1 induced podocyte structural changes **212**
6.11.1 ET_A receptor antagonism prevents ET-1 mediated human podocyte cytoskeletal rearrangements 212
6.11.2 ET_B receptor antagonism prevents ET-1 induced F-Actin reorganisation 212
6.12 ET receptor antagonism affects ET-1 induced podocyte dedifferentiation **216**
6.12.1 ET_AR antagonism prevents ET-1 mediated human podocyte nephrin loss 216
6.12.2 ET_BR antagonism does not affect ET-1 induced nephrin loss 216
6.12.13 Summary 219
6.13 Effect of ET-1 and selective ET receptor antagonism on human podocytes **220**
6.13.1 Human podocytes possess a functional ET system 220
6.13.2 ET-1 induces actin cytoskeleton abberations and ET-1 production in human podocytes 220

6.13.3 ET-1 induces nephrin down-regulation 221
6.13.4 ET-1 induces podocyte pro-inflammatory cytokine production 222
6.13.5 Mechanism of ET-1 mediated podocyte effacement 223
6.13.6 Putative ET-1 induced podocyte intracellular signalling mechanisms 224
6.13.7 Limitations and Future work 228

Chapter 7 230

7.1 Summary and Concluding Remarks 231

Chapter 8 234

8.1 References 235

Figures and Tables

Chapter 1: Introduction

Figure 1.1 Normal glomerular filtration

Figure 1.2 Structures of the glomerular filtration barrier

Figure 1.3 Podocyte structure and slit diaphragm

Table 1.1 Stages of chronic renal disease

Table 1.2 Common clinical syndromes of primary glomerular diseases

Table 1.3 Classification of primary glomerular disease based on clinical syndrome

Chapter 2: Materials and Methods

Figure 2.1 FACS staining of CD11b-DTR (macrophage deplete) mouse blood

Figure 2.2 Cartoon of experimental set up for invasive BP measurement

Figure 2.3 Representative figure of BP traces

Table 2.1 RT-PCR primer sequences

Table 2.2 Antibodies for FACS staining of whole mouse blood

Chapter 3: Selective ET_A receptor antagonism with Sitaxsentan in experimental nephrotoxic nephritis

Figure 3.1 Figure 3.1 Schematic of Experimental Design For NTN

Figure 3.2 Effect of STX treatment on NTS induced NTN

Figure 3.3 Effect of STX treatment on glomerular macrophage infiltration

Figure 3.4 Effect of STX treatment on NTS induced NTN

Figure 3.5 Effect of STX treatment on inflammation and fibrosis

Figure 3.6 Effect of STX treatment on high dose NTS induced NTN

Figure 3.7 Effect of STX treatment on high dose NTS induced inflammation and fibrosis in NTN

Chapter 4: Impact of ET-1 on human macrophage activation

Figure 4.1 Human Mϕ cell morphology

Figure 4.2 Human Mϕ ET_A and ET_B receptor expression
Figure 4.3 ET-1 induced Mϕ cytokine production
Figure 4.4 ET-1 induced Mϕ ET-1 production
Figure 4.5 ET-1 induced Mϕ migration
Figure 4.6 ET-1 induced Mϕ phagocytosis
Figure 4.7 Effects of chloroquine on Mϕ ET-1 handling
Figure 4.8 Effects of protease inhibitors on Mϕ ET-1 handling
Figure 4.9 Effects of Mϕ conditioned media on ET-1 degradation
Figure 4.10 Effects of ETR antagonism on Mϕ ET-1 uptake
Figure 4.11 Effects of nocodazole on Mϕ ET-1 handling
Figure 4.12 ET_AR antagonism of ET-1 induced Mϕ migration
Figure 4.13 ET_BR antagonism of ET-1 induced Mϕ migration

Chapter 5: Macrophage regulation of the pressor effects of ET-1

Figure 5.1 Effect of diptheria toxin on CD11b-DTR mice
Figure 5.2 Effects of DT on mouse monocyte expression
Figure 5.3 Effects of DT on mouse resident renal Mϕ e expression
Figure 5.4 Effects of DT on murine resident hepatic Mϕ expression
Figure 5.5 Effects of conditional Mϕ ablation on BP in response to ET-1

Chapter 6: Amelioration of cytotoxic and pro-inflammatory effects of ET-1 on human podocyte cells by ET_A receptor antagonism *in vitro*

Figure 6.1 Human podocyte cell morphological change
Figure 6.2 Human podocyte cell surface marker expression
Figure 6.3 Human podocyte structural protein expression
Figure 6.4 Human podocyte ET_A and ET_B receptor expression
Figure 6.5 Influence of ET-1 stimulation on ET-1 production over 48h
Figure 6.6 Effect of ET-1 on podocyte cytokine production
Figure 6.7 Effect of ET-1 on podocyte phalloidin staining
Figure 6.8 ET-1 effects on synaptopodin and nephrin localisation and expression

Figure 6.9 Selective ET receptor antagonism effects on ET-1 induced ET-1 production
Figure 6.10 Selective ET receptor antagonism effects on ET-1 induced podocyte cytokine production
Figure 6.11 Selective ET receptor antagonism effects on ET-1 induced cytoskeletal changes
Figure 6.12 Selective ET receptor antagonism effects on ET-1 induced nephrin loss

Chapter 7: Discussion

Figure 7.1 Effects of ET-1 on glomerular cells

Abbreviations

α-SMA	alpha-smooth muscle actin
β-ME	beta-mercaptoethanol
βIG-H3	TGF-β induced protein Ig-h3
ARRB 1/2	β-Arrestin 1/2
ACEi	Angiotensin converting enzyme inhibitor
ACH	Acetylcholine
ADR	Adriamycin nephropathy
AKT (PKB)	Protein kinase B
AMAC-1	Alternative macrophage activation-associated CC-chemokine-1
ANA	Antinuclear antibodies
ANCA	Antineutrophil cytoplasmic antibody
Ang II	Angiotensin-2
ANP	Atrial natriuretic peptide
Ap-1	Activator protein-1
APC	Adenomatous polyposis coli
ARB	Angiotensin receptor blocker
ARF	Acute renal failure
ARP 2/3	Actin related protein 2/3
Arg-1	Arginase-1
ATIIR	Angiotensin II receptors
ATN	Acute tubular necrosis
AXIN	Axis inhibition
BCG	Bromocresol green
BSA	Bovine serum albumin
BMDM	Bone marrow derived macrophages
CAV-1	Caveolin-1
CD	Collecting duct
CD2AP	CD2-associated protein
CDC42	Cell division control protein 42 homolog
CIN85/RukL	c-Cbl-interacting protein/ regulator for ubiquitous kinase
CKD	Chronic kidney disease
CME	Clathrin-mediated endocytosis
CQ	Chloroquine
CRF	Chronic renal failure
CVD	Cardiovascular disease
Cyr61	Cysteine-rich protein 61
DAB	3,3'-diaminobenzidine
DAI	Diffuse axonal injury
DALYs	Disability-adjusted life years
DAPI	4',6-diamidino-2-phenylindole
DEX	Dexamethasone
DM	Diabetes mellitus
DN	Diabetic nephropathy

DOCA	Deoxycorticosterone acetate
DPX	Distyrene, Plastciser, Xylene
DT(R)	Diptheria toxin (receptor)
ECE	Endothelin converting enzyme
ECL	Enhanced chemiluminescence
ECM	Extracellular matrix
EC	Endothelial cell
EDN1-3	Endothelin gene (1-3)
EDTA	Ethylenediaminetetraacetic acid
EGF	Epidermal growth factor
EMT	Epithelial to mesenchymal transition
ERK	Extracellular signal-regulated kinases 1/2
ESRD	End stage renal disease
ET-1	Endothelin-1
$ET_{A/B}R$	Endothelin $_{A/B}$ receptor
FAK	Focal adhesion kinase
FcRIIb	Inhibitor Fc receptor b
FACS	Flow activated cell sorting
FGF	Fibroblast growth factor
FITC	Fluorescein Isothiocyanate
fMLP	fMet-Leu-Phe
FSGS	Focal segmental glomerulosclerosis
Fizz-1	Found in inflammatory zone-1
GBM	Glomerular basement membrane
GEnC	Glomerular endothelial cells
(e)GFR	(estimated) glomerular filtration rate
GM-CSF	Granulocyte-macrophage colony stimulating factor
GN	Glomerulonephritis
GNo	Glomerulonephrosis
GPRC	G-protein coupled receptors
GRB2	Growth factor receptor bound protein 2
GSK-3β	Glycogen synthase kinase-3β
HEK293	Human embryonic kidney cell line 293
HGF	Hepatocyte growth factor
HIF	Hypoxia inducible factor
HMGB	High-mobility group box
hPBMC	Human peripheral blood mononuclear cells
HRP	Horseradish peroxidase
HO	Hemeoxygenase
HSA	Human serum albumin
HUS	Haemolytic uremic syndrome
IκB	Inhibitor of κB
ICAM	Intracellular adhesion molecule
ICGN	Immune-complex crescentic glomerulonephritis
IFN-γ	Interferon-γ

IGF1R	Insulin-like growth factor receptor 1
ILK	Integrin linked kinase
IMDM	Iscove's modified dulbecco's medium
JNK-C	c-jun-terminal kinase-C
LDL(R)	Low density lipoprotein (receptor)
LIFE	Losortan intervention for endpoint reduction in hypertension
LN	Lupus nephritis
LPS	Lipopolysaccharide
LY6c	Lymphocyte antigen 6c
LY6g	Lymphocyte antigen 6g
MAC	Membrane attack complex
MAP	Mean arterial pressure
MAPK	Mitogen activated protein kinase
MCD	Minimal change disease
MCP-1	Monocyte chemo-attractant protein
MDB	Membrane desalting buffer
MGN	Membranous glomerular nephropathy
MHC	Major histocompatibility complex
MMP	Matrix metalloproteinase
MPGN	Membranoproliferative glomerulonephritis
MPO	Myeloperoxidase
MVB	Multi-vesicular body
nAchR	Nicotinic acetylcholine receptor
NCK	Non-catalytic region of tyrosine kinase adaptor protein-1
NF-κB	Nuclear factor kappa B
NHE 1,5	Na+/H+ exchanger isoform 1,5
NIDDM	Non insulin dependent diabetes mellitus
NK	Natural killer cell
NKF-K/DOQI	National Kidney Foundations Kidney Disease Outcomes and Quality Initiative
NO	Nitric oxide
NPHS1	Nephrin gene
NPHS2	Podocin gene
NTN	Nephrotoxic nephritis
Nx	5/6 renal ablation model
NZ	Nocodazole
PACAP	Pituitary adenylate cyclase-activating polypeptide
PAF	Platelet activating factor
PAI	Plasminogen activator inhibitor
PAN	Puromycin aminonucleoside
Par3/6	Protease activated receptor 3/6
PCGN	Pauci-immune crescentic glomerulonephritis
PCNA	Proliferating cell nuclear antigen
PDGF	Platelet-derived growth factor
PEC	Parietal epithelial cells

PE-Cy7	Phycoerythrin Cy/7
PI3K	Phosphoinositol 3-kinase
PKA	Protein Kinase A
PKC	Protein Kinase C
PLC	Phospholipase C
PMA	Phorbol myristat acetate
PMSF	Phenylmethylsulphonyl fluoride
PRP	Platelet-rich plasma
RANTES	Regulated on Activation, Normal T Cell Expressed and Secreted
RAS	Renin-angiotensin system
RBC	Red blood cell
RBF	Renal blood flow
RENAAL	Reduction in endpoint in NIDDR with angiotensin II antagonist Losartan
RHO-GEF	RHO guanine nucleotide exchange factor
RIA	Radioimmunoassay
RME	Raft-mediated endocytosis
ROS	Reactive oxygen species
RPGN	Rapidly progressive glomerulonephritis
RPMI-1640	Roswell Park Memorial Institute medium
RRT	Renal replacement therapy
SD	Slit diaphragm
SH2/3	Src homology domain-containing adaptor proteins
SHR	Spontaneously hypertensive rate
SLE	Secondary lupus erythematosus
SOCS	Suppressor of cytokine signaling
SPARC	Secreted protein acid rich in cysteine
SRA	Scavenger receptor A
SRC	Proto-oncogene tyrosine protein kinase
SSH1	Slingshot-1
STAT 1-3	Signal transducers activators of transcription
STX	Sitaxsentan
SYNPO	Synaptopodin gene
TGF-β	Transforming growth factor beta
TGRs	Transgenic rats
TGBRIII	TGF beta receptor III
Th1/2	T-helper cell 1/2
TIMPs	Tissue inhibitors of metalloproteinases
TLR	Toll-like receptor
TNF-α	Tumour necrosis factor alpha
TNF-R	Tumour necrosis factor receptor
Ton-EBP	Tonicity-responsive enhancer binding protein
TRAF6	TNF receptor associated factor
TRAPS	TNF-receptor-associated periodic febrile syndrome

TRPV4	Transient receptor potential cation channel sub family V member 4
TSP	Thrombospondin-1
TTP	Thrombotic thrombocytopenic purpura
UUO	Unilateral ureteric obstruction
VCAM	Vascular cell adhesion molecule
VEGF(C)	Vascular endothelial growth factor (C)
VIP	Vasoactive intestinal peptide
VSMC	Vascular smooth muscle cell
vWF	von Willebrand factor
WASP	Wiskott-Aldrich syndrome protein
WHO	World Health Organisation
Wnt	Wingless-type MMTV (mouse mammary tumor virus) integration site
WT-1	Wilm's tumour 1
ZO-1	Zonula occludens-1

Abstract

A common feature of glomerular disease is a protein leak into the urine. Proteinuria occurs in kidney disease and is an important risk factor for cardiovascular disease (CVD). ET-1 is a potent vasoconstrictor/pressor peptide that is up-regulated in CVD and many forms of inflammatory renal diseases. The actions of ET-1 are mediated via two G-protein coupled receptors, the ET_AR which serves primarily in the pro-hypertensive actions of ET-1 and is often considered as the main pathological receptor subtype, with the ET_BR serving to clear circulating ET-1. Antagonism of one or both of receptors has been shown to be of clinical benefit in the treatment of hypertension. This research demonstrated a beneficial effect of selective ET_AR antagonism using Sitaxsentan in a rat model of GN. ET_AR blockade reduced blood pressure and importantly reduced glomerular inflammation as assessed by glomerular macrophage (Mϕ) infiltration. Further, we aimed to demonstrate that Mϕ, key mediators of inflammation are activated by ET-1 to adopt a pro-inflammatoy phenotype. However, early studies demonstrated that ET-1 does not activate Mϕ as hypothesised. Mϕ were more phagocytic, and ET-1 was chemokinetic for macrophages, an ET_BR medicated event. ET-1 was also removed by Mϕ, suggesting a potential regulatory role of Mϕ in the ET system. This phenomenon led to inclusion of additional *in vivo* studies to investigate the role of Mϕ in the regulation of ET-1 and its pressor effects. These effects were investigated in a murine model of Mϕ ablation using CD11b-DTR mice. These experiments determined *in vivo* that Mϕ ablation augments pressor responses to ET-1, suggesting that Mϕ are required to regulate ET-1*. In vitro*, Mϕ remove ET-1 by several mechanisms involving proteolytic degradation of the peptide and ET_BR mediated clearance, demonstrating a potential mechanism for the *in vivo* observation. Furthermore, proteinuria is believed to be due to damage or effacement of specialized visceral glomerular epithelial cells or podocytes. We identified *in vitro* that the ET_AR mediates ET-1 induced human podocyte cell effacement by actin cytoskeleton aberrations and slit-diaphragm protein down-regulation, ET-1 and pro-inflammatory cytokine production. This thesis provides evidence to support our initial hypotheses that selective ET_AR

antagonism ameliorates proteinuric renal disease via its effects on podocytes and macrophages. Continued studies both in vitro and *in vivo* will strengthen the body of evidence to promote the therapeutic use of ETR antagonists in inflammatory renal disease.

Lay Summary

Protein leak into the urine occurs in chronic kidney disease (CKD). This leak is caused by damage to the cells of the kidneys filter or the glomerulus. Leaked protein can also be a sign of high blood pressure and cardiovascular disease (CVD). A chemical found in the body that regulates blood pressure- Endothelin-1 (ET-1) is also higher in CVD and CKD patients. ET-1 enters cells by its receptors, the ET_AR - which is thought to cause constriction of the blood vessels, and the ET_BR -which is thought to mainly dilate blood vessels and to clear ET-1 from the circulation. The ET_AR is often considered as the disease causing receptor. Blocking one or both of receptors has been beneficial in treating high blood pressure. The research in this thesis tests the effects of a drug known to only block ET_AR and not ET_BR- Sitaxsentan, in rats with CKD. The inflamed glomeruli and protein in the urine of these rats, in addition to their high blood pressure, was reduced when treated with Sitaxstentan. The cells mainly responsible for filtering protein and other substances from the urine are called podocytes. ET-1 is known to damage these cells. This research also shows that in podocytes damaged with ET-1, blocking the ET_AR, but not the ET_BR prevents damage to these cells. It was expected that ET-1 would also cause the white blood cells mainly responsible for inflammation or macrophages (Mϕ) to become 'activated' to perform their pro-inflammatory functions. This however, was not the case. These cells did not become activated but instead moved in response to this drug and ingested more foreign objects-other key functions of these cells. The ET-1 was also removed by (Mϕ) and this was performed by the ET_BR and also by enzymes released by these cells that degraded ET-1. These studies suggested that these cells might in fact regulate this potent blood pressure agent. To test this, we measured the blood pressure in mice lacking Mϕ compared to healthy mice. We found that mice lacking Mϕ had higher blood pressure responses than healthy mice when given ET-1, suggesting that Mϕ are required to regulate ET-1. Continued studies will strengthen the evidence to promote the use of ETR blockers in inflammatory renal disease, and further investigations are essential to determine the role of Mϕ in ET-1 regulation.

Chapter 1
Introduction

1.1 The burden of chronic kidney disease

1.1.1 Definition of chronic kidney disease

Chronic kidney disease (CKD) is a major public health problem. CKD, also known as chronic renal failure (CRF), comprises a group of pathologies in which renal excretory function is severely compromised. Most forms of CKD eventually evolve towards a progressive and irreversible stage of increasing damage and renal dysfunction. Ultimately renal replacement therapy (RRT), namely dialysis or renal transplant, becomes necessary [1] and is termed as end-stage renal disease (ESRD).

Both CKD and ESRD are treated as functional diagnoses. In 2003, the publication of the National Kidney Foundations Kidney Disease Outcomes and Quality Initiative (NKF-K/DOQI) clinical practice guidelines for the evaluation, classification and stratification of CKD was a notable milestone for the treatment and management of CKD [2]. This work group defined CKD as the presence of markers of kidney damage (abnormalities in blood, urine, or imaging tests) for ≥3 months or a glomerular filtration rate (GFR) <60 mL/minute/1.73 m^2 for ≥3 months, with or without other signs of kidney damage. Following diagnosis, CKD progression is classified by its stage (1-5) according to the extent of renal dysfunction and renal damage, symptomatology and therapeutic guidelines (table 1.1). Stage 5, or ESRD occurs when GFR falls below 5% of normal function (<15ml min^{-1}) present on at least 2 occasions for ≥ 3 months with the uremic syndrome.

Uremia or uremic syndrome refers to the multitude of effects resulting from the inability to excrete products of the metabolism of proteins and amino acids. As a consequence, toxic substances usually eliminated through the urine become concentrated in the blood and cause progressive dysfunction of many other tissues and organs, seriously compromising quality of life and survival.

However, kidney damage must occur to a significant extent before function becomes altered. Uremic signs and symptoms start to be vaguely detectable when at least two thirds of the total number of nephrons is functionally lost. Until then, CKD runs apparently silent. This is due to the ability of the remaining nephrons to undergo hypertrophy and functionally compensate for those that are lost [3]. The multi-organ effects of uremia are also caused by the impairment of the wide range of metabolic and endocrine functions normally carried out by the kidney.

Table 1.1 Stages of chronic renal disease

Stages defined by the NKF according to the glomerular filtration rate (GFR, in mL/min per 1.73 m2 of body surface), and common manifestations observed in each stage. Table adapted from [2].

Stage	GFR	Symptoms
1	≥ 90*	-
2	60-89*	↑ Parathyroid hormone, ↓ renal calcium reabsorption
3	30-59	Left ventricular hypertrophy, anaemia secondary to erythropoietin deficiency
4	15-29	↑ Serum triglycerides, hyperphosphatemia, hyperkalemia, metabolic acidosis, fatigue, nausea, anorexia, bone pain
5	< 15	Renal failure: severe uremic symptoms

*CKD is defined as either GFR <60mL/min/1.73 m2 for 3 months or a GFR above those values in the presence of evidence of kidney damage such as abnormalities in blood or urine (e.g proteinuria) tests or imaging studies.

1.1.2 Hypertension

High blood pressure or hypertension (HTN) is common and is estimated to occur in approximately 1:3 middle-age adults, increasing to about 60% for those over 60. HTN is the most important risk factor for cardiovascular disease (CVD) i.e. stroke, ischaemic heart disease and heart failure, and importantly, is a common cause and consequence of CKD. According to the World Health Organization (WHO) in a recent report, blood pressure was responsible for half of all CVD cases worldwide [4].

Interventions such as lowering the salt content of processed foods or educating the general public to change diet in order to lower systolic blood pressure and cholesterol are cost-effective ways to limit CVD. Ultimately these interventions avert over 21 million DALYs (disability-adjusted life years) per year worldwide[5]. A meta-analysis in 61 prospective studies (over 1 million adults) demonstrates that the relationship between BP and CVD is stronger than previously thought and clearly quantifies the risk for systolic BP [6].

In England in 2011 Health Survey found that those aged over 35, 31% of men and 28% of women have high blood pressure, defined as systolic blood pressure ≥140 mmHg or diastolic (DBP) ≥90 mmHg or on blood pressure treatment [7]. The prevalence significantly increased with age in both sexes- approx. 33% of men and 25% of women aged 45-54 years have hypertension and approx. 66% of men and 78% of women aged ≥75 years or older have hypertension [7].

The relationship between hypertension and CKD will be discussed in the following sections. The current treatment regime for hypertension will also be discussed with reference to CKD in section 1.1.5.

1.1.3 Epidemiology and aetiology of CKD

Over 10% of the general adult population have an indicator of kidney damage and/or reduced GFR. In the newest CKD prevalence model, it is estimated that in 2011 there were 2.6 million people aged 16 years and older (equal to 6.1% of this population) living with CKD stage 3-5. Furthermore, there is evidence to suggest that a large number of patients with CKD stages 1 and 2 are grossly under-diagnosed. The most current data from the UK Renal Registry (2013) indicate that there were 56,940 adult patients receiving RRT, with a prevalence of 888 per million population (pmp) in the UK[8], with treatment costs accounting for over 2% of the total NHS budget[9]. CKD has a high global prevalence with a consistent estimated global CKD prevalence of between 11 to 13% with the majority stage 3 [10].

Diabetic nephropathy (DN) as a result of type 1 diabetes mellitus (DM) is thought to be the leading cause of CKD. The incidence of diabetes has also reached epidemic proportions throughout the world, with an expected doubling in the number of patients with type 2 diabetes in the next 25 years[11]. This will inevitably lead to an increased incidence of diabetic nephropathy. Currently, approximately 0.5% of patients with diabetes are on renal replacement in Scotland[12].

As noted, the second most common cause of CKD is thought to be hypertension and renovascular disease [13,14]. Approximately 50-60% of all patients with CKD are hypertensive, and this figure increases to 90% in patients over 65 years. All together DM and hypertension account for 40% of ESRD cases in the UK [13; 15].

For many years the leading cause of CKD was glomerulonephritis (GN) secondary to infections. However, antibiotics and improved sanitary conditions have led to GN now being the third most common cause of CKD in the general population. GN and unknown causes are more common in countries of Asia and sub-Saharan Africa[15]. Presently GN, which is twice as common in men, is still the most common cause of kidney disease in patients under 65 receiving RRT.

In the UK, the incidence of ESRD doubled between 1996 and 2006. The rise in incidence or diagnosis of CKD is multifactorial. It may be due to the development of guidelines and simple blood-test-based formulae (e.g. eGFR) that allow for easier and earlier diagnosis of CKD and, thus, increased reporting[16].

CKD prevalence also increases with age, and men with CKD have a worse prognosis and a more rapid decline in renal function and progression of their renal disease than women. In addition to gender and age differences, some ethnic populations have a higher prevalence of CKD [17]. For example, South Asian populations are at higher risk of CKD linked to diabetes, as there is a higher incidence of diabetes in this community [18]. Afro-Caribbean and Africans are at greater risk of CKD due to their higher prevalence of hypertension [18].

A variety of renal injuries may cause CKD. Disease or trauma may be of interstitial, tubular or glomerular origin and in some cases may originate in the renal vascular tree. As previously noted these may occur as a consequence of systemic diseases such as diabetes mellitus (DM), hypertension and inflammatory and infiltrative diseases. They may also occur as a result of renal and systemic infections, polycystic kidney disease, autoimmune diseases (e.g. systemic lupus erythematosus), renal hypoxia, trauma, nephrolithiasis and obstruction of the lower urinary tract, chemical toxicity and others [19].

1.1.4 Progression of CKD to ESRD

Once initiated, renal injury gradually aggravates even in the absence of the triggering insult and can be diagnosed independently from the knowledge of its cause. Patients with stage 5 or ESRD frequently manifest a wide range of pathological organ dysfunction, either caused by the primary disease, by intrinsic pathological effects of uremia, or a combination of the two.

A representation of GFR evolution over time is a helpful estimation of renal disease progression rate. It is useful to monitor CKD as well as to predict the time for RRT. Progression rate is highly dependent on the underlying cause but,

due to genetic heterogeneity, it is also very variable among subjects with the same etiology [20]. Furthermore, population studies have shown that CKD patients have a far greater likelihood of cardiovascular death than progression to established renal failure.

1.1.5 Proteinuria in CKD

The interplay between chronic disease processes is complex, and determining cause, consequence and association is challenging. However, it was noted by Go and colleagues (2004)[21] that CVD patients with comorbid CKD have inconsistently higher mortality rates, even after adjustment for adverse prognostic factors that co-occur with CVD. Proteinuria, a clinical marker of renal dysfunction can also be used to determine the rate of progression of CKD. In addition, there is a body of evidence to indicate that urinary protein itself is toxic to the kidney. Clinical support for this is exemplified in the RENAAL study [22] whereby patients were stratified for level of proteinuria on entry to the study, and demonstrates that >70% patients with high levels of proteinuria (>3.0g/g albumin/creatinine ratio) progress to ESRD compared with only ≈ 40% of those with moderate albuminuria (≥1.5<3.0 g/g) and as few as ≈ 10% of those with low albuminuria (<1.5g/g). When proteinuria was suppressed, there was a decrease in the risk of kidney failure.

Furthermore, urinary protein is also well recognised as an adverse prognostic indicator for poor CV outcomes i.e. stroke, myocardial infarction or cardiovascular death [23] as demonstrated in the LIFE study[24], and is classed as independent of other risk factors such as level of kidney function and hypertension. Reducing urinary protein therefore improves CKD outcomes and CVD risk. Thus, a complete diagnosis for CKD involves detection, determination of stage of disease and assessment of etiology, presence of comorbid conditions and an estimation of progression rate. Strategies aimed at earlier identification and, where possible, prevention of progression to established renal failure are clearly required.

1.1.6 Preventing the progression of CKD

Establishing the cause of CKD is paramount, as in some cases treating the primary disease prevents further renal damage. The main therapeutic focus for CKD patients is to reduce the rate of decline of renal function (or progression rate) and ensuing multi organ failure.

There are currently no therapies that are able to provide a curative benefit. Treatments for CKD are based on CVD treatments, primarily via blood pressure control. As hypertension is an established risk factor for both CKD progression and CVD risk, it could be considered a contributing cause to the development of CKD but also as a result of CKD. Regardless of whether it is a cause or a consequence, current clinical guidelines suggest that patients with CKD should aim to achieve BP below 130/80 mmHg.

Standard treatments target the renin-angiotensin-aldosterone system (RAS). Angiotensin converting enzyme inhibitors (ACEi) and angiotensin receptor blockers (ARBs) selectively interfere with or antagonise angiotensin II (Ang II) actions on systemic vasoconstriction, in addition to renal specific constriction of the efferent glomerular arteriole. [25] Combination ACE/ARB therapy significantly improves BP control and further reduces albuminuria when compared with ACE monotherapy. [25]

The key and yet unmet issue in CKD is why, and through which mechanisms, persistence of triggering damage, initially repairable as in acute events, ultimately progress beyond a point in which non-reversible chronicity ensues. The development of early diagnostic and prognostic markers, and effective curative therapies critically depend on answering these largely ignored questions. Information pertaining to new mechanisms and molecular pathways that mediate the development of chronic phenotypes has emerged over the last few decades. This knowledge is potentially useful for optimizing current, and developing new therapies.

CKD most commonly occurs as a result of glomerular disease whereas acute renal failure (ARF) is most commonly due to tubulointerstitial damage or acute tubular necrosis (ATN) [26], with glomerular diseases tending to progress more rapidly than tubulointerstitial diseases [1]. Proteinuria, both a marker of renal dysfunction, a predictor of progression rate and an independent risk factor for CKD occurs as a result of dysfunctional glomerular filtration.

The requirement for additional treatments that are able to further reduce proteinuria and protect renal and cardiovascular function are implicitly expected to extend beyond blood pressure control alone, and will be aimed at targeting other aspects of renal glomerular injury by preservation of glomerular structures or reversal of damage. These agents would also likely be used in conjunction with steroids and ACEi/ARB therapy. Molecule-specific approaches offer hope for more effective and safer treatments.

This thesis will therefore examine glomerular disease and the mechanisms leading to proteinuria and glomerular inflammation. Based on these observations, potential renoprotective agents (and their cellular targets) capable of improving proteinuria, reducing inflammation and resolving tissue injury is investigated. Furthermore, the *in vivo* and *in vitro* models in which to investigate these targets are also discussed.

1.2 Glomerular diseases

As previously discussed CKD most commonly occurs as a result of glomerular disease. Dysfunction of the normal physiological processes of the glomerulus is central to the cause of proteinuria.

1.2.1 Normal glomerular filtration

The principal functions of the kidney are accomplished by filtration, reabsorption, and secretion (Fig 1.1 A). In normal physiology blood enters the glomerulus at high pressure via the afferent arteriole, moving through to the glomerular capillaries, (Fig 1.1 B) and exiting via the efferent arteriole [27].

1.2.1.1 Glomerular filtration barrier

The glomerular microcirculation, unlike other capillary circulations, is highly permeable to water and small solutes. Yet, like other capillaries, is relatively impermeable to macromolecules. These properties are essential for filtration function and are a result of the unique three-layer structure of the glomerular capillary wall. This barrier comprises the luminal fenestrated glomerular endothelial cells (GEnC) with its glycocalyx, the glomerular basement membrane (GBM), and terminates in the ablumenal visceral epithelial cells or podocytes. In most CKDs, ultimately the size and charge selectivity and permselectivity of the glomerular filtration barrier becomes altered, and the glomerular structure collapses and leads to sclerosis and scarring, reduced glomerular flow and filtration, or even physical scission from the tubule. While the glomerular endothelium and GBM are important structures, much interest has more recently focused on the podocyte and particularly its slit diaphragm, the final barrier to macromolecular passage [28].

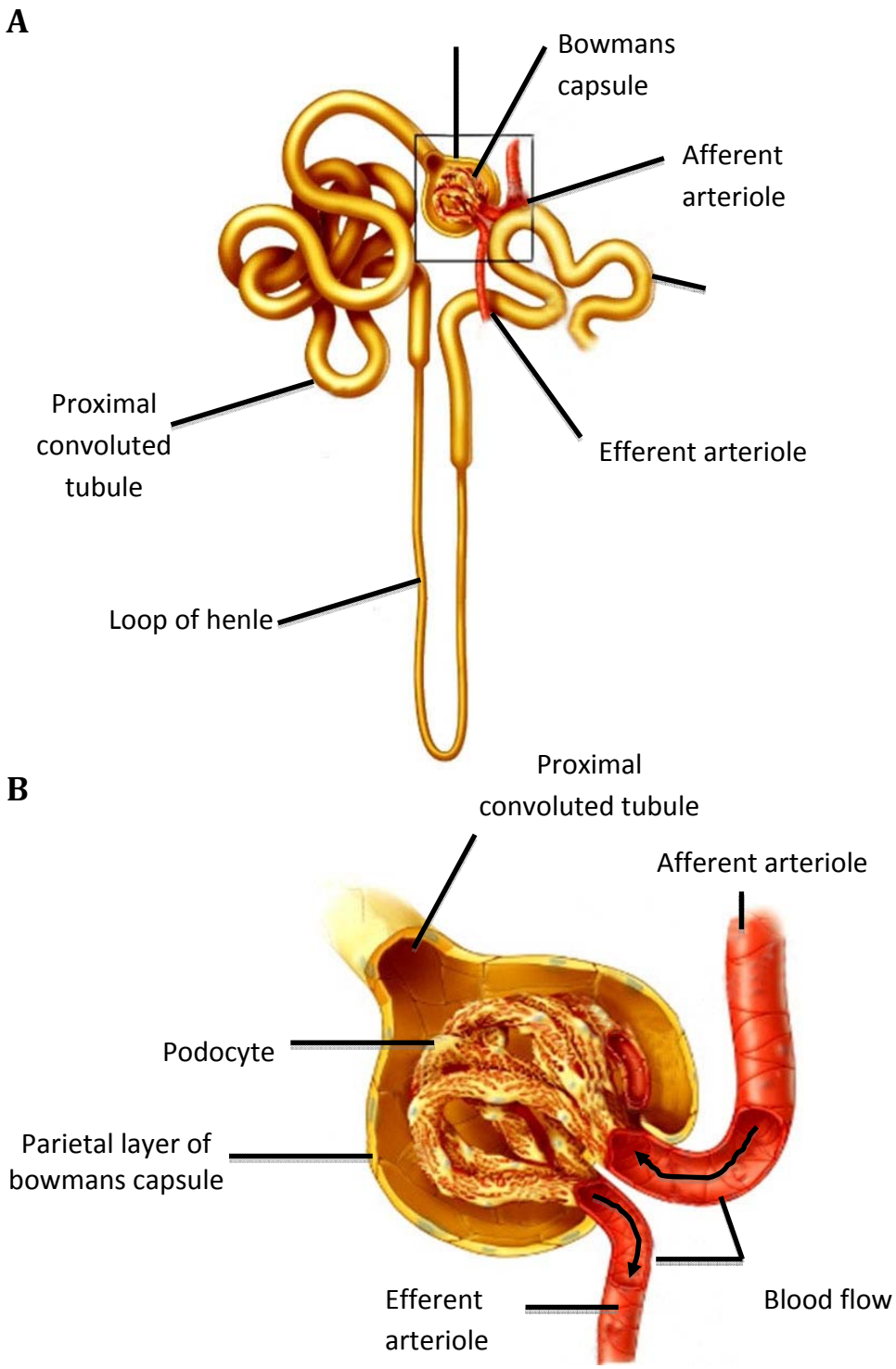

Figure 1.1 Normal glomerular filtration

A&B Diagrammatic representation of renal structures. (A) A single nephron, the repeating unit of the kidney (B) a single glomerulus, the filtration unit of the kidney. Images adapted from[29].

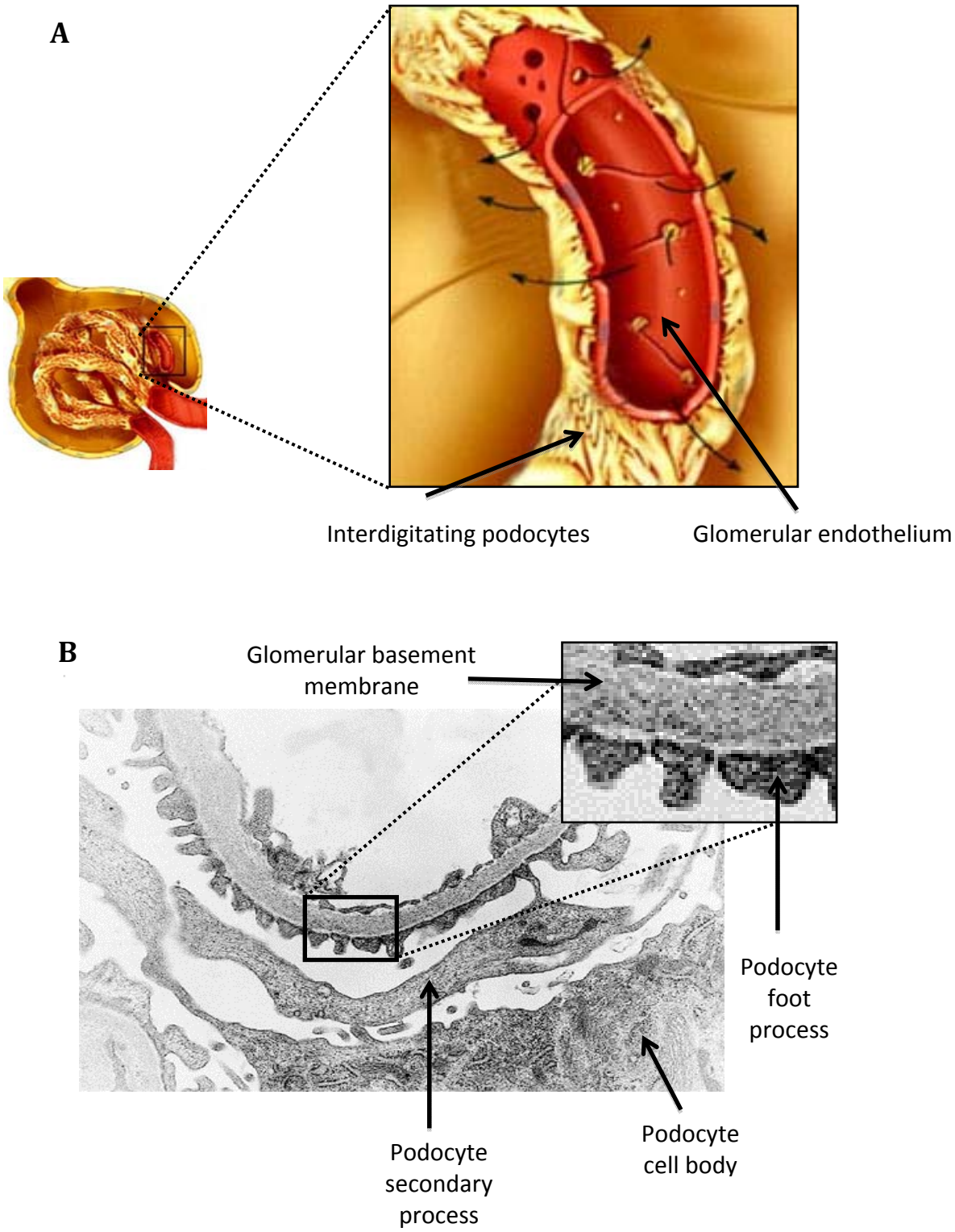

Figure 1.2 Structures of the glomerular filtration barrier.

A&B (A) Diagrammatic representation and (B) Electron microscope (EM) photomicrograph of the glomerular filtration barrier demonstrating glomerular endothelium, GBM and podocytes. Images A adapted from [29] Image B adapted from [30]

1.2.2 Glomerular disease classification

Glomerular diseases or glomerulonephritides are defined as diseases in which injury to the capillary bundle and Bowman's capsule (glomerulus) of the nephron occurs. They can be categorised as non-inflammatory glomerulonephrosis (GNo) or inflammatory glomerulonephritis (GN).

Non-inflammatory glomerular diseases comprise a repertoire of metabolic and systemic diseases that chemically or mechanically damage the glomerulus, such as diabetes and hypertension, toxins and neoplasias. The chronic form of GNo is glomerulosclerosis. Persistent hypertension is an important trigger of non-inflammatory glomerular disease, caused by pathologic remodelling of the capillary tuft as a response of an increased perfusion pressure and physical stress. Non-inflammatory glomerulopathies do progress with renal inflammation, which is a key mechanism of progression and an important target for therapeutics. This inflammation is, however, secondary to the injury inflicted by the initiating cause [31].

Inflammatory glomerular diseases or glomerulonephritides are renal diseases resulting in glomerular injury, in which inflammation is a primary component. GN is the third most common cause of CKD, after hypertension and diabetes. GN may occur in isolation (primary glomerular disease) or result from primary tubulointerstitial and renovascular diseases, i.e. polyarteritis nodosa and SLE (Secondary lupus erythematosus) [32] that contribute to the progression of the damage. Glomerular disease and GN are commonly used interchangeably, however, GN is synonymous with an inflammatory component of glomerular injury. In the glomerulus, inflammation exerts different effects that amplify the damage and directly contribute to the reduction in glomerular filtration. Initially, inflammation is probably activated as a normal repair mechanism upon cellular and tissue injury. However, undetermined pathological circumstances skew persistent inflammation into a vicious cycle of destruction and progression. In fact, inflammation activates many renal cell types to produce cytokines, which directly damage renal cells and exacerbate inflammation [33].

Renal and inflammatory cell activation and subsequent cytokine/chemokine release will be discussed in detail in section 1.2.5 -Pathogenesis of glomerulonephritis.

1.2.3 Clinical presentation of glomerulopathies

Glomerular diseases may present with one or more of the following; asymptomatic haematuria and/or proteinuria, nephrotic syndrome, nephritic syndrome and rapidly progressive glomerulonephritis (table 1.2).

Asymptomatic proteinuria is in the range of 150 mg to 3 g/d (in 24-hour urine collection) or as measured as spot protein-to-creatinine ratio ranging from 0.2 to 3 g protein/ gram creatinine is usually asymptomatic or non-nephrotic proteinuria. It may occur with glomerular or non-glomerular diseases such as tubulo-interstitial diseases (usually <1 g/d). Any type of glomerular disease can cause proteinuria in this range, with FSGS, membranous nephropathy, and diabetic nephropathy (DN) being common examples [34].

Asymptomatic haematuria is defined as >2 to 3 red blood cells (RBCs) per high-power field in spun urine (microscopic), or painless brown/red macroscopic haematuria without clots in patients who have normal renal function and no evidence of systemic diseases known to affect kidneys. The differential diagnosis is broad and urological problems (bladder, prostate, urethra, stones, and renal tumours) account for up to 80% of all cases of haematuria. The presence of RBC casts and/or dysmorphic RBCs indicates a glomerular cause for the haematuria. The most common diseases presenting as asymptomatic haematuria are thin basement membrane disease, IgA nephropathy, hereditary nephritis, and sickle-cell disease. Kidney biopsy is usually not performed to evaluate asymptomatic haematuria, unless there is concern for an unexplained systemic process that might warrant therapy [35].

Nephrotic syndrome is the major clinical syndrome produced by non-inflammatory glomerulopathies. This syndrome is a clinical pentad of proteinuria >3 g/d, hypoalbuminemia <3.5 g/dL, oedema, hypercholesterolemia, and lipiduria (most specific finding is presence of oval fat bodies in urinalysis). Complications of nephrotic syndrome include hypercoagulability due to loss of haemostasis control proteins such as antithrombin III and increased hepatic synthesis of protein C, fibrinogen, and von Willebrand factor (vWF). Venous thrombosis is more common than arterial thrombosis. Infection due to loss of immunoglobulins and immunosuppressive drugs, hyperlipidemia and atherosclerosis are also common complications. The most common glomerular diseases presenting as nephrotic syndrome are primary diseases such as minimal change disease, membranous nephropathy, and FSGS, as well as secondary forms such as diabetic nephropathy (DN), amyloidosis, and light-chain deposition disease (table 1.3). Contrarily to the nephritic syndrome, the nephrotic syndrome courses without haematuria. [36].

Nephritic syndrome is therefore the major syndrome produced by inflammatory GN. This syndrome presents gross or microscopic haematuria with dysmorphic RBCs and/or RBC casts, hypertension, and reduction in glomerular filtration rate with or without oliguria. Proteinuria (usually nonnephrotic) and oedema may also be present. Distinction between nephrotic and nephritic syndromes is usually based on clinical and laboratory evaluation. The most common diseases presenting as nephritic syndrome are post-streptococcal GN, other post-infectious diseases (endocarditis, abscess), IgA nephropathy, vasculitis, and lupus nephritis (LN). Generally, diseases presenting with nephritic syndrome tend be acute and rapidly progressive, and time is of the essence in diagnosis and early treatment, so as to avoid chronic renal damage [37].

Rapidly progressive glomerulonephritis (RPGN) is the most severe form of GN and usually presents as proteinuria <3 g/d and haematuria with dysmorphic RBCs and/or red cell casts, with or without systemic vasculitis. The appearance of crescents on biopsy are also present. RPGN can progress to ESRD within a

period of weeks to months if untreated. RPGN is usually due to one of the following disorders, which reflect different mechanisms of glomerular injury [38].

Type 1: Anti-GBM disease- in the setting of pulmonary involvement is also known as Goodpasture's syndrome. In this disorder histology demonstrates IgG positivity, and has a smooth, diffuse, linear pattern (ribbon-like appearance). Serology for serum anti-GBM antibodies is commonly positive.

Type 2: Immune complex GN- include mesangial IgA deposits in IgA nephropathy, antistreptococcal antibodies and subepithelial humps in postinfectious glomerulonephritis, antinuclear antibodies (ANA) and subendothelial deposits in lupus nephritis, and circulating cryoglobulins and intraluminal "thrombi" in mixed cryoglobulinemia.

Type 3: Pauci-immune GN- is a necrotizing glomerulonephritis with few or no immune deposits by IF or EM. The majority of patients with renal-limited vasculitis are antineutrophil cytoplasmic antibody (ANCA) positive, and many have or will develop the systemic symptoms of a vasculitis. Patients with ANCA-negative, pauci-immune RPGN are also considered part of this spectrum.

Type 4: Double–antibody-positive disease- has features of both types 1 and 3.

Table 1.2 Common clinical syndromes of primary glomerular diseases

Symptom	Nephrotic Syndrome	Acute GN	Rapidly Progressive GN	Asymptomatic Haematuria and/or Proteinuria
Proteinuria	>3.5 g/1.73 m^2/ day	May be in nephrotic range	May be in nephrotic range	No or non-nephrotic range
Haematuria	Variable and usually monomorphic if present	Micro- or macroscopic with RBC casts and dysmorphic RBCs	Micro- or macroscopic with RBC casts and dysmorphic RBCs	Micro- or macroscopic (may be dysmorphic with RBC casts)
Blood pressure	Normo- or hypertension	Hypertension	Hypertension	Normotension
GFR	Variable decline, depending on diagnosis	Rapid decline (days to weeks)	Progressive decline (weeks to months)	Decline uncommon

Table 1.3 Classification of primary glomerular disease based on clinical syndrome

Nephrotic syndrome
Minimal change disease (MCD)
Membranous glomerular nephropathy (MGN)
Focal segmental glomerulosclerosis (FSGS)
Membranoproliferative glomerulonephritis* (MPGN)
C1q nephropathy†
Fibrillary glomerulonephritis†

Acute Glomerulonephritis
Membranoproliferative glomerulonephritis
IgA nephropathy

Rapidly Progressive Glomerulonephritis
Antiglomerular basement membrane disease (anti-GBM disease)
Immune complex crescentic glomerulonephritis (ICGN)
Pauci-immune crescentic glomerulonephritis (PCGN)
Membranoproliferative glomerulonephritis
IgA nephropathy
Membranous glomerular nephropathy†

Asymptomatic Haematuria and/or Proteinuria
IgA nephropathy
Membranoproliferative glomerulonephritis

GFR, glomerular filtration rate; RBC, red blood cell.
*In children, >40 mg/m^2/hr; often accompanied by edema, hypoalbuminemia, hyperlipidemia, with or without lipiduria.
**Usually with active sediment; e.g., red blood cell casts, dysmorphic red blood cells), unlike other causes of nephrotic syndrome.*
†*Extremely rare disorders.*

1.2.4 Aetiology of glomerulonephritis

In the majority of cases of GN the aetiology is unknown. In a few cases however an aetiological agent can be identified**.** The known infectious agents including bacteria Staphylococcus spp., Lancefiled group A β-haemolytic streptococci, Streptococcus viridans, Treponema pallidum; viruses such as Coxsackie virus, Epstein Barr virus, hepatitis B virus, measles and mumps; and lastly parasites including Plasmodium malariae, Schistosoma spp. etc. [39]. Other aetiological agents can include drugs such as penicillamine and host antigens such as cryoglobulin, DNA and tumour antigens. Bacteria such as beta streptococci gives rise to poststreptococcal GN and viruses such as hepatitis C virus give rise to cryoglobulinemic membranoproliferative glomerulonephritis (MPGN). It is likely that most precipitating factors, such as infections and drug and toxin exposures, initiate similar immune responses that result in GN via shared common pathways [40].

1.2.5 Pathogenesis of glomerulonephritis

Although the pathogenesis is not fully understood, current evidence supports that most cases of GN are due to an immunologic reaction in response to a variety of different aetiologic agents. The immunologic response, in turn, activates a number of biological processes (complement activation, leukocyte recruitment, and release of growth factors and cytokines) that result in glomerular inflammation and injury [41]. GN may be isolated to the kidney (primary GN) or be a component of a systemic disorder (secondary GN). A large body of clinical, immunopathologic, and experimental data support the theory that most forms of human GN result from immunologic mechanisms [42; 43; 44; 45; 46; 47]. In these conditions glomerular injury is characterized by a primary immunological mechanism to the pathogenesis that often results in glomerular injury. Secondary mechanisms cause further glomerular damage by complement activation, platelet aggregation, neutrophil and Mϕ infiltration, fibrin deposition and activation of the kinin system.

1.2.5.1 Primary immunopathogenetic mechanisms

The nephritogenic immune response exhibits both humoral and cellular components, or T helper cell 2 (Th2)-regulated and T helper cell 1 (Th1)-regulated immune response [48].

1.2.5.1.1 Humoral/Antibody mediated injury

The humoral or Th2-regulated immune response occurs through regulation of B-cell differentiation and antibody production that leads to immune complex deposition and/or formation in the glomeruli.

In-situ immune complex deposition can occur as a result of circulating antibodies forming immune complexes with antigens of normal glomerular components, or with antigens of non-glomerular origin.

Fixed intrinsic tissue (Glomerular) antigens can be (1) Glomerular basement membrane antigens: NC1 domain of collagen type IV antigen (anti-GBM disease). These have linear patterns of immune-complex deposition on IF; (2) Podocyte antigens: Heymann antigen (membranous glomerulonephritis) these have a granular pattern of immune-complex deposition on IF [49]; (3) Mesangial antigens [50].

Planted (Deposited) antigens are non-glomerular antigens that are deposited in GBM from the circulation firstly and then circulating antibodies form immune-complex. These have a granular pattern immune-complex deposition. The trapped antigens are either exogenous antigens (i.e. infectious agents, drugs) or endogenous antigens (DNA, nuclear proteins, immunoglobulins, immune complexes, IgA). Antigen size, charge, molecular configuration and carbohydrate content of antigens are all factors influencing antigen trapping [50].

Circulating immune complex deposition occurs as a result of Type III hypersensitivity. Antigen-antibody complexes formed in the circulation are deposited in the glomeruli. These complexes have a granular pattern of

deposition on IF. Similarly, the antigen-antibody complexes formed in circulation are either from exogenous or endogenous antigens. Primary immune complex deposition in one site is often accompanied by deposition of lesser amounts in other sites. The factors influencing the localisation of complexes are molecular charge of complexes, size, avidity, blood flow, etc [51].

The site of complex formation or deposition can vary, and ultimately affect disease progression. Sites of formation or deposition can be (i) Subendothelial (between capillary endothelium and GBM): These are intermediate in size, highly anionic complexes excluded from GBM; (ii) Intramembranous (within GBM): These represent the transitional phase in which complexes migrate from subendothelial position to subepithelial and occur more frequently with increased blood flow; (iii) Subepithelial (between epithelial cells and GBM): These are small, highly cationic complexes which pass freely through the glomerulus without being trapped; (iv) Mesangial (within mesangium): These are large and neutral in charge and occur when there is decreased blood flow [52].

1.2.5.1.2 Cellular/T-cell mediated immune injury

The cellular or Th1-regulated immune response has a non-immune complex deposition mechanism whereby the infiltration of glomeruli is by circulating mononuclear inflammatory cells, including lymphocytes and macrophages (Mϕ). Here, crescent formation is observed [48]. The local Th1-regulated immunity involves the delayed-type hypersensitivity (DTH) reaction. This is initiated by CD4+ cells that activate monocytes or Mϕ to produce pro-inflammatory cytokines such as IL12 [53], IFN-γ [54] and TNF-α, with CD8+ cells acting by their cytotoxic ability [55]. Once activated, these cells are capable of producing cytokines that co-ordinate a local immune-inflammatory process. Mediators derived from lymphocytes such as IFN-γ induce an up-regulation of major histocompatibility complex (MHC) antigens by tubular cells, allowing these cells to act as antigen presenting cells. In addition, IFN-γ also activates Mϕ, which in turn trigger the synthesis of a variety of macrophage-derived growth factors, considered important mediators of fibrogenesis.

1.2.5.2 Secondary mechanisms mediating progression of glomerular damage

Secondary mechanisms cause further glomerular damage by both cellular components and soluble mediators produced by these cells. In early phases of GN, there is an influx of inflammatory cells irrespective of the nature of the initial renal insult. Cellular mediators include leucocyte infiltrates and platelet aggregates.

1.2.5.2.1 Neutrophils and platelets

In areas where antibodies that induce complement activation or immunoglobulin deposition at areas accessible to circulating inflammatory cells (e.g. subendothelial or mesangial immune complex deposits), neutrophil infiltration occurs [56]. It is well established that neutrophils cause much of the antibody-induced injury. Neutrophil involvement and localisation in glomeruli through interaction with a variety of leukocyte adhesion molecules (selectins, integrins, intracellular adhesion molecule (ICAM) and vascular adhesion molecule (VCAM)) has been demonstrated [57]. These molecules are overexpressed in response to cytokines and other inflammatory mediators. It is also established that neutrophils localized in glomeruli induce injury by undergoing a respiratory burst that results in release of toxic oxygen metabolites, particularly hydrogen peroxidase which is nephritogenic in its ability to interact with neutrophil-derived myeloperoxidase (MPO) [58; 59]. MPO is a cationic molecule that localizes in glome acids that directly damage GBM. It is also appreciated that in some settings platelets are essential for the occurrence of neutrophil mediated injury and apparently augment this process [60]. Finally, several neutrophil-derived serine proteases including elastase and cathepsin G can also cause capillary wall injury and proteinuria *in vivo* [61].

Thus neutrophils can cause damage to the GBM leading to proteinuria by generation of reactive oxygen metabolites and by release of proteolytic enzymes. These cells can also mediate acute changes in glomerular

hemodynamics. Glomerular filtration can be affected by mechanical obstruction of capillary lumens by neutrophils followed by attachment to the endothelium and ultimately stripping of endothelial cells from the underlying basement membrane. This leads to a reduction in the available surface areas for filtration.

1.2.5.2.2 Monocytes and macrophages

Monocytes and macrophages (Mϕ) are involved in the acute phase of the inflammatory response. Mϕ persist for months positioned in a variety of organs where they function as permanent 'sentinels' ready to initiate an inflammatory response via two main mechanisms. They protect the host through innate immunity and remove pathogens by engulfing them by phagocytosis. The development of acquired immunity with reciprocal interactions between macrophages and activated T and B lymphocytes provided novel levels of regulation and acquisition of enhanced antimicrobial resistance. The role of Th1-derived interferon-gamma (IFN-γ) [62] in cell-mediated immunity to intracellular infection and of interleukin-4 (IL-4) (Th2) [63] in extracellular parasitic infection gave rise to the concept of analogous M1 and M2 macrophages by Mills and Colleagues (2000)[64]. This terminology originated from an observation of differential macrophage arginine metabolism in various mouse strains with T helper type 1 (Th1) (C57BL/6 mice) and T helper type 2 (Th2) (Balb/c mice) backgrounds. Th1 mice with T cells producing mostly IFN-γ demonstrated macrophage activation in which nitric oxide (NO) was generated from arginine, versus ornithine production from Th2 mice with T cells producing IL-4 and tumor growth factor (TGF)-β 1. This finding led to a consensus within the scientific community that M1 (classically activated) macrophages exhibit inflammatory functions, whereas M2 (alternatively activated) macrophages exhibit anti-inflammatory functions.

This concept of M1 and M2 activation to mimic Th cell nomenclature was standard for many years, however, an ever-expanding body of evidence demonstrating that many stimuli combine to determine the phenotype of macrophages, and this M1/M2 polarisation view is now considered overly

simplistic. Recognition receptors, cytokines, and the signaling and genetic programs behind them control every aspect of cell activation, giving rise to a spectrum of macrophage activation phenotypes between the M1 and M2.

1.2.5.2.2.1 'Classical' M1 activation

The classical pathway of Mϕ activation occurs as a result of the combination of two stimuli. Firstly, interaction with interferon-γ (IFN-γ) from T-helper lymphocytes or natural killer (NK) cells [65]. This cytokine 'primes' Mϕ for activation, a dose dependant effect, and is able to enhance the inflammatory response, but does not in itself activate Mϕ [66]. The second signal is tumor necrosis factor (TNF-α) itself or an inducer of TNF-α. Exogenous TNF-α can act as the second signal, but the physiologically relevant signal is generally the result of Toll-like receptor (TLR) ligation, which induces endogenous TNFα production by the Mϕ itself. Thus, classically activated Mϕ are developed in response to IFN-γ, along with exposure to a microbe or microbial product such as endotoxin, a lipopolysaccharide (LPS)-containing molecule acting on TLR4 [67]. Consequently, ligand binding activates intracellular signalling pathways such as nuclear factor-κB (NF-κB) and leads to Mϕ activation [68]. This activation generates nitric oxide (NO) and reactive oxygen species (ROS), produces pro-inflammatory cytokines including tumour necrosis factor-α (TNF-α), IL-1, IL-12, IL-6, IL-8, IL-11ß and MCP-1 and finally induces expression of (MHC) class II and co-stimulatory molecules which promote antigen presentation including CD 80/86 and granulocyte-macrophage colony stimulating factor (GM-CSF) receptor CD116 [69]. M1 macrophages have also been shown to up-regulate the expression of the intracellular protein suppressor of cytokine signaling 3 (SOCS3), as well as activate inducible nitric oxide synthase (NOS2 or iNOS) to produce NO from L-arginine [70; 71]. Classically activated Mϕ are also a major source of the potent anti-inflammatory cytokine IL-10. This is generated in response to TLR signalling as a feedback mechanism to curtail the inflammatory response. In murine bone marrow-derived macrophages (BMDM), TLR4 stimulation by LPS induces the expression of IL-10 through the sequential induction of type I IFNs followed by induction and signalling through IL-27 via

two transcription factors, signal transducers and activators of transcription (STAT1) and STAT3, which are recruited to the IL-10 promoter [72].

1.2.5.2.2.2 'Alternative' M2 activation

In addition to the classical M1 Mϕ, these cells can undergo 'alternative' activation for an M2 phenotype. The first description of this phenotype reported Mϕ exhibiting an up-regulation of mannose receptor in response to an IL-4 or IL-13 stimulus [63]. Later studies showed that these Mϕ are distinct from classically activated Mϕ, and their phenotype is that of a 'regulatory' Mϕ [73]. These cells have a limited ability to destroy intracellular microbes and their antigen presenting ability is diminished compared to that of classically activated Mϕ. Unlike classically activated cells, M2 Mϕ do not produce NO as a result of arginase production [74]. These cells typically produce cytokines such as IL-10 and IL-1 receptor antagonist. Their main function is thus thought to be that of a pro-repair phenotype. These alternatively activated Mϕ are thought to mediate angiogenesis and deposit extracellular matrix (ECM) during wound healing. Alternatively activated Mϕ produce fibronectin and a matrix-associated protein TGFβ-induced gene-H3 (βIG-H3)[75], and they promote fibrogenesis from fibroblastoid cells [76]. The induction of arginase-1 (Arg-1) in these cells may lead to polyamine and proline biosynthesis, promoting cell growth, collagen formation, and tissue repair [77]. Markers to identify this cell type include Arg-1 induction, alternative macrophage activation-associated CC-chemokine-1 (AMAC-1) [78], CD163 and finally the transcription factors Found in inflammatory zone (FIZZ1) and Ym1- a chitinase family member [79]. It is noteworthy that these are largely murine markers, with alternatively activated human Mϕ being more difficult to characterise [80]. However, some molecules such as the multifunctional enzyme transglutaminase 2 (TGM2) serves as conserved markers for both human and mouse M2 macrophages and monocytes. Identification of human M2 macrophages can be performed by double staining for a combination of TGM2, mannose receptor C type 1 (MRC1/CD206), and CD68 [80].

1.2.5.2.2.3 'Type II' M2a activation

A third cell phenotype, the type II-activated Mϕ, gained recognition as an anti-

inflammatory cell. These cells are so named due to their ability to preferentially induce Th2 adaptive immune responses after initial activation in a Th1-type environment [81]. These Mϕ require two signals for activation. The first signal is the ligation of FcγRs with immune complexes. Receptor ligation also has to be coupled with a Mϕ stimulatory signal to influence cytokine production. Stimuli included those that signal through any of the TLRs, as well as through CD40 or CD44. The type II phenotypic switch following FcγR ligation occurs in un-primed and IFN-γ-primed Mϕ. Type II-activated Mϕ are clearly distinct from alternatively activated Mϕ described above, as they do not induce arginase. Activation also results in altered cytokine expression [81]. Cytokines produced by classically activated Mϕ, such as TNF-α, IL-1, and IL-6 are produced by these cells. However, production of IL-12, the Th1-promoting cytokine, is reduced and IL-10, the anti-inflammatory cytokine, is increased [81; 82]. Type II Mϕ also promote the differentiation of Th2 cells and subsequent IL-4 production [83].

It is now appreciated that the M2 terminology encompasses a functionally diverse group of macrophages rather than a unique activation state. Accordingly, M2 macrophages can be further divided into subsets specifically M2a, M2b, M2c and M2d based on their distinct gene expression profiles [84; 85]. Broadly speaking, as discussed the M2a subtype is elicited by IL-4, IL-13 or fungal and helminth infections. M2b is elicited by IL-1 receptor ligands, immune complexes and LPS whereas M2c is elicited by IL-10, TGF-β and glucocorticoids. The fourth type, M2d, is elicited by IL-6 and adenosine. M2d macrophages have phenotypic and functional attributes similar to ovarian TAMs but are distinct from M2a-c [86 87].

Rather than distinct macrophage populations, M1 and M2 are now though to not exclude each other and often are combined. The phenotype then depends on the balance of activatory and inhibitory activities and the tissue environment. The multipolar interplay between these and many other signals requires further studies *in vivo* and *in vitro*. The multitude of activating factors, known and proposed intracellular signaling pathways, chemokine receptor profiles and the

genes involved are exhaustive and beyond the scope of this thesis. Recent reviews by Martinez & Gordon (2014) [88] and Foey (2015) [89] indicate the spectrum of macrophage activation and the differences between the *in vitro* and *in vivo* environment.

In the context of renal disease, resident renal Mϕ may participate in the local presentation of antigen in (DTH) reaction. They are also responsible for hypercellularity of the glomerular tuft, particularly in diffuse proliferative GN and crescentic GN. Mϕ also play a central role in mediating the development of renal injury in animal models [90; 91; 92] as well as in human diseases. In rats subjected to 5/6 renal ablation (Nx), Mϕ infiltration begins 1 week after ablation and increases progressively with time [90]. Mϕ can mediate tissue injury through different pathways. Besides the ability of producing proteolytic enzymes, reactive oxygen ROS and vasoactive substances, Mϕ synthesize cytokines and fibrogenic growth factors responsible for a sustained inflammatory *milieu*. The maintenance of these cells in later phases of renal disease suggest that Mϕ are also involved in the chronic inflammatory process leading to the development of fibrotic changes.

The injurious role of infiltrating leukocytes has been discussed, however the contribution of resident glomerular cells to the disease states will also be addressed. These include the activation and loss and/or damage of endothelial cells [93] mesangial cells, and podocyte cells [94]. Both circulating inflammatory cells and resident glomerular cells can mediate glomerular injury acutely by release of oxidants, proteases and probably other chemo-attractant and GBM-degrading molecules.

1.2.5.2.3 Endothelial cell injury

GEnCs are primary sites of injury resulting in glomerulopathies and CKD. GEnCs serve to maintain glomerular perfusion, prevent leucocyte adhesion and platelet aggregation. As such, injury or insult to GEnCs results in alterations in haemodynamics i.e. hypertension and intravascular microthrombi as a result of dysregulated platelet aggregation.

1.2.5.2.4 Mesangial cell proliferation

Mesangial cells are contractile glomerular pericytes that play a major role in the regulation of renal blood flow and GFR. They also have a pivotal participation in the genesis of chronic glomerular diseases. Injury to these cells results in proliferation and increased matrix production and deposition. Mesangial proliferation is often considered an initial, adaptive response that eventually loses control and develops into a pathological process. It is a common feature during the initial phase of many chronic glomerular diseases, including IgA nephropathy, membranoproliferative GN [95; 96; 97], LN, and DN [98 99].

Numerous experimental models of glomerular damage have reported that proliferation of mesangial cells frequently precedes and is associated with ECM deposition in the mesangium and, therefore, leads to fibrosis and glomerulosclerosis. Reduction of mesangial cell proliferation in glomerular disease models ameliorates these pathological events [98].

Several cytokines, growth factors and complement proteins, through the activation of NF-κB-related pathways, initiate the damage stimulating mesangial cells to release chemotactic factors [100]. The recruited inflammatory cells amplify the proliferative response of mesangial cells [101], and also the expression of the epithelial to mesenchymal transition (EMT) marker α-smooth muscle actin (α-SMA) [102], [103] the production of ECM components [104; 105] and exacerbate cytokine and growth factor release [106].

Thus, proliferating mesangial cells are considered to be a central source of ECM production in both focal and diffuse glomerulosclerosis [104; 107]. Patients with mild glomerulonephritic damage show no interstitial collagen I and III [99]. Progressive renal damage correlates with increasing presence of collagen IV and VI, laminin and fibronectin in the mesangium. Finally, in later stages of glomerulonephritis, the amount of collagen IV, laminin and fibronectin gradually decreases, while focal expression of collagen I and III increases. Glomerular cell apoptosis also occurs in parallel to sclerosis, and ECM

progressively scars the spaces left by apoptotic and sloughed cells [108].

1.2.5.2.5 Podocyte loss and effacement

Podocytes have progressively gained attention in glomerulopathies and are considered to have a central role in the pathological process, as a result of both genetic and acquired alterations [96]. Podocytes form the terminal layer of the glomerular filtration barrier. It is the specialised structure and function of podocytes that makes them particularly attractive targets.

1.2.6 Podocyte structure and function

Podocytes are terminally differentiated and derive from embryonic mesenchyme. Consisting of a large cell body at the centre of the cell lying in the urinary space and large primary processes extending from the cell body, the processes then diverge into smaller secondary processes, and terminate in tertiary end foot processes [109] (Fig 1.3 A). These are polarised cells; the basal domain anchors podocytes to the matrix proteins in the underlying GBM via cellular adhesion molecules such as α3β1 integrin [110] and α- and β-dystroglycans [111; 112]. Pedicles of neighbouring podocytes interdigitate creating filtration slits, approximately 30nm wide, that are mainly responsible for the size selectivity of the filter [113]. Podocytes maintain their form by an actin fibre cytoskeleton, specifically comprising microfilaments, intermediate filaments and microtubules, in addition to actin binding proteins including α-actinin-4 [114] and synaptopodin [115]. Microfilaments are the predominant cytoskeletal constituents of the foot process, and contain a dense network of filamenous-actin (F-actin) and myosin (Fig 1.3 B).

1.2.6.1 Podocyte Slit diaphragm

Foot processes from adjacent podocytes interdigitate and connect via slit diaphragm proteins (Fig 1.3 B). This slit diaphragm consists of various protein-protein interactions, which connect and signal with the podocyte actin cytoskeleton [116].

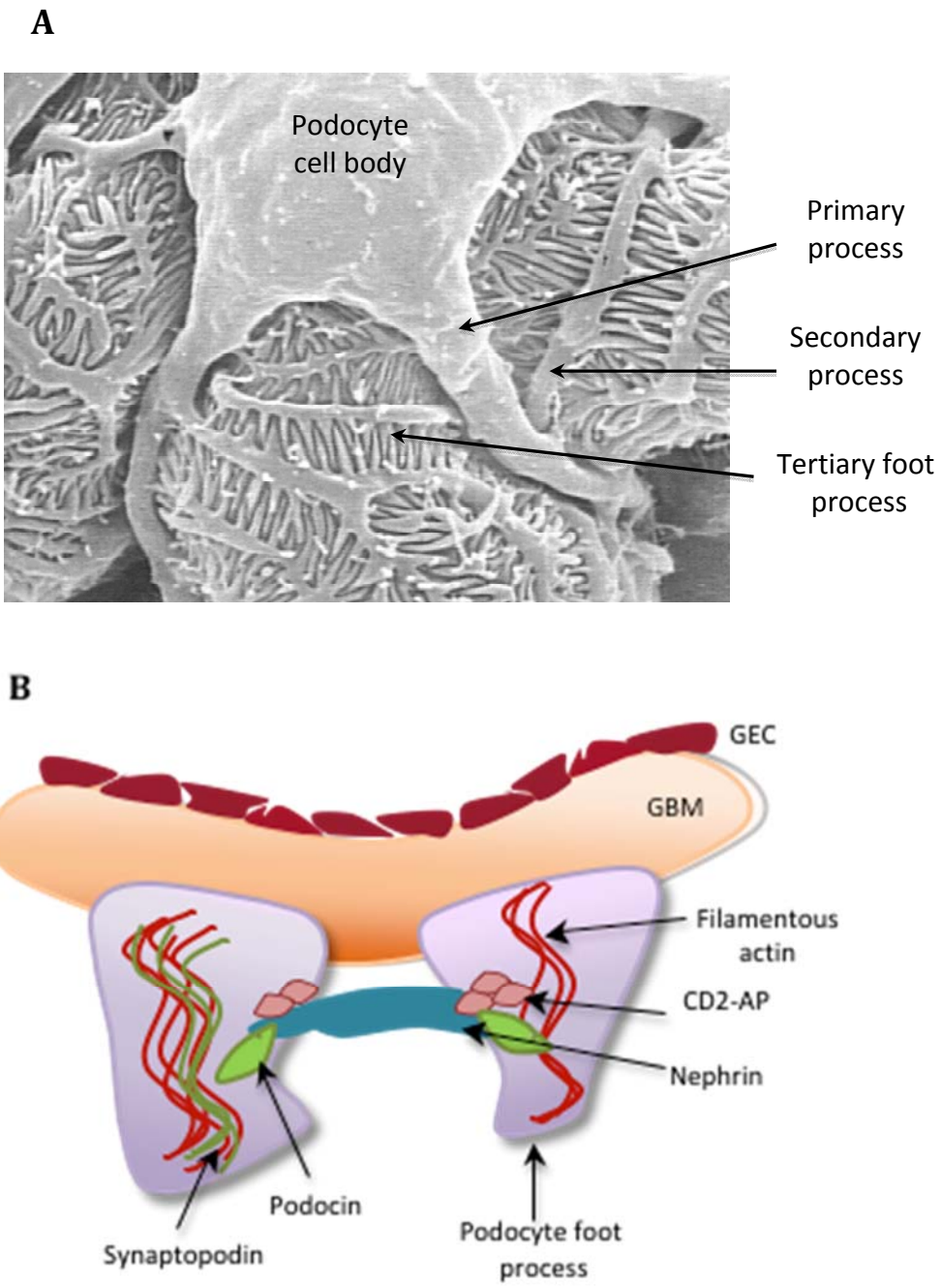

Figure 1.3 Podocyte structure and slit diaphragm

A&B (A) EM photomicrograph and (B) Diagrammatic representation of the glomerular podocyte and foot process slit-diaphragm proteins. Image A taken from [117]

Of the SD proteins, nephrin is well characterised [118]. While only one nephrin family gene exits in the human genome, there are 3 different gene loci encoding the Neph family proteins Nephrin, Neph 1, Neph 2. Nephrin and Neph 1 are structurally similar transmembrane Ig superfamily proteins. Neph2 is located at the podocyte-intercellular juncture, forms homodimers and its extracellular domain binds nephrin. A further member of this complex exists, the stomatin family member membrane-associated protein podocin[119; 120].

Like other stomatin family members it recruits its complex partners to cholesterol-enriched membrane domains at the podocyte foot process junction thereby creating a cluster that can act as a unique signalling platform [121; 122]. Consistently, mutations in the human podocin gene *NPHS2* were characterized which lead to foot process effacement, proteinuria and prevented the recruitment of Nephrin to lipid raft membrane domains [123; 121].

Also connecting this Nephrin-Neph1-Podocin complex are adaptor proteins[124]. Most adaptor proteins are localized at or near lipid rafts in podocytes and their interactions are regulated through phosphorylation and de-phosphorylation of crucial protein and lipid substrates [125; 126]. The adaptor proteins in podocytes including ZO-1- the tight junction protein expressed at the cell periphery; CD2-AP[127; 128], α-act-4- a protein linking F-actin filaments and others [129 130; 131; 132; 133] This receptor complex also associates with proteins involved in actin cytoskeleton dynamics. These include β-arrestins (1&2)- scaffold proteins that bind to and mediate internalization of plasma membrane receptors, and serve as molecular 'hubs' to organize complex signalling networks [134; 135] (reviewed in [136]) and synaptopodin- an actin associated protein encoded by the *SYNPO* gene.

In addition to size selectivity, there is also an element of charge selectivity. The apical membrane domain of podocytes is negatively charged due to surface anionic proteins podocalyxin [137] and podoplanin [138]. This causes neighbouring podocytes to remain separated in addition to preventing albumin passage (albumin is also anionic). Thus the podocyte is considered a target for an initial

insult, and loss or damage to these cells is a common feature of glomerulonephritides.

The nature of podocytes means that these cells are is considered a major target for an initial insult. Pathological podocyte involvement is mainly the consequence of podocytopenia resulting from podocyte apoptosis and EMT, or foot process effacement and alterations in podocyte dynamics [96; 139; 140]. Loss or damage to these cells is a common feature of glomerulonephritides, and a key component of the generation of proteinuria. The mechanism of podocyte loss and damage will be discussed in greater detail in section 1.3.1 Protecting or preserving podocytes from loss or effacement.

1.2.6.2 Fibrogenesis in progressive renal disease

The fibrotic mechanism of renal damage in glomerulopathies represents a final common pathway with the initial glomerular insult starting a cascade of events that include an early inflammatory phase. As discussed, resident glomerular cells such as mesangial cells and circulating inflammatory cells, including neutrophils, platelets and Mϕ mediate and perpetuate inflammatory responses leading to a fibrogenic response in the glomerular and the tubule-interstitial compartments of the kidneys [141 41; 142; 143]. This fibrotic response is oriented to an attempt towards resolution, with regression of fibrous tissue. In progressive renal diseases, however, this repair response is not halted.

The fibrogenic process is largely dependant on fibroblasts, which are considered to be the effector cells in fibrogenesis. Fibroblasts synthesize a variety of extracellular matrix components [144; 145; 146]. The overproduction of these proteins during fibrogenesis leads to excessive collagen accumulation and fibrosis. Progressive fibrosis then leads to tissue scarring with destruction of organ architecture. Fibroblasts and myofibroblasts can be derived from either resident interstitial fibroblasts or from perivascular cells. They can also be attracted into the interstitium by the action of locally produced cytokines,

particularly by platelet-derived growth factor (PDGF). The process of scar tissue remodelling involves tissue retraction [147] and is the result of the action of retractile fibroblasts derived from tubular cells. Through a process of transdifferentiation [148] these cells change their phenotype differentiating into myofibroblasts. Myofibroblasts can be recognized by their expression of α-SMA [90] and have been demonstrated in several experimental and clinical progressive renal diseases [92; 149]. The number of myofibroblasts present in renal tissue correlates with the prognosis of the disease progression preceding the development of renal scarring [90; 92]. This phenotypic transformation of fibroblasts and myofibroblasts is regulated by fibrogenic cytokines IL-l, TNF-α, PDGF, transforming growth factor-β (TGF-β), fibroblast growth factor (FGF) and others [147]. These fibrogenic cytokines also have mitogenic properties for these cells. Proliferation of fibroblasts and myofibroblasts is considered an active form of the fibrogenic response [147].

As noted, the interstitial wound in the fibrotic kidney is formed by excessive deposition of constituents of the interstitial matrix (e.g. collagen I, III, V, VII, XV, fibronectin), components restricted to tubular basement membranes in normal conditions (collagen IV and laminin), and *de novo* synthesized proteins (tenascin, certain fibronectin isoforms and laminin chains) [141]. Fibronectin has chemo-attractant and adhesive properties for the recruitment of fibroblasts and the deposition of other ECM components [150; 151; 152]. This is one of the first ECM proteins to accumulate in response to the initial damage. Fibroblasts, myofibroblasts, Mϕ, mesangial and tubular cells are sources of fibronectin [151; 152]. Other upregulated components include hialuronic acid [153; 154], secreted protein acidic and rich in cysteine (SPARC), thrombospondin (TSP) [155; 156], decorin and biglycan [157; 158].

Certain types of CKD are caused by a marked alteration of renal collagenase activity with little or no changes in collagen synthesis. Renal fibrosis in mice with unilateral ureteric obstruction (UUO) is also the result of decreased collagenolytic activity [159]. In damaged kidneys, up-regulation of TGF-β

activation also contributes to override the natural ECM homeostatic equilibrium by down-regulating the expression of matrix metalloproteinases (MMP) and activating the expression of the MMP-inhibitor plasminogen activator inhibitor 1 (PAI-1)[160]. Also tissue inhibitor of matrix metalloproteinases (TIMP)-1, an endogenous tissue inhibitor of MMPs, is actively synthesized by renal cells in progressive CKD [161], and its expression is stimulated by TGF-β, TGF-α, epidermal growth factor (EGF), PDGF, TNF-α, IL1, IL-6, oncostatin M, endotoxin, and thrombin[82]. However, its role is controversial as TIMP-1 deficient mice show no significant differences in interstitial fibrosis during induced renal damage [162; 163].

In wound-healing studies, an anti-fibrotic role for Mϕ is described, due to their participation in the resolution of the deposited ECM through phagocytosis [164]. Many short-term studies relate the number of infiltrated Mϕ with the extent of fibrosis and kidney dysfunction [165], supporting an etiological role of these cells in the pathogenesis of renal damage. Moreover, attenuated accumulation of Mϕ in experimental obstructive nephropathy is accompanied by enhanced renal interstitial fibrosis and pro-fibrotic activity [166]. However, longer-term studies reveal a reciprocal relationship between these two parameters, and raise questions about the function of infiltrating cells [167]. Thus, Mϕ probably play a dual effect, with a short-tem pro-fibrotic effect, and a long-term anti-fibrotic effect.

1.3 Therapeutic intervention

This introductory chapter summarizes the key pathophysiological events of CKDs compromising renal excretory function, at the tissue, cell and molecular levels. CKD may occur as a result of injury to the glomeruli, the tubules or the renal vessels. Most of the diseases in each of these groups have specific, but also common pathophysiological characteristics resulting from increasingly understood mechanisms of action. Moreover, all these diseases, regardless of aetiology, eventually affect all parts of the nephron and enter an irreversible course. As the disease progresses, a more uniform pathophysiological pattern occurs, characterized by increasing fibrosis, inflammation, nephron loss and parenchymal scarring.

The overall death rate increases as kidney function decreases, and the mortality in patients with ESRD remains 10-20 times higher than that in the general population. There is no cure for CKD; the natural course of the disease is to progress towards ESRD and death, unless RRT is implemented. It is essential then, that earliest possible diagnosis is critical for prognosis. The focus in recent years has shifted to optimizing the care of these patients during the phase of CKD, and to slow progression with the aim of avoiding the necessity of renal replacement therapy during the patient's lifespan.

Present treatments for CKD are only reasonably effective at slowing progression. Treatments are given substantially after irreversibility ensues, mostly because clear pathological signs only arise after more than half of the nephrons are functionally nulled. In many cases, it is possible to slow the progression of CKD to ESRD if kidney disease is diagnosed and treated in its earlier stages. The necessity for aggressive blood pressure control in CVD and CKD patients is undisputed. As discussed, current treatments for proteinuric renal diseases focus on blood pressure control via blockade of the renin-angiotensin system[168] primarily with RAS blockers [169]. Thus, early CKD identification has potentially enormous socioeconomic and medical benefits. Still, the development of earlier diagnostic tools and better drugs for preventing

and, ideally, reversing renal damage and restoring renal function needs a better knowledge of pathophysiological mechanisms of CKD genesis and progression. In this sense, reversal of CKD in the clinical setting is still an unmet goal.

Thus in chronic disease, an initial insult to the kidney, whether by injury or infection, is not repaired but rather leads to persistent, irreversible inflammation, sclerosis and necrosis. This no-return point in the fate of injured kidneys probably holds the key to a conceptual therapeutic drift from slowing progression towards regression and, along with a sufficiently early diagnosis, prevention of entering the vicious cycle of deterioration.

This thesis therefore aims to identify and investigate potential cellular and molecular targets and renoprotective agents capable of preserving renal structure and function and/or reversing damage and improving proteinuria.

1.3.1 Protecting the glomerulus from podocyte loss and effacement

Molecular insights have established the podocyte as a key component of the glomerular filtration barrier, and hence have progressively gained attention in glomerulopathies. The specialised structure of podocytes creates a filter (see section 1.4.1.2 podocyte structure and function). Pathological podocyte involvement is mainly the consequence of podocytopenia resulting from podocyte apoptosis and EMT, or foot process effacement and alterations in podocyte dynamics [96; 139; 140].

1.3.1.1 Podcytopenia

The loss of α3β1 integrin anchoring of podocyte foot processes to the GBM, followed by podocyte detachment (podcytopenia) and shedding into the urine is now recognized as an early pathologic feature in the progression of glomerular diseases (including experimental and human diabetes [170; 171]) to glomerulosclerosis [172]. Loss of these cells is believed to cause the adhesion of a glomerular capillary to Bowman's capsule at a podocyte deprived basement membrane point. These adhesions create spaces in the parietal epithelium that allow ectopic filtration out of Bowman's capsule into the paraglomerular,

interstitial space, which may be extended over the glomerulus and may also initiate tubulo-interstitial injury. In human diabetic nephropathy and IgA nephropathy, decreased podocyte number correlates significantly with poor prognosis [173; 174]. These data suggest that podocyte injury is critical not only in podocyte-specific diseases such as MCNS and FSGS but also in podocyte-nonspecific diseases such as IgA and DN.

In the process of podocyte effacement, the interconnecting foot processes detach due to loss of slit diaphragm proteins. Ultimately, these cells detach from the underlying GBM and are replaced by ECM components leading to sclerosis. There is increasing interest in therapy that specifically targets and protects the podocyte [175]. By delineating molecular mechanisms leading to these cellular events of podocyte injury and loss, therapies may be developed to reduce the burden of proteinuric renal diseases.

1.3.1.2 Podocyte Effacement

Podocyte effacement occurs as a reaction to injury or damage characterized by flattening of foot processes due to gradual simplification of the interdigitating foot process; the whole podocyte appears flattened due to retraction, widening, and shortening of the processes of each podocyte while the frequency of filtration slits is reduced, giving the appearance of a continuous cytoplasmic sheet covering the glomerular basement membrane. These cells may also become detached from the GBM which then forms a 'tuft adhesion' to the parietal cells of Bowman's capsule, leading to misdirected filtration of protein from the denuded capillary to the periglomerular or peritubular space. This results in degeneration of the affected tubule, interstitial fibrosis and eventual sclerosis [176]. The podocytes restricted capacity to replicate and/ or repair may underlie the tendency for glomerular diseases to progress to scarring (glomerulosclerosis) [177].

Effacement, injury or loss of cells results in perturbations in the complex filtration system, and is a common feature of nephrotic range (>3 g/day)

proteinuric GN [178]. Not all cases of nephrotic range proteinuria are accompanied by podocyte disease or damage-the glomerular filtration barrier also comprises the GEN and GBM and damage to these structures also contribute to proteinuria as seen in thrombotic microangiopathy or anti-GBM disease, respectively. However in the majority of glomerular diseases, podocyte loss or effacement is a frequent finding. Human acquired proteinuric glomerulopathies, such as DN, minimal-change nephrotic syndrome (MCNS), FSGS, and membranous nephropathy (MN), commonly exhibit foot process effacement of podocytes and loss of slit diaphragm in electron microscopy. These glomerulopathies therefore are considered as podocyte injury diseases (podocytopathies) [139; 179].

Therapeutic intervention by means of protection of the podocyte has therefore become an area of increasing interest in renal pathophysiology. There are several lines of evidence to demonstrate the mechanism by which podocyte effacement occurs. In experimental models, podocytes are highly susceptible to a variety of injurious agents, including complement, reactive oxygen species (ROS), and toxins such as puromycin aminonucleoside (PAN).

Podocytes up-regulate their expression of C5a receptors and become the major target of complement-mediated immune injury in membranous nephropathy [180]. In Heymann nephritis, a rat model of human membranous nephritis, the combined insults of sublytic amounts of complement membrane attack complex and ROS induce podocyte injury and proteinuria.[181]

Banas *et al* [182] suggest that podocytes may aggravate immune and nonimmune glomerular injury and contribute to their own effacement through expression of receptors linked to pathways that induce pro-inflammatory molecules using an immune complex–initiated injury in thymic stromal lymphopoietin transgenic mice that develop cryoglobulinemia and membranoproliferative glomerulonephritis. Expression of mRNA encoding Toll-like receptor (TLR)-1, -2, and -4 are markedly upregulated early in the development of disease, and their expression is further increased when the severity of GN is augmented by

deletion of an inhibitory Fc receptor (FcRIIb). TLR-4 expression is found on podocytes in nephritic glomeruli, and *in vitro* studies using immortalized mouse podocytes demonstrate induction of chemokine expression in response to lipid A, the specific TLR-4–binding component of LPS ligand. Interestingly, fibrinogen, an endogenous TLR-4 ligand, is prominently deposited in glomeruli in this model and exhibits a similar ability to induce chemokine production by podocytes. These studies demonstrate the potential of podocytes to contribute actively to recruitment of inflammatory cells and glomerular injury by upregulating TLR-4 and production of pro-inflammatory chemokines in response to stimulation by either endogenous or exogenous TLR-4 ligands.

In rat PAN nephropathy- used as a model of idiopathic nephrotic syndrome, and murine adriamycin (ADR) nephropathy, direct oxidative mechanisms induce podocyte foot process effacement[183] and apoptosis[184] leading to proteinuria, and have provided insights into the cellular and intracellular mechanisms of podocyte injury disease. Sustained proteinuria gives rise to tubulo-interstitial injury, eventually leading to renal failure [185]. Second, podocyte injury impairs mesangial structure and function. In anti-Thy-1 GN, the induction of minor podocyte injury with PAN pre-treatment results in an irreversible mesangial alteration [186]. In addition, cysteine-rich protein 61 (Cyr61), a potent angiogenic protein that belongs to the CCN family of matrix-associated secreted protein family, is expressed in podocytes and upregulated in anti-Thy-1 glomerulonephritis [187]. Cyr61 inhibits mesangial cell migration, suggesting that Cyr61 may play a modulatory role in limiting mesangial activation.

Evidence from knockout mice and rare single human gene disorders emphasizes the importance of podocytes in nephrotic syndrome: defects of the podocyte-specific gene nephrin [188] cause congenital nephrotic syndrome of the Finnish type; mutations in CD2AP, which associates with nephrin [189] gives rise to proteinuria in patients who have CD2AP haploinsufficiency [190] in addition to causing congenital nephritic syndrome in mice [191]. Mutations in α-actinin-4 (α-act-4) cause autosomal-dominant FSGS [114], and mutations in podocin cause

autosomal recessive steroid-resistant nephrotic syndrome and FSGS in children [123]. In addition to slit diaphragm protein abnormalities, podocytes can be injured by a number of mechanisms:

Proteinuria itself may contribute to podocyte effacement. Transmission electron microscopic studies reveal that proteinuria is associated with the accumulation of protein droplets within podocyte cells [192] most likely mediated by podocyte endocytosis [193]. Protein overload, both *in vivo* [194] and *in vitro* [195; 196], has been shown to induce podocyte de-differentiation and rearrangement of the F-actin cytoskeleton, in addition to stimulating upregulation of TGFβ.

Pro-inflammatory cytokines and oxidative stress are also causes of podocyte damage and de-differentiation [197; 198; 199]. Stress–tension caused by increased intraglomerular pressure seen in e.g. systemic hypertension and diabetic and non-diabetic nephropathy can lead to podocyte injury [200; 201]. Various soluble factors such as the vasopressor Ang II have also been shown to induce alterations or damage to podocytes by inducing depolarization [202], cytoskeletal rearrangements [203], and stimulation of TGFβ [204]. Furthermore, in murine podocyte cell lines these effects are paralleled with increased albumin permeability across podocyte monolayers[205]. For example, Ang II and high glucose exposure increase podocyte production of TGF-β1 [206] and vascular endothelial growth factor (VEGF) [207].

Lastly, endothelins (ETs), a family of structurally related vasoconstrictor peptides, also have implicated roles as both a stimulus, and a product of stimulation of podocytes. ETs are implicated in the pathophysiology of renal disease [208; 209; 210], and their role in the development of GN will be discussed in greater detail in the following sections.

1.3.2 The Endothelin System

The endothelins are potent vasoconstrictor/pressor peptides. There are currently 3 known isoforms encoded by distinct genes (*EDN1*, *EDN2* and *EDN3*), of which ET-1 is the most potent and widely distributed [209]. ET-1 was originally characterised from the culture supernatant of porcine aortic endothelial cells and consists of 21 amino acid residues with two sets of intrachain disulfide linkages [208]. Human *EDN1* encodes the 212 amino acid peptide ET1 precursor pre-pro-ET1 and is located on chromosome 6, spanning 6.8 kb and containing five exons. PreproET-1 is cleaved to the biologically inactive precursor big ET-1 (38 amino acids)[211]. Finally, conversion of big ET-1 to the biologically active ET-1 and C-terminal fragment occurs via the endothelin converting enzyme (ECE).

EDN1 is thought to be regulated primarily at the level of transcription, which is induced by various stimuli [212; 213], each acting in certain cells and tissues and each are regulated by different transcription factors. These include Ang II, pro-inflammatory cytokines (TNF-α, IL-1b), hypoxia, ROS, pro-fibrotic cytokines (TGF-β, PDGF) and others. Gene transcription is inhibited by prostacyclin, NO and the natriuretic peptides.

EDN1 is under the transcriptional control of a TATA box-containing promoter. Within the proximal promoter, a functional activator protein 1 (Ap-1) site has been identified, which can be bound by the c-fos and c-jun transcription factors. This promotes the transcription of *EDN1* in response to various stimuli, including phorbol esters, thrombin, Ang II and insulin, which signal through different pathways, including protein kinase C (PKC) and c-jun N-terminal kinase (JNK) pathways for transcriptional control of a TATA box-containing promoter. Other regulatory elements in the proximal *EDN1* promoter include binding sites for GATA family transcription factors TGFβ, activated SMAD transcription factors and hypoxia-inducible factor 1 (HIF-1).

ET-1 is produced by a variety of cell types including vascular smooth muscle cells, cardiomyocytes and epicardial cells, glial cells and pituitary cells [209; 214], however vascular endothelial cells are the major source. ET-1 secretion from

endothelial cells is largely abluminal [215], towards the adjacent vascular smooth muscle. Thus, ET-1 acts in an autocrine and a paracrine manner to elicit cellular responses via stimulation of two G-protein coupled receptors (GPRCs); the endothelin A receptor (ET_AR) and endothelin B receptor (ET_BR) [216; 217]. Tissue distribution of receptor subtypes varies, but both are widely expressed. ET_AR are found primarily on VSMCs and interaction with ET-1 causes vasoconstriction. ET_BR are found on VSMCs and ECs where their activation is principally involved in vasodilatation via the release of NO and prostacyclin. Both of these vasoactive peptides result in sustained vasodilation and anti-proliferative effects on vascular smooth muscle cells, in essence serving to offset the effects of smooth muscle cell ET_AR activation [218]. Furthermore, because the majority of ET-1 is released ablumenally, plasma concentrations of ET-1 do not accurately reflect ET-1 production. Some ET-1 is released into the circulation and the ET_BR also acts to clear this circulating ET-1.

The result of the ET-1 ligand binding to ET_BR is complex internalization and intracellular degradation, accounting for the majority of clearance, particularly in the pulmonary [219] and renal [213;220] circulation. Therefore, reductions in ET_BR numbers or ET_BR blockade may reduce ET-1 clearance, increasing plasma concentrations without altering production.

1.3.3 Endothelins in the Kidney

Vascular ET-1 production (plasma ET-1) is believed to be independent of renal ET-1 production and urinary excretion of ET-1 is thought to reflect renal ET-1 synthesis [221]. Within the renal system, ETs are involved in the regulation of various functions including vasoconstriction [222], natriuresis/diuresis [223; 224], inflammation and fibrosis [225]. ET-1 is produced by glomerular epithelial, endothelial and mesangial cells, renal tubular and medullary CD cells [226] and, potentially, resident and infiltrating Mϕ [227].

The cortical renal vasculature is the most sensitive vascular bed to ET-1 and the highest local concentration is found in the collecting duct epithelial cells of the inner medulla [228]. ET-1 is known to contribute to the control of renal blood flow

and glomerular filtration rate through constriction of glomerular afferent and efferent arterioles. ET_AR are predominantly located in cells of the renal vasculature throughout the cortex and medulla, including the large arcuate arteries, adjacent veins and arterioles, the vasa recta and glomeruli [229]. Activation of ET_AR leads to constriction of pre-glomerular arteries and efferent arterioles [230] and proliferation of mesangial cells [231]. ET_BR are predominantly located in the collecting ducts [229], and function predominantly in Na+ and K+ excretion [232].

1.3.4 Therapeutic intervention by ET receptor blockade

Various ET receptor antagonists are currently under investigation and have provided further insight as to the role and actions of ET-1 and the ET receptors. The ET receptor antagonists were originally licenced for and are used primarily in the treatment of pulmonary arterial hypertension (PAH) (reviewed by Humbert *et al.* 2015 [233]). PAH patients have higher plasma and lung ET-1 levels than controls. Excessive ET-1 could be due to increased production, reduced clearance or a combination of the two processes in the lung vasculature [234; 235; 236]. Furthermore, ET-1 levels in the circulation correspond to severity of disease and prognosis [237; 238; 239]. In experimental pulmonary hypertension the same trend of increased ET-1, ET_AR, and ET_BR expression can be seen [240; 241; 242].

Receptor antagonists are classified as either ET_AR or ET_BR selective, or non-selective $ET_{A/B}R$ antagonists. There is significant debate as to whether a selective ET_AR or mixed $ET_{A/B}R$ antagonist has most benefit.

1.3.4.1 ET-1 antagonism in hypertension

In addition to the observations in PAH, in humans, systemic studies using bosentan (dual $ET_{A/B}R$ antagonist) and darusentan (selective ET_AR antagonist) in hypertensive patients caused significant reduction of blood pressure (BP) [243; 244]. In a study by Haynes *et al*. (1996) [245] BQ123 has been shown to cause arterial vasodilation in both healthy volunteers and hypertensive patients.

BQ123 is a synthetic derivative of BE 18257B, a product of *Streptomyces misakiensisis* and is a cyclic pentapeptide that is highly selective for the ET_A receptor (IC50: ET_A = 7.3 nM) [246]. Studies with radiolabelled BQ123 demonstrate that it binds competitively to the ET_A receptor, achieving steady state within 7 minutes of injection and dissociates with a half-time of 1.4 min [247]. BQ-788 is an ET_B receptor antagonist which prevents binding of ET-1 at the ET_B receptor (IC50: ET_B = 18 μM) [246].

In animal models of hypertension, selective ET_AR antagonists BQ123 and darusentan were shown to decrease mean arterial pressure (MAP). The nonselective ET antagonists bosentan and SB209670 also lowered BP in the hypertensive rat, presumably as a result of the reduction of peripheral resistance, whereas cardiac output was unaltered [248].

Thus, the detrimental effects of ET-1 in the development of hypertension may be mediated by ET_AR, whereas the role of ET_BR may be the mediation of peripheral vasorelaxation. Because the two receptors have synergistic and alternate functions, it is difficult to delineate how the effect is mediated. Non-selective blockade not only attenuates the deleterious effects of ET-1 mediated by ET_AR but also concomitantly blocks the anti-hypertensive effects mediated by ET_BR. Although this seems an expected effect, at present the data regarding selective ET_A and non-selective $ET_{A/B}$ receptor blockade are variable, the relative beneficial effects of selective versus non-selective ET receptor blockade remain to be determined.

Furthermore, evidence suggests that ET-1 is involved in the pathogenesis of renal disease. Urinary ET-1 reflects renal ET-1 production. In salt-dependent models of experimental hypertension such as Deoxycorticosterone acetate (DOCA)-salt hypertension or Dahl salt-sensitive rats, renal ET synthesis is increased in animals maintained on a high-salt diet [249; 250] and urinary ET-1 concentrations are increased in many renal diseases [251].

1.3.4.2 ET-1 antagonism in CKD

Goddard & Johnston (2004) [252] examined the effects of BQ123 and BQ788 alone and in combination in healthy subjects and patients with CKD. Both selective ET_AR and combined $ET_{A/B}R$ antagonism significantly reduces BP and systemic vascular resistance in CKD patients compared healthy subjects. These changes were not consistent with renal vasoconstriction. Combined $ET_{A/B}R$ antagonism had no effect on renal blood flow (RBF) or renal vascular resistance, whereas selective ET_AR antagonism produced an increase in RBF. The results of this study showed the possible renoprotective effect of selective ET_AR antagonism as there was also reduced filtration fraction and proteinuria, suggesting vasodilatation at the efferent arteriole and reduction in intra-glomerular filtration pressure. A sustained effect may be associated with a reduced rate of progression of renal disease.

As previously discussed, the most common causes of CKD are hypertension, DM and GN. The effects of ET receptor antagonism have been investigated in hypertensive renal disease, ET_AR antagonism results in a reduction in proteinuria and glomerulosclerosis in a renal mass reduction rat model of hypertensive nephropathy[253]. Since these early studies, many other preclinical data have emerged confirming the renoprotective effects of both ET_AR and $ET_{A/B}R$ antagonism in several forms of experimental hypertension and have been reviewed elsewhere [254]. Opocensky *et al*. [255] demonstrated that hypertensive rats also developed podocyte injury, an effect observed prior to the development of proteinuria. Treatment with atrasentan (selective ET_AR antagonist) prevented podocyte injury and reduced proteinuria whilst hypertension persisted [255], an effect not seen with bosentan (mixed $ET_{A/B}R$ antagonist). In these animals, podocyte protection was observed in the earlier stages of glomerular damage (prior to glomerulosclerosis) and in the presence of established hypertension. These, and other lines of evidence in hypertensive renal disease [256;257] suggest that the renoprotective effects of ETR blockade may be independent of blood pressure reduction.

In models of DN mixed $ET_{A/B}R$ antagonists showed reduced proteinuria, glomerular injury and hypertension [258; 259]. When comparing ET receptor antagonists to ACE inhibitors, ET receptor antagonists were not superior to ACE inhibitors when measuring proteinuria as an endpoint, however some studies demonstrated equal efficacy [260; 261]. Overall, ACE inhibitors were superior in efficacy [262], however the combination of ACE inhibition with ET receptor antagonism is additive [260]. ET receptor antagonists also affect glomerular injury and inflammation in models of DN. In streptozocin-induced DN, ET_AR antagonism resulted in reduced expression of ICAM-1 and monocyte chemo-attractant protein (MCP-1), whilst preserving expression of nephrin [263]. Furthermore, the selective ET_AR antagonist sitaxentan reduced renal Mϕ infiltration and expression of pro-inflammatory cytokines in different models of DN[262; 264]. These BP-independent, anti-inflammatory and podocyte protective effects of ET receptor antagonism may provide additional longer-term benefits in DN.

As noted, studies investigating ET receptor antagonism have largely been performed in animal models of either hypertension or DN, and there are very few studies in inflammatory GN. The following studies in rats demonstrated similar effects of ET receptor antagonism. Studies in immune complex GN using a mixed $ET_{A/B}R$ antagonist demonstrated reduced proteinuria and glomerular injury[265]. In Anti-Thy1 nephritis using a selective ET_AR antagonist demonstrated reduced glomerular cell proliferation[231]. Similarly, studies in membranous nephropathy using an ACE inhibitor and ET_AR antagonist, alone and in combination demonstrated reduced proteinuria, lower serum creatinine and less glomerular and tubulointerstitial injury. Combination therapy was found to be more effective to either intervention alone[266]. Finally, studies examining Heymann nephritis using an ACE inhibitor, an ARB, and an ET_AR antagonist alone and in combination, demonstrated a similar reduction in BP. The ACE inhibitor was more effective in reducing proteinuria and glomerulosclerosis. ET_AR antagonism had an additive effect when used in conjunction with either the ACE inhibitor or the ARB [267]. Whether ET receptor antagonists are able to

alter Mϕ infiltration and function and podocyte biology in GN has not been assessed. Finally, a single study to assess renal inflammation by ETR antagonism exists in the context of lupus nephritis. This study shows that urinary ET-1 as a reflection of renal ET-1 synthesis [268] [269] is increased in those with renal inflammation. Urinary ET-1 levels decreased following successful treatment of the inflammation.

1.3.4.3 ET-1 antagonism in podocytes

Podocytes have been shown to express both ET_AR[195] and ET_BR[270] in rodents. There is limited data lacking definitive expression of receptors for human podocytes [271; 272]. However, it is likely that human podocytes also possess both ET_AR and ET_BR [273]. ET-1 is also implicated as both a stimulus, and a product of stimulation of podocytes. As previously discussed, murine podocytes exposed to an albumin (or IgG) load leads to disruption of the actin cytoskeleton and activation of focal adhesion kinase (FAK). This activates transcription of pre-proET-1 mRNA leading to ET-1 secretion [195]. Furthermore, shiga toxin treatment leads to ET-1 secretion. In turn, ET-1, acting in an autocrine manner via the ET_AR, causes disruption of the podocyte actin cytoskeleton [274].

ET-1 may also affect proteins of the slit diaphragm including nephrin, podocin, CD2AP and synaptopodin. Of these, nephrin particularly is often used in experimental models as a marker of podocyte injury. *In vitro* studies demonstrate that glomerular endothelial cells incubated with pre-eclamptic sera induced ET-1 production. Treatment of murine podocytes with this conditioned sera induced shedding of nephrin [272]. Furthermore, infusion of ET-1 into rats caused nephrin excretion into the urine [263]. In both instances these effects were inhibited by ET_A receptor antagonism.

In addition to the studies previously mentioned (section 1.3.4.2 ET-1 antagonism in CKD), there is further evidence that the beneficial effects of ET antagonists may be, in part, due to protection of podocyte structure and function. Aged Wistar rats spontaneously develop glomerulosclerosis,

proteinuria and podocyte injury, [275] and treatment with darusentan reduced BP and proteinuria and preserved podocyte number. In a separate study, nephrin loss was also attenuated in this model of spontaneous hypertension[263].

1.3.4.4 ET-1 in macrophages

ET-1 is known to be involved in the regulation of various functions including vasoconstriction[222], natriuresis and diuresis [223; 224] and importantly in inflammation and fibrosis [225]. Mϕ infiltration is a near universal feature of renal disease and is involved in both progression and resolution of renal injury. Although the data is limited, Mϕ are believed to have an ET-1 system. Human Mϕ have been shown to express ET_BR, but there is currently no data demonstrating the presence of the ET_AR [276]. In human and animal studies activated Mϕ have been shown to synthesise ET-1 in response to LPS, phorbol myristate acetate (PMA) and low-density lipoprotein (LDL)[277; 278; 227; 279] Furthermore, ET-1 is also considered to be pro-inflammatory and chemotactic for Mϕ /monocytes [280; 281;282]. ET-1 is also a potent mitogen, and partly mediates the proliferative effects of several cytokines [283; 284; 285]. It is thus suggested that in instances of chronic inflammation, ET-1 promotes the pro-inflammatory phenotype of Mϕ, which in turn exacerbates chronic inflammation. It is hypothesised then that selective ET_AR antagonism with BQ123 will be beneficial in limiting the pro-inflammatory effects of ET-1 in Mϕ. Studies to this end have not yet been investigated.

1.4 Overview

Podocyte effacement underlies the pathology of numerous forms of renal disease, notably various forms of GN. By delineating the events leading to injury in podocytes, therapies may be developed to reduce the burden of proteinuric renal diseases by protecting or preserving these cells. Podocyte injury can occur via protein loading, inflammatory cytokines and growth factors, in addition to vasoconstrictors such as Ang II.

ET-1 also has implicated roles as both a stimulus, and a product of stimulation of podocytes. Podocytes cells have been described as targets for ET-1, given that ET_A and ET_B receptors are present on the surface of podocyte cells in humans and in animals [270; 273]. Inflammatory cytokines and proteinuria augment renal ET-1 production [286]. ET-1 may therefore cause podocyte effacement by direct interaction with the cells, and a resultant increase in ET-1 production. Furthermore, activated Mϕ have been shown to synthesize ET-1, and ET-1 may activate and be chemotactic for Mϕ/monocytes [277 280]. The pathophysiology of the ET system in renal disease is not yet fully understood, there is a body of evidence supporting a beneficial role for manipulation of the ET system, exemplified by studies involving selective ETR antagonism.

1.5 Hypothesis and Aims

This thesis will examine the effects of selective ET_AR antagonism using orally active Sitaxsentan in a rat model of GN. We hypothesise that ET_AR antagonism ameliorates proteinuric renal disease. The study also intends to further clarify the action of ET-1 in human podocytes and human peripheral blood monocyte derived Mϕ. We hypothesise that ET-1 will mediate podocyte effacement and macrophage inflammation. We further aim to investigate the mechanism by which ET-1 mediates its effects. We hypothesise that these effects will be mediated via the ET_AR; blockade with the selective ET_AR antagonist BQ123 will attenuate these effects, with the selective ET_BR antagonist BQ788 conferring no effect.

Chapter 2
Materials and Methods

2.1 In vitro studies

All cell culture was performed in a Class II tissue culture hood (ICN microflow). All chemicals, sera and plastics were tissue culture grade unless otherwise stated.

2.1.1 Cell Culture

2.1.1.1 Human Immortalised Podocyte Cells

All experiments in this study utilise a conditionally immortalized human podocyte cell line initially described by Saleem *et al.* (2002)[287]. Briefly, cells were cultured under growth-permissive conditions to promote cell propagation as a cobblestone phenotype (undifferentiated) in uncoated 75-cm^2 flasks (Falcon; BD Biosciences, Bedford, MA) at 33°C (5% CO_2) in RPMI 1640 medium supplemented with 10% foetal bovine serum (FBS), insulin, transferrin, selenium (Sigma Chemicals, Dorset, UK), L-glutamine, 100 µl/ml penicillin and 0.1 mg/ml streptomycin (P/S). Cells were grown to 70-80% confluence, then trypsinized for 5 min and re-suspended in supplemented media. The cells were then centrifuged 300 x *g,* supernatant removed, and cell pellet re-suspended. The cells were seeded into fresh flasks at a dilution of between 1:3 and 1:5, and/or seeded to varying sizes (depending on the assay) of uncoated tissue culture plates. Cells were seeded onto type I rat tail collagen coated glass coverslips for immunofluorescence studies. To induce differentiation, podocytes were maintained in non-permissive conditions at 37°C (5% CO_2) to inactivate the temperature sensitive SV40 T antigen. Experiments were conducted on day 14 of differentiation. In this culture condition, cells were identified as differentiated podocytes by their arborized morphology under light microscopy (LM). Cells were rinsed with phosphate buffered saline (PBS) without Ca and Mg (-), and medium replaced 3 times per week. Images were obtained using a Zeiss Axiovert 25 inverted light microscope fitted with a coolsnap photometrics camera using Openlab software.

2.1.1.2 Human peripheral blood macrophages (Mϕ)

All experiments with Mϕ were of human peripheral blood mononuclear cell (hPBMC) origin. Blood was taken under the remit of an on-going clinical research trial for which ethical approval was obtained. Blood was drawn by a qualified phlebotomist also registered in the trial. Consent was obtained from healthy volunteers in each case. For each experiment 160ml of peripheral venous blood was drawn from a single volunteer. Sodium citrate (0.31%) was used as an anti-coagulant. Blood was centrifuged at 350 x *g* for 20 min at room temperature. The top layer of platelet rich plasma (PRP) was removed. Autologous serum was prepared by adding 10ml of PRP to 200µl 1M $CaCl_2$, inverted, and maintained at 37°C for 2h or until a platelet plug is formed. Cells were diluted 1:2 with normal saline and 6 ml dextran (6%) added to lyse RBCs. After RBC sedimentation (20-30 min), leukocyte-rich upper layer was removed and centrifuged at 350 x *g* at 20°C for 6 min, and RBCs were discarded. The cell pellet was layered on a Percoll (GE Healthcare) gradient (81% 68% and 55%) and the upper layer containing monocytes was obtained following centrifugation at 720 x *g* for 20 min. Cells were re-suspended in 1 x PBS (-) and centrifuged at 230 x *g* for 6 min. Cells were counted using a haemocytometer with trypan blue exclusion. Cells were re-suspended in serum free Iscove's modified Dulbecco's medium (IMDM) ($4x10^6$/well) and purified by adhesion in culture flasks for 90 min at 37°C. Non-adherent cells were removed and medium replaced by fresh IMDM containing 10% autologous serum. Serum containing medium was changed every 2–3 days. After 4-6 days of culture, monocytes acquired a Mϕ phenotype [288]. Cells were used on d7 for all experiments.

2.1.2 ET-1 stimulation assay

To investigate the effect of exogenous ET-1 administration on podocytes and Mϕ, confluent differentiated cells were exposed for 2-48 hours to medium alone, or in the presence of 5-50,000 pg/ml of ET-1 depending on the specific assay. The cell supernatant was then removed and centrifuged at 13,000 x *g* for 20 minutes. The supernatant fraction was removed and stored at -80°C for

further analysis of ET-1 and cytokine content. Additionally, Mϕ were classically activated as a positive control by exposure to LPS (100ng/ml) and rIFNγ (5ng/ml) for the same time periods.

2.1.3 ET-1 stability assay

To estimate the natural attrition rate of ET-1 in culture over time, 10 pg/ml of ET-1 in supplemented media was measured at 0h and after 48h incubation at 37°C (5% CO_2) standard culture conditions.

2.1.4 ET-1 quantification

ET-1 protein from cell supernatants was assessed by standard radioimmunoassay (RIA) (Peninsula Laboratories Europe, St Helens, UK) using ^{125}I radiolabelling [252; 289; 290]. Either standard compounds or unknown samples (100µl) were added to 100µl of antiserum (Peninsula Laboratories Inc., Belmont, CA) diluted in phosphate buffer, pH 7.2 (RIA buffer), at a final dilution of 1:72,000. The reaction mixture was incubated for 24h at 4°C, then 15,000 cpm (^{125}I) ET-1 in 100µl was added and the incubation prolonged for 24h at 4°C. Separation of free from antibody-bound (^{125}I) ET-1 was achieved by addition of a second antibody (500µl of immunoprecipitating mixture consisting of a sheep anti-rabbit IgG and polyethylene glycol) for 30 min at room temperature. Finally, 500µl of RIA buffer was added to the stop reaction, and the immunoprecipitates were centrifuged at 5000 x *g* for 30 min. Supernatants were discarded, and pellet radioactivity detected by γ-counter (Beckman, Irvine, CA). Results were expressed as pg/ml quantities. The sensitivity of the assay was 1 fmol/tube with inter- and intra-assay coefficients of variation of 13% and 9%, respectively. Cross-reactivity with endothelin-3 and non-endothelin peptides was less than 1%.

2.1.5 Enzyme-linked immunosorbent assay (ELISA)

The detection of cytokines were performed by capture ELISA according to manufacturers protocol (ELISA Duoset, R&D Systems). Briefly, 96 well ELISA plates were coated with 100µL per well of capture antibody diluted to the

working concentration in PBS without carrier protein. Plates were then sealed and incubated overnight at room temperature. Wells were then aspirated and washed with wash buffer (x3). Antibodies were then blocked by addition of 300µL reagent diluent to each well and incubated at room temperature for a minimum of 1 hour. Plates were then washed (x2) with wash buffer and 100µL of sample or standards in reagent diluent were added per well. Plates were re-sealed and incubated for 2 hours at room temperature. Following sample incubation plates were washed (x2) in wash buffer then 100µL of the detection antibody diluted in reagent diluent was added. Plates were incubated for 2h at RT. Plates were washed (x2) with wash buffer then 100µL of the working dilution of Streptavidin-HRP was added to each well. Plates were re-sealed and incubated for 20 min at RT. Plates were washed (x2) with wash buffer then 100µL of Substrate Solution was added to each well and incubate for 20 min at RT. Finally, 50µL of Stop Solution was added to each well. Samples were quantified by optical densitometry at 450nm (Molecular device spectra 340 microplate reader, USA) and GEN5 software, and standard curve generated using Microsoft Excel software. Cytokines measured were IL-6 (9.38-600 pg/ml), IL-8 (31.2-2000 pg/ml), IL-10 (31.2-2000pg/ml), TNFα (15.6-1000pg/ml) & VEGF (31.2-2000 pg/ml).

2.1.6 ET receptor antagonist assays

Where ET-1 effects were observed, investigations into the effect of ET_A and ET_B receptor antagonism on ET-1 induced ET-1 and cytokine protein production were conducted using the selective ET_AR antagonist BQ-123 (IC50: ET_A = 7.3 nM) [246] (1µM) (Merck Biosciences, Beeston, Nottingham), [246; 252] and BQ-788 (0.1µM) (IC50: ET_B = 18 µM) [246] (Merck Biosciences, Beeston, Nottingham), a selective ET_BR antagonist. The doses used were based on previous studies as having maximal haemodynamic effect [252]. ET-1 and cytokine production was determined as in previous experiments. Cells were incubated in the absence or presence of receptor antagonists in supplemented media 1h prior to stimulation with ET-1 at various concentrations (0, 5, 50, 100 pg/ml).

Sitaxentan sodium is a highly selective ET_AR antagonist that has been developed for the treatment of patients with pulmonary arterial hypertension classified as WHO functional class III, to improve exercise capacity. It binds to and blocks selectively (ratio $ET_{A/B}$ is ~6,500 fold) and competitively ET_AR with high affinity (Ki 0.43 nM), and potently inhibits receptor signalling (Ki 0.43 nM; 0.686 nM). Animal studies (using rats and pigs) have shown that sitaxentan sodium (mg/kg range) is effective for pulmonary hypertension (PAH) in response to hypoxia [291].

2.1.7 Immunofluorescence (IF) studies

Podocytes and Mϕ were fixed with 2% paraformaldehyde (PFA), 4% sucrose in PBS (-) for 30 min at 37°C, then permeabilised with 0.3% Triton X-100 (Sigma) in PBS (-) for 10 min. Non-specific binding sites were blocked with block solution (4% FBS + 2% bovine serum albumin (BSA) + 0.1% Tween x 20 (Sigma) in PBS (-)) for 30 min. Coverslips were washed x1 in PBS (-). Primary antibodies: polyclonal mouse α human ET_A and ET_B receptor (Sigma) (1:200), polycolonal mouse α human nephrin (Sigma) (1:200), rabbit α human podocin (Santa Cruz) (1:200), polyclonal goat α human Synaptopodin (1:200) Rhodamine conjugated Phalloidin (Biotium) (5units/ 300µl), and isotype controls: mouse, rabbit and goat IgG1 negative control (Serotec) (1:200) were diluted in block solution and applied (50µl) overnight at 4ºC. Coverslips were washed 2x in PBS (-) followed by incubation with secondary antibodies: goat α mouse or rabbit Alexa-488 (green) and Alexa-542 (red) were applied (50µl) for 30 minutes at the appropriate dilutions. Coverslips were washed 3x in PBS (-). Nuclei were stained for 5 sec with methanolic 4',6-diamidino-2-phenylindole (DAPI). Coverslips were washed x3 in dH_2O and mounted on glass slides with VECTASHIELD (Vector Labs) mounting medium for fluorescence. Images were obtained using a Zeiss Axioskop fluorescence photomicroscope attached to a Spot 2 slider digital camera (Diagnostic Instruments Inc., Sterling Hts. MI) with Openlab software, and were processed with Adobe Photoshop 5.0 software.

2.1.8 Cellular protein extraction

Cellular proteins were extracted by washing with PBS followed by incubation in cell lysis buffer (1% saponin (Sigma), 75 mM NaCl, 5 mM ethylenediaminetetraacetic acid (EDTA), 50 mM Tris (pH 7.6), 1 mM phenylmethylsulfonyl fluoride (PMSF), 1 µg/ml aprotinin, 1 µg/ml leupeptin, 1 µg/ml pepstatin, 1 mM Na Orthovanadate) at 4°C for 20 min. Cells were scraped from the wells. The suspension collected and centrifuged at 14000 x *g* for 20 min. The supernatant containing protein was collected and stored (-80°C).

2.1.9 Total protein quantification

Whole protein content was quantified by the Bradford assay using the Bio-Rad protein assay reagent (Richmond, CA) according to manufacturer's protocol. To reduce proteolysis, all buffers contained protease inhibitor cocktail (Roche, UK). Human serum albumin (HSA) (Sigma) was used as a standard. Protein content was determined colorimetrically at 720nm (Molecular device spectra 340 microplate reader, USA).

2.1.10 SDS-PAGE and Western blot

Following whole protein content quantification samples were diluted to 1µg total protein/ µl, and Laemmli Buffer (LB) added (1:5) and denatured by heating to 95°C. 25µl (20µg total protein) was loaded onto 9% sodium dodecyl sulfate–polyacrylamide gels and electrophoresed (SDS-PAGE) under standard conditions (120V, 1h). Following running, gels were equilibrated in transfer buffer (15 min) and prepared for wet transfer to nitrocellulose membranes at 40mA for 3 h. Membranes were rinsed in reagent diluent (Tris-buffered saline + 0.05% Tween 20 (TBST)) followed by blocking (5% milk powder in TBST) for 1 h before incubation with primary antibodies: polyclonal mouse α human ET_AR and ET_BR (Sigma; 1:200; each 50kDa), rabbit α- human podocin (Santa Cruz; 1:200; 42kDa) and mouse α-β-actin (Sigma, 1:10,000; 50kDa). Membranes were washed x2 then incubated in horseradish peroxidase (HRP)-conjugated secondary antibody (mouse and rabbit) (Amersham Biotech, Buckinghamshire, UK; 1:2,500) for 1h. After final washing (x3), membranes were developed using

enhanced chemiluminescence (ECL) reagent or West Femto Supersignal (Pierce) to XAR5 film (Kodak) for 30s-10min.

2.1.11 RNA extraction and RT-PCR

Total RNA was extracted using NucleoSpin Mini Spin columns according to the manufacturers instructions. Briefly, cells were lifted using trypsin and centrifuged 13,000 x *g.* The cell pellet was then washed (x2) with PBS (-). The cell pellet was then re-suspended in 350µl RA1 buffer, and 3.5µl β-mercaptoethanol (β-ME) and vortexed for cell lysis. The lysate was then filtered through a Nucleospin filter column at 11,000 x *g* for 1 min to reduce viscosity and clear the lysate. RNA was then precipitated from lysate by addition of 350µl ethanol (70%) and vortexing. Precipitated RNA was then loaded onto Nucleospin silica membrane columns and centrifuged at 11,000 x *g* for 30s. Salt residues on silica membranes containing bound RNA were then removed by incubation (1min) with membrane desalting buffer (MDB) and centrifugation at 11,000 x *g* for 30s. DNA was then digested by addition of 95µl of reconstituted DNAse to the membrane for 15 min at room temperature. Following DNA digestion, the RNA on the silica membrane was washed in 200µl RA2 buffer, then 600µl RA3 buffer, then 250µl RA3 buffer, each time centrifuging for 1 min at 11,000 x *g.* The purified RNA was then eluted in 30µl dH_2O. Eluted RNA was then quantified by spectrophotometry using NanoDrop. The purity of the RNA was determined by A260/A280 values being 1.7-2.0. Similarly, A260/A230 values between 1.3-1.7. RNA was then diluted to 100ng/µl in nuclease-free H_2O. 1µg total RNA was reverse transcribed using MultiScribe RT Kit (Promega) according to manufacturers instructions. Briefly 10µl (100ng/µl) RNA was added to 10µl 2X RT Mix containing 2 µl 10X RT buffer, 0.8µl 25X dNTP Mix (100mM), 2µl 10X RT Random Primers, 1µl MultiScribe RT, 1µl RNAse Inhibitor and 3.2µl nuclease-free H_2O on ice in thin-walled eppendorff PCR tubes. The samples were heat cycled as follows: 1) -25°C for 10 min, 2) 37°C for 2h, 3) 85°C for 5 sec, 4) 4°C ∞. cDNA was stored at -80°Cor used for PCR. The PCR reaction was performed using the 5'-3' primers shown in table 2.1.

In each PCR reaction, 2µl cDNA template was added to 12.5µl 2X PCR master mix containing Taq DNA polymerase (pH 8.5), 400µM of each dATP, dGTP, dCTP, dTTP and 3mM MgCl2. Additionally, 1µl sense and 1µl antisense primers, and 8.5µl nuclease-free H_2O were added. Amplification was carried out using the following PCR program: Denaturation- 94ºC for 5 minutes Annealing- 94ºC for 30 sec, 56ºC for 30 sec, 72ºC for 30s (35 cycles) Extension- 72ºC for 5min sec, 4ºC ∞. Following amplification, 5µl of nuclease free water 2µl of orange loading buffer (Thermo-Fisher) were added to 5µl of each sample. 25µl of each sample were loaded in to a 1.2% agarose gel (1.2g/100ml 0.5x TBE) containing 3µl ethidium bromide. In addition, 4µl 1Kb DNA ladder + 2µl loading buffer was loaded in to the first lane. The samples were electrophoresed at 120V for approx. 30mins, and visualised under UV light. The product sizes are ET_AR-242bp, ET_BR-260bp and β-Actin-250bp. Gel band densitometry was then assessed using image J software.

Table 2.1 RT-PCR primer sequences

Gene	Sense	Antisense	Product Size (bp)	Annealing Temp. (˚C)
hNephrin	GTG-AAC-GAG GGC-TCC-CAG-C	GCAGTCCATC CATGACTGTC	520	56
hSynaptopodin	TGCCCAAC CTGCCCAA	CGCATTGATG ATGTTTCGC	497	52
hPodocin	GGCATGGGAA TGTAGCAAGT	TCTCCAAATC CAATTCCTCG	433	54
hET_A Receptor	CCTTTTGATCA CAATGACTTT	TTTGATGTGGCA TGAGCATACAG	242	56
hET_B Receptor	ACTGGCCATTT GGAGCTGAGAT	CTGCATGCCACT TTTCTTTCTCAA	260	56
β-actin	GCGGGAAATCGT GCGTGACATT	GATGGAGTTGAA GGTAGTTTCGTG	250	56

2.1.12 Mϕ migration assay

Test media (600µl) was added to 12 of the lower chambers of a 24 well TC plate. Test media are all serum free IMDM + P/S and contain either monocyte chemo-attractant protein (MCP-1) (100ng/ml) as a positive control, ET-1 (10-10,000 pg/ml) or media alone. 8µm pore size transwell filters (Costar) were placed into the media containing wells. Mature Mϕ were lifted from TC flasks using EDTA buffer for 5 min followed by cell scraping. Cells were re-suspended in Mϕ assay medium (IMDM + 10% autologous serum + 1% P/S), counted using a haemocytometer, centrifuged at 350 x *g* for 5 min, supernatant discarded and cell pellet re-suspended in at $1x10^6$/ml. 100µl (100,000 cells) of cell suspension was added to the upper chamber of each transwell. Methanol fixed cells were added to media containing MCP-1 as a negative control. Plates were incubated at 37ºC for 12h. At the end point transwell filters were removed and cells were allowed to adhere for a further 12h. Non-adherant cells were then washed with PBS (-). Adherent cells were incubated with 0.5% DAPI in dH_2O for 10 sec. DAPI was removed and cells were washed x2 in dH_2O and visualised under a Zeiss inverted fluorescence microscope. Low power images were captured using Openlab software. Experiments were performed in duplicate. One image per well was taken and the number of nuclei per low power field were counted and expressed as mean of duplicate wells.

2.1.13 Mϕ phagocytosis assay

Mature Mϕ were treated with dexamethosone (DEX) (100ng/ml) as positive control, ET-1 (10-1000 pg/ml) or media alone for 24h in assay medium containing (IMDM + 10% Autologous Serum + 1% P/S). Following this incubation period, GFP–tagged *Escherichia coli* bacterial particles (Sigma) were added to each well and incubated for 1h. The cells were then washed x3 PBS and stained with LysoTracker Red for visualisation of Mϕ. The cells were then fixed by addition of ice cold (1:1) methanol (100%) and acetone (100 %). Following 1h fixation cells were washed x2 in dH_2O and visualised under a Zeiss inverted fluorescence microscope. Low power images were captured using Openlab software. Experiments were performed in triplicate. Mϕ area was quantified by

using image J software. GFP signal was assessed by colour image analysis using Adobe Photoshop. Data are expressed as GFP/ Mϕ area.

2.1.14 Mϕ Endocytosis assays

Mature Mϕ were treated with Chloroquine (CQ) (100μg/ml; Sigma Chemical, St. Louis, MO) or Nocodazole (NZ) (10μM; Sigma Chemical, St. Louis, MO) 2h prior to addition of ET-1 (30-30,000 pg/ml) for 2h and 24h in assay medium containing (IMDM + 10% autologous serum + 1% P/S). CQ or NZ plus ET-1 (3000 pg/ml) alone (no Mϕ) were also incubated as internal controls.

2.1.15 Mϕ protease inhibitor assay

Mature Mϕ were treated with protease inhibitors (PI) (1 tablet/50ml; Roche Diagnostics Ltd, Welwyn Garden City, UK) 2h prior to addition of ET-1 (30-3000 pg/ml) for 2h and 24h in assay medium containing (IMDM + 10% autologous serum + 1% P/S). PI plus ET-1 (3000 pg/ml) alone (no Mϕ) was also incubated as internal controls.

2.2 *In vivo* studies

All animal experiments were carried out in accordance with the British Home Office Animals (Scientific Procedures) Act 1986.

2.2.1 Rat nephrotoxic nephritis (NTN)

In vivo experiments were performed using a telescoped model of Nephrotoxic serum (NTS)-induced nephritis in rats [292]. This is a basic experimental model first described by Masugi and colleagues[293], that resembles human diffuse glomerulonephritis (GN). Briefly, in this model the GN is induced by the injection of a rabbit antibody raised against rat GBM. Within hours from the injection of the anti-GBM antibody, the initial heterologous phase of the nephritis takes place. It is mediated by the binding of the heterologous antibody to the rat GBM. Proteinuria also occurs in this heterologous phase and coincides with the binding of rabbit antibody to the GBM [294; 295; 296]. Furthermore, a complement-dependent attraction of polymorphonuclear leucocytes to the glomeruli also occurs [297].

Schreiner *et al*. [298], In a model of nephrotoxic nephritis resembling the autologous phase, demonstrated a mononuclear (MN) cell infiltrate in the glomerulus and proposed a role for cell-mediated immunity in experimental GN. In addition to being used to study the cause and developing mechanisms of GN, this model is also used to evaluate the anti-nephritic effects of various agents. The nephritic effects of NTS in different species and strains can vary significantly its ability to induce proteinuria, hypertension, crescent formation etc [299]. These experiments were conducted in Sprague-Dawley rats to determine whether a selective ET_AR antagonist sitaxsentan (STX), would ameliorate proteinuria, hypertension, and renal inflammation and fibrosis.

The importance of the autologous phase in occurrence or chronic progression has also been shown by Unanue & Dixon[296] in accelerated types of nephrotoxic serum nephritis wilh the atcive immunisation of rats with heterologous (rabbit) immunogiobulins.

2.2.1.1 Generation of rat NTN

Male Sprague Dawley rats (weight, 200-250g) were obtained from animal house stock. Rats were pre- immunised with s.c. injection 7d prior to induction of NTN with 1mg of rabbit IgG. NTN was induced by single i.v. injection of 1ml/200g nephrotoxic serum (NTS) containing rabbit anti-rat glomerulus antibodies under halothane anesthesia (Zeneca, Macclesfield, UK). Three days prior to induction of NTN animals were treated with either selective ET_AR antagonist STX (30mg/kg) or placebo by gavage, and every day thereafter for 17d. This work was carried out under the supervision of David Kluth and William Mungall.

2.2.1.2 Production of nephrotoxic serum

Nephrotoxic serum contains high titres of anti-rat GBM antibodies and was produced by immunisation of rabbits with homogenate of rat glomeruli. Rat GBM antigen was prepared from frozen kidneys of Sprague-Dawley rats. The capsules were removed from the kidney and the renal cortex dissected away. The glomeruli were purified from the renal cortex by sieving through meshes of 250μm, 150μm and 63μm diameter with the glomeruli caught by the 63μm sieve. Glomeruli were recovered into ice cold PBS and the suspension spun at 500 rpm for 5 minutes in a Jouan CR 312 centrifuge. This washing procedure was repeated on 2 more occasions. The glomeruli were then sonicated on ice for 3-5 minutes until complete disruption of glomeruli was confirmed by microscopic examination. The sonicated glomeruli were washed x2 in PBS (-) followed by centrifugation at (1000 rpm, 5 min). The GBM pellet was lyophilised and stored at –20°C until use.

Nephrotoxic serum was raised in New Zealand white rabbits. They were initially immunised with subcutaneous injection of 1 mg of prepared GBM in 1ml of Freund's complete adjuvant (Sigma, Poole, Dorset, UK) and then at 2 weekly intervals the rabbits were boosted with 1mg of GBM in 1ml of Freund's incomplete adjuvant (Sigma, Poole, Dorset, UK). After 4-5 injections a blood

sample was taken by bleeding of the ear vein and the titre of serum determined. This was assessed by determining the binding of dilutions of the serum to cryostat sections of normal rat kidney followed by staining with anti-rabbit IgG FITC (Sigma, Poole, Dorset, UK). A titre of at least 1:1000 was required and if this level was obtained the animals were boosted on one further occasion 2 weeks later and the rabbits the sacrificed by cardiac puncture under anaesthesia. The blood was centrifuged at 2500 rpm in Jouan CR 312 and the serum removed. Complement within the serum was heat inactivated by heating to 56°C for 30 minutes. The serum was then absorbed against rat red blood cells at 4°C overnight and then repeated for 1 hour at room temperature. The serum was stored in aliquots at -80°C. The LPS level was assessed using the limulus amoebocyte lysate assay using a test kit with a lower limit of detection of 50 pg/ml (Sigma, Poole, Dorset, UK). Nephrotoxic serum contained less than 50 pg/ml in all samples analysed.

2.2.1.3 Sample collection and quantification

Rats were housed in metabolic cages for the duration of the experiments. Animals were weighed daily and timed urine collections were made every 2-4 days. The sample volumes were measured then stored (-80°C) for later analysis. Furthermore, blood pressure was sampled by tail-cuff plethysmography every 3-5 days. 14d after treatment, the animals were sacrificed by cervical dislocation. Prior to sacrifice, a minimum of 1ml of blood from the tail vein was collected into sodium citrate. Blood was centrifuged (300 x g) for 10 min and the serum removed and stored. The urinary and serum albumin and creatinine concentrations were determined. Albuminuria was expressed as an albumin creatinine ratio. Kidneys were removed and fixed in methylcarnoys. Routine sections were cut at 2 μm and stained with H&E.

2.2.1.4 Serum and urinary albumin and creatinine quantification

Rat urinary albumin measurements were determined using a commercial serum albumin kit (Alpha Laboratories Ltd., Eastleigh, UK) adapted for use on a Cobas Fara centrifugal analyser (Roche Diagnostics Ltd, Welwyn Garden City, UK). All measurements were performed by Forbes Howie. Measurement of serum albumin was based on its quantitative binding to bromocresol green (BCG). Albumin-BCG-complex absorbs maximally at 578nm, the absorbance being directly proportional to the concentration in the sample. Within run precision was CV < 2.5% while intra-batch precision was CV < 4%.

Serum creatinine was determined using the creatininase/creatinase specific enzymatic method [300] utilising a commercial kit (Alpha Laboratories Ltd. Eastleigh, UK), also adapted for use on a Cobas Fara centrifugal analyser (Roche Diagnostics Ltd, Welwyn Garden City, UK). Within run precision was CV < 3% and intra-batch precision was CV < 5%. The normal reference range for Sprague Dawley rat serum creatinine is 0.27mg/dl or 23.8 μmol/L [301]

2.2.1.5 Blood pressure by tail cuff plethysmography

Rats were pre- heated in a chamber at 35 °C for 5 min, then placed on a heat blanket. A cuff with a pneumatic pulse sensor was attached to the tail. Rats were allowed to habituate to this procedure for 7d prior to experiments. BP and HR values were recorded on a Model MK-2000 with heating and were averaged from three consecutive readings obtained from each rat.

2.2.1.6 Mϕ infiltration immunohistochemistry

Glomerular Mϕ infiltration in NTN animals was assessed by immunohistochemical (IHC) staining for ED-1 (CD68) a rat Mϕ marker. Kidneys from STX and placebo treated rats were removed on d14, formalin fixed and paraffin wax embedded. 4μm serial sections were cut and mounted onto poly-l-lysine coated slides. Sections were dewaxed through xylene, rehydrated through

graded strengths of ethanol (99%, 90%, 70%), and rinsed in distilled water for 5 min. IHC staining was performed using the streptavidin–biotin–peroxidase method using the Vectastain Avidin-Biotin Complex (ABC) kit for peroxidase (rabbit IgG) (Vector Laboratories, Burlingame, USA) according to the manufacturer's protocol. Briefly, antigen was retrieved by citrate treatment (Citric acid (2.94g in 1000ml dH2O, pH6)) 15min (microwave 800w). Slides were then blocked with peroxidase (1.6% H_2O_2 in dH_2O) 15min at room temp followed by washing with d H_2O for 15min. Slides are then loaded into sequenza racks. Primary antibody (ED-1; Santa Cruz Biotechnology) was diluted 1:200 in PBS and sections were incubated overnight at 4ºC. Sections were washed twice in PBS then incubated with appropriate dilution of HRP-conjugated secondary antibody and finally developed with 3,3'-diaminobenzine (DAB). Sections were counterstained with haematoxylin, cleared through to xylene, and mounted using DPX mounting medium. Slides were viewed under LM. Images (50 glomeruli identified morphologically per slide) were taken using a Spot 2 slider digital camera (Diagnostic Instruments Inc., Sterling Hts. MI), and analysed using Image J software. ED-1 positive cells/glomerulus were counted, and glomerluar areas measured. Data are expressed as ED-1 positive cells/glomerular area (100μm^2).

2.2.1.7 Glomerular sclerosis- Picrosirius Red staining

Glomerular sclerosis in NTN animals was assessed by picrosirius red histological stain for collagen fibres. Kidneys from STX and placebo treated rats were removed on d14, formalin fixed and paraffin wax embedded. 4µm serial sections were cut and mounted onto poly-l-lysine coated slides. Sections were dewaxed through xylene, rehydrated through graded strengths of ethanol (99%, 90%, 70%), and rinsed in distilled water for 5 min. First, the nuclei were stained with Weigert's haematoxylin for 8 min, slides were then washed for 10 min in running tap water. Sections were then stained in picro-sirius red (Sirius red F3B (C.I. 35782) 0.5 g + 500ml saturated aqueous solution of picric acid) (Direct red 80, Sigma) for 1h. Sections were then washed in two changes of acidified water

(5 ml glacial acetic acid (glacial) + 1l dH_2O). Slides were then cleared through to xylene, and mounted using DPX mounting medium. Slides were viewed under LM. Images were taken using a Spot 2 slider digital camera (Diagnostic Instruments Inc., Sterling Hts. MI), and analysed using semi-quantitave colour image analysis in photoshop. Briefly, a range of red pantones were determined. This colour spectrum was identified in each image and recorded as red pixels. The relative red pixel number to total pixel number was then determined for each image. 10 images from random fields were taken per slide. The data are converted to percentage red staining per image and the mean of 10 images calculated.

2.2.2 Murine Mϕ depletion in CD11b-DTR mice

These experiments use transgenic mice expressing the human diphtheria toxin receptor (DTR) under the control of the CD11b promoter on an FVB background. Experiments were conducted to determine whether monocytes/ Mϕ affect pressor responses to ET-1. In this model, DT binds to the human DTR and results in blood monocyte and resident tissue Mϕ depletion. Following Mϕ depletion, examination of the pressor response to endothelin-1 was studied by invasive carotid bp measurement.

2.2.2.1 Generation of monocyte/ macrophage depletion

Diptheria toxin (DT) (1.0mg) (List Biological Laboratories, Campbell, CA) was reconstituted with 1.0ml sterile distilled water and then diluted to 2ng/ml in sterile PBS. DT (20ng/g i.p) was administered to mice to induce monocyte/ Mϕ depletion in CD11b-DTR transgenic mice and FVB strain controls 24h prior to experiments. This dose of DT was chosen based on previous studies. The original studies by Duffield *et al.* [302] using this model in the context of liver fibrosis used does of DT between 10ng/g and 25ng/g. Further studies from the Duffield lab by Guo *et al.* [303] used mice transgenic for thymic stromal lymphopoietin (TSLP), under regulation of the lymphocyte-specific promoter Lck. These Lck-TSLP transgenic mice also expressed the human diphtheria toxin receptor (DTR) under control of the monocyte/macrophage-restricted CD11b promoter (Lck-TSLP;CD11b-DTR). Treatment with 20ng/g DT resulted in a marked reduction of monocytes/macrophages in the peritoneal cavity of both CD11b-DTR and Lck-TSLP;CD11b-DTR mice and marked reduction of macrophage infiltration in glomeruli of Lck-TSLP;CD11b-DTR mice compared to controls.

2.2.2.1.1 Sample collection and quantification

To ensure efficacy of DT treatment blood leucocyte populations were assessed by FACS. Flow cytometric analysis of precisely measured citrate anticoagulated blood allowed absolute leukocyte counts to be determined (gating criteria are summarised in Fig 2.1 A-G). Furthermore, F4/80 immunohistochemical staining was used to assess tissue Mϕ depletion.

2.2.2.1.2 Fluorescence activated cell sorting (FACS)

Whole mouse blood was assessed by flow cytometry. Briefly, to avoid coagulation 30μl of 3.9% sodium citrate was taken up into a p100 pipette set at 60μl. Mouse tails were nicked using a scalpel. A further 30μl of blood was then taken up into the pipette to give a total volume of blood and citrate of 60μl. Citrate anticoagulated blood was aliquoted (20μl) into FACS staining tubes. To allow careful characterisation of inflammatory and resident monocytes a combination of lymphocyte antigen 6C (Ly6C) to represent inflammatory monocytes, Ly6G to represent neutrophils, CD115 to represent total monocytes and CD11b to represent total leukocytes is used (table 2.2). Antibodies to stain mouse blood were prepared into a mastermix depending of the number of tubes/samples to stain. The diluted FACS antibodies (50μl) were then added directly to the Blood. Tubes were vortexed and stained for 25min on ice. RBCs were then lysed by adding 1ml of 1x lysis buffer (10x lysis buffer stock from BD Biosciences dilute to 1x with distilled water). Tubes were then vortexed again and lysed for 8min at RT in the dark. Cells were then centrifuged at 300 x *g* for 5min at 4°C. The supernatant fraction was then discarded and cells were analysed by FACS on the same day, or fixed with formalin (5% final concentration) and analysed within 2-3 days. FACS results were analysed (BD FACStation and FlowJo software).

Table 2.2 Antibodies for FACS staining of whole mouse blood

Antibody	Dye	Volume
Anti-Ly6C (BD Biosciences)	PerCP Cy5.5	1:100 (0.5µl)
Anti-CD11b (Invitrogen)	AF-488	1:200 (0.25µl)
Anti-Ly6G (BD Biosciences)	PE Cy7	1:100 (0.5µl)
Anti- CD115 (Sigma)	PE	1:100 (0.5µl)
10% Mouse Serum		48.25µl
		50µl

2.2.2.1.2.1 Flow cytometry gating parameters

Initially, polymorphonuclear cells (PMC) were gated on the basis of size or forward scatter (FSC) and granularity or side scatter (SSC) profiles. The un-gated population represents small less granular lymphocytes (Fig 2.1A). This 'PMN' population was then plotted against CD11b and Ly6G. Co-positive cells are inversely gated out and labelled as neutrophils (Fig 2.1B). CD11b single positive Ly6G negative populations were labelled CD11b+ (Fig 2.1C). Both 'Neutrophil' and CD11b+ populations were then displayed on FSC SSC plot of the entire blood sample, to ensure they were represented in the appropriate place (Fig 2.1D). Neutrophils (blue) are approximately the same size but more granular than the CD11b+ cells (orange). This was to be expected and the analysis continued. The remaining CD11b+ cells are expected to represent monocytes. This was ensured by plotting CD115 against Ly6C- a monocyte specific marker (Fig 2.1E) Co-positive cells are considered Ly6C + monocytes. The profile is expected to show 3 distinct monocyte populations 1) Ly6C hi CD115 hi 2) Ly6 intermediate CD 115 low and 3) Ly6C lo CD115 hi. The blood sample in these experiments always showed an anomalous population (gated population in Fig 2.1E). When this population was shown on the FSC SSC profile of the whole blood sample, these cells appeared where neutrophils would be expected (Fig 2.1F). These cells were labelled as Ly6C+ neutrophils (blue) with the likelihood of the Ly6C antibody cross reacticting with Ly6G (neutrophil marker) antibody. This population was then gated out, and the remaining ungated population were labelled Ly6 C+ neutrophil - (orange). This population were CD11b+, CD115+, Ly6C+ and therefore represented monocyte cells. This remaining population was gated into 1) Ly6C hi, CD115 hi 2) Ly6 intermediate, CD 115 low and 3) Ly6C low, CD115 hi and the relative percentages were recorded (Fig 2.1G). These figures were also converted to cells per ml blood.

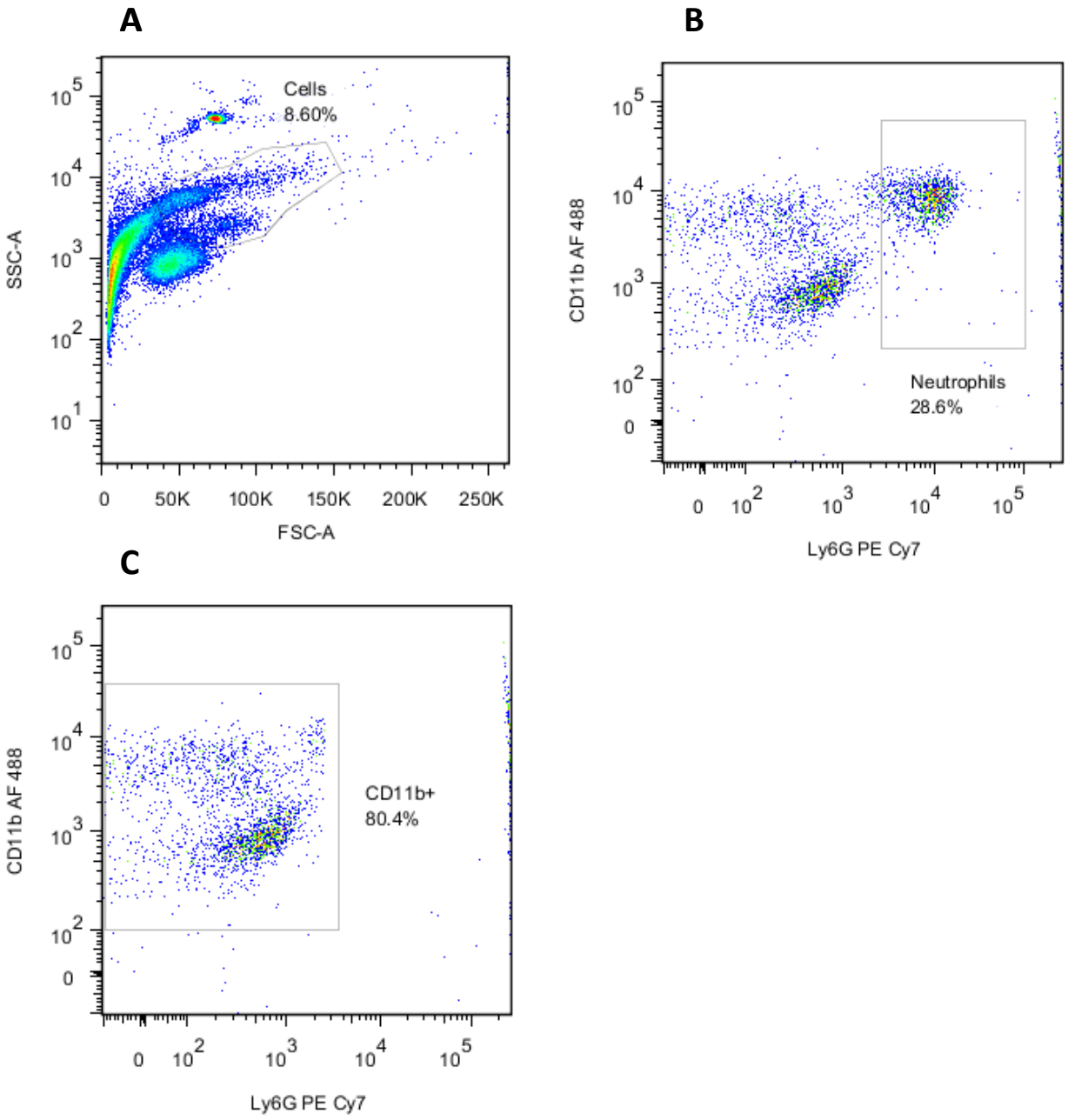

Figure 2.1 FACS staining of CD11b-DTR (macrophage deplete) mouse blood

A-C FACS plots of stained whole mouse blood. (A) PMNs initially gated on the basis of FSC SSC profiles (ungated population representing lymphocytes) (B) 'PMN' population plotted against CD11b and Ly6G. Co-positive cells inversely gated out and labelled as 'neutrophils'. (C) CD11b single positive Ly6G negative population labelled as CD11b +.

D

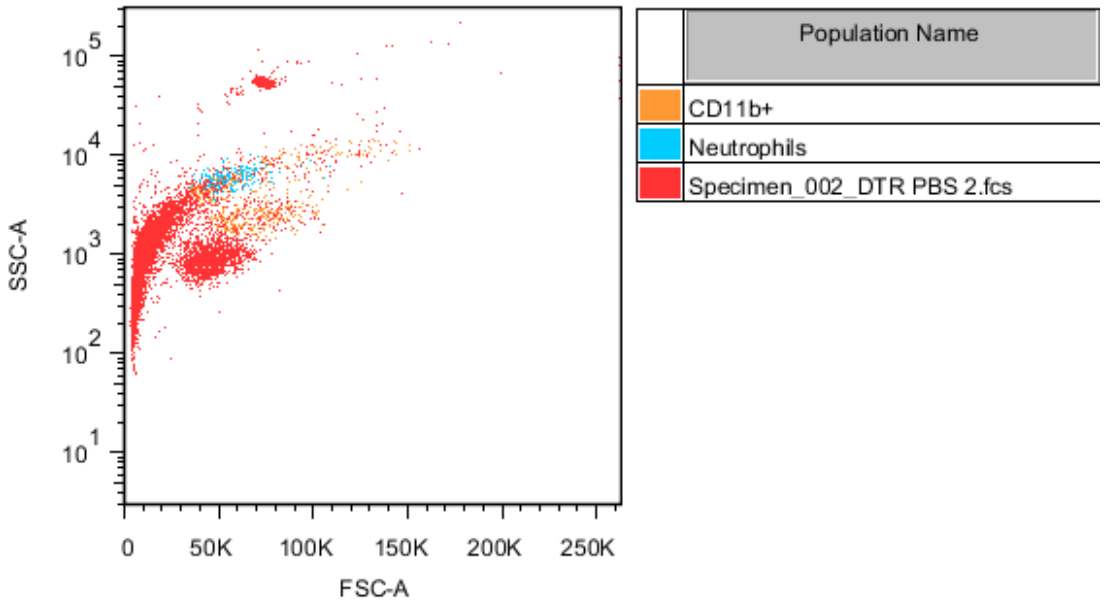

Figure 2.1 (cont.) FACS staining of CD11b-DTR (macrophage deplete) mouse blood

D FACS plots of stained whole mouse blood. (D) 'CD 11b+' (orange) and 'neutrophil' (blue) populations plotted on FSC SSC with whole sample background.

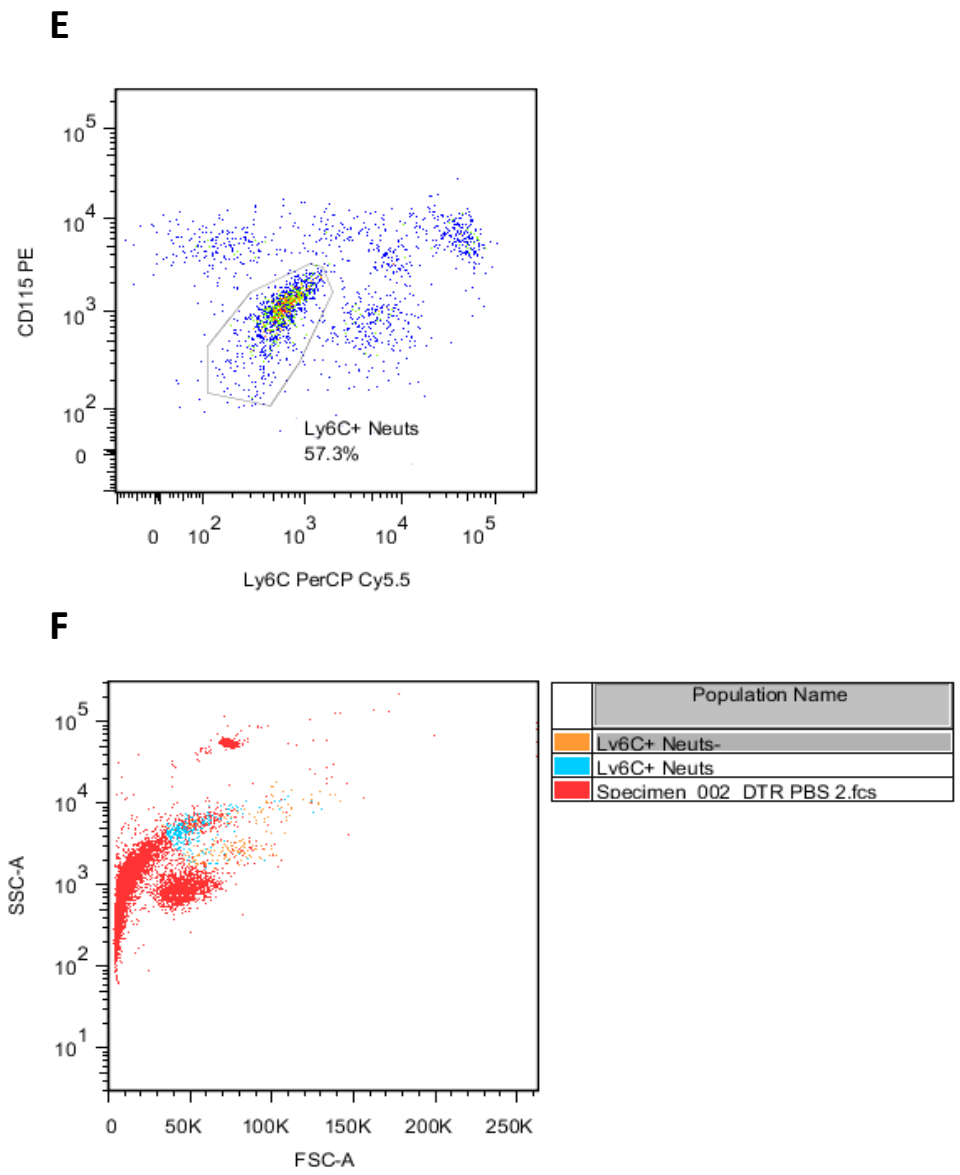

Figure 2.1 (cont.) FACS staining of CD11b-DTR (macrophage deplete) mouse blood

E-F FACS plots of stained whole mouse blood showing (E) 'CD 11b+' population plotted against CD115 and Ly6C. An anomalous population appeared (gated population). (F) The anomalous (gated) population visualised on FSC SSC of whole blood sample. The size and granularity of this population suggests they are neutrophils not monocytes. This population was gated out and labelled Ly6C+ neutrophil+ (blue). The remaining population was labelled Ly6C+ neutrophil- (orange) and this population were considered to be purely monocytes.

G

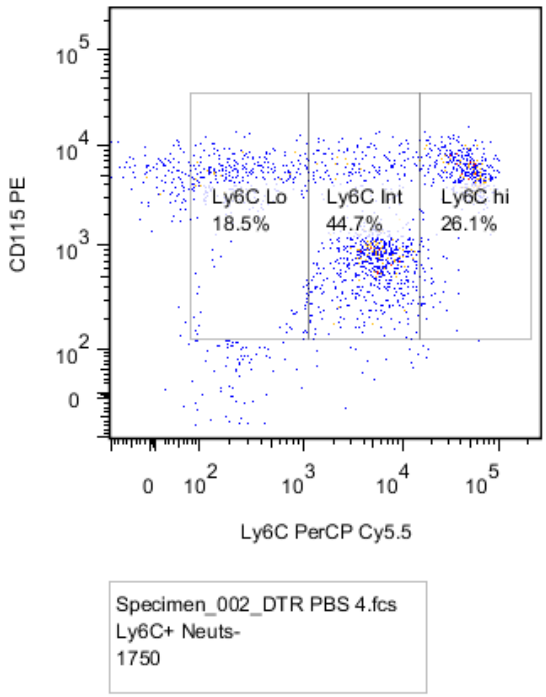

Figure 2.1 (cont.) FACS staining of CD11b-DTR (macrophage deplete) mouse blood

G FACS plot of stained whole mouse blood showing (G) The pure monocyte population labelled Ly6C + neut - plotted against CD115 and Ly6C and gated into 1) Ly6C hi CD115 hi 2) Ly6 intermediate, CD 115 low and 3) Ly6C low CD115 hi. The relative percentages of these cells are also shown.

2.2.2.1.3 Immunohistochemistry for resident tissue macrophage depletion

Resident renal, hepatic and splenic Mϕ in CD11b-DTR and wildtype mice were assessed by immunohistochemical (IHC) staining for F4/80 a murine Mϕ marker. Organs from DT and placebo treated mice were removed 24h post DT/saline injection, formalin fixed and paraffin wax embedded. 4μm serial sections were cut and mounted onto poly-l-lysine coated slides. IHC staining was performed using the streptavidin–biotin–peroxidase method using the Vectastain Avidin-Biotin Complex (ABC) kit for peroxidase (rabbit IgG) (Vector Laboratories, Burlingame, USA) according to the manufacturer's protocol (see section 2.2.1.6). Primary antibody (F4/80; Santa Cruz Biotechnology) was diluted 1:200 in PBS. F4/80 positive cells/section were counted from 10 representative sections per slide.

2.2.2.1.4 Invasive blood pressure measurement

Mice were initially anaesthetized with Thiobutabarbital (100mg/kg i.p.). Following this a tracheotomy was performed and the jugular vein and carotid artery were cannulated for administration of drugs and bp measurement.

Briefly, a small incision (1.5–2 cm) was made in the neck of the mouse for tracheostomy. A slit incision was then made in the mouse platysma muscles. The trachea was then identified and a small incision was made on the cartilage tissue, and the tracheostomy was performed using a small piece of paediatric Ryle's tube or rodent tracheal intubation tube.

The jugular vein was cannulated and used for drug administration. Briefly, after making a small incision in the neck, the thick veins are located bilaterally in the incised region. These are visible just below the dermis, and are separated from the underlying tissues using artery forceps or curved, blunt forceps. When the jugular vein was isolated, the cephalic end was tied off with 5-0 vicryl suture. A small cut was made on the vein to insert the rodent catheter (PE catheter fabricated with 26 G × 1/2″ needle) up to 1′′ towards the heart using a catheter

pre-filled with heparinized normal saline (0.5 IU/ml), and the vein was then tied with along with the catheter [304]. After cannulation, the cannulation line is flushed with normal saline (0.1 ml) to prevent thrombosis [305; 306]

The carotid artery was then cannulated for invasive BP measurement. The carotid was identified along with the vagus nerve on either side of the trachea. One side of the carotid artery was separated from the adjacent connective tissue and carefully cleaned without stimulating the vagus nerve. The blood vessel was separated from the vagus using a small needle, and the cephalic end of the blood vessel was tied. The blood vessel was similarly cannulated using a cannula pre-filled with heparinized normal saline (0.5 IU/ml). The opposing end of the cannula was connected to a three-way stopcock/saline filled tuberculin syringe. Then the carotid artery cannulation site was tied. After cannulation, the tied suture at the cardiac end of the blood vessel was released slowly, ensuring that there was no bleeding at the cannulation site.

The three-way stopcock was connected to the pressure transducer and a syringe filled with heparinized saline. The heparinized saline aids in application of a positive pressure to maintain it at the baseline value. The three-way stopcock works as a bridge connecting the carotid cannula and the pressure transducer. During the experiment, the positive pressure is to be blocked to avoid transmission of BP to the syringe. The pressure transducer unit of the student physiograph/data acquisition system (AD instruments) converts BP into an electrical signal. The animals are allowed to stabilize for 10–20 min, during this time the animals are also monitored for any bleeding and respiratory problems. Following this stabilisation, baseline recordings are carried out for 10–15 min to ensure the stability of the preparation. The baseline BP of the animals is also essential when considering treatment or use of different strains. In this instance, the baseline blood pressure of CD11b-DTR mice pre-treated with either DT or saline, and FVB strain controls treated with DT required comparison to ensure accuracy and relevance of BP readings.

30 minutes after surgery the effect, duration of the action of the drugs were observed and recorded. First, The lowest dose of ET-1 (0.01 nmol/kg) is injected i.v. and b.p is recorded over a 20-minute period. The second dose (0.1 nmol/kg) is injected, followed 20 minutes later by the highest dose (1nmol/kg). The final drug to be administered was ang II (1nmol/kg). After each drug administration, the BP of the animal was allowed to return to the normal baseline value. Following these experiments the animals were then sacrificed by cervical dislocation, and tissues were harvested for further analysis. This work was carried out under the supervision and with the assistance of Matthew Bailey and Michael Clay.

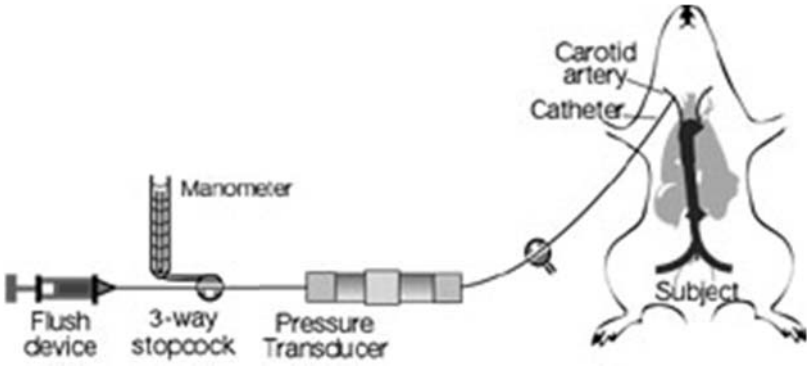

Figure 2.2 Cartoon of experimental set up for invasive BP measurement

Cartoon demonstrating equipment setup for electrophysiological blood pressure measurement.

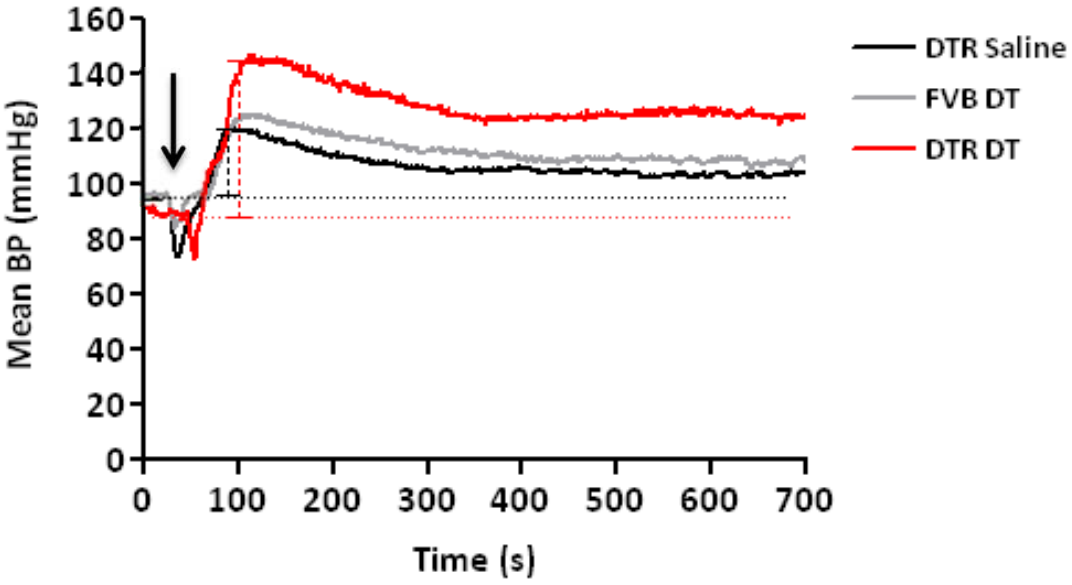

Figure 2.3 Representative figure of BP traces

Representative traces of BP response to ET-1 at 1nmol/kg. Following ET-1 administration (Arrow) a classic dip in ET-1 is observed. Following this, a rapid rise in BP up to a peak point was observed. The amplitude and duration of pressor response in each group was measured by analysing the area under the curve (AUC) by measuring from the point at which the BP rises back to baseline and thereafter for 10 min.

2.2.3 Statistical analyses

Data are given as mean ± SD unless otherwise indicated. All Statistical analyses were performed using Graphpad Prism software. Data were analysed by either Students T-test, 1-way analysis of variance (ANOVA) with post-hoc Dunnetts comparisons, or 2-way ANOVA with pairwise comparisons using bonferroni or Tukey corrections. D'Agostino and Pearson normality test was used to determine Gaussian distribution. A two-tailed p value of < 0.05 was considered statistically significant.

Chapter 3

Selective ET_A receptor antagonism with Sitaxsentan in experimental nephrotoxic nephritis

3.1 Introduction

In human and experimental models of GN, the potent vasoconstrictor ET-1 is up-regulated [251]. In addition to its vasoactive properties, this peptide is known to have pro-inflammatory and pro-fibrotic potential. Vascular ET-1 production is independent of renal ET-1 production, and as such urinary excretion of ET-1 is thought to reflect renal ET-1 production [221]. The actions of renal ET-1 are mediated via the ET_AR [229; 230; 231] with the ET_BR functioning to clear circulating ET-1 [220; 229]. ET_AR and ET_BR antagonists have emerged as potential therapeutic agents with renoprotective effects [231; 243; 244].

Various ET receptor antagonists are currently under investigation and have provided further insight as to the role and actions of ET-1 and the ET receptors. Receptor antagonists are classified as either ET_AR or ET_BR selective, or nonselective $ET_{A/B}R$ antagonists. The majority of studies using ETR antagonists are performed in models of hypertensive nephropathy and diabetic nephropathy with few in models of GN. This chapter will investigate the use of a selective ET_AR antagonist sitaxsentan (STX) as a renoprotective agent *in vivo* in a telescoped model of rat NTN. The immediate or heterologous phase of nephrotoxic nephritis is characterised by the accumulation of PMCs, primarily neutrophils within the glomeruli, hypertension and overt proteinuria [307; 308; 309]. Proteinuria then rapidly declines and the autologous phase commences, whereby less obvious glomerular polymorph accumulation also occurs, and shifts from primarily neutrophils, to monocytes [310]. Proteinuria then gradually and progressively increases. Of these immunologic events, the autologous phase is most comparable to the autoimmune response in human GN.

3.1.1 Experimental hypothesis and aims

We hypothesise that STX treatment will reduce BP in STX treated animals. Furthermore, STX will improve renal function, ameliorate proteinuria and reduce glomerular inflammation and glomerular and interstitial fibrosis.

3.2 Experimental protocol

I. Rats were pre- immunised with s.c. injection 7d prior to induction of NTN with 1mg of rabbit IgG.
II. Three days prior to induction of NTN animals were treated with either selective ET_A antagonist sitaxsentan (30mg/kg) or placebo (n=5 per group) (gavage) and every day thereafter for 17d.
III. NTN was induced by single i.v. injection of 1ml/200g nephrotoxic serum (NTS) containing rabbit anti-rat glomerulus antibodies under halothane anaesthesia (AstraZeneca, Macclesfield, UK).
IV. Rats were weighed daily and housed in metabolic cages and timed urine collections were made every 2-3 days.
V. Blood pressure was recorded by tail cuff plethysmography prior to STX treatment and thereafter every 3-4 days. Rats were allowed to habituate to this measurement procedure for 3d prior to experiments to ensure accurate BP not related to stress responses. BP and HR values were recorded on a Model MK-2000 and were averaged from three consecutive readings.
VI. 14 days after NTN induction, animals were culled, and blood collected for analysis. The final urine sample was collected and kidneys removed for analysis. Urinary and serum albumin and creatinine were analysed.
VII. Kidneys were formaldehyde (FA) fixed and paraffin wax embedded. 4μm serial sections were cut and mounted onto poly-l-lysine coated slides.
VIII. Renal inflammation was determined by glomerular Mϕ infiltration by IHC for CD68 (rat Mϕ marker), and determined as Mϕ n/glomeruli from 50 glomeruli from a representative section.
IX. Glomerular sclerosis was assessed by picrosirius red staining for collagen accumulation. Picrosirius red was analysed using semiquantitave colour image analysis using Photoshop software. 10 images from random fields were taken per slide. Data were converted to percentage red staining per image with the mean of 10 images calculated.
X. Slides were viewed under LM. Images were taken using a Spot 2 slider digital camera (Diagnostic Instruments Inc., Sterling Hts. MI).

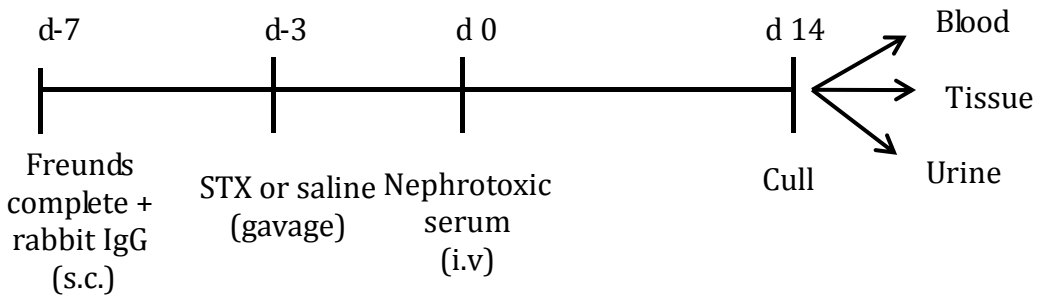

Figure 3.1 Schematic of Experimental Design For NTN

3.3 Preliminary studies with NTN model

Initial pilot studies were undertaken using this telescoped model of rat NTN to determine the efficacy of the NTS (1ml/200g) and tolerability of STX (30mg/kg).

3.3.1 NTS treated animals develop progressive glomerulonephritis

NTN control animals gained weight over the course of the experiment (d-3 *vs* d14; 253.2 ± 15.7g *vs* 301.4 ± 20.5g) (Fig 3.2 A). On d1 following NTS treatment, a slight reduction in body weight was observed along with a rapid increase in urinary albumin excretion (Fig 3.2 B), consistent with the heterologous phase of NTN. Proteinuria then rapidly decreases on d2. From d3 and thereafter until d14 the animals progressively develop proteinuria throughout the autologous phase of disease (d0 *vs* d14; 13.7 ± 13.4 mg/mmol *vs* 350.0 ± 403.5 mg/mmol) (Fig 3.2 B). Over the course of the experiment a significantly increased BP in NTS treated control animals was also apparent (d0 *vs* d14; 135 ± 14.9 mmHg *vs* 172.4 ± 23.8 mmHg) (Fig 3.2 D). Lastly, evidence of Mϕ infiltration in NTN treated rats was apparent on d14 (Fig 3.3 A).

3.3.2 Sitaxsentan improves renal function and glomerular inflammation

NTN animals treated with STX also gained weight normally throughout the study (d-3 *vs* d14; 273.8 ± 26.1g *vs* 328.8 ± 34.0g) (Fig 3.2 A). On d1 following NTS treatment, a reduction in body weight was also observed accompanied by a less prominent increase in urinary albumin excretion (Fig 3.2 B) compared to control. As in control animals, proteinuria then rapidly decreases on d2. From d3 and thereafter until d14 the animals develop proteinuria (d0 *vs* d14; 7.2 ± 9.5 mg/mmol *vs* 210.8 ± 118.3 mg/mmol) (Fig 3.2 B). Proteinuria appears to be decreased compared to control, however this trend was not statistically significant. Renal function measured by serum creatinine was significantly reduced in STX treated animals compared to control (d14 NTN *vs* STX; 73.2 ± 13.2 μmol/l *vs* 51.8 ± 9.8 μmol/l) (Fig 3.2 C). In these preliminary experiments, BP was unaffected by STX treatment by d14 (NTN Control *vs* NTN STX; 172.4 ± 23.9 mmHg *vs* 164.8 ± 21.2 mmHg) (Fig 3.2 D). Furthermore, glomerular inflammation measured by Mϕ infiltration in STX treated animals was also

significantly reduced compared to control (NTN control *vs* STX NTN d14; 21.05 ± 8.6 Mϕ/glom *vs* 10.2 ± 4 Mϕ/glom) (Fig 3.3 A-C).

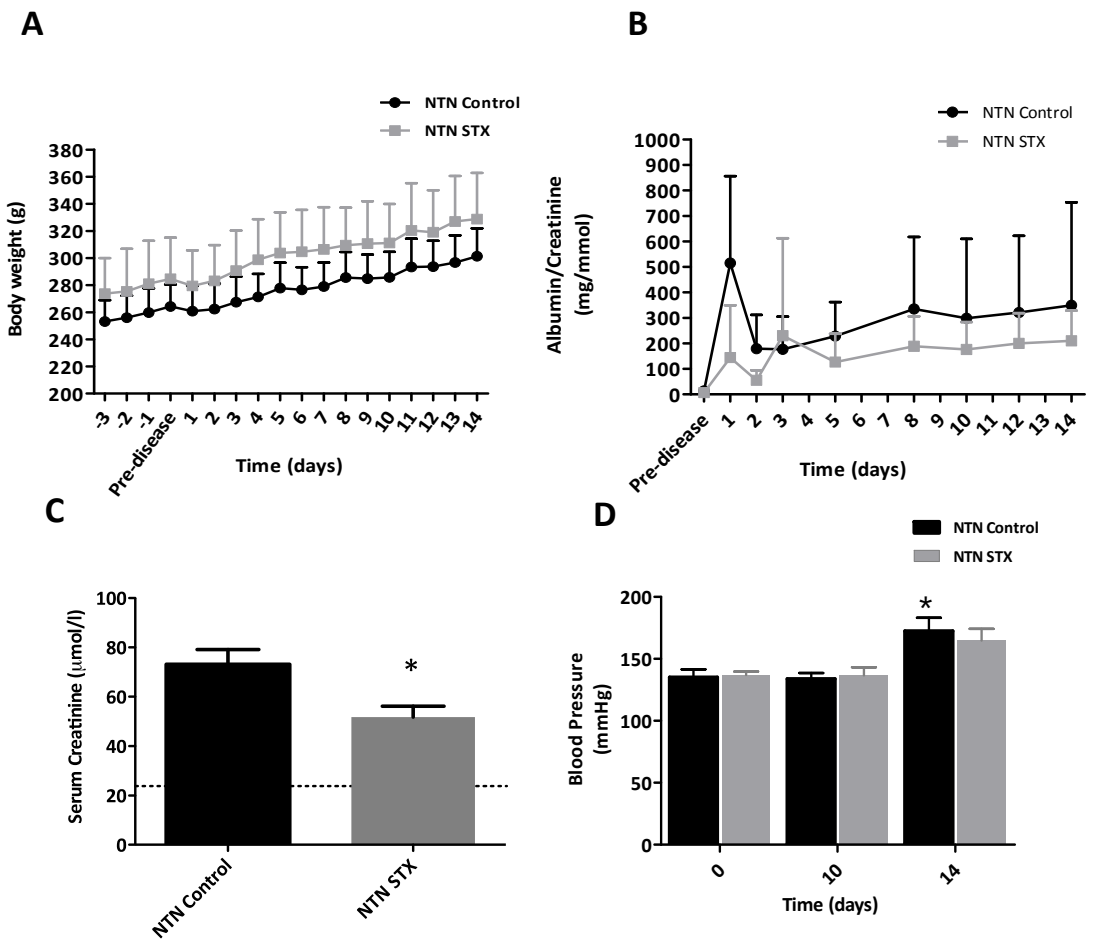

Figure 3.2 Effect of STX treatment on NTS induced NTN

A-D Body weight and measures of GN. (A) Control animals treated with NTN and animals treated with STX gained weight normally over 14 d (B) NTS treatment induces progressive albuminuria. Treatment with STX prevents severe development of albuminuria over 14d. (C) Serum creatinine (d14) is significantly reduced by STX treatment compared to control. (D) NTS treated controls develop an increase in BP in the latter stages of disease. STX treatment did not significantly lower blood pressure by d14. Serum creatinine data are analysed by Students T-test. Data are mean ± SD (n=5/group) Symbols displayed above bars represent significance compared to respective control * $p < 0.05$. All Other data analysed by 2-way ANOVA. Dotted line in (C) represents normal serum creatinine. Symbol in (D) are significance compared to day 0.

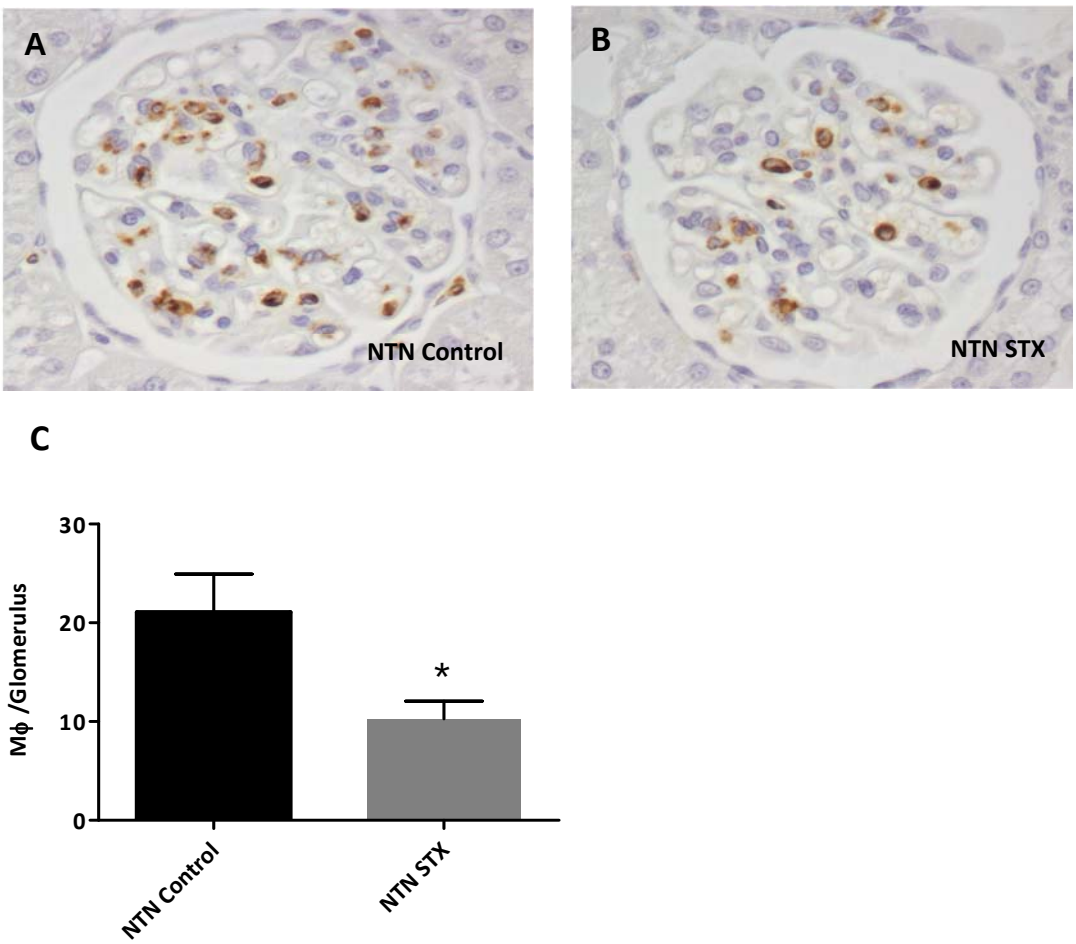

Figure 3.3 Effect of STX treatment on glomerular macrophage infiltration

A-C Photomicrographs of glomeruli (A) Control animals treated with NTN and (B) animals treated with STX contained demonstrated glomerular Mϕ infiltration by ED-1 staining. (C) Mϕ numbers in the glomeruli are significantly reduced by STX treatment. Data analysed by Students' T-test. Data are mean ± SD (n=5/group). Symbols displayed above bars represent significance compared to control * $p < 0.05$.

3.4 Selective ET_AR antagonism in nephrotoxic nephritis studies

Our initial experiments were replicated in this model. We aimed to demonstrate similar findings with additional measures. In our interim experiments we did not detect a reduction in BP as anticipated. Therefore, in these experiments we acclimatised the animals to the tail-cuff BP measurement procedure for 7 days prior to the first measurement to ensure greater accuracy of readings. Furthermore, we investigated glomerular and interstitial fibrosis by measurement of collagen accumulation.

3.4.1 NTS treated animals develop progressive GN

As in our previous studies, NTN control animals gained weight over the course of the experiment (d-3 *vs* d14; 227.2 ± 15.6g *vs* 284.4 ± 16.9g) (Fig 3.4 A). The heterologous phase of NTN was not apparent on d1 following NTS treatment; no significant increase in proteinuria was observed and no body weight reduction (Fig 3.4 B). The animals progressively developed proteinuria over 14d (Fig 3.4 B) throughout the autologous phase of disease (d0 *vs* d14; 6.1 ± 4.4 mg/mmol *vs* 458.9 ± 340.4 mg/mmol). Over the course of the experiment a significant increase in BP in NTN controls was detected (d-1 *vs* d14; 156.7 ± 8.9 mmHg *vs* 182.0 ± 9.7 mmHg) (Fig 3.4 D). Animals also demonstrated glomerular Mϕ staining and glomerular collagen staining (Fig 3.5 A &D)

3.4.2 STX treatment reduces hypertension

NTN STX animals also gained weight normally throughout the study (d-3 *vs* d14; 219.4 ± 11.8g *vs* 274.8 ± 7.8g) (Fig 3.2 A). Similar to control animals, STX treated animals showed no significant increase in proteinuria and no body weight reduction on d1 following NTS treatment (Fig 3.4 B). In this study STX treatment did not reduce proteinuria; these animals progressively developed proteinuria over 14d throughout the autologous phase similar to controls (d0 *vs* d14; 7.1 ± 5.5 mg/mmol *vs* 448.0 ± 303.6 mg/mmol) (Fig 3.2 B). Renal function measured by serum creatinine was also not significantly reduced in STX treated animals compared to control (d14 NTN control *vs* NTN STX; 24.4 ± 4.7 μmol/l *vs* 25.4 ± 2.8 μmol/l) (Fig 3.2 C). Despite proteinuria reduction not being detected and no improvement in renal function, STX animals did not develop

hypertension (d-1 *vs* d14; 155.7 ± 12.5. mmHg *vs* 155.6 ± 12.1 mmHg) (Fig 3.4 D). This BP was significantly lower than NTN control animals on days 9 and 13. In addition to a reduction in blood pressure, STX also significantly reduced glomerular inflammation. Glomerular Mϕ numbers were significantly reduced in STX treated animals compared to controls (NTN control *vs* STX NTN d14; 34.8 ± 13.1 Mϕ/glom *vs* 17 ± 6 Mϕ/glom) (Fig 3.5 A-C). Glomerular and interstitial fibrosis assessed by picrosirius red staining for collagen accumulation was not altered by STX treatment (NTN control *vs* STX NTN d14; 15.2 ± 1.5 % Pic red *vs* 13.7 ± 1.6 % Pic red) (Fig 3.5 D-F).

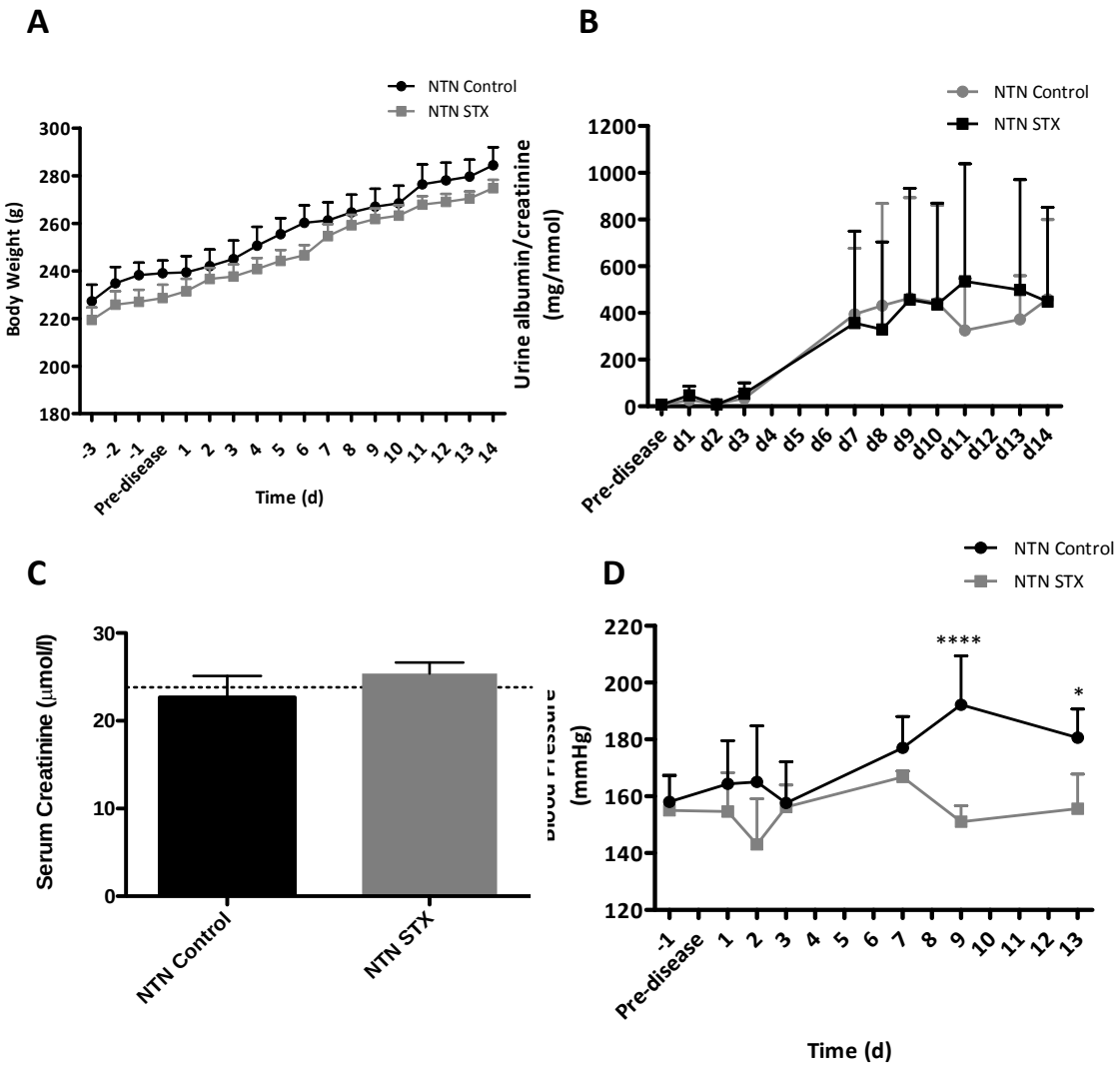

Figure 3.4 Effect of STX treatment on NTS induced NTN

A-D Body weight and measures of GN. (A) NTN Control and NTN STX animals gained weight normally over 14 d (B) NTS treatment induces progressive proteinuria. STX treatment does not affect development of proteinuria over 14d. (C) Serum creatinine is not affected by STX treatment compared to control. (D) NTN Control animals develop hypertension. Over 14 d STX treatment significantly reduces BP. Serum creatinine data are analysed by Students T-test. Data are mean ± SD (n=5/group) Symbols displayed above bars represent significance compared to respective control * $p < 0.05$, **** $p < 0.001$. All Other data analysed by 2-way ANOVA. Dotted line in (C) represents normal serum creatinine.

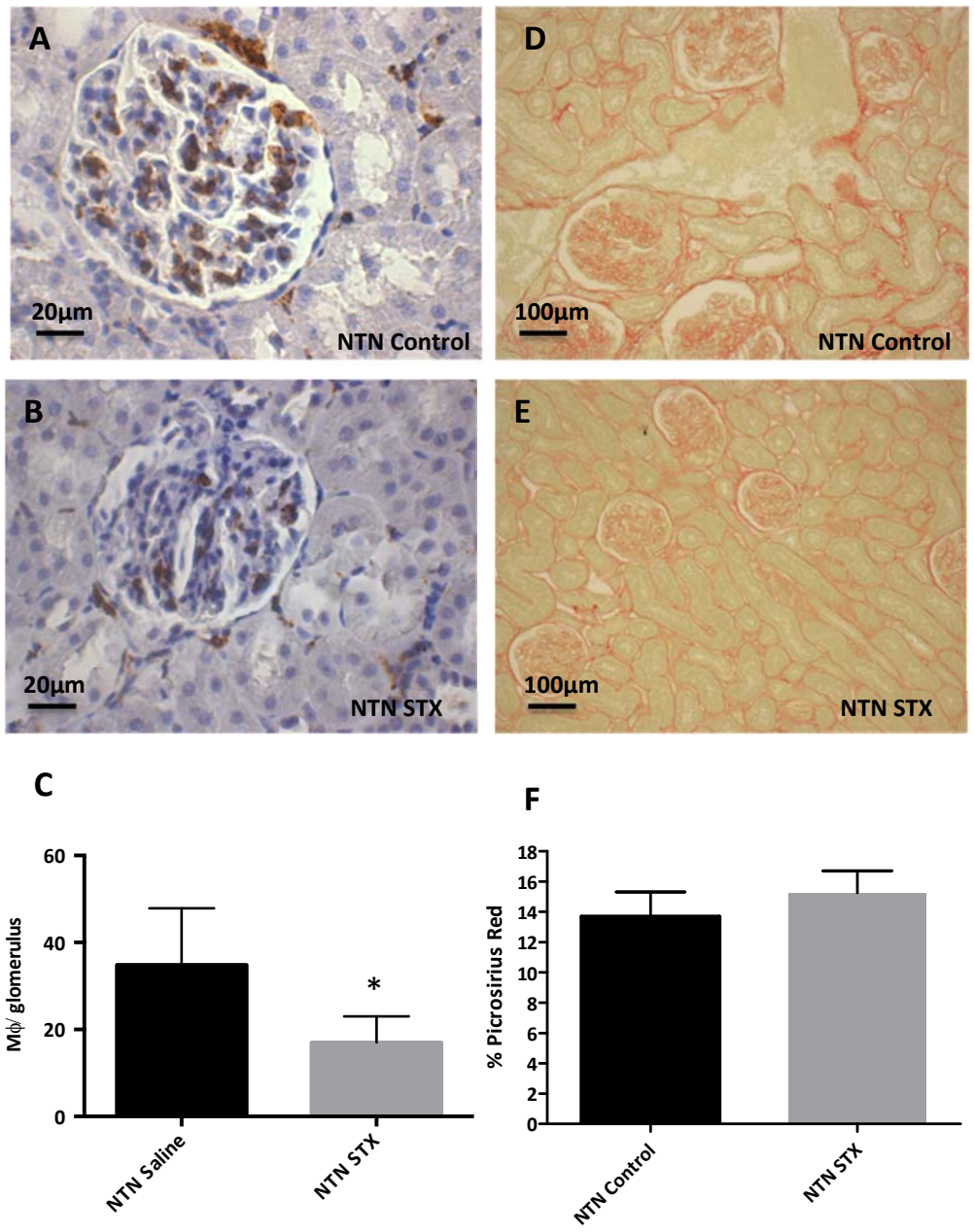

Figure 3.5 Effect of STX treatment on inflammation and fibrosis

A-F Photomicrographs of ED-1 and picrosirius red staining for (A&D) Control animals treated with NTN and (B&E) animals treated with STX demonstrated glomerular Mϕ infiltration by ED-1 staining. (C&F) Mϕ numbers in the glomeruli and picrosirius red staining in the glomerular and interstitial compartments are significantly reduced by STX treatment. Data analysed by Students' T-test. Data are mean ± SD (n=5/group). Symbols displayed above bars represent significance compared to control * $p < 0.05$.

3.5 Selective ET_A receptor antagonism in severe NTN

Our previous study demonstrated an effect of STX in NTN. Contrary to our initial findings however, we were unable to detect a reduction in proteinuria and serum creatinine. In this last study more severe disease developed. The animal groups were not comparable to the previous experiments and have therefore remained separated.

3.5.1 NTS treated animals develop progressive proteinuria

NTN control animals gained weight over the course of the treatment (d-3 *vs* d14; 283.5 21.27g *vs* 308 ± 25.4g) (Fig 3.5 A). On d1 following NTS treatment, a significant reduction in body weight was observed along with a rapid increase in urinary albumin excretion (Fig 3.5 B). In the previous experiment this heterologous phase was not observed. Proteinuria then rapidly reduces on d2. From d3 and until d14 the animals progressively develop severe proteinuria (d-3 *vs* d14; 13.6 ± 24.4 mg/mmol *vs* 2217.7 ± 1329.3 mg/mmol). A significant increase in BP in NTN controls was also detected (d0 *vs* d14; 151.1 ± 4.6 mmHg *vs* 190.1 ± 9.4 mmHg) (Fig 3.5 D). Animals also showed marked glomerular Mφ infiltration and fibrosis (Fig 3.6 A&D)

3.5.2 STX improves proteinuria and blood pressure

NTN STX animals also gained weight throughout the study (d-3 *vs* d14; 277.6 ± 3.2g *vs* 296.2 ± 9.7g) (Fig 3.5 A). Similar to control animals, STX treated animals showed a significant increase in proteinuria and a body weight reduction on d1 following NTS treatment (Fig 3.5 B). The animals progressively developed proteinuria over 14d throughout the autologous phase. Similar to our pilot studies, a non-significant trend towards reduced proteinuria was observed (Fig 3.5 B). Furthermore, STX animals did not develop hypertension (d-1 *vs* d14; 15 151.0 ± 4.5 mmHg *vs* 190.13 ± 9.4 mmHg) (Fig 3.4 D). This BP was significantly reduced compared to NTN control animals on days 9 and 13. In addition to a reduction in blood pressure, Mϕ infiltration in STX treated animals was significantly reduced compared to control (NTN control *vs* STX NTN d14; 39.9 ± 3.4 Mϕ/glom *vs* 17.7 ± 2.6 Mϕ/glom) (Fig 3.6 A-C). Renal function measured by serum creatinine was not significantly reduced in STX treated animals

compared to control (d14 NTN *vs* STX; 41.2 ± 12.3 µmol/l *vs* 37.8 ± 7.2 µmol/l) (Fig 3.5 C). Furthermore, no significant reduction in fibrosis assessed by picrosirius red staining for collagen accumulation was observed (NTN control *vs* STX NTN d14; 28.8 ± 1 % Pic red *vs* 28.7 ± 1.1 % Pic red (Fig 3.5 D-F).

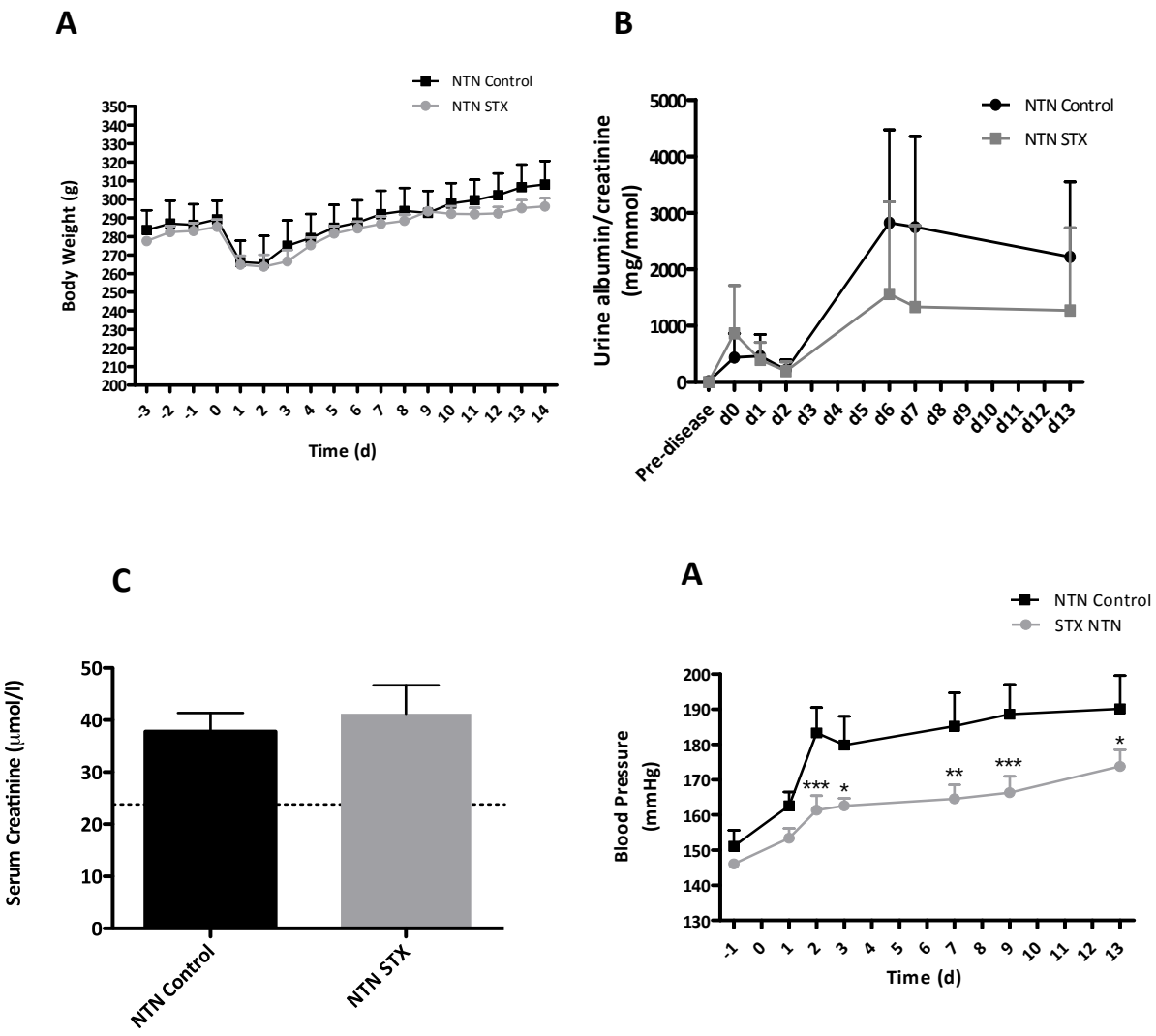

Figure 3.6 Effect of STX treatment on NTS induced NTN

A-D Body weight and measures of GN. (A) NTN Control and NTN STX animals gained weight normally over 14 d (B) NTS treatment induces progressive proteinuria. STX treatment results in a trend towards reduced proteinuria over 14d. (C) Serum creatinine is not affected by STX treatment compared to control. (D) NTN Control animals develop hypertension. Over 14 d STX treatment significantly reduces BP. Serum creatinine data are analysed by Students T-test. Data are mean ± SD (n=4-5/group). Symbols displayed above bars represent significance compared to respective control * $p < 0.05$, ** $p < 0.01$, *** $p < 0.005$. All other data analysed by 2-way ANOVA. Dotted line in (C) represents normal serum creatinine.

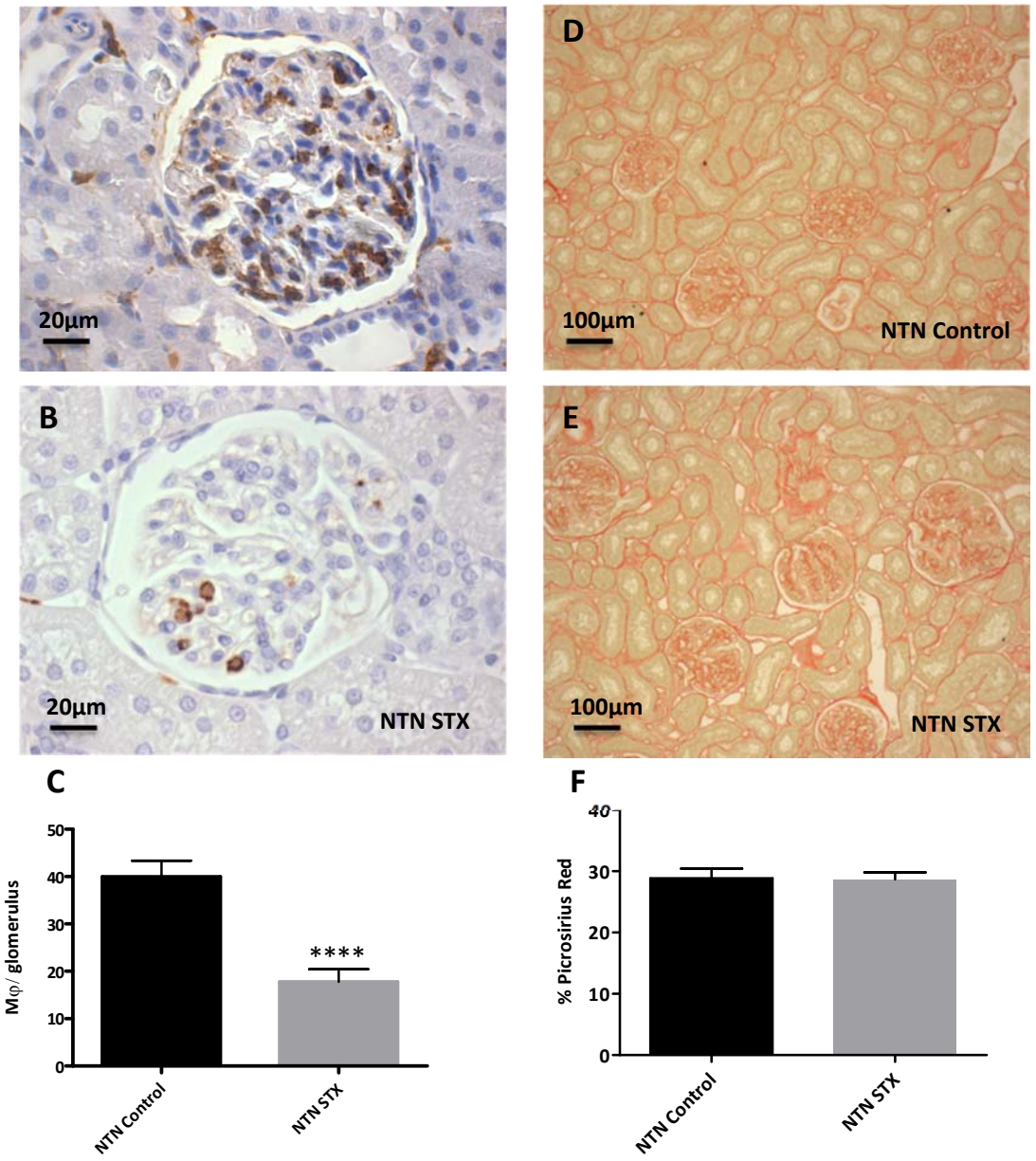

Figure 3.7 Effect of STX treatment on inflammation and fibrosis

A-F Photomicrographs of ED-1 and picrosirius red staining for (A&D) Control animals treated with NTN and (B&E) animals treated with STX demonstrated glomerular Mϕ infiltration by ED-1 staining. (C) Mϕ numbers in the glomeruli are significantly reduced by STX treatment. (F) STX treatment does not affect collagen deposition in the glomerular and interstitial compartments Data analysed by Students' T-test. Data are mean ± SD (n=4-5/group). Symbols displayed above bars represent significance compared to control * $p < 0.05$, **** $p < 0.001$.

3.6 Summary

In pilot studies, NTS treated animals developed GN. These animals demonstrated:-

- Proteinuria, hypertension, elevated serum creatinine and glomerular Mϕ infiltration.
- With the exception of hypertension, these measures were all ameliorated by treatment with an ET_A receptor antagonist.

Further experiments aimed to reproduce the pilot study and to accurately measure BP by acclimatising the animals to the tail cuff procedure. These animals demonstrated:-

- Reduced hypertension and glomerular Mϕ infiltration
- Unable to detect a reduction in proteinuria and serum creatinine in response to STX treatment.

In our final experiment, animals were treated with a higher dose of NTS to generate overt proteinuria. These studies demonstrated:-

- Serum creatinine was similarly not reduced in these animals.
- A trend towards proteinuria reduction was observed, however this was not a significant event.
- Hypertension and glomerular inflammation were significantly reduced in these animals.

The results of these experiments investigating the use of a selective ET_AR antagonist have suggested a role for selective ET_AR antagonism in GN however these data demonstrated some conflicting evidence. A consistent finding in these experiments was reduced glomerular macrophage infiltration. There are limited data examining the role of ET-1 in macrophage biology. The next chapter will address this role of ET-1 in human macrophages *in vitro.*

3.7 Discussion

3.7.1 ET_AR antagonism in experimental NTN

ET-1 contributes to hypertension and CKD. In experimental hypertension [249] and renal disease [311; 312; 313; 314] an up-regulation of urinary ET-1 in observed, likely reflecting increased renal ET synthesis. The role of ET-1 in regulating BP and renal haemodynamics is well understood, however the effects of ET-1 that are important in the development and progression of CKD are less well defined, and are likely the result of BP independent effects. Current data suggest that the majority of the pathological effects of ET-1, at least within the kidney, are mediated via the ET_AR [229; 230; 231], with the ET_BR functioning to clear circulating ET-1 [220; 229]. ET_AR and ET_BR antagonists have therefore emerged as potential therapeutic agents with renoprotective effects [231; 243; 244].

ET-1 also contributes to the development of inflammation and fibrosis [315; 316;317] in the absence of hypertension[318]. The mechanism for these changes is not well defined but is the focus for future research. This involves studies examining the effects of ETR antagonists on inflammatory cell infiltrates and resident renal cell inflammatory responses.

Hypertension and DN are the leading causes of CKD, and studies investigating ET receptor antagonism have largely been performed in animal models of these diseases, with very few studies in inflammatory GN [265;231;266;267]. We therefore utilised an *in vivo* model of GN, the NTN model (described in Chapter 2 section 2.1.1) and its subsequent use to study the effect of selective ET_AR antagonism using sitaxsentan. NTN was achieved by administering nephrotoxic serum (containing anti-GBM antibodies) to rats pre-immunised with rabbit IgG. In addition to BP and proteinuria, we also aimed to assess the effects of STX on glomerular inflammation, fibrosis and resident renal cell injury.

3.7.2 NTS induces progressive GN

Our experiments demonstrate the establishment of a model of progressive GN. Animals develop hypertension, progressive proteinuria, elevated serum creatinine, glomerular inflammation, and glomerular and interstitial fibrosis.

Initial pilot studies demonstrated promising results with the selective ET_AR antagonist, showing a significant improvement in renal function (assessed by measurement of serum creatinine levels), significant albuminuria reduction and attenuation of glomerular Mϕ infiltration.

3.7.3 Sitaxsentan reduces hypertension and macrophage infiltration in experimental nephrotoxic nephritis

Hypertension is a hallmark of GN and is apparent in experimental NTN. In our pilot studies, we were unable to detect a reduction in BP in response to the ET_AR antagonist, leading us to conclude that the animals required acclimatisation to the tail cuff procedure. Further experiments aimed to reproduce the pilot study and to accurately measure BP by acclimatising the animals to the tail cuff procedure. These animals also demonstrated a reduction in hypertension and glomerular Mϕ infiltration. The method of drug delivery in this model was by oral gavage. This was used in favour of administration via drinking water, to better account for the dose received by each animal. Despite using this technique, our *in vivo* studies did not yield a significant reduction in proteinuria and renal function (assessed by serum creatinine) in response to STX treatment. These findings were largely unexpected and have been attributed, in part to the cohort size and, potentially, the dose of STX used. Future experiments would aim to utilise a higher dose of STX.

3.7.4 Podocyte cell structure and function remain un-assessed

An important aspect of this experimental design was to also include assessment of the effect of this drug on podocyte cell structure and function. We aimed to assess podocyte numbers, hypothesising that NTN would lead to podcytopenia and foot process retraction and effacement. We hypothesised that STX treatment would likely protect the podocyte from loss and damage. In an effort

to quantify podocyte number, we used a monoclonal murine anti- Wilms' tumour-1 (WT-1) antibody on sections of rat kidney. This antibody was reported to cross-react with rat WT-1, however despite using several antigen retrieval techniques (Sodium Citrate and Borg decloaking), and alternative fixatives (4% FA and Methylcarnoys), we were unable to detect nuclear WT-1 staining the podocytes of these glomeruli, with only weak non-specific cytoplasmic staining apparent. Furthermore, kidneys were also fixed in glutaryaldehyde for transmission electron microscopic examination of podocyte structural abnormalities, however this EM service was unavailable at the time when required, and these studies were not carried out.

3.7.5 Glomerular inflammation is reduced in STX treated NTN animals

A consistent finding in these studies was reduced glomerular Mϕ numbers in STX treated animals. These findings are consistent with the literature, however, the mechanisms by which ET_AR antagonists improve glomerular inflammation are likely multifactorial and investigations into the role of ET-1 and ETR antagonism in macrophages and podocytes is discussed in the following sections.

3.7.6 Further Work

As noted, studies investigating ET receptor antagonism have largely been performed in animal models of either hypertension or DN, and there are very few studies in inflammatory GN. In models of DN mixed $ET_{A/B}R$ antagonists showed reduced proteinuria, glomerular injury and hypertension [258; 259]. ET receptor antagonists also affect glomerular injury and inflammation in models of DN.

In a previous study using immune complex GN, a mixed $ET_{A/B}R$ antagonist demonstrated reduced proteinuria and glomerular injury[265]. Our studies demonstrated a similar effect of selective ET_AR antagonism although our findings were more inconsistent than those shown in this study.

This NTN model has been used as a tool to study glomerulonephritis [292] is notorious for its inconsistency in generation of disease severity and associated mortality. This is most likely due to the differing titres of anti-glomerular basement membrane antibody between batches of nephrotoxic serum, and that the titre is not measured. The nature of the disease course, from an acute inflammatory phase, to a progressive phase also means that a considerable degree of variability will be apparent by the end of the experiment. Our results demonstrated significant variability in generation of disease severity. Initially, an n of six was chosen based on preliminary work by our lab. Furthermore, only five of the six animals in each group survived the experiment. While these studies were deemed appropriately powered at the outset, the variability has shown that these studies should be repeated with an increased n to account for this variability and mortality.

Future studies using this NTN model would benefit from determination of urinary ET-1 concentrations, to detect the effect of ET_AR antagonism on renal ET-1 production. Furthermore, an additional experimental group using a calcium channel blocker (Nifedipine, Efonidipine, Amlodipine) as an active blood pressure control should be pursued. This would allow for comparison of blood pressure effects against a known standard agent used in the management of CKD. Expansion of these experiments would also include a Sham operated group. Sham controls were not performed in this instance, as these were preliminary experiments to determine the efficacy of Sitaxsentan in this disease context, thus time and funding constraints would not allow for further analysis.

As proteinuric diseases vary in their degree of proteinuria and associated glomerulosclerosis, an alternative *in vivo* model of glomerular disease using ADR (doxorubicin) nephropathy, a rodent model of FSGS [319; 320] would be advantageous. It is characterized by rapid onset of glomerular podocyte damage and proteinuria, which progresses to segmental glomerular sclerosis. Accompanying this there is early tubulo-interstitial damage with subsequent tubular atrophy, accumulation of myofibroblasts around damaged tubules, and interstitial fibrosis. It is of particular interest as it is thought to provide an

animal model of the way in which glomerular proteinuria is associated with progressive tubulo-interstitial scarring and inflammation. This model would allow for the investigation of the effects of selective ET_AR antagonism on other aspects of glomerular injury in addition to hypertension and proteinuria.

Histological analysis of podocyte number is desirable in the context of these studies, however there remains no rat equivalent commercially available WT-1 antibody. An antibody generated in house may be necessary to perform these analyses. Staining of podocytes for SD proteins may be of use, but would not determine discrete cells. These would have to be semi-quantitatively assessed by image analysis for degree of expression. EM analysis of podocyte structure in this model is also a useful indicator of the effects of ET_AR antagonism on podocyte protection and should be pursued.

ED1 (rat CD68) recognizes a cytoplasmic antigen in monocytes and in most Mϕ, free and fixed[321]. ED2[322] and ED3[323] recognize membrane antigens of tissue Mϕ, discriminating between distinct subpopulations of Mϕ, each with a characteristic localization in the compartments of lymphoid organs[324]. No other cell types except cells of the mononuclear phagocyte system are positive for any of the three monoclonal antibodies. Further studies would benefit from staining of tissue sections to determine the distinct sub populations of glomerular Mϕ origin [325].

The role of the ET system in Mϕ is not well defined. The second chapter of this thesis investigated human blood monocyte derived Mϕ ET system biology, using exogenous ET-1 administration *in vitro*. In human and animal studies Mϕ have also been shown to synthesise ET-1 [227; 279]. Additionally, ET-1 has been shown to stimulate the biosynthesis of pro-inflammatory cytokines such as TNFα from Mϕ [282]. ET-1 is a potent mitogen, and partly mediates the proliferative effects of several cytokines [283; 284; 285]. It is thus suggested that in instances of chronic inflammation, ET-1 promotes the pro-inflammatory phenotype of Mϕ, which in turn exacerbate chronic inflammation. [320]

Chapter 4

Impact of ET-1 on human macrophage (Mϕ) activation

4.1 Introduction

ET-1 is known to be involved in the regulation of various functions including vasoconstriction[222], natriuresis and diuresis [223; 224] and importantly in inflammation and fibrosis [225]. Mϕ infiltration is a near universal feature of renal disease and is involved in both progression and resolution of renal injury. Although the data is limited, Mϕ are believed to have an ET-1 system. Rat Mϕ have been shown to express ET_BR but not the ET_AR [276] and there is currently no data demonstrating the presence of either receptor in humans. In human and animal studies activated Mϕ have been shown to synthesize ET-1 in response to LPS, phorbol myristate acetate (PMA) and low-density lipoprotein (LDL)[277; 278; 227; 279] Furthermore, ET-1 is also considered to be pro-inflammatory and chemotactic for Mϕ /monocytes [280; 281;282].

4.1.1 Experimental hypothesis and aims

The experiments described in this chapter were designed to investigate the hypothesis that ET-1 activates Mϕ. Specifically, in human Mϕ ET-1 will – 1) stimulate production of ET-1 2) promote a pro-inflammatory phenotype 3) induce macrophage chemotaxis. The action of ET-1 on Mϕs will be ameliorated by selective ET_AR, but not selective ET_BR antagonism.

Specifically the chapter aims to:

- Demonstrate ET_AR and ET_BR expression on the human monocyte derived Mϕ.
- Determine whether ET-1 administration would induce Mϕ IL-6, IL-8, TNFα and IL-10 up-regulation.
- Investigate whether ET-1 will induce ET-1 production
- Using a transwell assay system, determine whether ET-1 induces chemotaxis.
- Where ET-1 effects are observed, determine whether the effects are ET_AR and/or ET_BR mediated using selective antagonists. The selective ET_AR antagonist BQ123 (IC50: ET_A = 7.3 nM) was used at a concentration of 1μM [246; 252] and the selective ET_BR antagonist BQ-788 (IC50: ET_B = 18 μM) [246] was used at a concentration of 0.1μM. The doses used were based on previous studies as having maximal haemodynamic effect [252].

In the absence of ET-1 effects on macrophages, we aimed to investigate the mechanism by which ET-1 is handled by Mϕ *in vitro*.

The specific aims of these i*n vitro* studies were to determine whether Mϕ would:-

- Remove ET-1 by bulk phase endocytosis
- Degrade ET-1 by proteases either transiently released, or in response to an ET-1 stimulus
- Remove ET-1 by ET receptor mediated clearance

To determine whether ET-1 is taken up by bulk phase endocytosis, we used the lysosomotropic agent chloroquine (CQ) and an inhibitor of microtubule formation Nocodazole (NZ).

To study the effect of proteases on ET-1 degradation, we used a protease inhibitor cocktail (Roche complete) that inhibits a broad spectrum of serine, cysteine and metalloproteases as well as calpains.

Furthermore, the role of ET_AR and ET_BR in Mϕ mediated ET-1 uptake was conducted. We hypothesise that ET receptor involvement in clearance will be mediated by the ET_BR.

4.2 Experimental Protocol

I. Mϕ were cultured ($4x10^6$/well) in IMDM in $75cm^2$ flasks (37°C, 5% CO_2) and purified by adhesion in culture flasks for 90 min at 37°C. Non-adherent cells were removed and medium replaced by fresh IMDM containing 10% autologous serum.

II. Serum containing medium was changed every 2–3 days. After 4-6 days of culture, monocytes acquired a Mϕ phenotype [288] before exposure to ET-1.

III. Cells were used on d7 for all experiments.

IV. ET_AR and ET_BR expression was confirmed by WB, IF and RT-PCR.

V. Mϕ were stimulated with ET-1 (0-10,000pg/ml) at a 24h time-point for detection of pro-inflammatory cytokines by ELISA.

VI. ET-1 induced macrophage migration was assessed using a transwell assay system

VII. Mϕ phagocytosis in response to ET-1 was assessed by semi-quantitative analysis of ingestion of GFP tagged e. coli.

VIII. Where ET-1 effects were observed, Mϕ were incubated with selective ET_AR (BQ123, 1μM) and ET_BR (BQ788, 0.1μM) antagonists 1h prior to stimulation with ET-1.

Where ET-1 effects were not observed, the mechanism by which Mϕ handle ET-1 were investigated. Three basic mechanisms were investigated 1) Bulk phase endocytosis 2) proteolytic degradation and 3) ET receptor mediated clearance.

Bulk phase endocytosis experiments

Experimental groups:

- Chloroquine (CQ) + ET-1 (0, 30, 300, 3000 pg/ml)
- ET-1 (60, 600, 6000pg/ml) BASELINE
- CQ + ET-1 (3000 pg/ml) (No Mϕ) INTERNAL CONTROL

- Nocodazole (NZ)+ ET-1 (0, 30, 300, 3000 pg/ml)
- ET-1 (60, 600, 6000pg/ml) BASELINE
- NZ + ET-1 (3000 pg/ml) (No Mϕ) INTERNAL CONTROL

Protease inhibitor experiments

Experimental groups:

- PI + ET-1 (0, 30, 300, 3000 pg/ml)
- ET-1 (60, 600, 6000pg/ml) BASELINE
- PI + ET-1 (3000 pg/ml) (No Mϕ) INTERNAL CONTROL

ET receptor experiments

Experimental groups:

- No Blockade + ET-1 (0, 15, 15,000 pg/ml)
- ET_AR Blockade- BQ123 + ET-1 (0, 15, 15,000 pg/ml)
- ET_BR Blockade- BQ788 + ET-1 (0, 15, 15,000 pg/ml)
- BQ123 + ET-1 (1500pg/ml) INTERNAL CONTROL
- BQ788 + ET-1 (1500pg/ml) INTERNAL CONTROL
- ET-1 (30, 300, 3000 pg/ml) BASELINES

IX. All samples not requiring incubation with cells (baseline and internal controls) were aliquoted into eppendorfs and incubated for appropriate timepoints.

X. For each experiment, cells were incubated in either 0.5ml chloroquine (CQ) (100μg/ml), 0.5ml PI (1 tablet/50ml) or 0.5ml BQ123, BQ788 or No antagonist for 2h prior to addition of ET-1

XI. ET-1 (0, 60, 600 and 6000 pg/ml) was diluted in autologous serum supplemented IMDM and baseline samples were aliquoted.

XII. After 2h 0.5 ml media containing ET-1 was then added to each well (giving the correct final ET-1 concentration in 1 ml).

NB: All ET-1 dilutions were made in media containing appropriate dilutions of CQ, NZ, PI or antagonists.

NB: Blockade experiments used 0, 30, 30,000 pg/ml baselines to give 0, 15 and 15,000 pg/ml final concentrations

At 2h and 24h media was removed and analysed by RIA for ET-1 content. Detailed methods can be found in Chapter 2 (section 2.1-2.2)

4.3 Human monocyte/macrophage (Mϕ) cell culture

All experiments in this study utilise human PBMC. Immature monocytes were cultured under growth-permissive conditions (37°C) in uncoated standard tissue culture flasks for 7 days to differentiate into mature Mϕ. The characteristics of the mature Mϕ phenotype were identified morphologically under LM (Fig 4.1 A&B).

4.4 Mϕ express ET_A and ET_B receptors

Mϕ have previously been shown to express the ET_B [326], but not ET_A receptor protein. Here, human peripheral blood Mϕ expression and localization of ET_A and ET_B receptor protein and mRNA by is shown *in vitro* (Fig 4.2 A-F) by IF, RT-PCR and WB.

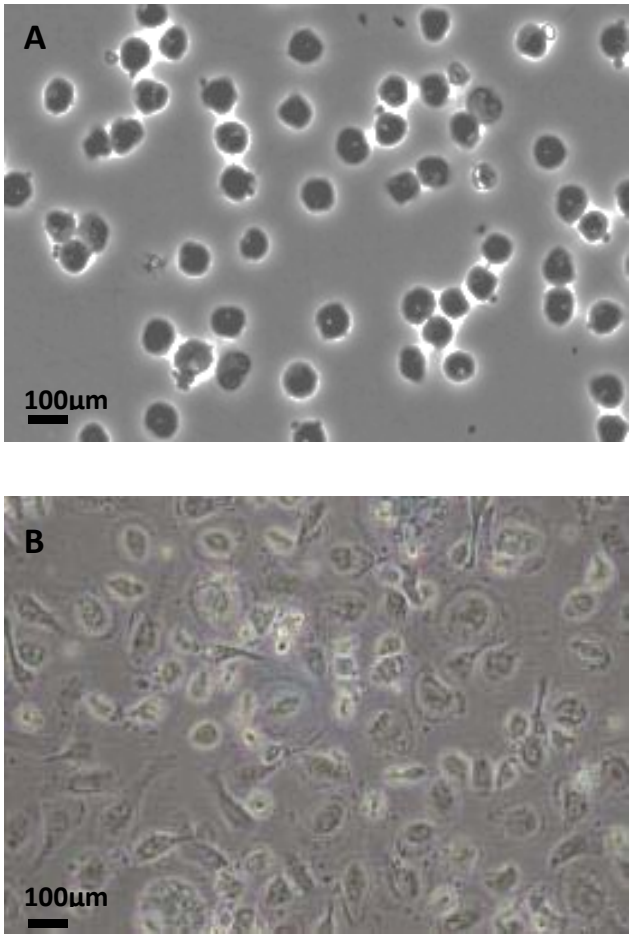

Figure 4.1 Human Mϕ cell morphology

A&B Differing Mϕ cell phenotypes. Photomicrographs (400x) of (**A**) Undifferentiated and (**B**) Differentiated cells under LM. Scale bar represents 20µm.

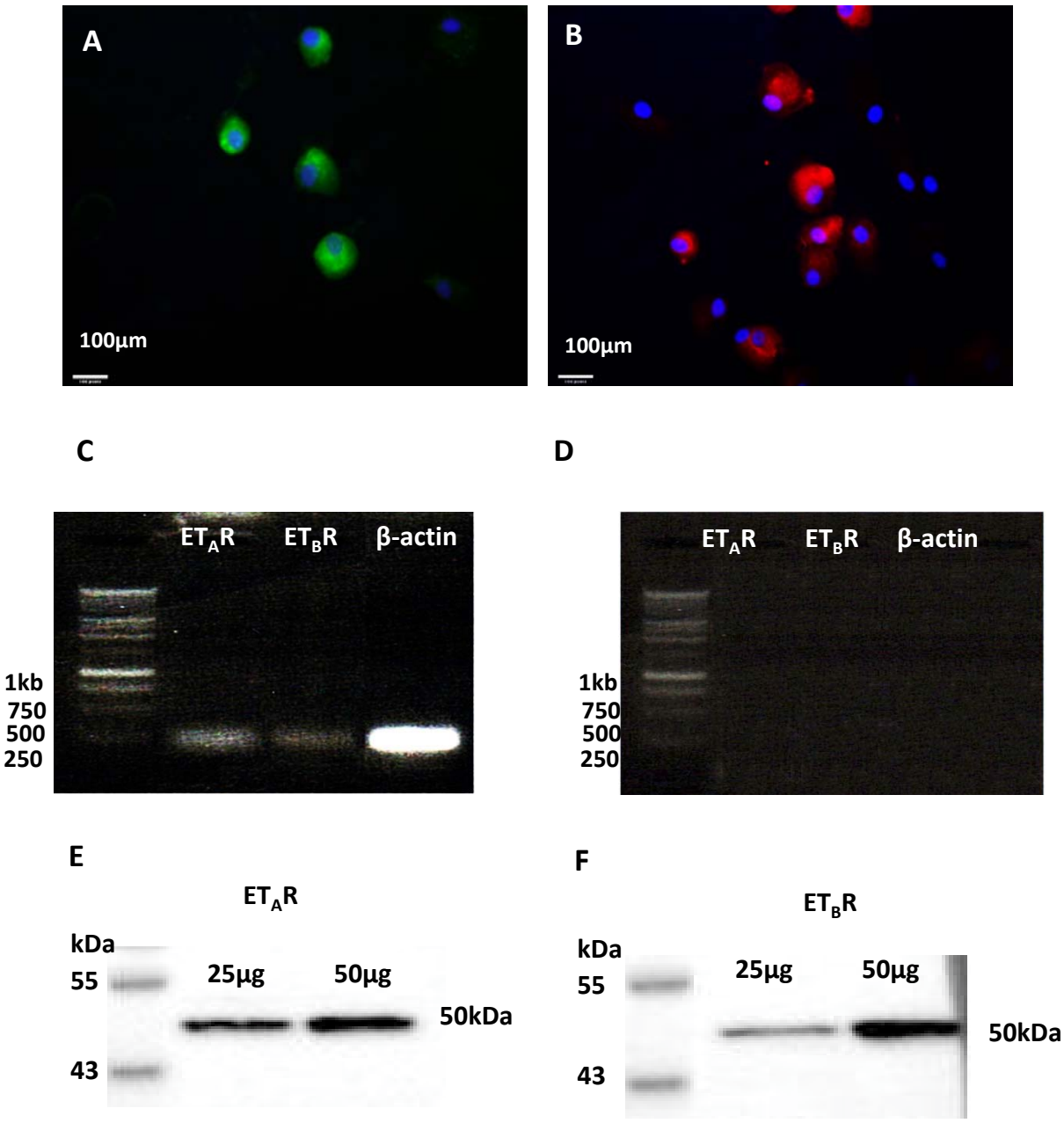

Figure 4.2 Mϕ ET_A and ET_B receptor expression

A-F Photomicrographs (400x) of (**A**) IF staining of ET_AR (green) (**B**) ET_BR (red) and nuclei (blue) (**C**) RT-PCR and (**D**) No RT control of Mϕ RNA using primers for human ET_AR (242bp), ET_BR (260bp) and control 'housekeeping' gene β-actin (250bp) and (**E**) Western blot on whole cell lysates for ET_AR and (**F**) ET_BR. Both receptors are expressed in all experiments. All images are representative of 3 replicates

4.5 ET-1 effects on Mϕ activation

Classical Mϕ activation results in production of pro-inflammatory cytokines and up-regulation of antigen presentation molecules. ET-1 has been shown to stimulate production of pro-inflammatory cytokines in various cell types [282; 327]. We tested the hypothesis that ET-1 activates human Mϕ to adopt a pro-inflammatory phenotype.

4.5.1 ET-1 does not classically activate human Mϕ

Mϕ stimulated with physiological and pharmacological ET-1 doses ranges (10-50,000 pg/ml) did not demonstrate classical activation by production of pro-inflammatory cytokines and chemokines (IL-6, IL-8, TNFα, IL-10) (Fig 4.3 A-D).

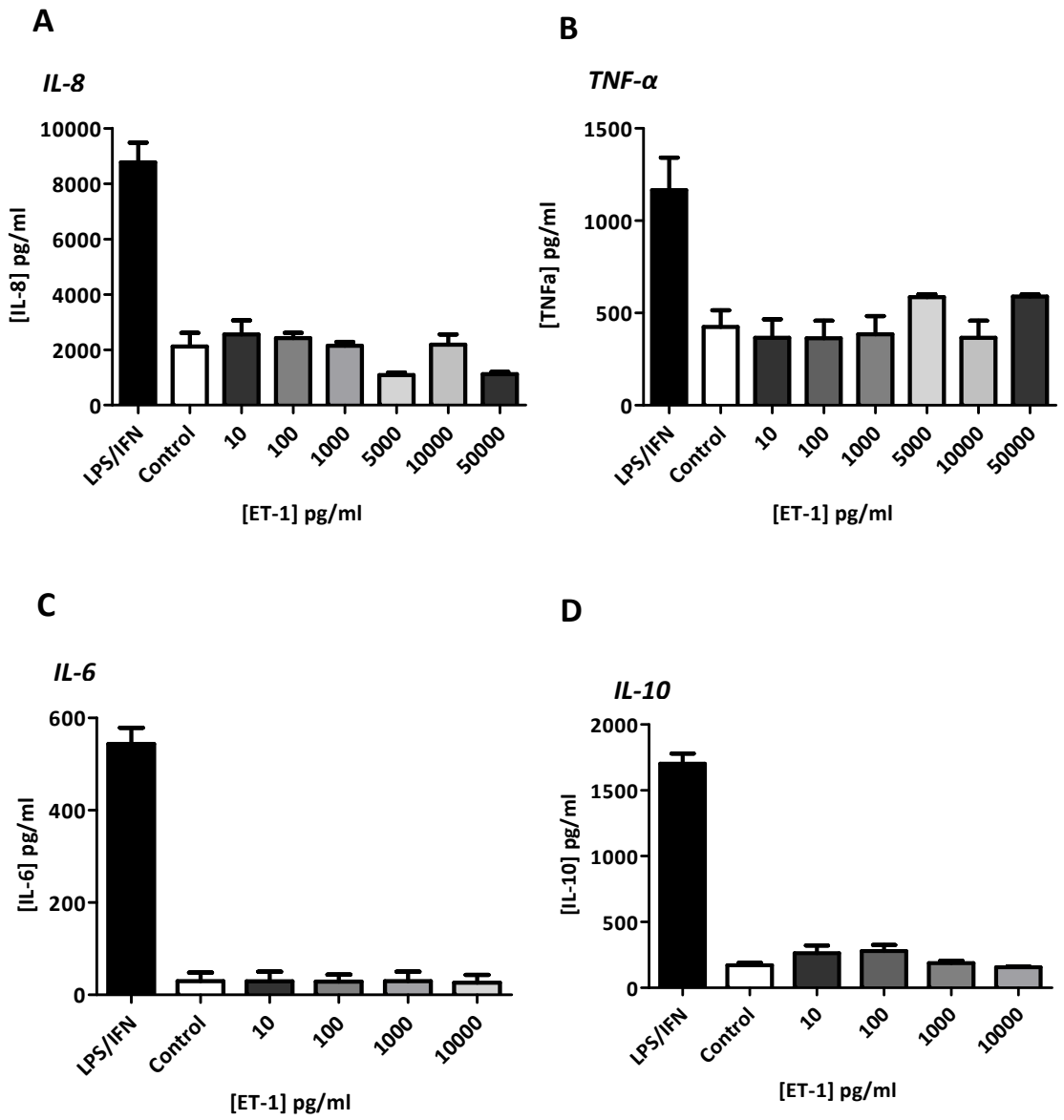

Figure 4.3 ET-1 induced Mϕ cytokine production

A-D Cytokine content assessed by ELISA. ET-1 stimulation at physiological (10 & 100pg/ml) and pharmacological (1000 & 10,000pg/ml) doses did not elicit production of (**A**) IL-8 (**B**) TNFα (**C**) IL-6 or (**D**) IL-10 in human Mϕ. Data are mean ± SD, analysed by 1-way ANOVA, n=8-12.

4.6 ET-1 effects on Mϕ ET-1 production

Mϕ produce ET-1 in response to various stimuli including LPS and PMA [227]. In this assay we tested the hypothesis that ET-1 would stimulate production of ET-1 in human Mϕ.

4.6.1 Mϕ eliminate ET-1 from culture media

Mϕ stimulated with 100 and 500pg/ml ET-1 did not produce ET-1 (Fig 4.4 A&B). Interestingly, little or no ET-1 was detectable in the culture media after 24h incubation. This may be representative of proteolytic ET-1 degradation or cellular uptake and destruction. Of note in this assay is that these were preliminary studies and the 0h ET-1 concentration was not measured. The 0h time-point shown in Fig 4.4 A&B is the assumed concentration of ET-1 added. However, this phenomenon led to further assays with accurate ET-1 measures detailed in the following sections.

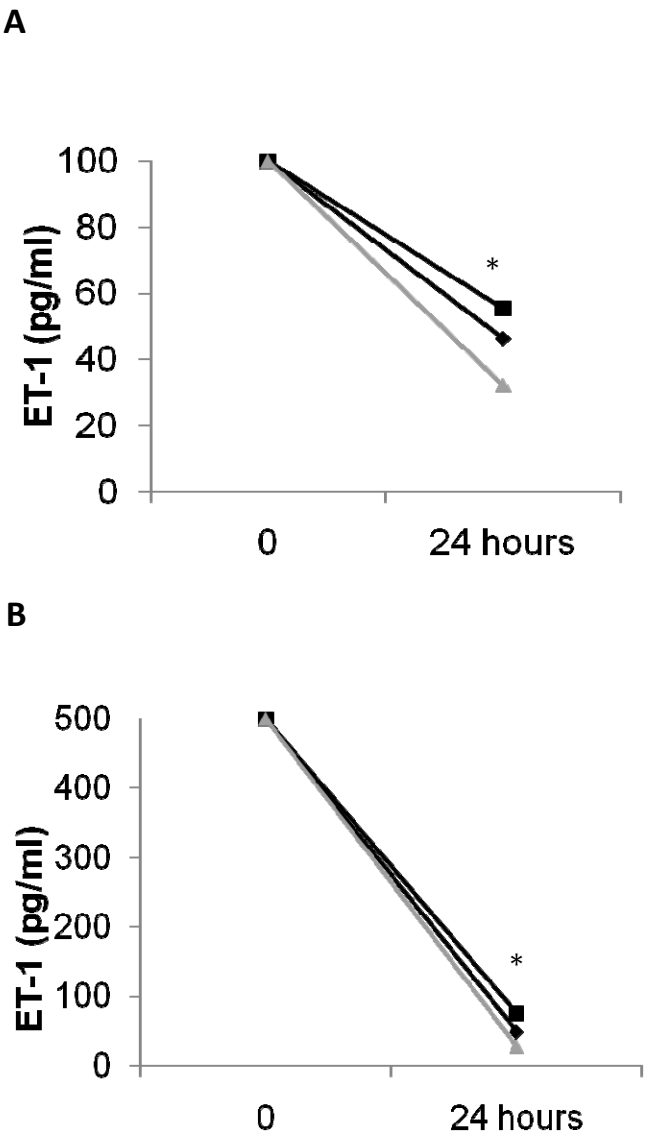

Figure 4.4 ET-1 induced Mϕ ET-1 production

A&B ET-1 content assessed by RIA. ET-1 does not stimulate Mϕ to produce ET-1 at (**A**) 100pg/ml or (**B**) 500pg/ml. Data analysed by Students T-test , (n=3) * $p < 0.05$ Symbols displayed above bars represent significance compared to baseline.

4.7 ET-1 effects on Mϕ migration

Mϕ motility and signalling are influenced by various soluble factors. ET-1 has been implicated as a chemoattractant [280]. Here we investigated the effect of ET-1 on Mϕ chemotaxis/chemokinesis. Monocyte chemoattractant protein (MCP-1). MCP-1, a member of the C-C chemokines [328; 329] is a potent chemoattractant acting on monocytes/ Mϕ [330] and was used in this assay as a positive control.

4.7.1 ET-1 is chemokinetic for Mϕ

In the presence of ET-1 (10-1000pg/ml) cells migrated across the transwell membrane (Fig 4.5 A-G). This was a dose dependent effect with significantly more cells transmigrating at 1000pg/ml compared to control (389.5± 73.5 *vs* 68± 6 nuclei/lpf). This was an approximately 2-fold greater effect than with the positive control MCP-1 (158.5 ± 8.5 nuclei/lpf). Mϕ migration across the membrane only became apparent after 12h, suggesting that the effects of ET-1 are chemokinetic rather than chemotactic. Non-viable methanol fixed cells did not migrate towards MCP-1.

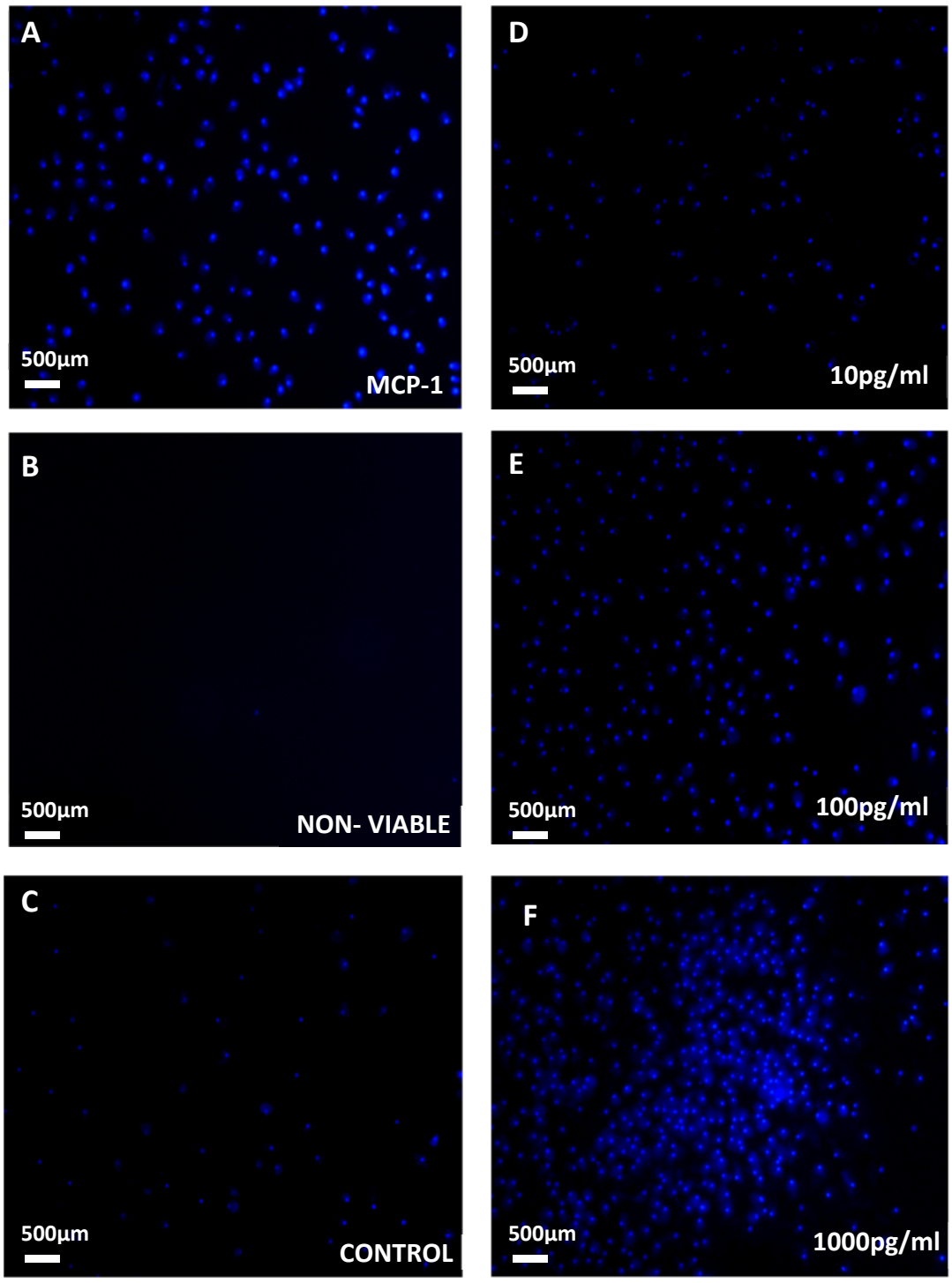
A
500µm
MCP-1
D
500µm
10pg/ml
B
500µm
NON- VIABLE
E
500µm
100pg/ml
C
500µm
CONTROL
F
500µm
1000pg/ml

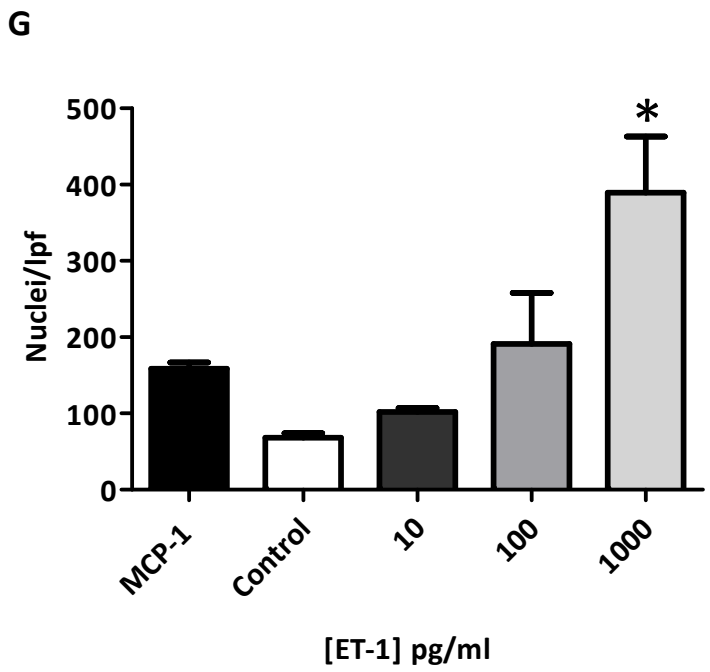

Figure 4.5 ET-1 induced Mϕ migration

A-G Mϕ migration assessed using transwell system to determine number of DAPI stained nuclei/lpf. Mϕ migrate towards a chemo-attractant stimulus as in (**A**) MCP-1. Non- viable cells (**B**) cannot transiently pass through the membrane, whereas low levels of viable cells without a stimulus can migrate (**C**). In the presence of ET-1 however, cell migration is increased at (**D**) 10 and (**E**) 100pg/ml. This is a statistically significant effect at (**F**) 1000pg/ml compared to control. Data are mean ± SD (n=2) analysed by 1-way ANOVA, *p < 0.001 Symbols displayed above bars represent significance compared to control.

4.8 Effects of ET-1 on Mϕ phagocytosis

We have shown the presence of ET receptors on human macrophages and have demonstrated some functional effects of ET-1 administration and ET receptor blockade. In addition to their migratory capacity, another key physiological function of Mϕ is their phagocytic ability. Here we investigated the effect of ET-1 on Mϕ phagocytosis of bacterial particles labelled with GFP. Dexamethasone (DEX), is a steroid capable of enhancing Mϕ phagocytosis [331] and was used in this assay as a positive control.

4.8.1 ET-1 induces increased phagocytosis in human Mϕ

Quiescent Mϕ phagocytose GFP E-coli particles. A phagocytosis positive control dexamethasone (DEX) was used. Compared to no stimulation, DEX significantly increased phagocytosis. The capacity to induce phagocytosis by DEX was not significantly different to that of 100pg/ml (physiological) ET-1 doses. At an ET-1 concentration of 1000pg/ml (pharmacological dose) bacterial particle ingestion was approximately 2-fold higher than control and 1 fold higher then both DEX and 100pg/ml ET-1 (Control *vs* DEX *vs* 100pg/ml *vs* 1000pg/ml; 1.5±0.3 *vs* 5.8±0.8 *vs* 5.8±0.9 *vs* 10.9±0.9) (Fig 4.6 A-E).

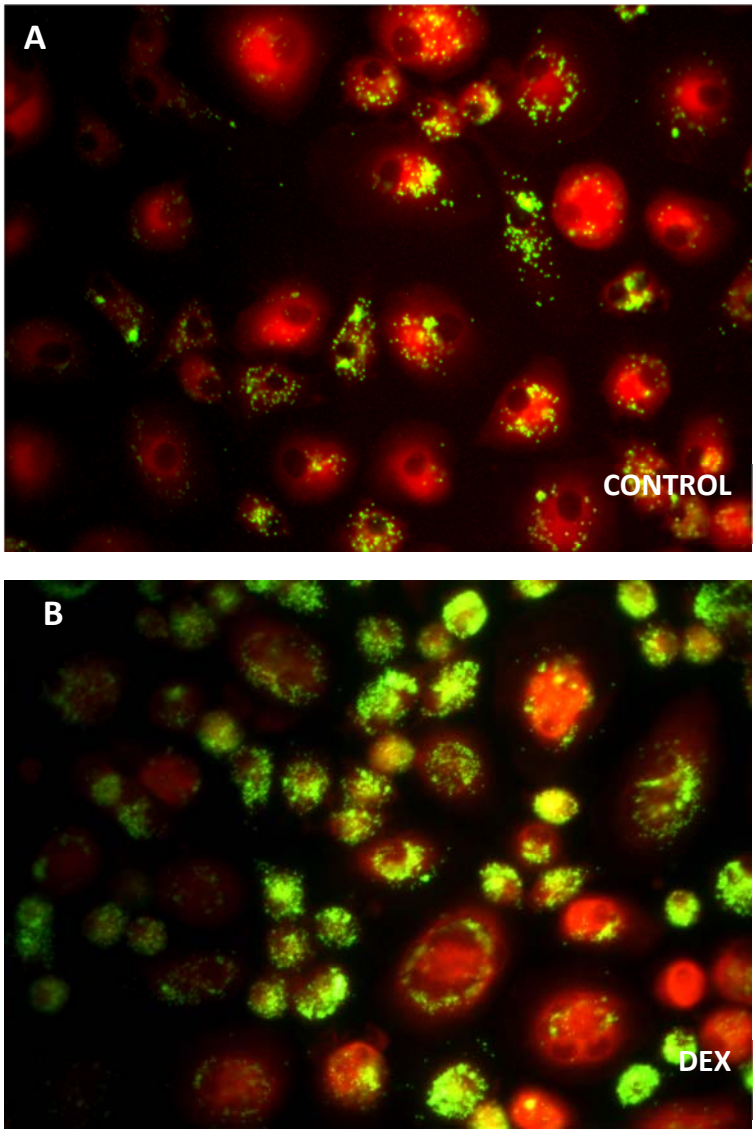

Figure 4.6 ET-1 induced Mϕ phagocytosis

A&B Photomicrographs (600x) of Mϕ phagocytosis of GFP bacterial particles (**A**) Quiescent Mϕ phagocytose e-coli particles. (**B**) Dexamethasone significantly increases phagocytic activity.

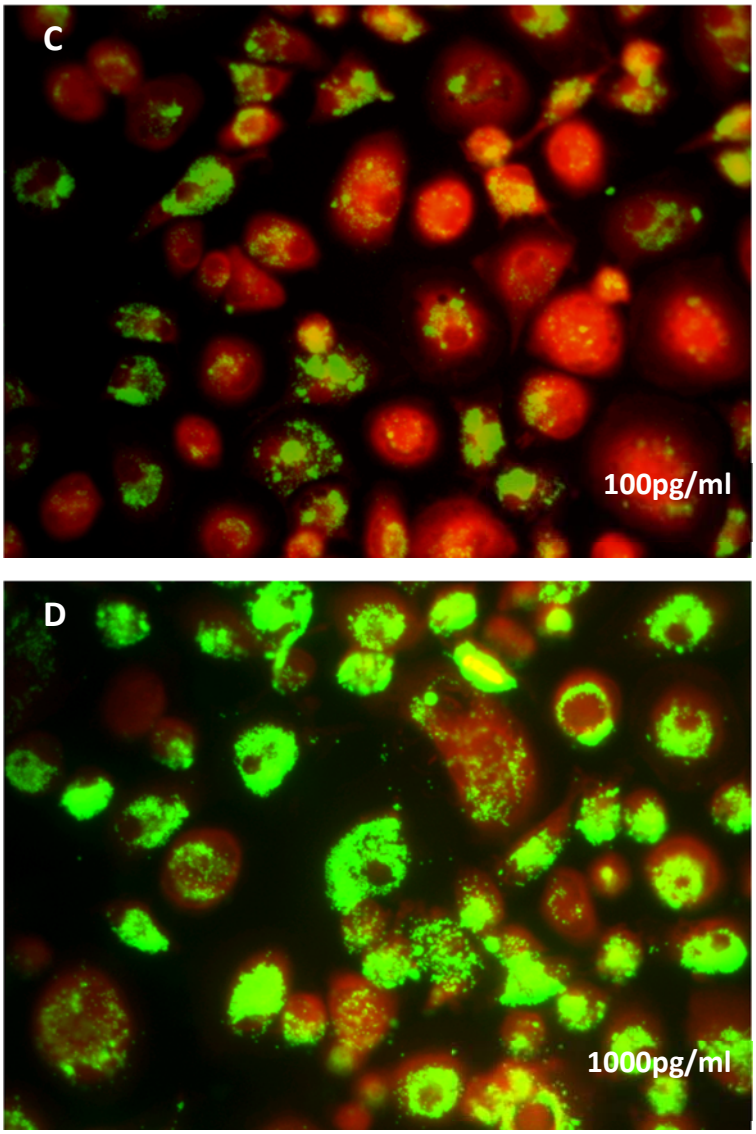

Figure 4.6 Cont. ET-1 induced Mϕ phagocytosis

C&D Photomicrographs (600x) of Mϕ phagocytosis of GFP bacterial particles and (**C**) In the presence of physiological concentrations of ET-1 (100pg/ml), Mϕ phagocytosis is comparable to treatment with dexamethasone. (**D**) Pharmacological doses of ET-1 (1,000pg/ml) induce phagocytosis further.

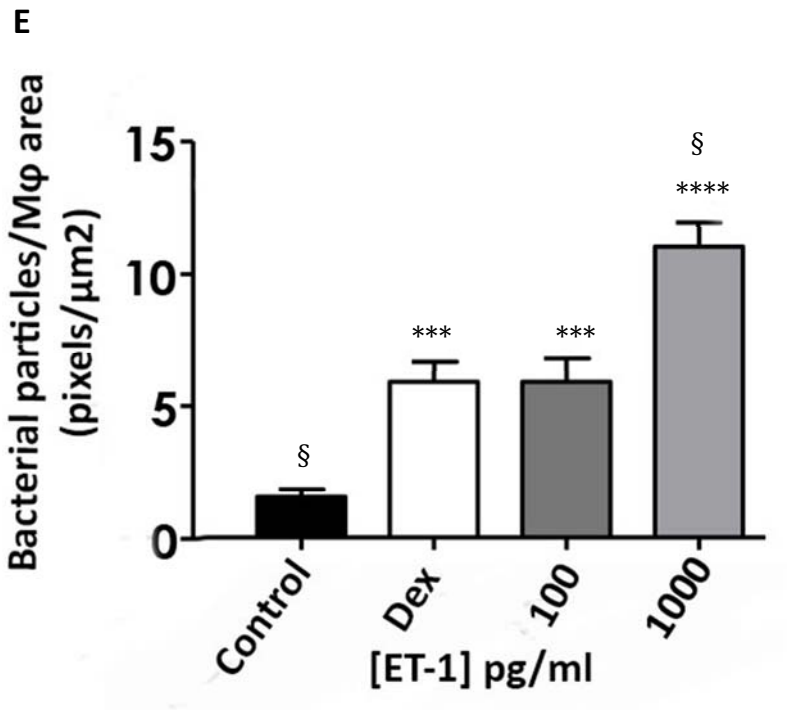

Figure 4.6 Cont. ET-1 induced Mϕ phagocytosis

E Graph of Mϕ phagocytosis of GFP bacterial particles. (**E**) Semi-quantitative image analysis of Mϕ phagocytosis. Data are mean ± SD (n=2), analysed by 1-way ANOVA, Stars displayed above bars represent significance compared to control, *** $p<0.005$, **** $p<0.001$. Symbols represent significance compared to DEX positive control § $p<0.005$.

4.9 Mechanisms of Mϕ ET-1 handling

Our studies have shown that ET-1 added to cultured human monocyte derived Mϕ was absent after 24h. We hypothesised then that Mϕ may regulate ET-1 and aimed to investigate the mechanism by which Mϕ clear or remove ET-1 from the culture media. We investigated three basic mechanisms of ET-1 clearance:- 1) bulk phase endocytosis, 2) proteolytic degradation and 3) cellular uptake by the $ET_{A/B}R$.

4.9.1 Chloroquine does not prevent ET-1 loss

Initially, to study the role of bulk phase endocytosis in Mϕ ET-1 clearance, we used the lysosomotropic agent chloroquine (CQ). The process of bulk phase endocytosis is largely pH dependant. CQ is an agent that prevents endosomal acidification [332]. It accumulates inside the acidic components of the cell, including endosomes and lysosomes. This accumulation leads to inhibition of lysosomal enzymes that require an acidic pH, and prevents fusion of endosomes and lysosomes. CQ is commonly used to study the role of endosomal acidification in cellular processes [333; 334] such as the signalling of intracellular TLRs. CQ also inhibits autophagy as it raises the lysosomal pH, which leads to inhibition of both fusion of autophagosome with lysosome and lysosomal protein degradation [335].

Initially, to ensure CQ did not affect ET-1 in culture conditions, we incubated ET-1 and CQ alone. ET-1 concentrations remained stable after 24h in culture with CQ (CQ+ ET-1 30,000 pg/ml; 0h *vs* 24h; 46442 *vs* 40711.0 pg/ml). Mϕ exposed to chloroquine alone for 24 did not elicit production or release of ET-1 (no ET-1 detectable in the media). Mϕ exposed to CQ did not prevent removal of ET-1 across all concentrations (Fig 4.7 A-D).

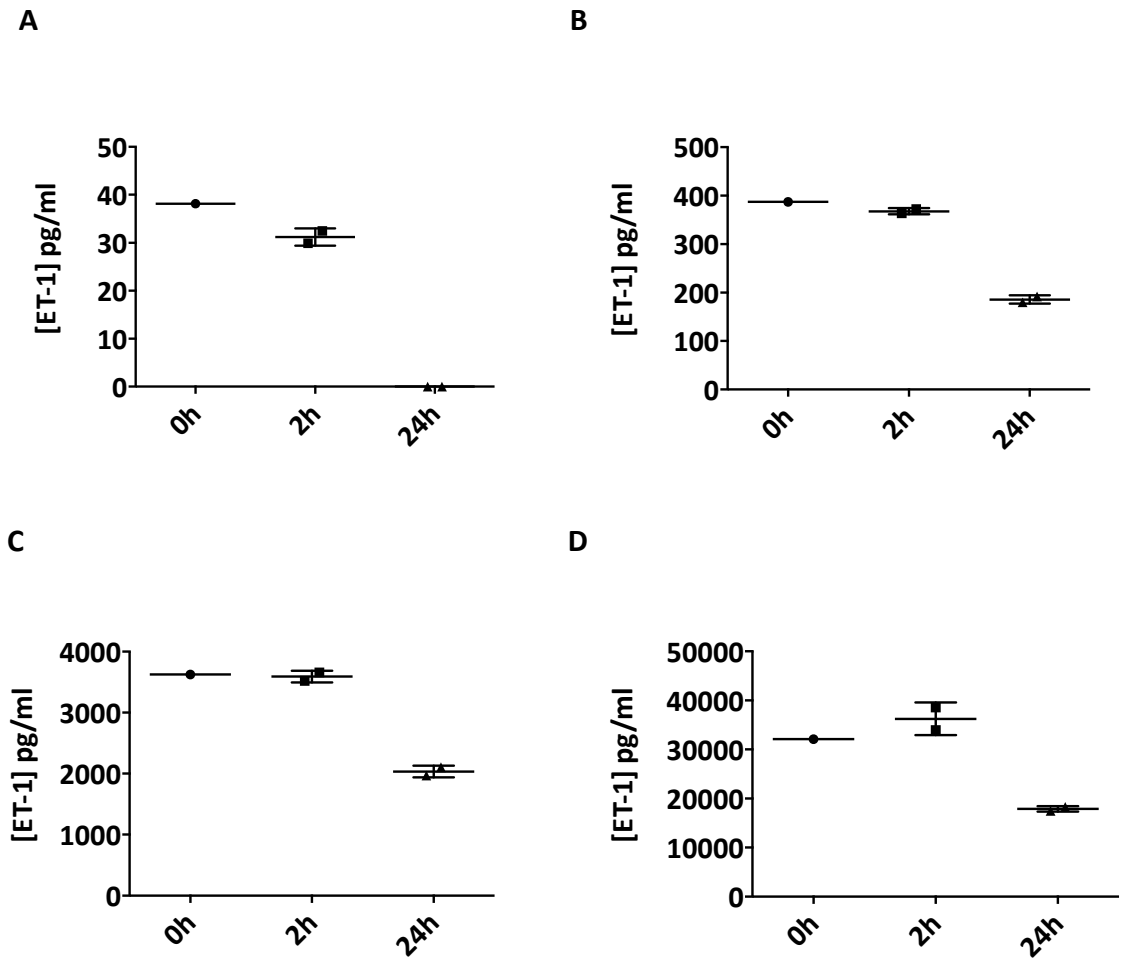

Figure 4.7 Effects of chloroquine on Mϕ ET-1 handling

A-D Mϕ handling of ET-1 by RIA. Mϕ supplemented with chloroquine degrade/remove physiological (**A**) 30pg/ml (**B**) 300pg/ml and supraphysiological/ pharmacological (**C**) 3000pg/ml (**D**) 30,000pg/ml does of ET-1. (n=2) Data are mean ± SD.

4.9.2 ET-1 degradation is prevented by protease inhibition

To study the role of proteolytic degradation of ET-1 by Mϕ, we used a broad-spectrum protease inhibitor (PI). Initially, to ensure PI did not affect ET-1 in culture conditions, we incubated ET-1 and PI alone. ET-1 concentrations remained stable after 24h in culture with PI (PI+ ET-1 30,000pg/ml; 0h *vs* 24h; 31425 *vs* 28053). Mϕ exposed to PI alone for 24 did not elicit production or release of ET-1 (no ET-1 detectable in the media). Mϕ exposed to PI prevent degradation of ET-1 at 300, 3000 and 30000 pg/ml concentrations (Fig 4.8 A-D).

4.9.3 Quiescent Mϕ do not release proteases responsible for degrading ET-1

It is unclear whether the protease(s) released by Mϕ responsible for degrading ET-1 are transiently released by quiescent unstimulated Mϕ, or whether they are released in response to an ET-1 stimulus. For this reason we incubated ET-1 at various concentrations with Mϕ conditioned media for 24h. ET-1 concentrations remained stable over 24h across all dose ranges (Fig 4.9 A-D), indicating that Mϕ at rest do not release proteases capable of degrading ET-1, but rather require stimulation by ET-1 in order to remove/degrade it via a negative feedback mechanism.

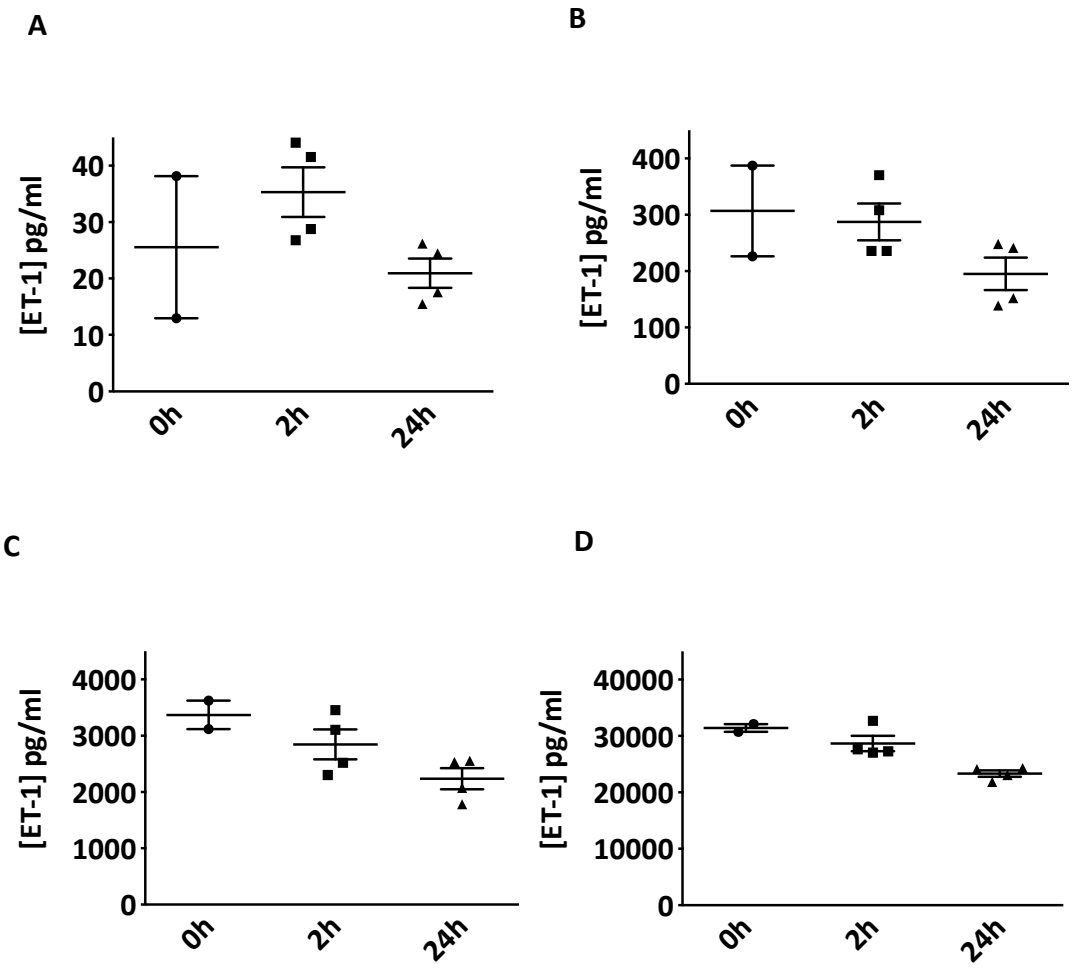

Figure 4.8 Effects of protease inhibitors on Mϕ ET-1 handling

A-D Mϕ handling of ET-1 by RIA. Mϕ supplemented with protease inhibitors prevent degradation/removal of (**A**) 30 pg/ml (**B**) 300 pg/ml (**C**) 3000 pg/ml and (**D**) 10,000 pg/ml ET-1. (n=2-4) Data are mean ± SD.

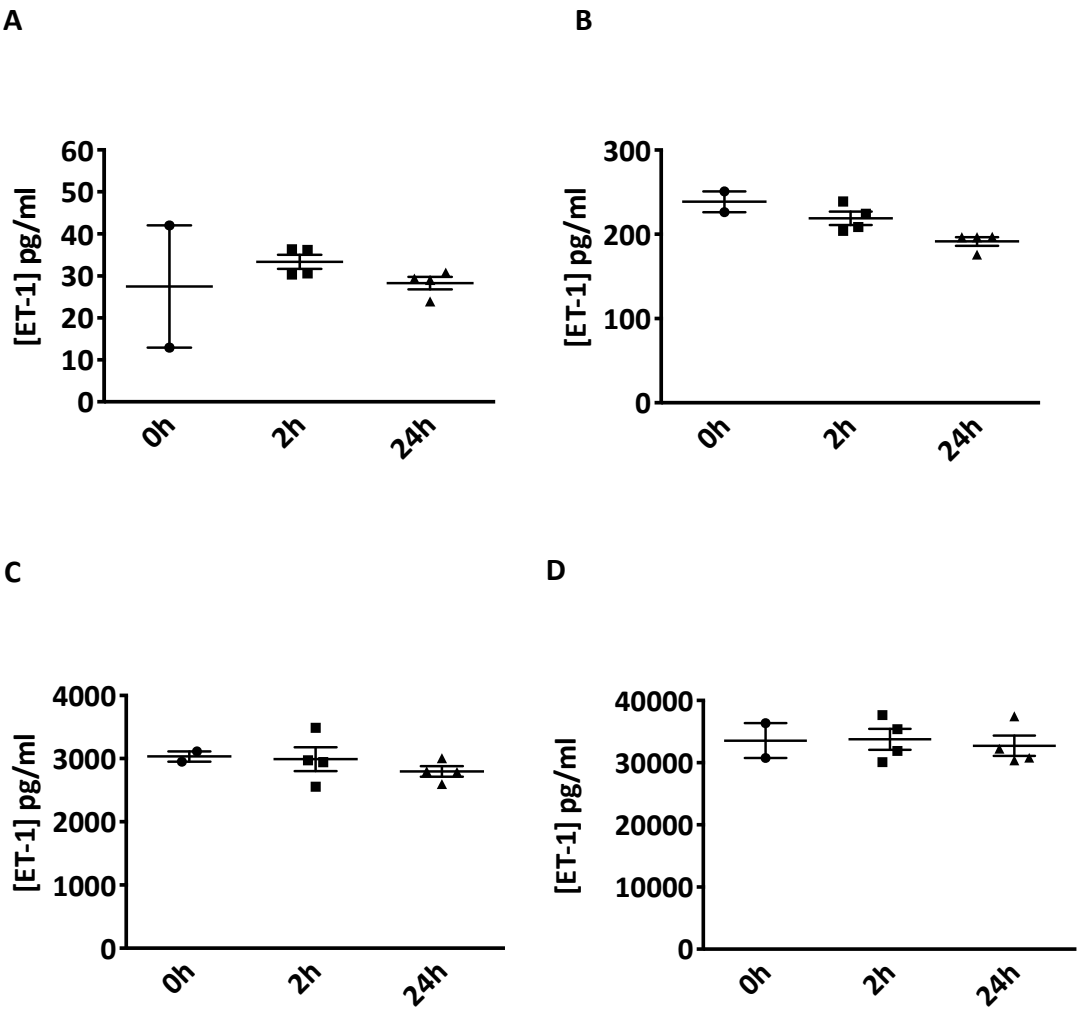

Figure 4.9 Effects of Mϕ conditioned media on ET-1 degradation

A-D ET-1 concentrations in Mϕ CM by RIA. Mϕ CM did not degrade ET-1 at (A) 30 pg/ml (B) 300 pg/ml (C) 3000 pg/ml and (D) 30,000 pg/ml ET-1. (n=2-4) Data are mean ± SD.

4.9.4 Selective ET_BR Blockade partially prevents ET-1 loss

Mϕ ET-1 uptake does not appear to occur by bulk phase endocytosis. Mϕ require stimulation with ET-1 in order to elicit protease release. The ET receptors may therefore be required to clear/uptake ET-1. We investigated the mechanism by which ET-1 was taken up using selective ETR antagonists. At physiological (15 pg/ml) and pharmacological (15,000 pg/ml) doses, ET-1 was removed by Mϕ treated with ET_AR (BQ123), ET_BR (BQ788) antagonists or vehicle control (Fig 4.10). However, after 24h with no antagonist ET-1 removal was complete. However, a significant difference between no blockade and ET_BR blockade was observed at 15pg/ml (24h; No antagonist *vs* ET_AR *vs* ET_BR; 0±0 *vs* 1.45 ± 1.76 *vs* 3.2± 1.5**) and 15,000pg/ml (24h; No antagonist *vs* ET_AR *vs* ET_BR; 8662 ± 1336 *vs* 7595 ± 514 *vs* 10,165 ± 965**)

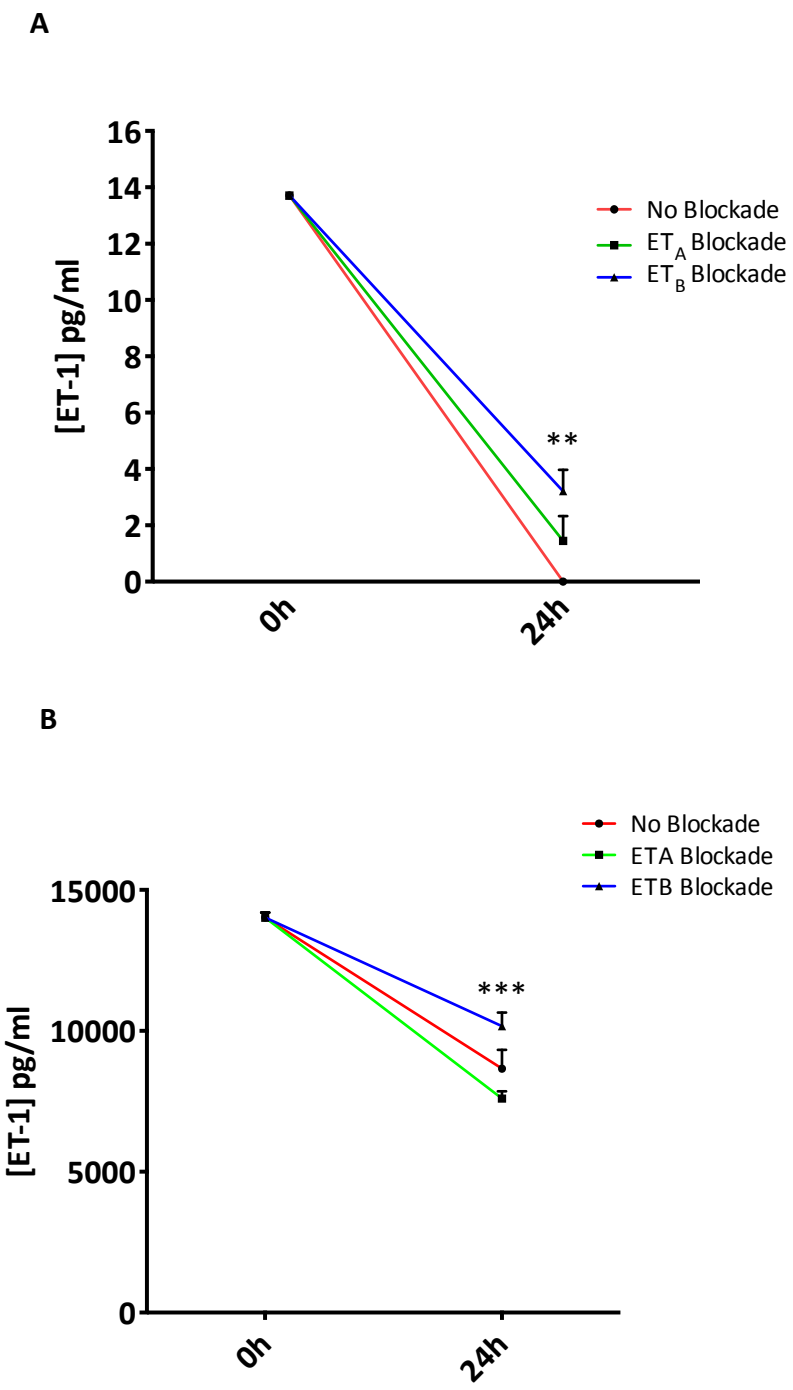

Figure 4.10 Effects of ETR antagonism on Mϕ ET-1 uptake

A&B ET-1 concentrations measured by RIA. After 24h ET-1 (15pg/ml and 15000 pg/ml) added to Mϕ alone, and those pre-treated with BQ123 or BQ788 is removed after 24h. However, at 24h BQ788 attenuates ET-1 removal at (A) 15 pg/ml (B) 15,000 pg/ml ET-1 compared to BQ123 or no antagonist. Data are mean ± SD analysed by 2-way ANOVA, n=4. Stars represent significance compared to control (No Blockade) **p<0.01; ***p<0.005.

4.9.5 Inhibition of microtubule formation prevents ET-1 loss

We concluded that ET-1 was not removed by endocytosis when initially assessed. However, upon addition of an agent (Nocodazole) responsible for disrupting the actin cytoskeleton by inhibiting microtubule formation, we were able to show that Mϕ were not able to remove ET-1 under these conditions (Fig 4.11 A-D). ET-1 uptake did not occur the presence of Nocodazole (100 μM), with no significant reduction in ET-1 concentrations after 24h across the dose range.

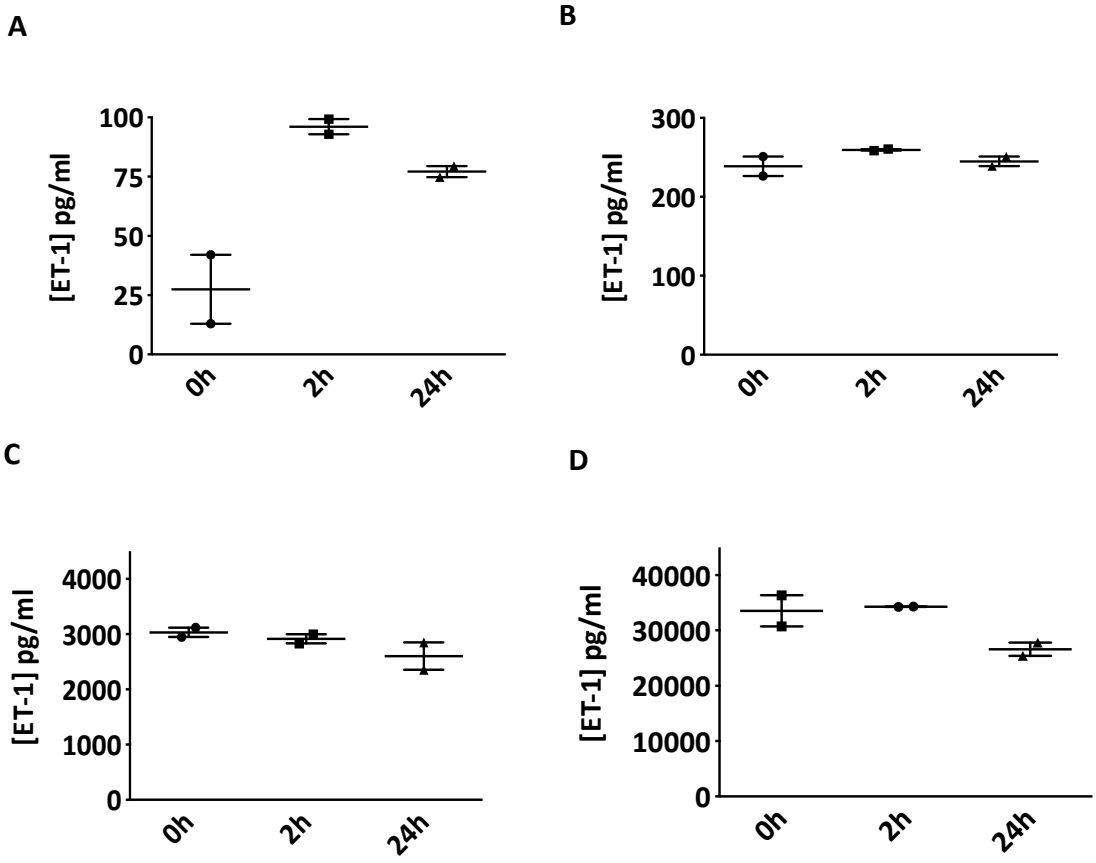

Figure 4.11 Effects of nocodazole on Mϕ ET-1 handling

A-D Mϕ handling of ET-1 by RIA. Mϕ supplemented with NZ prevent ET-1 removal at physiological (A) 30pg/ml (B) 300pg/ml and supraphysiological (C) 3000pg/ml (D) 30,000pg/ml does of ET-1; (n=2) Data are mean ± SD.

4.9.6 ET-1 induced Mϕ chemokinesis is ET_BR mediated

ET-1 induced Mϕ chemokinesis was not affected by the presence of an ET_AR antagonist (BQ123), with cells migrating across the transwell membrane towards increasing doses (10-1000pg/ml) of ET-1 (Fig 4.12 A-G). This effect reached significance at higher doses (Control *vs* 100pg/ml *vs* 1000pg/ml; nuclei/lpf) compared to control (70.5± 3.5 *vs* 247± 9* *vs* 668.5 ± 10.6***). Conversely, Mϕ chemokinesis was attenuated when incubated with an ET_BR antagonist BQ788 across all doses (Fig 4.13 A-G).

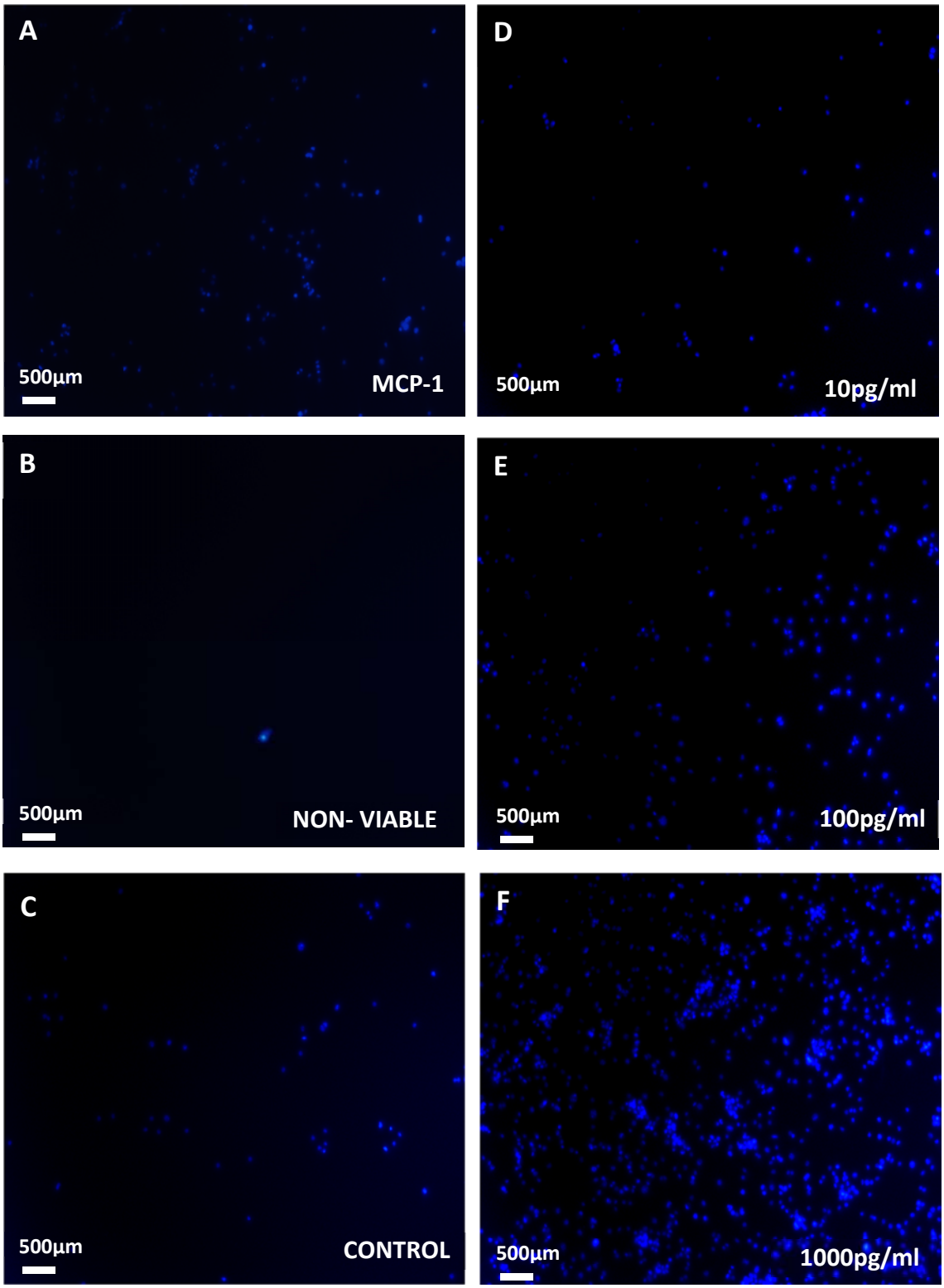
A
500µm
MCP-1
D
500µm
10pg/ml
B
500µm
NON- VIABLE
E
500µm
100pg/ml
C
500µm
CONTROL
F
500µm
1000pg/ml

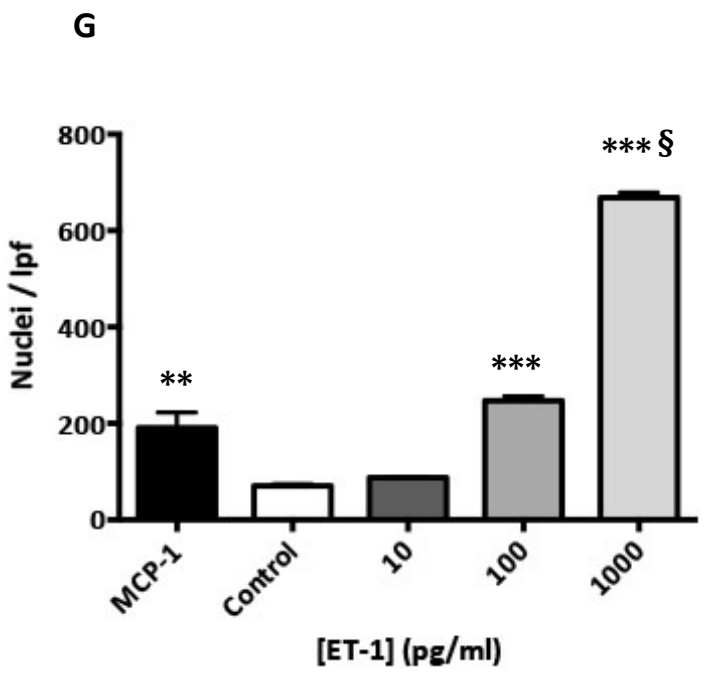

Figure 4.12 ET_AR antagonism of ET-1 induced Mϕ migration

A-G Mϕ migration assessed using transwell system to determine number of DAPI stained nuclei/lpf. Mϕ migrate towards a chemo-attractant stimulus as in (**A**) MCP-1. Non- viable methanol fixed cells (**B**) cannot transiently pass through the membrane, whereas low levels of viable cells without a stimulus (Control) can migrate (**C**). In the presence of BQ123 (1μM), cell migration is increased in response to ET-1 stimulation at (**D**) 10 pg/ml. This is a statistically significant effect at (**E**) 100 pg/ml and (**F**) 1000 pg/ml compared to control. (**G**) Data are mean ± SD, analysed by 1-way ANOVA (n=2), **p < 0.01, ***p < 0.005 compared to control, § p < 0.001 compared to MCP-1. Symbols displayed above bars represent significance compared to control.

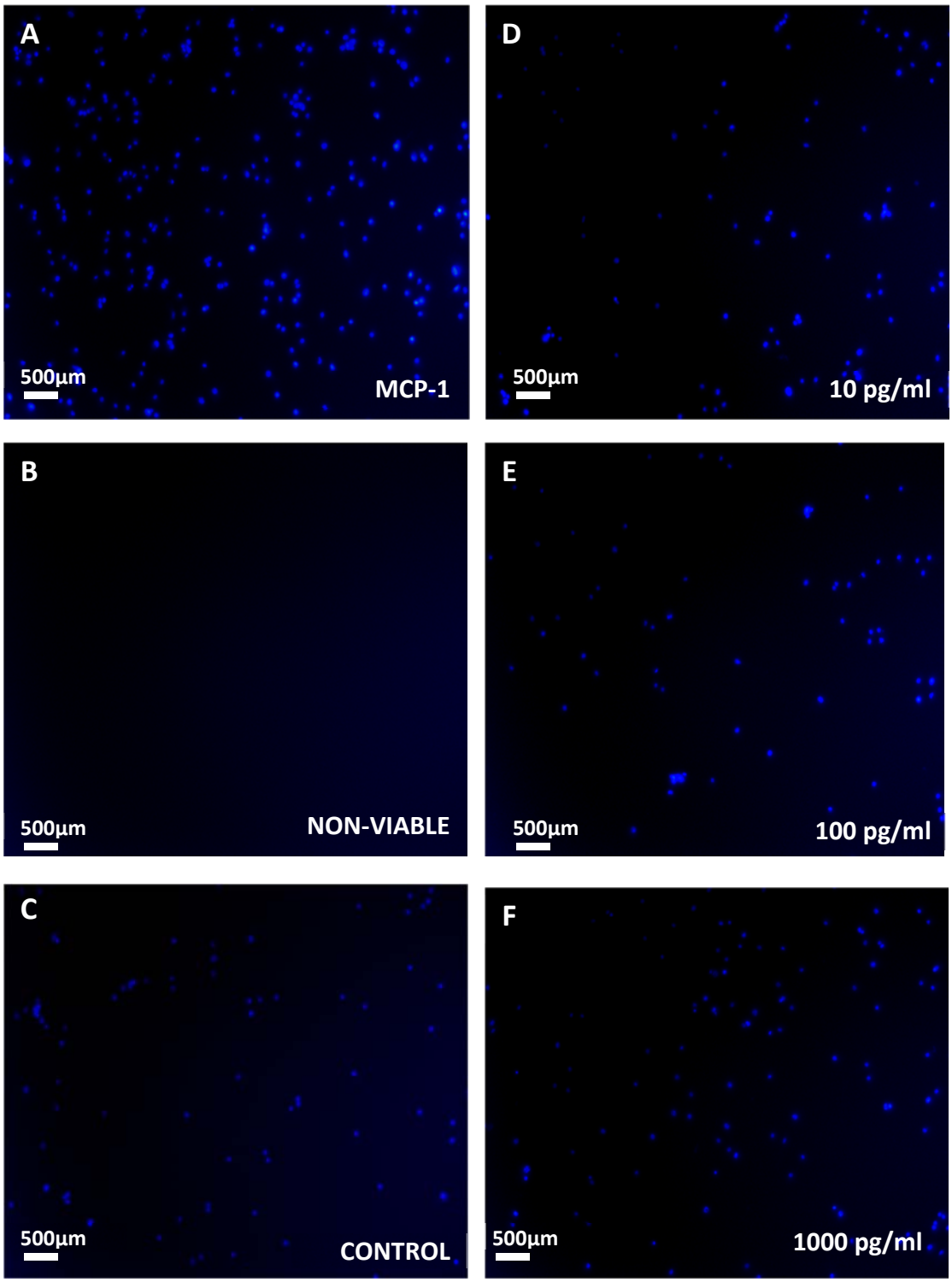
A
500µm
MCP-1
D
500µm
10 pg/ml
B
500µm
NON-VIABLE
E
500µm
100 pg/ml
C
500µm
CONTROL
F
500µm
1000 pg/ml

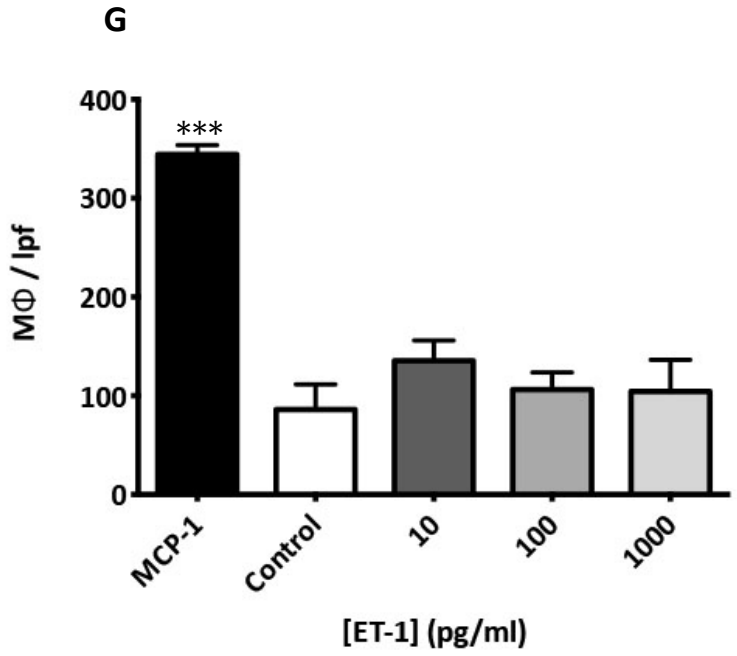

Figure 4.13 ET_BR antagonism of ET-1 induced Mϕ migration

A-G Mϕ migration assessed using transwell system to determine number of DAPI stained nuclei/lpf. Mϕ migrate towards a chemo-attractant stimulus as in (**A**) MCP-1. Non- viable methanol fixed cells (**B**) can not transiently pass through the membrane, whereas low levels of viable cells without a stimulus (Control) can migrate (**C**). The addition of BQ788 (0.1μM) results in the inhibition of ET-1 induced cell migration at (**D**) 10 pg/ml and (**E**) 100 pg/ml and (**F**) 1000 pg/ml compared to control. (**G**) Data are mean ± SD (n=2), analysed by 1-way ANOVA. Symbols displayed above bars represent significance compared to control ***p < 0.005.

4.10 Summary

- Human Mϕ express ET_AR and ET_BR and functionally respond to ET-1.
- Contrary to our initial hypothesis, in response to ET-1 Mϕ are not classically activated. They do not do not produce pro-inflammatory cytokines demonstrative of classical activation.
- The cells do respond to ET-1. ET-1 may be chemokinetic for Mϕ and may augment phagocytosis.
- ET-1 mediated macrophage migration is an ET_BR mediated event.
- Furthermore ET-1 is removed from the media. The mechanism for this removal may be ET_BR mediated, and involving proteolytic degradation of this peptide.

While our initial hypothesis was not supported, these results suggest a role for Mϕ in regulation of ET-1. The physiological effects of ET-1 may be affected by Mϕ. To address this we investigated the effect of macrophage depletion on the physiological pressor response to ET-1 *in vivo*.

4.11 Discussion

4.11.1 Human Mϕ possess ET receptors, but are not classically activated by ET stimulation

ET-1 exerts a number of pro-inflammatory effects. It is a widely held contention that the action of ET-1 is mediated, at least in part, by its ability to classically activate Mϕ to adopt an M1 phenotype. Rodent Mϕ have been shown to express ET_BR, but there is currently no data demonstrating the presence of the ET_AR [276]. These studies demonstrate that human Mϕ express both ETR at the protein and mRNA level.

Of note, all experiments described in this chapter utilised human blood derived macrophages separated by heperosmolar Percoll gradient and purified by adhesion (See 2.1.1.2 for method). Obtaining macrophages by this method is common practice [336] . Following an initial serum-free adhesion step and removal of non-adherent cells (primarily lymphocytes), a 6d adhesion protocol was used. After this time cells a >90% population assessed morphologically was observed. There are, however other methods including FACS sorting to allow for a purer macrophage population. This cell population purity issue should be taken into account when considering this data.

There is some evidence to suggest that ET-1 can elicit classical pro-inflammatory Mϕ activation by the NF-κB signalling and subsequent release of TNF-α [337; 338], although this result has not been consistently observed [339;340]. ET-1 has been shown to stimulate Mϕ production of the chemokine macrophage inflammatory protein-1β (MIP-1β). These changes may be part of an ET-1-induced alteration in Mϕ phenotype. However, data to this end are scarce but are of interest in light of the potential role for Mϕ in renal repair [341]. In these *in vitro* experiments, Mϕ stimulation with ET-1 across physiological and pharmacological doses does not elicit classical Mϕ activation.

4.11.2 ET-1 is cleared by Mϕ and induces migration in an ET_BR dependant manner

Human Mϕ and DCs have been shown to synthesise ET-1 in response to LPS, PMA and LDL [277; 278; 340]. Based on these studies, we hypothesised that ET-1 would induce Mϕ ET-1 synthesis. ET-1 production did not occur and 24h after addition of ET-1 to the culture media, the ET-1 peptide was not detected in the supernatant, suggesting that Mϕ remove this peptide. Therefore, the mechanism(s) by which Mϕ remove ET-1 were investigated.

Initially, we investigated the role of bulk phase endocytosis in the clearance of ET-1 using CQ. This weakly basic compound is used experimentally to inhibit clathrin-mediated endocytosis (CME). Experiments demonstrated that CQ did not prevent ET-1 loss.

We also investigated the role of proteolytic degradation in Mϕ handling of ET-1. While broad-spectrum PI prevented ET-1 loss, Mϕ CM did not effect ET-1 concentrations, implying that ET-1 is removed upon contact with the cells. We hypothesised that this initial cell contact and subsequent proteolytic degradation was likely mediated by the ET_BR, the receptor primarily responsible for clearing ET-1. These observations were confirmed in antagonist studies, whereby ET-1 removal was partially prevented by ET_BR blockade.

While ET-1 does not induce pro-inflammatory cytokine production, it does affect other functions of macrophages. We demonstrate that Mϕ migrate toward an ET-1 gradient. The mechanism by which ET-1 induced Mϕ movement was via the ET_BR; antagonism of this receptor but not the ET_AR prevented ET-1 induced chemokinesis. The literature surrounding this effect are sparse, however stimulation of human neutrophils with safrotoxin S6c, a selective ET_BR agonist induces chemotaxis, an effect that is similarly inhibited upon addition of an ET_BR antagonist IRL1038[342].

Early studies by Bremnes *et al.* (2000) demonstrated that in CHO cells, the ET receptor subtypes follow an arrestin and dynamin/clathrin-dependent mechanism of internalisation. Following ET-1 stimulation, ET_AR and ET_BR

subtypes were targeted to different intracellular routes. While ET_AR followed a recycling pathway and co-localised with transferrin in the pericentriolar recycling compartment, ET_BR was targeted to lysosomes after ET-induced internalization. Both receptor subtypes co-localized with Rab5 in classical early endosomes, indicating that this compartment is a common early intermediate for the two ET receptors during intracellular transport [343]. The opposing intracellular routes of ET-1 stimulated ET_AR and ET_BR may explain the persistent signal response through the ET_AR and the transient response through the ET_BR thus lysosomal targeting of the ET_BR serves as a biochemical mechanism for clearance of plasma endothelin via this subtype [343].

As CQ is a weak base that prevents late endocytic processes, i.e. it prevents endosomes from moving into the multi-vesicular body (MVB)/lysosome stage, it is likely that the observed ET-1 loss from the culture media upon addition of CQ corresponded to ET-1 uptake into early endosomes via the $ET_A/_BR$, but likely prevented ET-1/ETR complex movement to other intracellular compartments (including lysosomes) at this stage. The ETR may then recycle back to the plasma membrane to further bind and internalise more ET-1.

Investigations into the protease(s) responsible for ET-1 degradation require further investigation. In addition to degradation of ET-1, proteolytic activity is required for several key processes in macrophages, including cell migration. The best characterized extracellular protease families - MMPs, cathepsins and urokinase-type plasminogen activator are reviewed in reference to their involvement in macrophage migration [344].

We therefore speculate that ET-1 engagement of the ET_BR leads to receptor internalisation and initiation of signalling pathways that induce macrophage migration and associated expression of proteases. Cathepsins and other serine proteases usually presented on the leading edge of migrating macrophages involved in degradation of extracellular matrix may also lead to subsequent degradation of ET-1.

The role of the cytoskeleton has been extensively studied and was long thought not to be involved in endocytosis. Experiments in the 1990s demonstrated that the actin cytoskeleton and its binding partners do play a role at different stages along the endocytic pathway in polarized and non-polarized cells and in yeast [345; 346; 347]. Microtubules are involved in late steps of endocytosis, in the traffic between early and late compartments. When microtubules are disrupted, translocation of endosomes and lysosomes is inhibited [348; 349;350].

We demonstrated that NZ, an inhibitor/disruptor of microtubule formation prevented ET-1 uptake suggesting that late endocytic processes and engagement/activation of the cytoskeleton and related intracellular signalling events are required for subsequent removal/degradation of larger quantities of ET-1.

In addition to potentially being an active component of endocytosis of ET-1/ET_BR and associated cell signaling events, the actin cytoskeleton of these cells also plays a central role in locomotion, phagocytosis, and the regulation of cell shape. We demonstrated that ET-1 induced macrophage chemokinesis. When assessed, this appeared to be an ET_BR mediated event.

4.11.3 Further investigations

The phenotype of ET-1 stimulated Mϕ remains to be determined and further investigations into the phenotype and mechanisms of ET-1 handing should be determined. ET-1 may induce a more 'M2' type macrophage. In murine cells, markers of alternative activation such as Fizz-1, YM-1 etc. are readily available. Alternatively activated murine Mϕ produce fibronectin and a matrix-associated protein, βIG-H3 [75], arginase [77], AMAC-1 [78] CD163, transcription factors FIZZ1 and Ym1, [79]. Alternatively activated human Mϕ are more difficult to characterise. When considering M2 phenotypes in human cells, it is more likely that the ratio of a given set of receptors is altered. Human M2 Mϕ may up-regulate mannose receptor (CD206), Scavenger receptor-A (SRA) (CD204) and down-regulate co-receptors CD80/CD86. This is not always the case and depends on the degree of skew of the Mϕ towards M2. More recently, M2

polarised Mϕ have also been shown to express suppressor of cytokine signalling (SOCS 1 and 2) but not SOCS 3[351]. Whether ET-1 activates an M2 macrophage remains to be elucidated.

We have described potential mechanisms of ET-1 handling via endocytic, proteolytic and ET receptor mediated processes. All studies performed were preliminary and require further analysis with increased numbers and alternative reagents. For this reason the assays described in these mechanistic investigations are described in terms of their trends and were not statistically assessed with an n of 2 only. The specific limitations of each assay will be addressed in this section.

When considering the role of the actin cytoskeletons in receptor endocytosis, repeated experiments with NZ, and alternative reagents such as colchicine, cytochalasin B[352] and Brefeldin A [353] to target microtubule disruption and clathrin-coated pit internalisation should be considered. The pharmacological inhibitor of dynamin (Dynasore) may be employed to determine whether these are clathrin-mediated processes. Downstream intracellular signalling events and proteins may also be investigated. siRNA knockdown of β-arrestin 2 in human cells may be a useful tool in this process [354]. Reagents for these experiments are all commercially available (Santa Cruz Biotch, CA).

Our Mϕ migration assays utilised transwell inserts containing a micro-porous membrane. We concluded that these assays demonstrated chemokinesis due to the duration of time taken for migration to occur. To definitively determine whether these are truly chemokinetic or or chemotactic processes, the use of Dunn chemotaxis chambers with time-lapse photography is required [353]. Furthermore, these migration experiments may be expanded further to include addition of e.g. culture of parietal epithelial cell layers on the transwell inserts to mimic passage of Mϕ from the interstitial space to the glomeruli.

We also investigated the phagocytic activity of human Mϕ in response to ET-1 using GFP bacterial particles. There were several issues relating to these

experiments. While this was a suitable means of assessing phagocytosis in principle, there were issues relating to determining whether the particles were truly internalised, or whether they were membrane bound. To attempt to address this issue, after particle ingestion the cells were treated with trypan blue. This theoretically quenches any external dye without compromising internalised bacterial GFP. In this assay we used direct immunofluorescence to assess GFP signal. A more accurate way to assess ingested particles would be to use confocal microscopy. Furthermore, this assay could be expanded to include different particulate matter including apoptotic cells and/or latex beads. Further investigations into the receptor mechanism of increased phagocytosis are also required.

In this chapter we propose that ET-1 does not directly activate Mϕ in a classical sense. Rather, the pro-inflammatory potential of ET-1 is mediated by its ability to induce up-regulation of pro-inflammatory pathways in a number of other cell types including resident renal glomerular and interstitial cells. Rather, the role of ET-1 in Mϕ alone is to signal Mϕ for migration to an injured/inflamed environment, an ET_BR mediated event. Here Mϕ may be classically activated by other pro-inflammatory mediators, or by ET-1 in an as yet unclear fashion. ET-1 activated Mϕ may exhibit more M2 phenotypic changes to a pro-resolution phenotype, as ET-1 clearance and phagocytosis are increased. Whether ET-1 is capable of inducing strong M2 phenotypic changes or not remains to be elucidated. However, it is apparent that ET-1 is cleared by Mϕ and may serve as regulatory cells in the ET system. These observations may ultimately be of more relevance in limiting the pro-hypertensive effects of ET-1.

Chapter 5

Macrophage regulation of the pressor effects of ET-1

5.1 Introduction

In the previous chapter we aimed to demonstrate that ET-1 would classically activate human blood monocyte derived Mϕ. Our studies showed human Mϕ expressed the ET_AR and ET_BR. However, despite repeated experiments, Mϕ did not respond to ET-1 as hypothesised. In response to physiological and pharmacological dose ranges of ET-1, these cells were not activated to produce pro-inflammatory cytokines, did not express surface markers of classical (M_1) activation, and did not produce ET-1. Furthermore, ET-1 did not induce ET-1 production, but rather depleted ET-1 from the media.

5.1.1 Experimental hypothesis and aims

These initial observations led to the consideration that Mϕ could potentially serve to regulate ET-1. We hypothesise that Mϕ regulate ET-1, and the vasoactive properties of ET-1 are exacerbated in the absence of Mϕ. With only a few examples in the literature of an indication that inflammatory cells may be involved in the regulation of blood pressure via regulation of vasopressors [355; 356], these experiments would indicate a paradigm shift in the way blood pressure control is viewed and potentially provide a rationale for immune cell modification in therapy for hypertension and hypertensive nephropathy.

To investigate the potential of Mϕ in ET-1 handling and regulation, a selective Mϕ depletion strategy was employed *in vivo* using transgenic mice expressing the diphtheria toxin receptor under the control of the CD11b promoter[302]. In this model, administration of DT results in blood monocyte and resident tissue Mϕ depletion. Following Mϕ depletion, we aimed to examine the pressor response to ET-1 by invasive carotid BP measurement.

The specific aims of these experiments were to:

- Determine whether Mϕ depletion would exacerbate the pressor response to ET-1

5.2 Experimental Protocol

I. Diptheria toxin (DT) (20ng/g i.v.) was administered to mice to induce monocyte/ Mϕ depletion in CD11b-DTR transgenic mice and FVB strain controls, and an equal volume of saline was administered to treatment control CD11b-DTR mice 24h prior to BP measurements.

II. After 24h mice were initially anaesthetized with Thiobutabarbital (100mg/kg i.p.).

III. Following this a tracheotomy was performed and the jugular vein and carotid artery were cannulated for administration of drugs and BP measurement.

IV. The animals were then allowed to stabilize for 10–20 min.

V. Following this stabilisation, baseline recordings were carried out for 10–15 min to ensure the stability of the preparation.

VI. After baseline measurements were recorded, the effect and duration of the action of the drugs were observed and recorded. The doses of ET-1 (0.01, 0.1 and 1 nmol/kg) were injected in order of increasing concentration via the jugular cannula.

VII. BP was recorded over a 20-minute period and allowed to normalise back to baseline.

VIII. The final drug to be administered was Ang II (1nmol/kg).

IX. After each drug administration, the BP of the animal was allowed to return to the normal baseline value before injection of the subsequent dose.

X. Following these experiments the animals were then sacrificed by cervical dislocation, and tissues were harvested for further analysis.

XI. To assess the efficacy of DT treatment on Mϕ depletion blood leucocyte populations were assessed by FACS.

XII. Tissues (liver, kidney and spleen) were fixed in 4% FA and F4/80 immunohistochemical staining was performed to assess tissue Mϕ depletion.

5.3 Effects of diptheria toxin administration on monocyte/ macrophage ablation

5.3.1 Monocytes are depleted by diphtheria toxin

Experiments were conducted using transgenic mice expressing the DTR under the control of the CD11b promoter on an FVB/nj background. DT (20ng/g) was administered to induce monocyte/ Mϕ depletion in transgenic mice 24h prior to experiments. FVB/nj mice treated with DT were used as strain controls and a CD11b-DTR treated with vehicle (saline) were used as transgenic controls.

Monocytes were identified according to their size, granularity and immunophenotype by flow cytometry (see gating parameters in Chapter 2 Methods section 2.2.2.1.2.1) and gated into subsets 1) CD11b+, CD115+, Ly6G-, $Ly6C^{hi}$ 2) CD11b+, CD115+, Ly6G-, $Ly6C^{int}$ and 3) CD11b+, CD115+, Ly6G-, $Ly6C^{lo}$. Administration of DT to CD11b-DTR animals resulted in significant ablation of circulating monocytes at 24h compared to control DTR mice treated with saline, and sham DT treated FVB/nj mice (Fig 5.1 A-D). Analysis of the three main monocyte subsets ($Ly6C^{lo}$; $Ly6C^{int}$; $Ly6C^{hi}$) demonstrated that all subsets are significantly depleted at 24h, and there were no significant differences in monocyte number between control groups (Fig 5.2 A-C).

5.3.2 Resident renal macrophages are depleted by DT

Tissue sections were stained for Mϕ using F4/80. Administration of DT to CD11b-DTR animals resulted in significant ablation of Mϕ at 24h compared to control DTR mice treated with saline, and sham DT treated FVB/nj mice in the cortex (Fig 5.3 A-D) and medulla (Fig 5.3 E-H). Resident hepatic Mϕ however were not significantly affected in any group (Fig. 5.4 A-D).

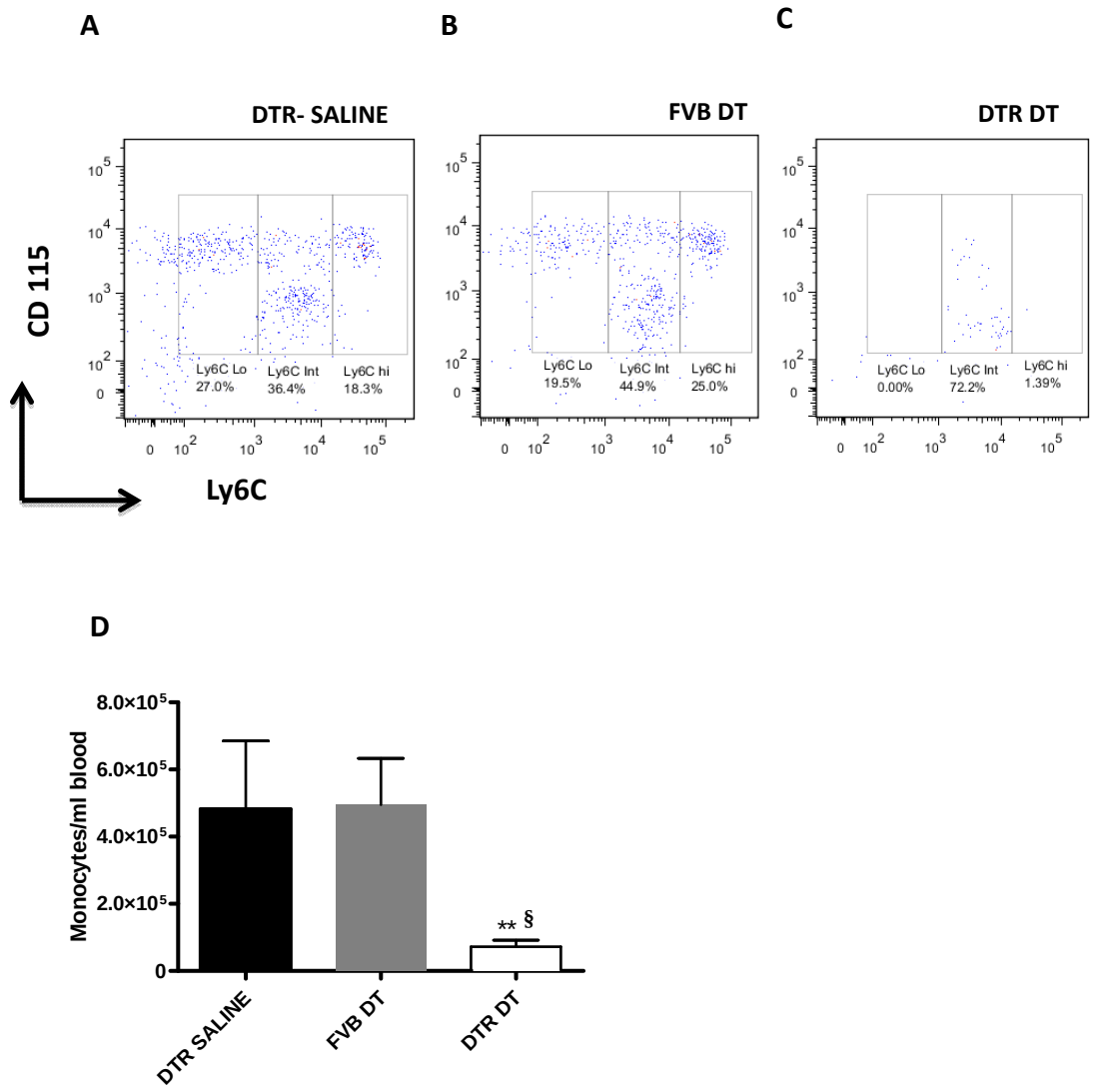

Figure 5.1 Effect of diptheria toxin on CD11b-DTR mice

A-F FACS analysis of whole mouse blood. Representative dot plots of (**A**) CD11b-DTR mice treated with saline and (**B**) FVB/nj strain controls treated with DT demonstrating distinct Ly6C^{hi}, Ly6C^{int} and Ly6C^{lo} monocyte populations. Monocytes are ablated by (**C**) DT treatment of CD11b-DTR mice. (**D**) Data are Mean ± SD analysed by 1-way ANOVA with Bonferroni corrections; n=4-6; stars represent significance compared to DTR saline controls; symbols represent significance compared to FVB DT controls. ** $p<0.01$; § $p<0.01$.

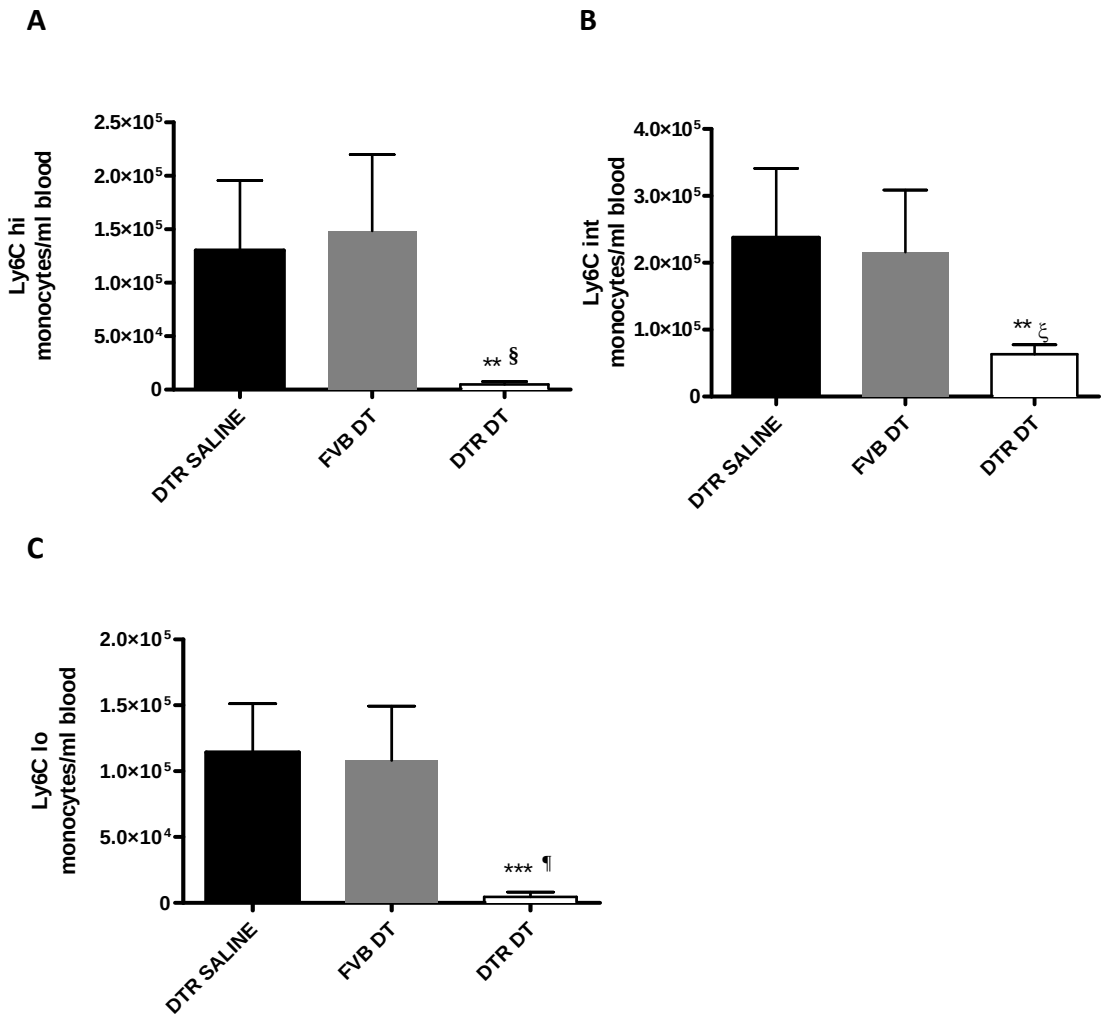

Figure 5.2 Effects of DT on mouse monocyte expression

A-C Ablation of monocyte subsets by DT. (**A**) Ly6C^{hi} (**B**) Ly6C^{int} and (**C**) Ly6C^{lo} monocyte subsets were depleted by DT treatment of CD11b-DTR mice compared to DTR mice treated with saline and FVB/nj strain controls treated with DT. Data are mean ± SD (n=4-6) analysed by 1-way ANOVA and Bonferroni post-tests. Stars represent significance compared to DTR saline controls; symbols represent significance compared to FVB DT controls. ** $p<0.01$; ***$p<0.005$; ξ $p<0.05$; § $p<0.01$; ¶ $p<0.005$.

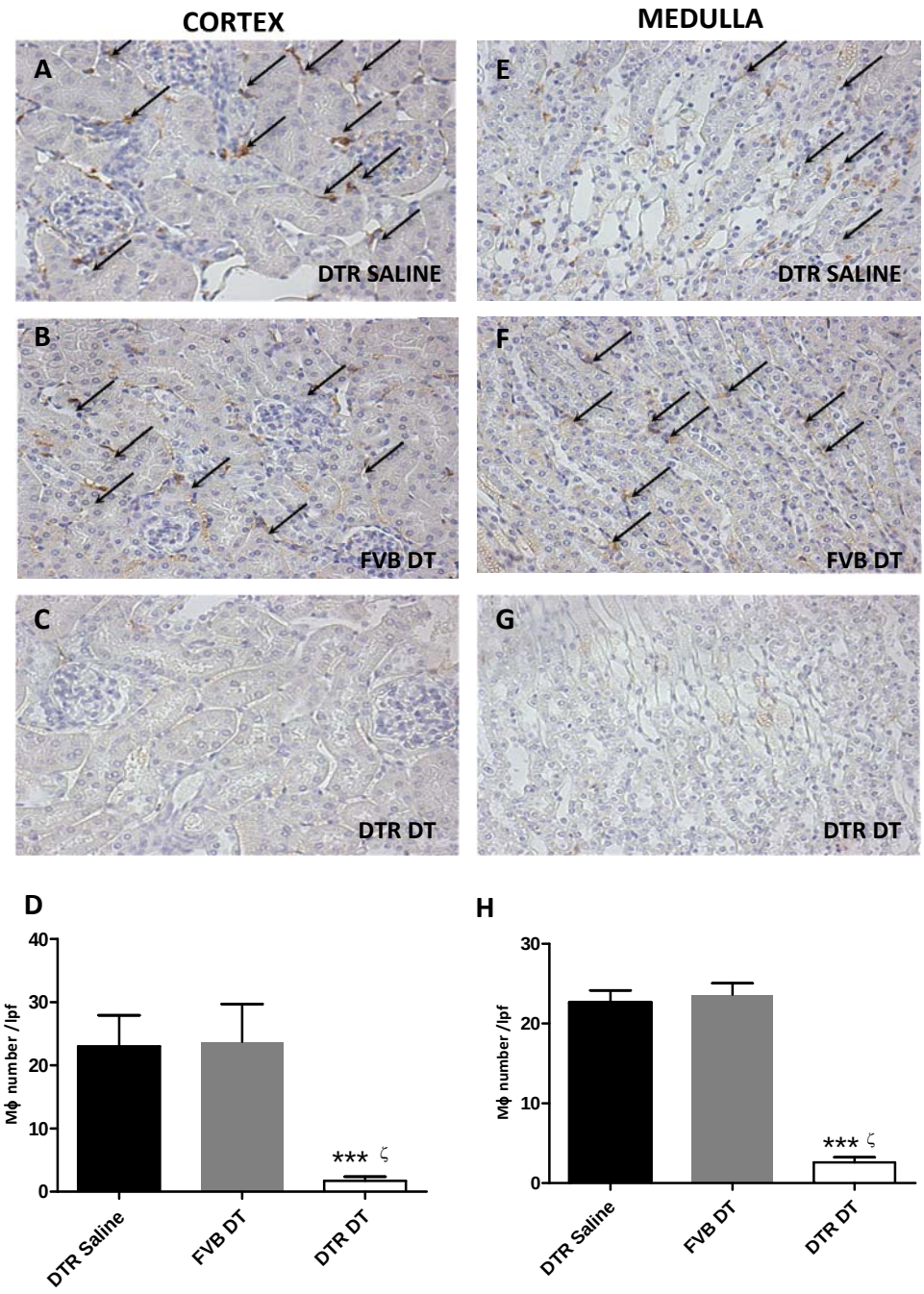

Figure 5.3 Effects of DT on mouse resident renal Mϕ expression

A-H Ablation of resident renal Mϕ by DT. F4/80 staining for murine Mϕ in the cortex and medulla of (**A&E**) DTR saline treated control (**B&F**) FVB/nj DT treated control and (**C&G**) DTR DT treated mice (**D&H**). Arrows represent individual Mϕ. Images are representative of 10 fields/slide. Data are mean ± SD analysed by 1-way ANOVA and Bonferroni post tests; n=4-6; Stars represent significance compared to DTR saline controls; symbols represent significance compared to FVB DT controls. ***p<0.005; ξ p<0.005.

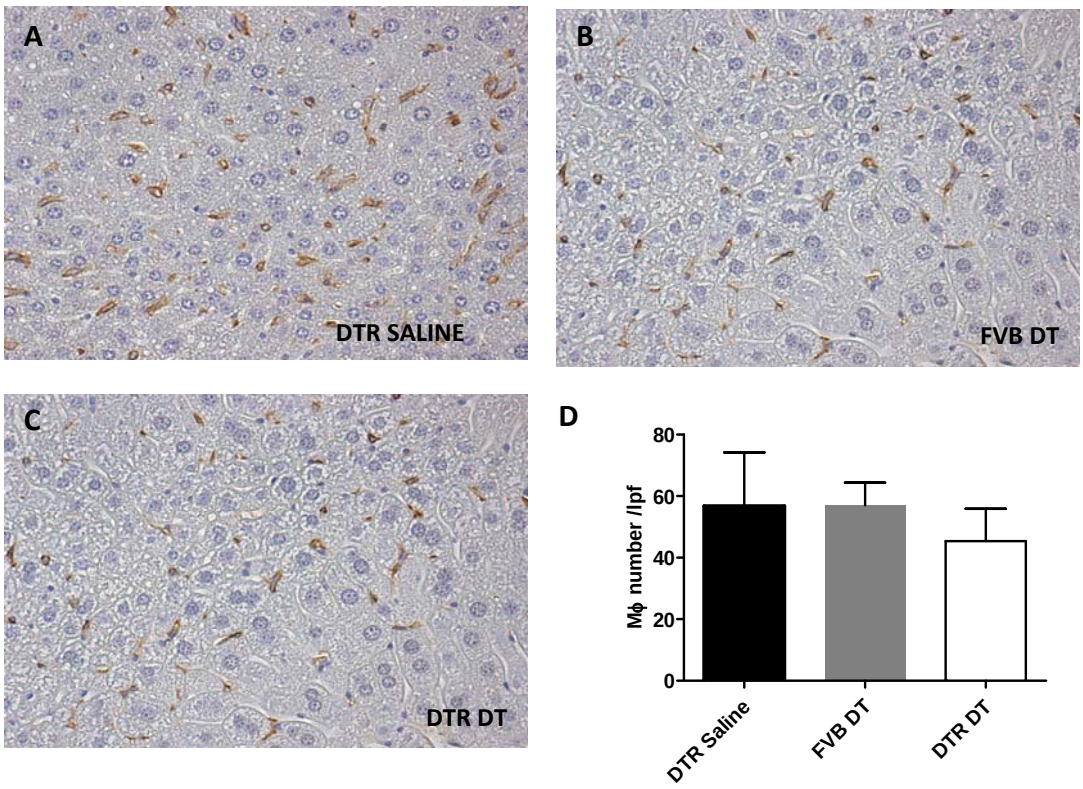

Figure 5.4 Effects of DT on murine resident hepatic Mϕ expression

A-D Ablation of resident renal Mϕ by DT. F4/80 staining for murine Mϕ in the cortex of (**A**) DTR saline treated control (**B**) FVB/nj DT treated control and (**C**) DTR DT treated mice. Images are representative of 10 fields per slide (**D**) Data are mean ± SD (n=4-6) analysed by 1-way ANOVA.

5.4 Effects of Mϕ depletion on physiological responses to ET-1

5.4.1 Monocyte/ Mϕ ablation exacerbates the pressor response to ET-1

In vivo, basal blood pressure was unaffected by DT treatment in DTR mice compared to controls (Fig 5.5 A). The pressor response to ET-1 in these animals was then assessed (see supplementary Fig 2.2 for BP trace analysis parameters). Administration of ET-1 did not produce a pressor response in control DTR saline treated and sham DT treated FVB/nj strain control animals (Fig 5.5 B). DT treated DTR mice were more sensitive to the pressor effect of ET-1 and at the lower doses (0.01 and 0.1 nmol/kg) as a pressor response was observed in these animals. At the highest dose (1nmol/kg) all mice responded to ET-1. In Mϕ deplete mice however a significantly greater pressor response compared to control and sham-operated was observed. To determine whether this was an effect specific to ET-1, animals were also exposed to Ang II at an eqimolar concentration (1nmol/kg). All animals responded equally to Ang II at this dose (Fig 5.5 C).

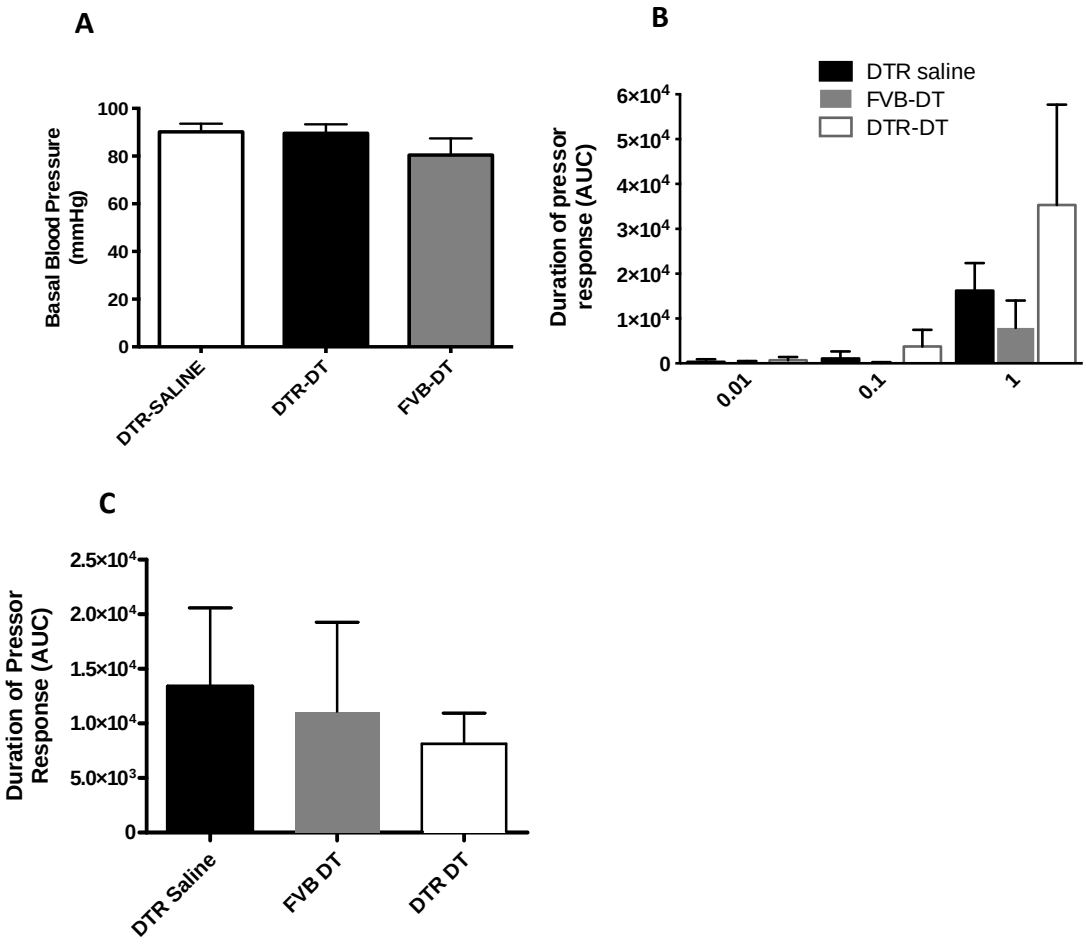

Figure 5.5 Effects of conditional Mϕ ablation on BP in response to ET-1

A-C Pressor response to ET-1 and Ang II. (**A**) Baseline BP of DTR saline treated control FVB/nj DT treated control and DTR DT treated mice. (**B**) Duration of the pressor response to ET-1 (0.01 0.1 and 1 nmol/kg) expressed as area under the curve (AUC). (**C**) Duration of pressor response to Ang II (1nmol/kg). Data are mean ± SD (n=4-7) analysed by 1-way ANOVA (**A&C**) and 2-way ANOVA with Bonferroni post-tests (**B**). Stars represent significance compared to DTR saline controls; symbols represent significance compared to FVB DT controls ****p<0.001; ξ p<0.005;

5.5 Summary

In the previous chapter we examined the effects of ET-1 on human Mϕ phenotype and function. In response to ET-1 Mϕ are not classically activated as hypothesised, but do migrate towards ET-1. When in contact with ET-1 Mϕ are more phagocytic. ET-1 is then cleared from the media via the ET_BR and proteolytic degradation.

This chapter investigated the impact of conditional Mϕ ablation on the pro-hypertensive actions of ET-1. *In vivo*, Mϕ ablation resulted in an exacerbation of the pressor response to ET-1. BP was significantly lower in mice possessing Mϕ. This effect was significant in terms of the duration and amplitude of the response, and in the peak change in BP in response to an ET-1 bolus. This effect was not observed with Ang II. These early studies indicate a previously undocumented role of macrophages in BP regulation.

In addition to the role and action of ET-1 in macrophages, we also aimed to investigate the effects of ET-1 in resident renal cells, specifically in human podocyte cells.

5.5.1 Mϕ regulation of the pressor effects of ET-1

There is a single example in the literature describing a protective phenotype of immune cells in relation to ET-1. Maurer *et al.* 2004 [357] found that mast cells were shown to limit ET-1 mediated lethality *in vivo* both by receptor-mediated uptake and through the action of proteolytic enzymes. Mast cells increase in number in many renal inflammatory diseases and may have a role in limiting renal injury [357]. Regulating the effects of ET-1 may form part of this mechanism. This protective role of mast cells with regards to ET-1 may be translatable to Mϕ. To address this hypothesis, we used a model of CD11b-DTR [302] mediated conditional Mϕ ablation. In this model we monitored the pressor response to ET-1, hypothesising that, in the absence of Mϕ ET-1 mediated pressor responses are dysregulated and exacerbated.

There are few examples in the literature whereby inflammatory cells may have a new physiological role in acting as mediators or regulators of vasoconstrictors. Machnik *et al.* (2009)[358] describes experiments whereby Mϕ regulate salt-dependent volume and blood pressure. The authors attribute this phenomena to a Tonicity-responsive enhancer binding protein (TonEBP)/VEGFC mechanism. In line with this work, they have now extended their work demonstrating that the mononuclear phagocyte system depletion induces salt-sensitive hypertension in rats [359]. Crowley *et al.* (2010) demonstrate chronic angiotensin II infusion in mice lacking ATII1 on bone marrow cells results in augmented hypertension [356]. These findings promote a new view on a protective role for macrophages in hypertension. An important feature in this scenario is also sodium homeostasis. Therefore, it is relevant to know whether the observed blood pressure effects after macrophage depletion in salt-sensitive models of hypertension are reproducible in models where macrophage action has been associated with deleterious effects.

In a letter to Hypertension Schmaderer and colleagues[360] joined this debate, demonstrating that Mϕ depletion by liposomal clodronate did not improve hypertension in SHR. The sparse data to this end are conflicting.

Our data demonstrate that conditional renal Mϕ and monocyte depletion prior to administration of ET-1 was achieved by administering diphtheria toxin to mice carrying the CD11b-DTR transgene, or controls on the same genetic background. *In vivo*, basal blood pressure was unaffected by DT treatment in DTR mice compared to controls. The pressor response to ET-1 in these animals was then assessed. Administration of low dose ET-1 did not produce a pressor response in control DTR saline treated and sham DT treated FVB/nj strain control animals. DT treated DTR mice were more sensitive to the pressor effect of ET-1 and. At the highest dose (1nmol/kg) all mice responded to ET-1. In Mϕ deplete mice however a significantly exaggerated pressor response compared to control and sham-operated was observed. To determine whether this was an effect specific to ET-1, animals were also exposed to Ang II at an equimolar concentration (1nmol/kg). All animals responded equally to Ang II at this dose. The results of these pilot studies showed promising translatable effects of Mϕ regulation of ET-1 in the context of its pro-hypertensive actions.

5.5.2 Future studies

These studies were designed to assess the ability of Mϕ to regulate BP responses to ET-1. Initial pilot studies were promising however would require further analysis. First, the method of drug delivery and BP measurement was via an invasive jugular route with carotid BP measurement. In this model, animals respond to a bolus of pressor. These conditions are an extreme and a more appropriate method of delivery would be via osmotic minipump. The use of osmotic minipumps has many advantages over other methods of delivery including i.p. and i.v. injection. Minipumps deliver drugs at a constant, controlled rate and reduce researcher intervention during the experimental period. Chronic infusion of ET-1 over a longer period of time, as opposed to an acute exaggerated pressor response would provide a more accurate picture of ET-1 regulation.

Observations from Schmaderer's group [360] demonstrate a lack of effect in a model of established hypertension. Our experiments show an effect to the

contrary and would require BP measurement by radiotelemetry allowing for accurate real-time BP measurement. It may be the case that Mϕ have a role to play in specifically limiting the early pro-hypertensive effects of ET-1 prior to established hypertension.

To ensure that the CD11b-DTR mice and control animals have similar baseline vascular responses to ET-1, wire myography estimation of ET-1 responses is required. Small resistance vessels are more sensitive to ET-1 than larger vessels; therefore murine femoral and/or mesenteric vessels may be an appropriate option to directly measure ET-1 effects on the vasculature.

An important aspect of these experiments would also be to ensure ET-1 levels are reduced in DT treated DTR mice. Urinary ET-1 excretion may be assessed if animals were to be housed in metabolic cages for timed urine collections. We were unable to quantify serum ET-1 in these animals, as ET-1 quantification by RIA requires a sample size of 0.5ml to detect pg/ml quantities. Dilution of murine serum to this level would not give ET-1 quantities in the working range. Method development for use of a novel ET-1 ELISA kit specifically designed for neonate samples is underway and would allow for murine serum ET-1 quantification (Enzo Life Sciences).

Lastly, future studies to investigate not only the role of macrophages, but also the role of the respective ET receptors in hypertension may be addressed. Strategies include the generation of mice with targeted deletions of the ET_AR and ET_BR in neutrophils and Mϕ through crossing a LysM-Cre line [361] with strains carrying the floxed ET_AR [362] and ET_BR [363] alleles. Primary culture of murine macrophages with these targeted deletions, and/or siRNA gene knockout are strategies that may be employed to assess the effects of ET receptors on macrophage function.

Chapter 6

Amelioration of cytotoxic and pro-inflammatory effects of ET-1 on human podocyte cells by ET_A receptor antagonism *in vitro*

6.1 Introduction

In this final chapter, the role of ET-1 in human podocytes is investigated. Podocytes have been shown to express both ET_A R[195] and ET_B R[270] on rodent podocytes. There is limited data lacking definitive expression of receptors for human podocytes [271; 272]. However, it is likely that human podocytes also possess both ET_AR and ET_BR [273]. ET-1 is also implicated as both a stimulus, and a product of stimulation of podocytes. As previously discussed, murine podocytes exposed to an albumin (or IgG) load leads to disruption of the actin cytoskeleton. This activates transcription of preproET-1 mRNA leading to ET-1 secretion [195]. Furthermore, shiga toxin treatment leads to ET-1 secretion. In turn, ET-1, acting in an autocrine manner via the ET_AR, causes disruption of the podocyte actin cytoskeleton [274].

ET-1 may also impact slit diaphragm proteins including nephrin, podocin, CD2-AP, synaptopodin etc. One of the key podocyte proteins at the slit diaphragm is nephrin and mutations of the nephrin gene lead to congenital nephrotic syndrome [188]. Nephrin is often used in experimental models as a marker of podocyte injury. *In vitro* studies conducted using glomerular endothelial cells as a source of ET-1 were cultured in pre-eclamptic sera. Treatment of murine podocytes with conditioned sera induced shedding of nephrin [272]. Furthermore, infusion of ET-1 into rats caused nephrin excretion into the urine [263]. In both instances these effects were inhibited by ET_A receptor antagonism.

Lastly, ET-1 is known to participate in renal inflammation [364]. Podocytes exposed to various mediators are able to produce pro-inflammatory cytokines. It is likely that podocytes may adopt a pro-inflammatory phenotype in response to an ET-1 stimulus.

6.1.1 Experimental hypothesis and aims

The experiments described in this chapter were designed to investigate the hypothesis that ET-1 is detrimental to podocyte health.

In response to an initial insult podocyte effacement or de-differentiation, ET-1 production and pro-inflammatory cytokine production occurs. This increased ET-1 production, likely mediated by stimulation of the ET_AR, may act in an autocrine and paracrine manner to perpetuate podocyte ET-1 production, de-differentiation and inflammatory cytokine production and eventually leading to a breakdown of the glomerular filtration barrier.

Specifically, in human podocytes, ET-1 will- 1) stimulate production of ET-1, 2) induce de-differentiation and re-organise cytoskeletal structure and 3) promote a pro-inflammatory phenotype. The detrimental effects of ET-1 on podocytes will be ameliorated by selective ET_AR, but not selective ET_BR antagonism.

Specifically the chapter aims to:

- Demonstrate ET_AR and ET_BR expression on the human podocyte cell line
- Establish whether ET-1 causes podocyte ET-1 production, effacement via alterations in filamentous actin and slit diaphragm (SD) protein nephrin loss.
- Determine whether ET-1 administration would induce podocyte ET-1, IL-6 and IL-8 and up-regulation.
- Where deleterious ET-1 effects are observed, determine whether the effects are ET_AR and/or ET_BR mediated using selective antagonists.

6.2 Experimental Protocol

I. Podocytes were cultured in supplemented RPMI in 75cm^2 flasks (33°C, 5% CO_2) to propagate. At 80-90% confluence cells were trypsinised and either reseeded into 75cm^2 flasks at a ratio of 1:5 and maintained at 33°C, or reseeded onto rat-tail collagen type I-coated TC plates and maintained in non-permissive conditions at 37°C for 14 days before exposure to ET-1.

   NB: cells were matured in 6 well plates for WB and RT-PCR studies, 12 well for IF and 24 well plates for RIA/ELISA experiments, respectively

II. Presence of podocyte specific markers nephrin, podocin, synaptopodin and non-specific F-Actin were confirmed by WB, IF and RT-PCR.

III. ET_A and ET_B receptor expression was subsequently confirmed as above.

IV. Podocytes were stimulated with ET-1 (5-100pg/ml) over a 2-48 hour timecourse to determine (maximal) ET-1 production by RIA.

V. Subsequent ET-1 stimulation experiments were performed at a 24h timepoint for detection of
   - Pro-inflammatory cytokines by ELISA.
   - Cytoskeletal reorganisation and de-differentiation by IF, PCR and WB.

VI. Where deleterious ET-1 effects were observed, podocytes were incubated with selective ET_AR (BQ123, 1µM) and ET_BR (BQ788, 0.1µM) antagonists 1h prior to stimulation with ET-1 (5, 50, 100 pg/ml).

NB. The concentration of ET-1 and ETR antagonists were chosen based on pharmacological profile data and previous studies. This is detailed in the methods section 2.1.6.

6.3 Podocytes propagate under growth permissive conditions and differentiate under non-permissive conditions

All experiments described in this chapter utilise a conditionally immortalized human podocyte cell line initially described in detail by Saleem *et al.* (2002)[287] to study the effects of exogenous ET-1 administration on podocyte cell structure and function. Podocyte cells were cultured under growth-permissive conditions (33°C) where they propagated as a typical cobblestone monolayer (undifferentiated), and grew to 70-80% confluence after 3-4 days (Fig 6.1 A). Thermoswitching to 37°C resulted in arrest of proliferation, followed by differentiation over 14d. The characteristics of the phenotype were identified morphologically under LM (Fig 6.1 B).

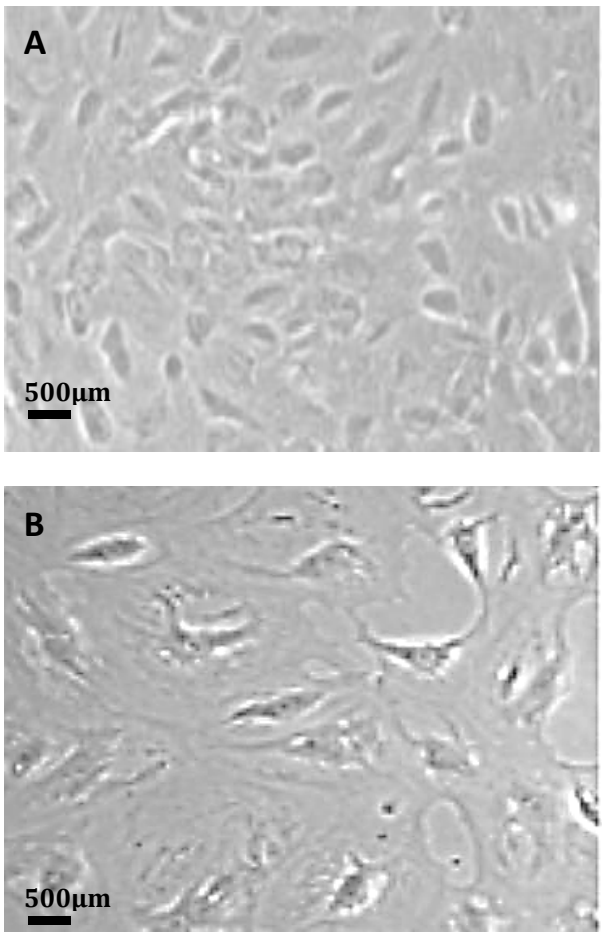

Figure 6.1 Human podocyte cell morphological change

A&B Differing podocyte cell phenotypes. Photomicrographs (400x) of (A) Undifferentiated and (B) Differentiated cells under LM. Differentiated cells were identified morphologically displaying enlarged, irregular cell bodies with short rounded and/or long spindle-like projections. Scale bar represents 20µm. Arrow indicates short rounded process extending from cell body.

6.4 Podocyte specific structural and functional proteins are expressed by the immortalised human podocyte cell line.

Replication of the results seen by Saleem and colleagues (2002)[287] demonstrating the presence of podocyte specific structural and functional proteins in the immortalised cell line was an essential validation step for these experiments.

6.4.1 Podocytes express functional proteins nephrin and podocin

Nephrin is one of the more recently described podocyte specific transmembrane proteins located at the slit diaphragm [188]. Nephrin, a product of the *NPHS1* gene, undergoes homophilic interaction on neighbouring podocyte foot processes and binds to Podocin [119; 120]. Podocin is the protein product of the *NPHS2* gene, first discovered as the gene aberration responsible for familial FSGS [123]. The immortalised human podocytes express nephrin and podocin protein and mRNA (Fig 6.2 A-H). IF demonstrates positive staining for nephrin (Fig 6.2 A), and podocin (Fig 6.2 B), with no primary antibody controls demonstrating negative staining with weak auto-fluorescence (Fig 6.2 C&D respectively). Nephrin and podocin were also detected by Western blot as 195kDa and 42 kDa proteins respectively (Fig 6.2 E&F). Lastly, using primers for the *NPHS1* and *NPHS2* genes, nephrin and podocin mRNA was detected by RT-PCR (Fig 3.2 G&H).

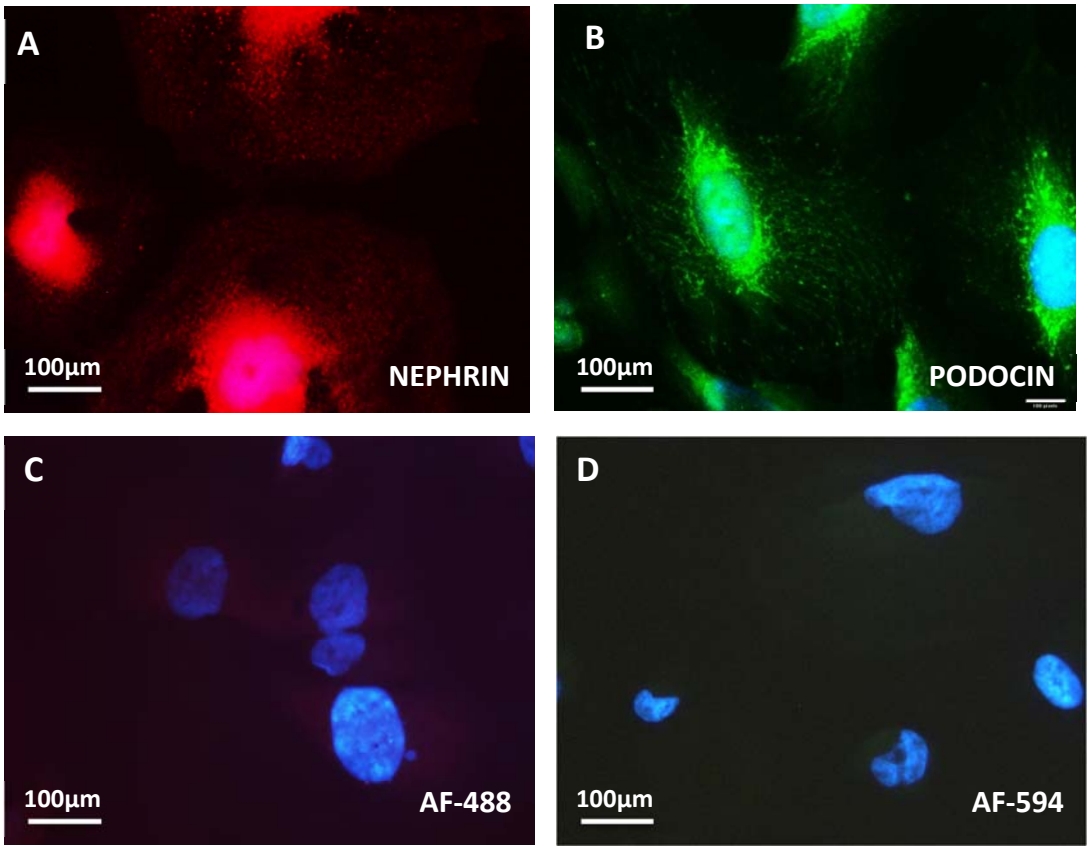

Figure 6.2 Human podocyte SD protein expression

A-F Photomicrographs 600x of (**A**) IF staining of Nephrin (red) and (**B**) Podocin (green) both with nuclear stain DAPI (blue). Secondary antibody alone controls for (**C**) anti mouse aleaxa-fluor-488 (AF-488) and (**D**) anti-rabbit alexa-fluor-594 (AF-594) demonstrate no staining with a weak auto-fluorescence detectable. All images are representative of 3 replicates.

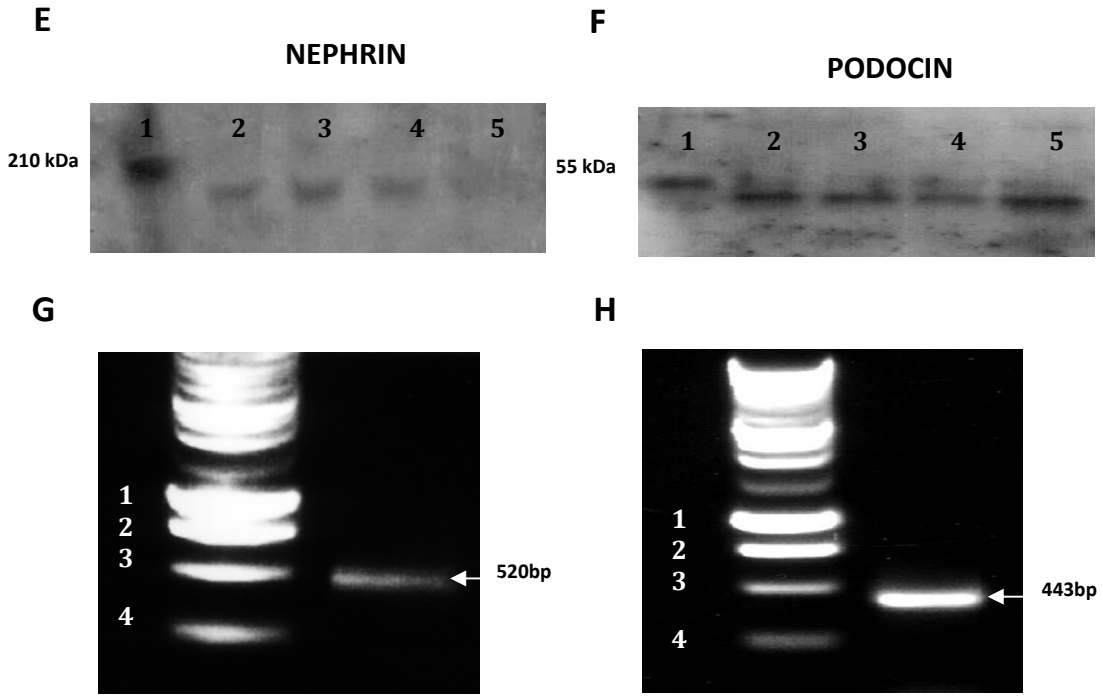

Figure 6.2 Cont. Human podocyte SD protein expression

E-H WB analysis of (**E**) Nephrin and (**F**) Podocin (lane 1: ladder, lanes 2-5: 1:100, 1:200, 1:300, 1:400 antibody dilution respectively. RT-PCR (**G**) of *NPHS1* gene encoding nephrin (520bp) and (**H**) *NPHS2* gene encoding podocin (443bp). Lanes represent 1) 1kb; 2) 750bp; 3) 500bp; 4) 250bp. All blots and gels are representative of 3 replicates

6.4.2 Podocytes express structural proteins synaptopodin and filamentous actin.

One of the most sensitive markers for differentiated podocytes is synaptopodin. This has been found to be expressed in mature podocyte foot processes and to co-localize with the actin cytoskeleton [115]. Podocytes demonstrated strong cytoplasmic expression of synaptopodin, extending from the cell body into large primary processes, beyond the large processes, expression is filamentous (Fig 6.3 A) with a comparable staining pattern to F-actin (Fig 6.3 B). An α-goat alexa-fluor-488 secondary antibody alone control was also employed to demonstrate negative staining, with vague auto-fluorescence detectable (Fig. 6.3 C). The antibody used to detect synaptopodin by IF was only able to detect the epitope on non-denatured protein, therefore synaptopodin was not detectable by WB. Synaptopodin mRNA was detectable by RT-PCR, using primers for the *SYNPO* gene (Fig 6.3 D).

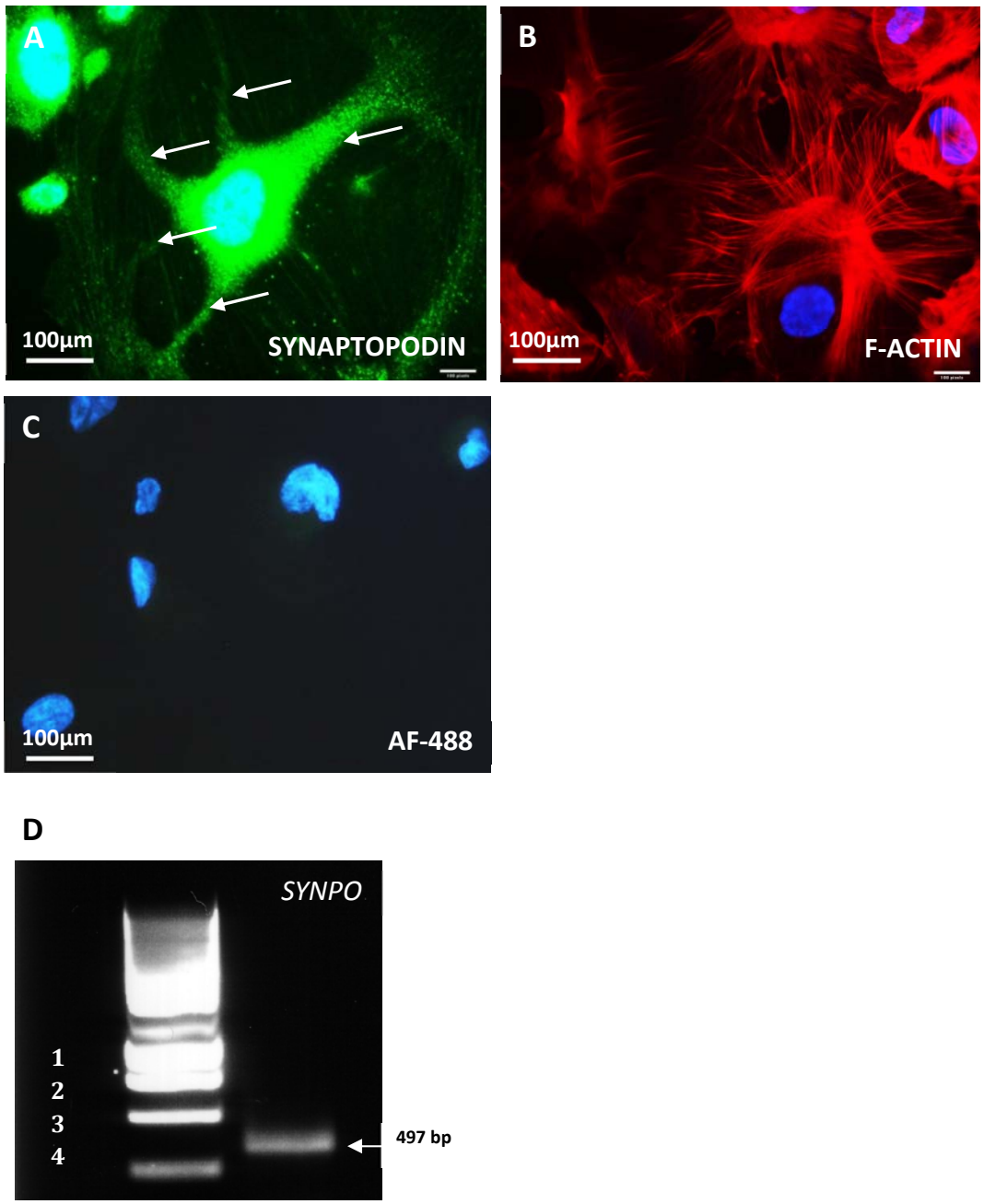

Figure 6.3 Human podocyte structural protein expression

A-D Photomicrograph 600x of (A) IF staining of synaptopodin (green) and (B) filamentous actin (red) with nuclear stain DAPI (blue). Arrows indicate sypnaptopodin expression along the large primary processes. (C) Secondary antibody alone demonstrating negative staining (D) RT-PCR products of *SYNPO* gene encoding synaptopodin (497bp). Lanes represent 1) 1kb; 2) 750bp; 3) 500bp; 4) 250bp. All images are representative of 3 replicates

6.5 Podocytes express ET_A and ET_B receptors

Previously reported data regarding ET receptor expression by podocytes is somewhat sparse and inconclusive. Rebibou and colleagues[273] demonstrate the presence of ET receptors in human podocytes, however, these studies do not discriminate which receptor type is expressed. ET_BR-like immunoreactivity has been demonstrated in podocytes from rat kidney sections [270]. Prior to stimulation of podocytes with ET-1, it was essential to determine whether the cells expressed ET_AR and ET_BR. Receptor expression and localisation was therefore investigated *in vitro*. Positive staining of both receptor subtypes was observed by two stage IF (Fig 6.4 A&B). ET_AR and ET_BR protein was also detected by WB (Fig 6.4 C&D). Furthermore, RT-PCR revealed mRNA expression of both receptor subtypes in the podocyte cell line (Fig 6.4 E&F).

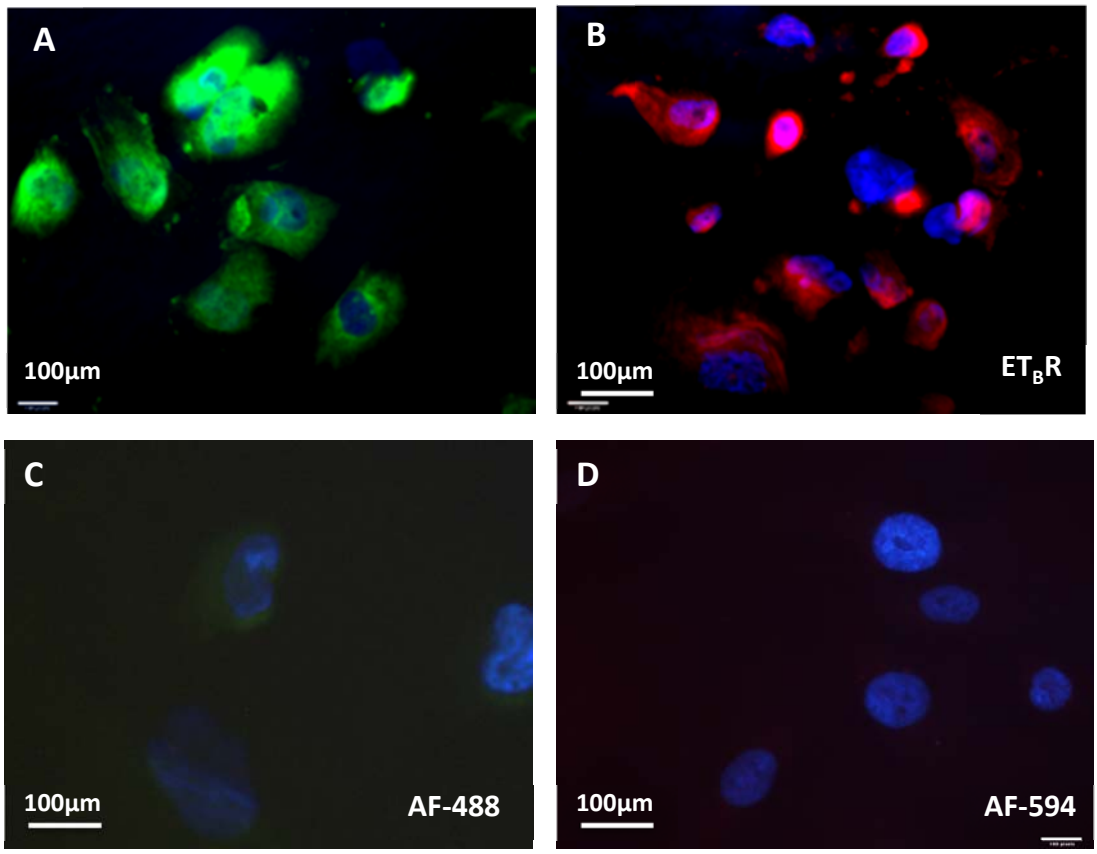

Figure 6.4 Human podocyte ET_A and ET_B receptor expression

A-E Photomicrographs (400x) of (**A**) IF staining of ET_AR (green) DAPI (blue) (**B**) IF staining of ET_BR (red) DAPI (blue). Secondary antibody alone controls for (**C**) anti-mouse aleaxa-fluor-488 (AF-488) and (**D**) anti-mouse alexa-fluor-594 (AF-594) demonstrate no staining with a weak auto-fluorescence detectable. Both receptors are expressed in all experiments. Images are representative of 3 replicates.

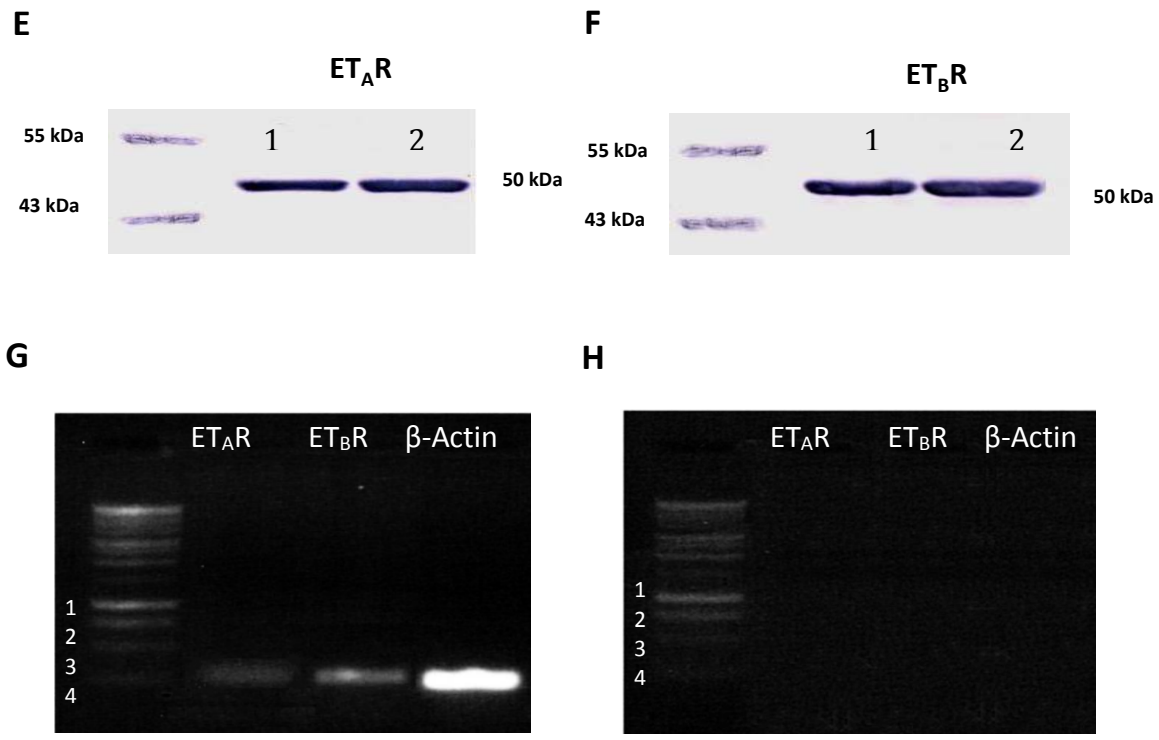

Figure 6.4 Cont. Human podocyte ET_A and ET_B receptor expression

E-H (**E**) Western blot on whole cell lysates (x2 replicates) for ET_AR (50kDa) and (**F**) ET_BR (50kDa). (**G**) RT-PCR and (**H**) No RT control using primers for human ET_AR, ET_BR and 'housekeeping' gene β-actin. Markers represent 1) 1kb; 2) 750bp; 3) 500bp; 4) 250bp. Both receptors are expressed in all experiments. All gels and blots are representative of 3 experiments.

6.6 Exogenous ET-1 induces podocyte ET-1 production

In response to various initial insults, podocytes have been shown to produce ET-1 [195]. ET-1 production occurs in an autocrine and paracrine manner to elicit cellular responses via stimulation of ET_AR and ET_BR [216]. Thus, in this assay podocytes were exposed to exogenous ET-1 (5-100 pg/ml) to determine whether an ET-1 insult would elicit ET-1 protein production. This was measured by RIA over a period of 48h. The time course of ET-1 protein synthesis by podocytes was assessed by RIA using ^{125}I radiolabelling. A detailed description of ET-1 stimulation and quantification can be found in Chapter 2 (see section 2.1.2 & 2.1.4 respectively).

6.6.1 Podocytes produce ET-1 over time, preceded by cellular ET-1 uptake

Over a period of 48h, administration of exogenous ET-1 to cultured podocyte cells induces net secretion of ET-1 (Fig 6.5). In this assay the stimulant is the same as substrate. In order to correct for this the concentration of ET-1 added to the media was deducted from the measured concentration to give a net ET-1 concentration. Furthermore, to correct for any differences in cell number/well, total cellular protein was extracted and quantified. Net ET-1 values were then normalised for protein content/well to give a final net ET-1 / protein (pg/mg) value. After 2h incubation, cells stimulated with all concentrations of ET-1 are net negative ET-1/protein. This suggests cellular uptake of ET-1. Un-stimulated cells showed no ET-1 production at this time. After 6 hours, a similar trend can be seen in all concentrations; however the net negative ET-1 values decrease across all concentrations. This suggests that ET-1 is being produced by podocyte cells, however as the values do not exceed the initial concentration added this cannot be confirmed as true production. This apparent ET-1 production continues to occur up to 12 hours. Cells stimulated with 10 and 20pg/ml ET-1 after 12 hours show net positive ET-1/protein levels, demonstrating that ET-1 levels exceed that of the concentration initially added, establishing definitive ET-1 production/release. After 24 hours in culture, with the exception of 100pg/ml, cells stimulated with all concentrations of ET-1 appear to be

producing ET-1. Furthermore, unstimulated cells demonstrate ET-1 production at 24 hours (40.70 ± 3.292 pg/mg). At 48h all cells produce ET-1, with peak ET-1 production occurring when stimulated with 10pg/ml. This increase in ET-1 production over 48h is observed across all concentrations, and is statistically significant irrespective of concentration of ET-1 ($p=<0.001$) following a 2-way ANOVA.

6.6.2 ET-1 induces ET-1 production in a dose dependant manner

In addition to the increase in ET-1 production across all concentrations over time, there is a significant main effect of ET-1 stimulus concentration ($p<0.001$). At 2h there is a linear dose response to ET-1 stimulation, which corresponds to ET-1 uptake. This effect is also seen at 6h, but the effect is decreasing. By 12h the trend alters and by 24h an inverted U dose response becomes apparent, however, this does not become statistically significant until 48h with peak ET-1 production at 10pg/ml ET-1 stimulation. Post-hoc Bonferroni comparisons reveal significantly higher ET-1 concentrations at 5, 10 and 20pg/ml ET-1 stimulation compared to control. When ET-1 stimulus doses exceed 20pg/ml, results are attenuated to baseline and there is no significant difference in ET-1 production when compared to control.

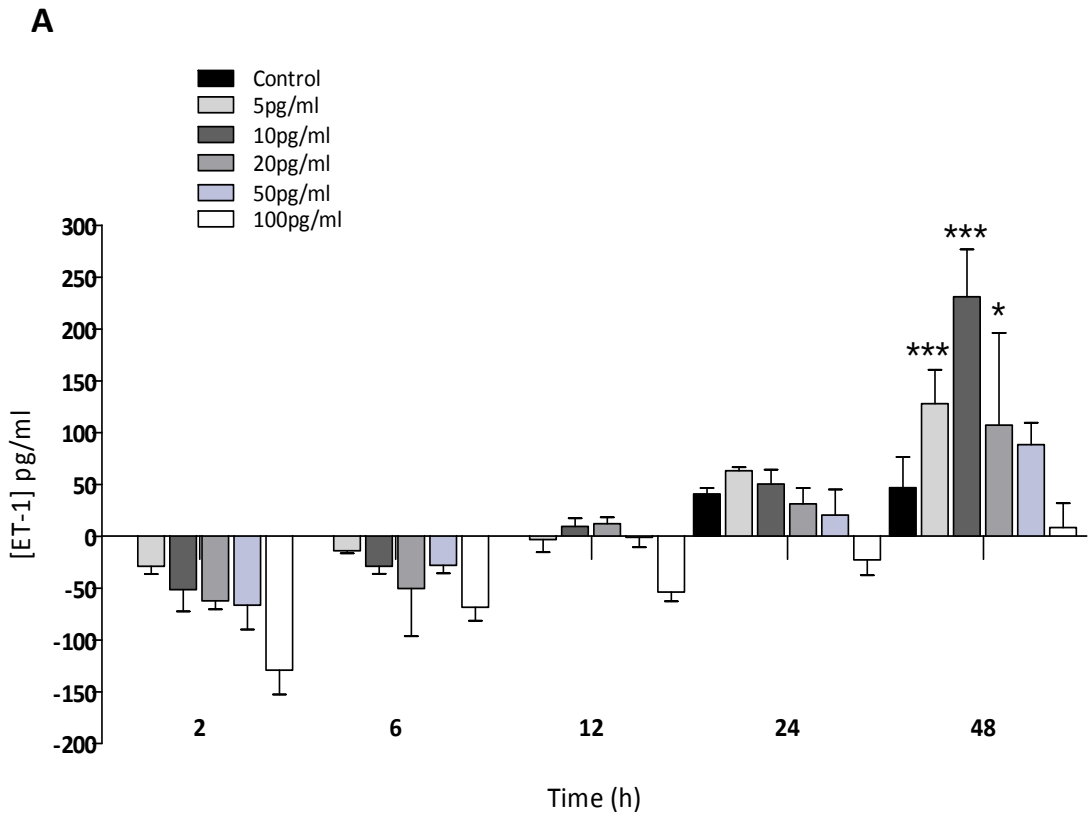

Figure 6.5 Influence of ET-1 stimulation on ET-1 production over 48h

A ET-1 content of podocyte supernatant as assessed by standard RIA. (A) ET-1 was detected at all concentrations of ET-1 stimulation. Cells were incubated in the absence, or presence of ET-1 stimulation at various concentrations (5, 10, ,20, 50, 100 pg/ml). There is a time and concentration dependent increase in ET-1 production, with peak ET-1 production occurring at 10 pg/ml after 48h stimulation ($p<0.001$ to control). Data are mean ± S.D. ET-1 values are adjusted for protein content. Data analysed by 2-way ANOVA with Bonferroni corrections (n=3). Symbols displayed above bars represent significance compared to 0 pg/ml control * $p<0.05$, ** $p<0.01$, *** $p<0.005$, **** $p<0.001$

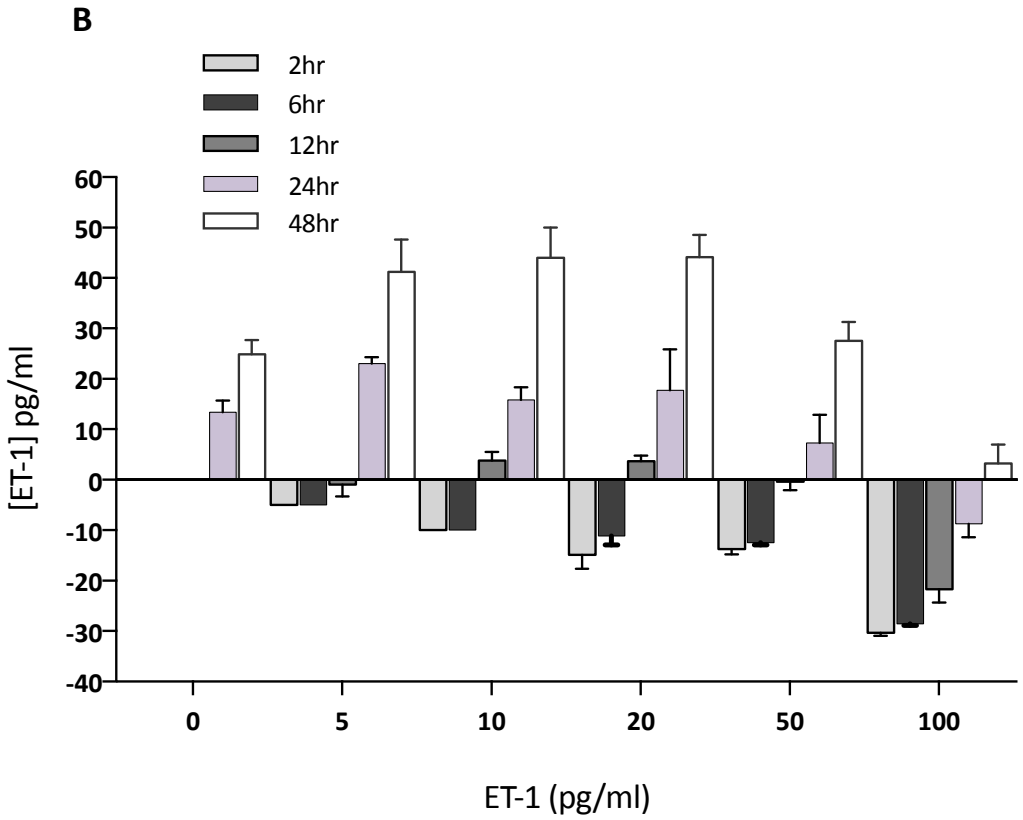

Figure 6.5 Influence of ET-1 stimulation on ET-1 production over 48h

B Data are re-presented to demonstrate the effect of time-course on ET-1 production in podocytes. Data are mean ± S.D. ET-1 values are adjusted for protein content.

6.7 Exogenous ET-1 induces podocyte cytokine production

In response to various initial insults, podocytes have demonstrated production of pro-inflammatory cytokines [365; 366]. In this assay, IL-6 and IL-8 protein was measured in response to stimulation of human podocytes with increasing concentrations (0-100 pg/ml) of exogenous ET-1 compared to media alone over 48h. The effect of ET-1 treatment of mature cells for 48 h was tested because cytokine expression was expected to be rapid and maximal within this time period. Furthermore, the short half-life of secreted cytokines made it important to test at early time periods. In these assays the 24h time-point was determined based on both the results of the ET-1 production time-course assay, and observations of peak cytokine production in inflammatory cells *in vitro.*

6.7.1 ET-1 induces podocyte IL-6 and IL-8 production

At 24h in standard culture conditions podocytes synthesize IL-6 (3633 ± 310.9 pg/ml). Administration of exogenous ET-1 to cultured podocyte cells upregulates production of IL-6 in a dose dependant manner and becomes statistically significant at 100 pg/ml (Fig 6.6 A). Podocyte IL-8 production (7378 ± 886.4 pg/ml) also occurs at baseline. ET-1 dosing results in a similar trend towards a dose dependant increase in IL-6, reaching significance at 100pg/ml (Fig 6.6 B).

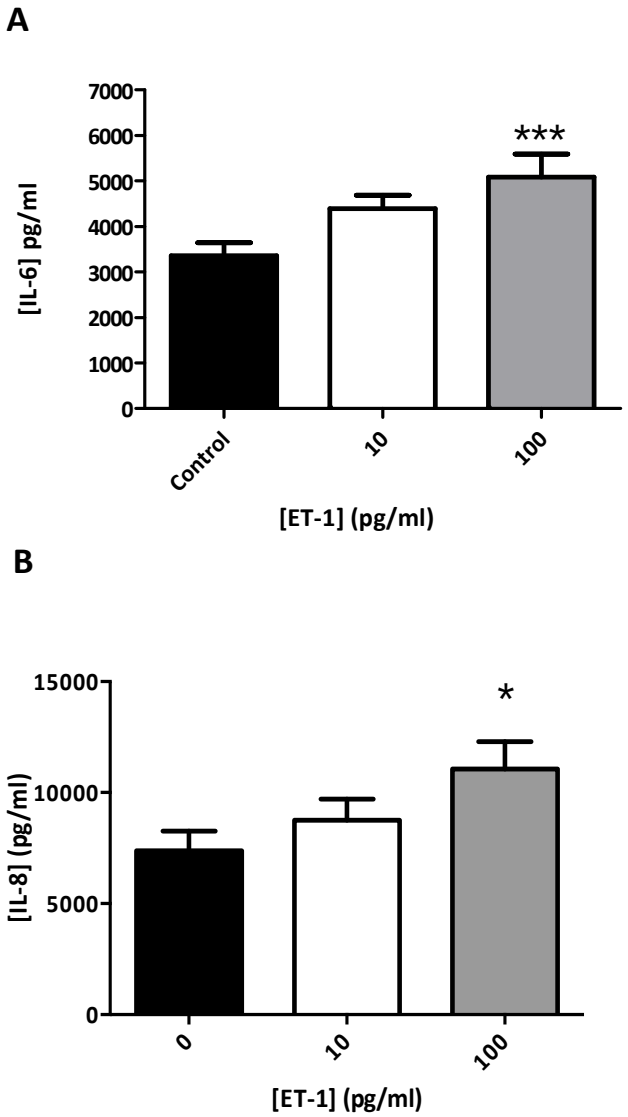

Figure 6.6 Effect of ET-1 on podocyte cytokine production

A&B Cytokine content in podocyte supernatant assessed by ELISA (A) Podocytes up-regulate IL-6 production in response to ET-1 stimulation (B) Podocyte IL-8 production also increases in response to ET-1 stimulation. Data are mean ± SD (n=13-15) analysed by 1-way ANOVA and Dunnetts comparisons Symbols displayed above bars represent significance compared to control * $p<0.05$, *** $p<0.005$.

6.8 ET-1 induces podocyte de-differentiation

In response to soluble factors such as angiotensin II [205] and albumin [195] the cytoskeleton of podocytes undergo rearrangement. Further studies by Morigi and colleagues in 2006 demonstrated a re-organisation of F-actin, with corresponding intercellular spaces in mouse podocytes treated with Shigatoxin, a promoter of ET-1 production [274]. In this assay, filamentous actin organisation in podocytes exposed to ET-1 is assessed by direct IF phalloidin staining. To detect disruptions in tight junctions, dual staining with Zonula Occludens-1 (ZO-1) is performed. In addition to the cytoskeleton, ET-1 may also cause alterations in mature podocyte slit diaphragm proteins. Expression and localisation of nephrin and synaptopodin from podocytes treated with ET-1 (10-1000 pg/ml) for 7 days was assessed by IF and PCR. Further WB analysis of nephrin expression was performed.

6.8.1 ZO-1 staining was not sufficient to show abberations in tight junctions

Prior to stimulation of cells with ET-1, podocytes were dual stained with ZO-1 and phalloidin. Following permeablisation, the cells were exposed to mouse anti- ZO-1 primary antibody (Invitrogen) for 24h at 4°C. Rhodamine conjugated phalloidin (Biotium) was then added for for 30 min. Cells were washed, then incubated with goat anti-mouse Alexa 488 secondary antibody (Invitrogen). As expected with most ZO-1 staining, some cytoplasmic and nuclear staining could be seen. However, tight junctions could not be appreciated as no cell periphery staining was observed (Fig 6.7 A). Dual antibody staining can occasionally cause interference with one or both of the antibodies used. For this reason, the cells were then stained solely with ZO-1. In the absence of rhodamine phalloidin staining, the cells demonstrated a similar cytoplasmic and nuclear staining pattern, but no cell periphery staining (Fig 6.7 C). Appropriate IgG1 control staining was also negative (Fig 6.7 E). For this reason we were unable to quantify cell-cell contact disruptions in response to ET-1. Alterations in cell structure, demonstrated by F-actin staining, are described qualitatively.

6.8.2 In response to ET-1 stimulation, podocytes undergo cytoskeletal re-arrangements

Unstimulated podocytes display linear F-actin fibres arranged in parallel (Fig 6.7 B). ET-1 stimulation for 2h, alters actin fibre arrangement to peripheral distribution and lack of trans-cytoplasmic staining (Fig 6.7D). Higher doses of ET-1 (100pg/ml) can cause complete loss of linear distribution to a disorganized abberant fibre distribution (Fig 6.7 F).

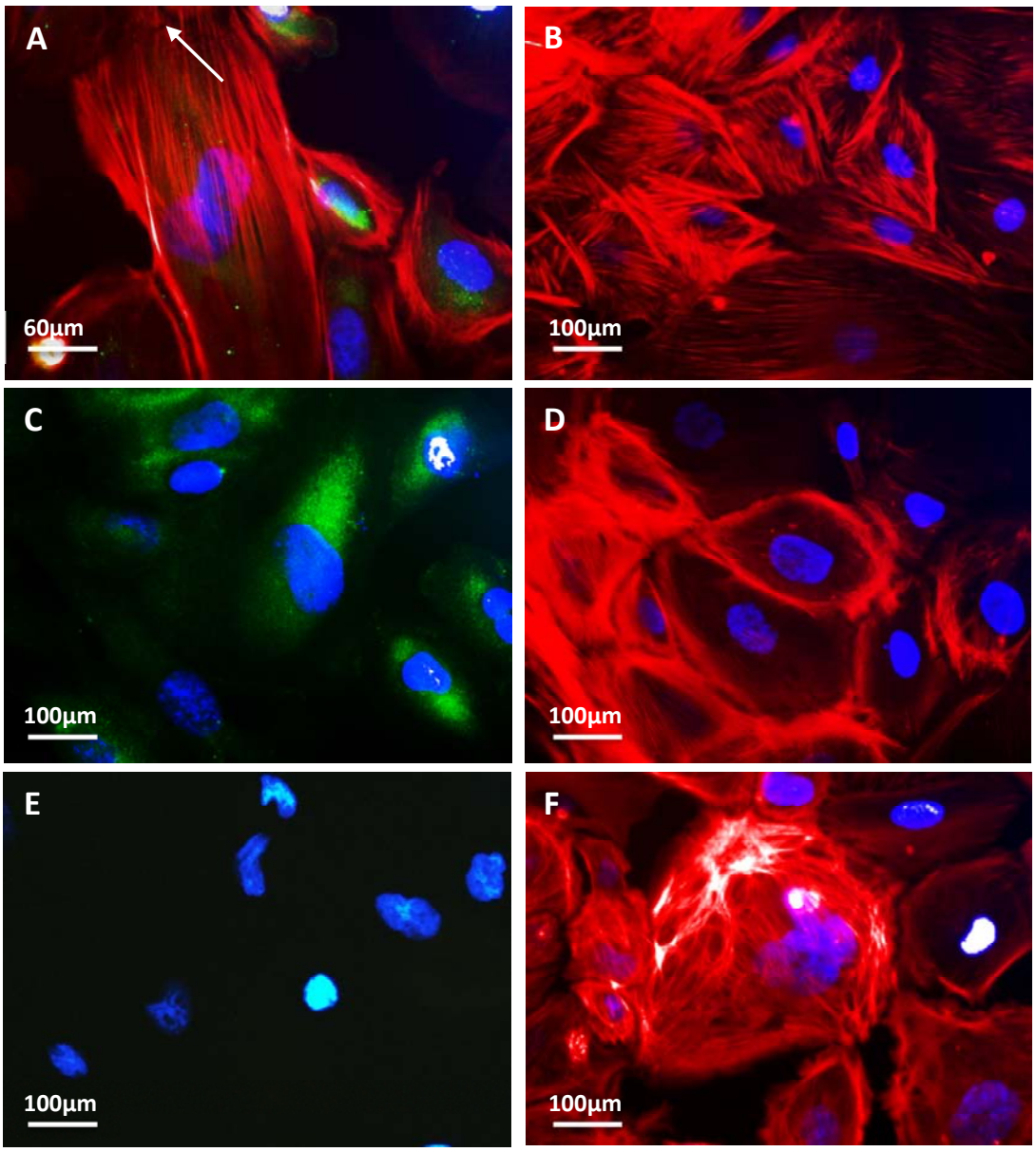

Figure 6.7 Effect of ET-1 on podocyte F-actin

A-E Phalloidin and ZO-1 tight junction protein IF staining of ET-1 treated podocytes. (A) Dual filamentous actin (red) and ZO-1 (green) staining. Arrow indicates lack of ZO-1 staining at the cell periphery. (C) Single ZO-1 (green) staining demonstrating no tight junction staining and (E) IgG1 negative control. (B) Untreated podocyte F-actin filaments are linearly arranged. (D) 10pg/ml ET-1 results in filament disorganization and redistribution to the cell periphery. (F) 100pg/ml ET-1 leads to complete fibre disorganization. Nuclear stain DAPI (blue) in all images. Representative images of n=6.

6.8.3 ET-1 reduces synaptopodin expression

ET-1 induces acute structural changes in the cytoskeleton, with rearrangements apparent after 2h incubation. No changes in synaptopodin localisation were appreciated under IF in ET-1 treated cells compared to untreated controls (Fig. 6.8A A-D). WB was performed to quantify changes at the protein level. As previously described, synaptopodin cannot be shown by WB. To quantify gene expression of synaptopodin following ET-1 treatment, RT-PCR was performed. Synaptopodin mRNA expression decreased following ET-1 treatment in a dose dependant manner (Fig 6.8 E). Band analysis indicates a significant main effect of ET-1 treatment on synaptopodin mRNA expression ($p=0.0003$) following a 1-way ANOVA. Dunetts post-test revealed a significant reduction in synaptopodin following treatment with ET-1 at 100 pg/ml ($q=3.312$, $p<0.05$), 1000 pg/ml ($q=4.827$, $p<0.01$) and Ang II ($q= 6.058$, $p<0.005$) $n=3$, relative to untreated controls (Fig 3.8A F).

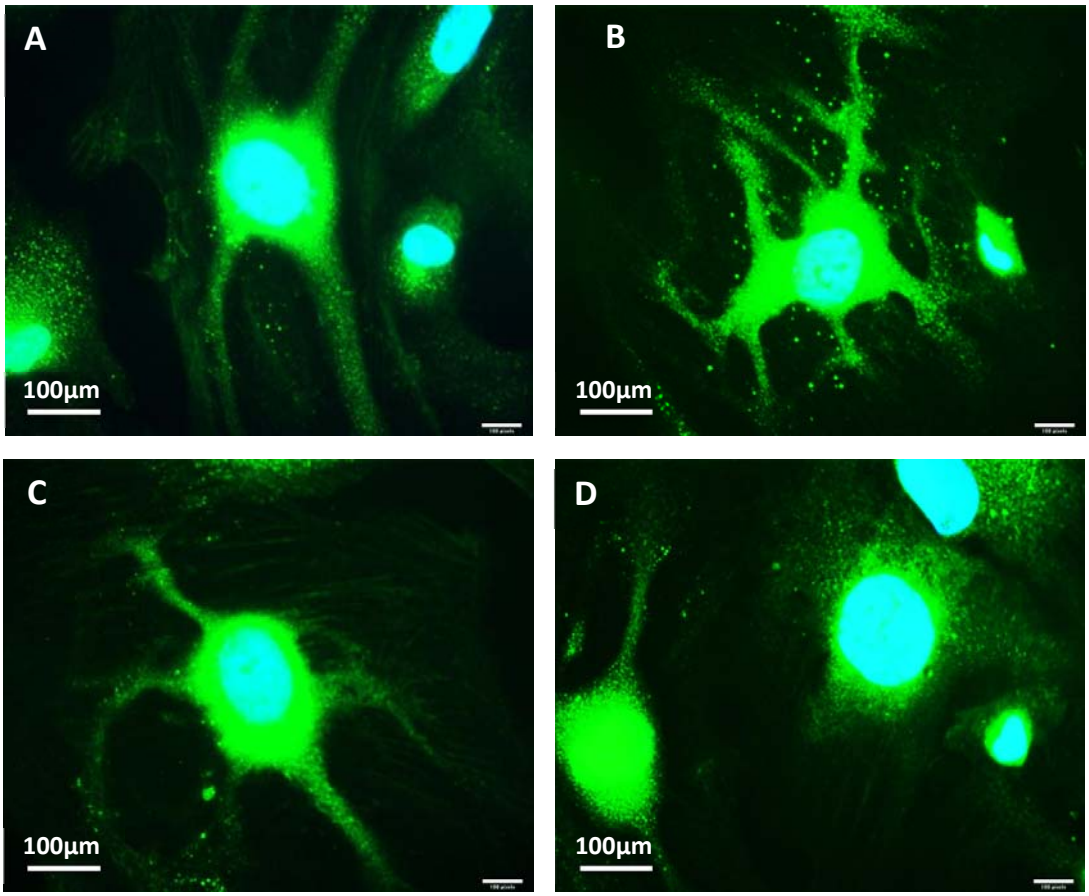

Figure 6.8A ET-1 effects on synaptopodin localisation and expression

A-D Photomicrographs (600x) of synaptopodin localization and expression by IF. Staining demonstrates unstimulated cells express nephrin (A) Expression is unaltered in ET-1 treated cells at (B) 10pg/ml, (C) 100pg/ml and (D) 1000pg/ml. representative images of n=3.

E

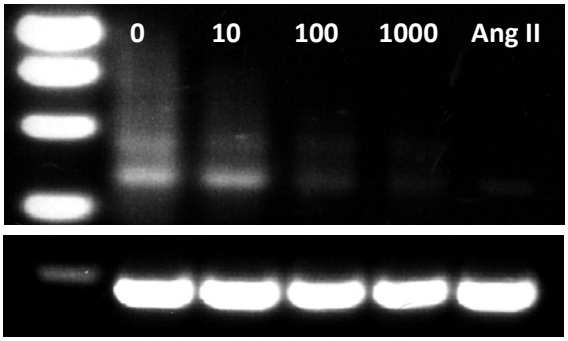

F

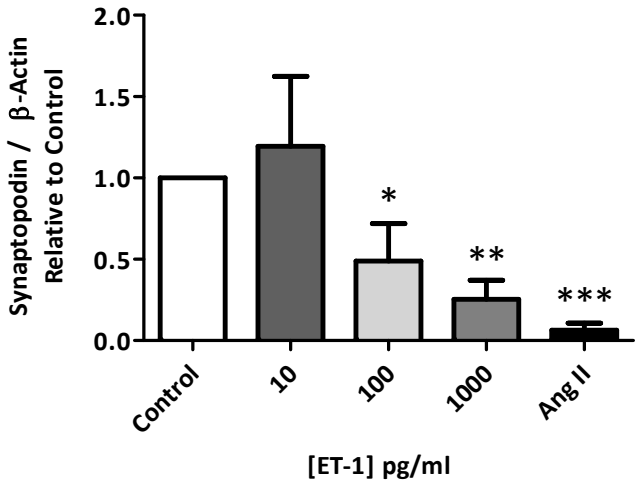

Figure 6.8A cont. ET-1 effects on synaptopodin localisation and expression

E&F Synaptopodin mRNA expression. RT-PCR of (E) *SYNPO* gene encoding synaptopodin (F) mean band intensity relative to β-actin, expressed as a ratio of the untreated control. Reduction in synaptopodin expression increases with with increasing ET-1 concentration. Data are mean ± SD, analysed by 1-way ANOVA followed by Dunnetts post hoc test (n=3). Symbols displayed above bars represent significance compared to control * $p<0.05$, ** $p<0.01$, *** $p<0.005$,

6.8.4 ET-1 treatment reduces SD protein nephrin expression

ET-1 induces acute structural changes in the cytoskeleton, with rearrangements apparent after 2h incubation. No changes in nephrin localisation were appreciated under IF in ET-1 treated cells (24h) compared to untreated controls (Fig. 6.8B G-J respectively). WB was performed to quantify changes at the protein level. Nephrin protein expression decreased dose dependently following ET-1 treatment (Fig 6.8B K). Semi-quantitative band analysis indicates a significant main effect of ET-1 treatment on nephrin expression ($p<0.0001$) following a 1-way ANOVA. Dunetts post-test revealed a significant reduction in nephrin following treatment with ET-1 at 100 pg/ml ($q=3.646$, $p<0.05$), 1000 pg/ml ($q=8.601$, $p<0.005$) and Ang II ($q=15.46$, $p<0.005$) n=3, relative to untreated controls (Fig 6.8 M). To quantify gene expression of nephrin following ET-1 treatment, RT-PCR was performed. Nephrin mRNA expression decreased dose dependently following ET-1 treatment (Fig 6.8B L). Band analysis indicates a significant main effect of ET-1 treatment on nephrin expression ($p=0.0086$) following a 1-way ANOVA. Dunetts post-test revealed a significant reduction in nephrin following treatment with ET-1 at 1000 pg/ml ($q=3.688$, $p<0.05$) and Ang II ($q=4.794$, $p<0.01$) n=3, relative to untreated controls (Fig 6.8B N). Although not a significant effect, there is a trend towards reduced expression at 100 pg/ml ET-1 treatment.

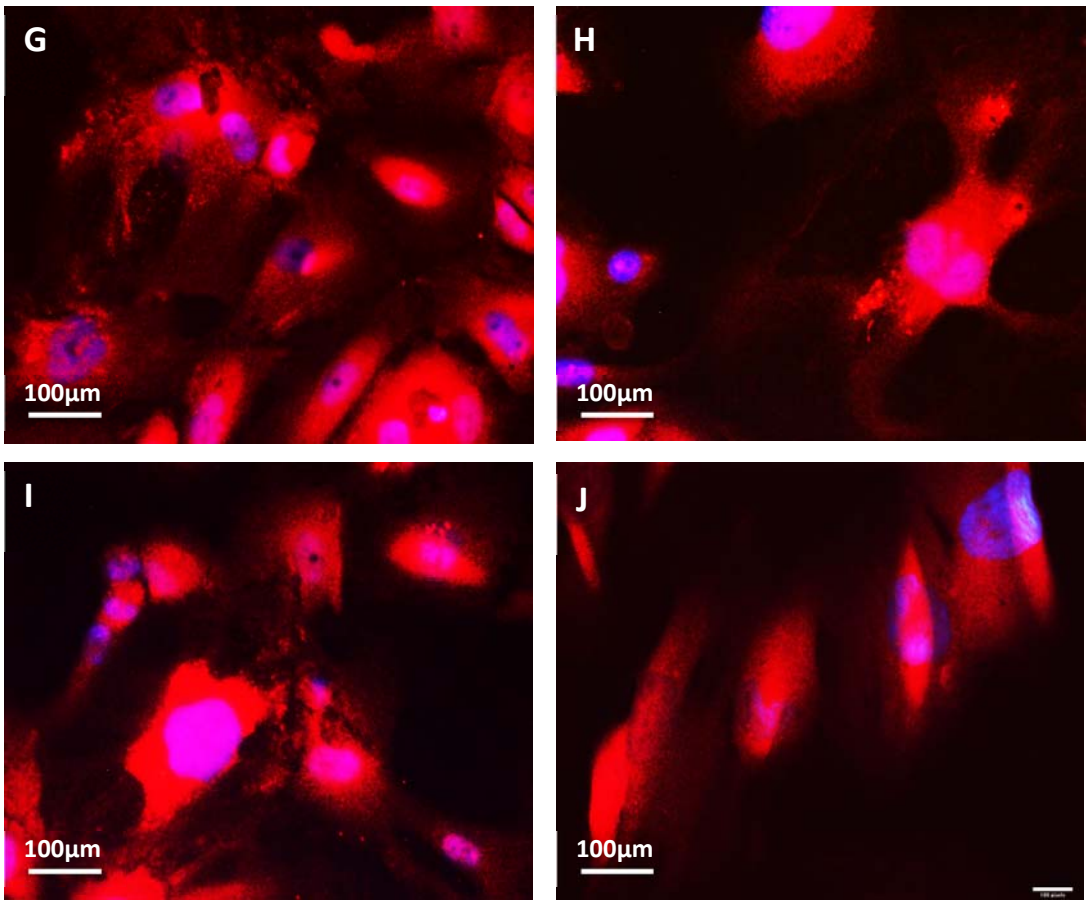

Figure 6.8B ET-1 effects on Nephrin localisation and expression.

G-J Photomicrographs (600x) of Nephrin localization and expression by IF. Un-stimulated cells express nephrin (G) Expression is unaltered in cells treated with (H) 10pg/ml (I) 100pg/ml and (J) 1000 pg/ml. Representative images of n=3.

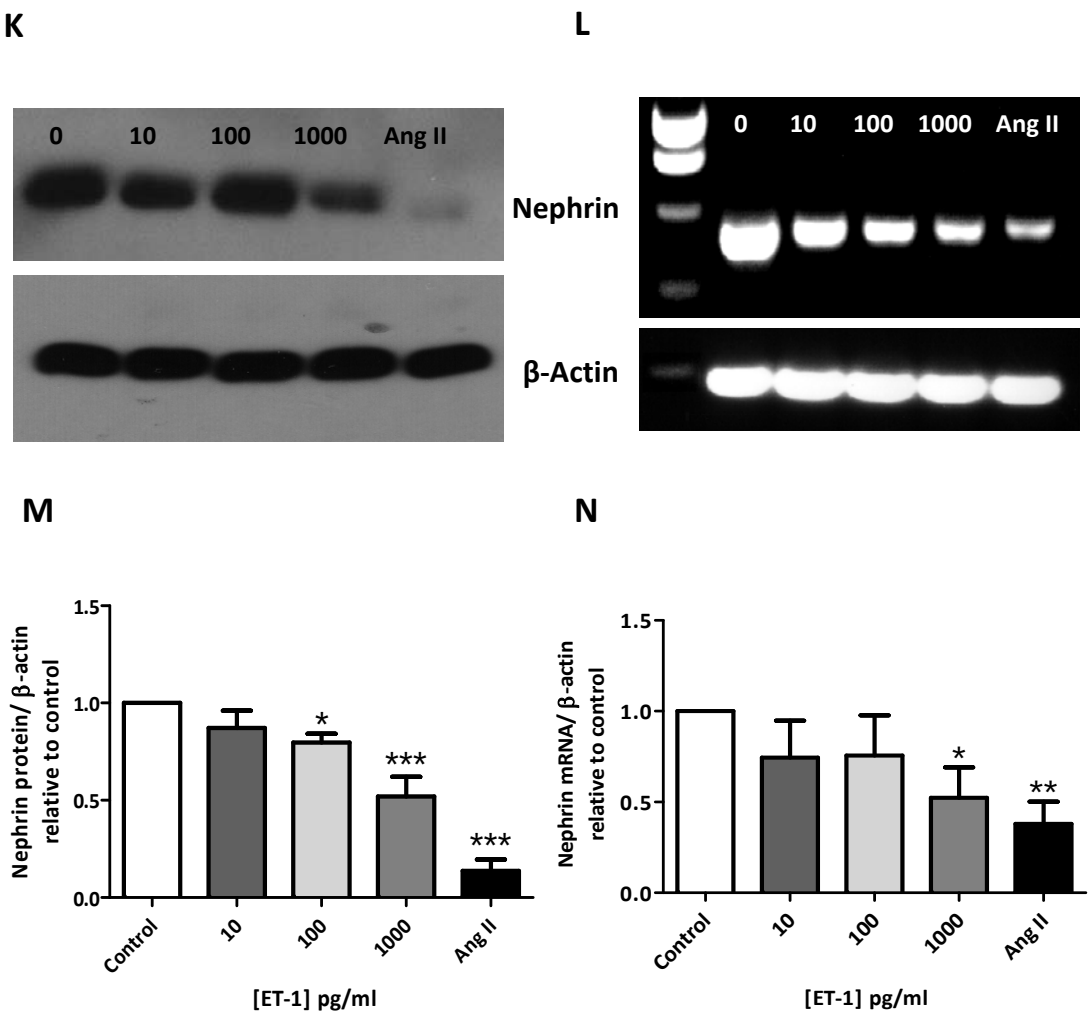

Figure 6.8B cont. ET-1 effects on Nephrin localisation and expression.

K-N Nephrin protein and mRNA expression. WB of (K) nephrin protein expression and RT-PCR of (L) *NPHS1* gene encoding nephrin. Mean band intensity of protein (M) and mRNA (N) relative to β-actin, expressed as a ratio of the untreated control. Both protein and mRNA nephrin levels are reduced in response to ET-1 stimulation. Loss of nephrin expression is more profound with increasing concentration. Data are mean ± SD, analysed by 1-way ANOVA followed by Dunnetts post hoc test (n=3). Symbols displayed above bars represent significance compared to control * $p<0.05$, ** $p<0.01$, *** $p<0.005$, **** $p<0.001$

6.9 ET receptor antagonism influences podocyte ET-1 induced ET-1 production

A beneficial role for selective ET receptor antagonism in renal disease has been suggested. In the current study we have demonstrated ET-1 mediated ET-1, IL-6 and IL-8 production, F-actin reorganisation, and a reduction in markers of podocyte differentiation. The following experiments aim to determine a mechanism by which ET-1 mediates its effects on podocytes. In the following studies, previous experiments were replicated with the addition of BQ123 (ET_AR) and BQ788 (ET_BR) antagonists.

6.9.1 Selective ET_AR antagonism reduces ET-1 induced ET-1 production

Cells incubated for 24h in the absence or presence of the selective ET_AR antagonist BQ123 show no significant difference in ET-1 production (53.06± 6.781 *vs* 46.89± 11.50 pg/ml respectively). When stimulated with ET-1 however, ET_AR antagonism significantly reduces the amount of ET-1 produced, and this effect is seen across all concentrations with the exception of 100 pg/ml (Fig 6.9 A).

6.9.2 Selective ET_BR antagonism prevents clearance of ET-1

Unstimulated cells in the presence of ET_B antagonist produced approximately threefold higher ET-1 concentrations compared to control (158.4 ± 12.22 *vs* 53.06 ± 6.781 pg/ml respectively), although this is not statistically significant. When stimulated with 5pg/ml ET-1, significantly higher ($p < 0.001$) concentrations of ET-1 were detected in the supernatant with ET_BR antagonism (554.4 ± 46.09 pg/ml) compared to control (222.0 ± 27.29 pg/ml). This likely reflects an inability to clear ET-1, as opposed to an up-regulation of production. ET-1 stimulation at 10 pg/ml and 50 pg/ml confers no change from baseline, and 100 pg/ml does not stimulate ET-1 production (Fig 6.9 B).

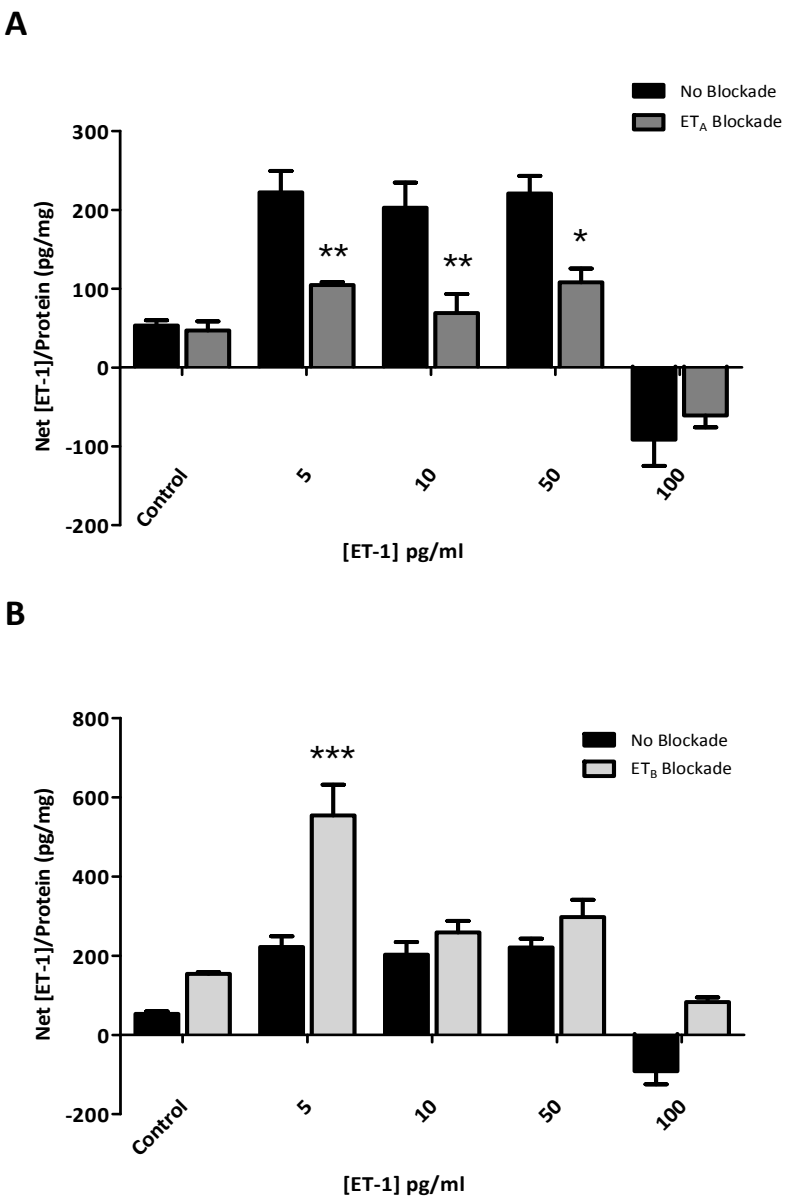

Figure 6.9 Selective ET receptor antagonism effects on ET-1 induced ET-1 production

A&B ET-1 content in podocyte supernatant assessed by RIA. Podocytes up-regulate ET-1 production in response to ET-1 stimulation at 24h. This effect is reduced by (A) selective ET_A antagonism, whereas (B) selective ET_B antagonism confers no change, with the exception of 5pg/ml whereby ET-1 production is greater. Data analysed by 2-way ANOVA and Bonferroni post-tests (n=6). Symbols displayed above bars represent significance compared to control * $p<0.05$, ** $p<0.01$, *** $p<0.005$, **** $p<0.001$.

6.10 ET receptor antagonism affects ET-1 induced cytokine production

The following assays were performed in order to determine whether ET-1 induced cytokine production is mediated by the ET_AR and/or ET_BR via selective antagonism with BQ123 and BQ788 respectively.

6.10.1 Selective ET_AR antagonism reduces ET-1 induced IL-6 and IL-8 production

Cells incubated for 24h in the absence or presence of the selective ET_A antagonist BQ123 show no significant difference in IL-6 (4431 ± 188.9 *vs* 3106 ± 663.8 pg/ml) or IL-8 (7823 ± 1091 *vs* 4743 ± 538.4 pg/ml) production. When stimulated with ET-1 however, ET_A antagonism significantly reduces the amount of IL-6 produced, and this effect is seen across all concentrations (Fig 6.10 A). Similarly, a trend towards decreased IL-8 production is also observed, and reaches significance at 5 pg/ml (Fig 6.10 C).

6.10.2 Selective ET_BR antagonism does not affect IL-6 or IL-8 production

Cells incubated under the same culture conditions challenged with the ET_B antagonist produced comparable IL-6 concentrations to control (5732±313.5 *vs* 4431 ± 188.9 pg/ml respectively). A similar effect was seen with IL-8 (5693± 3499 *vs* 7823 ± 1091 pg/ml). Conversely, when stimulated with ET-1 ET_BR antagonism failed to reduce cytokine production over all concentrations, (Fig 6.10 B & 6.10 D), demonstrating that ET-1 induced cytokine production is ET_AR mediated.

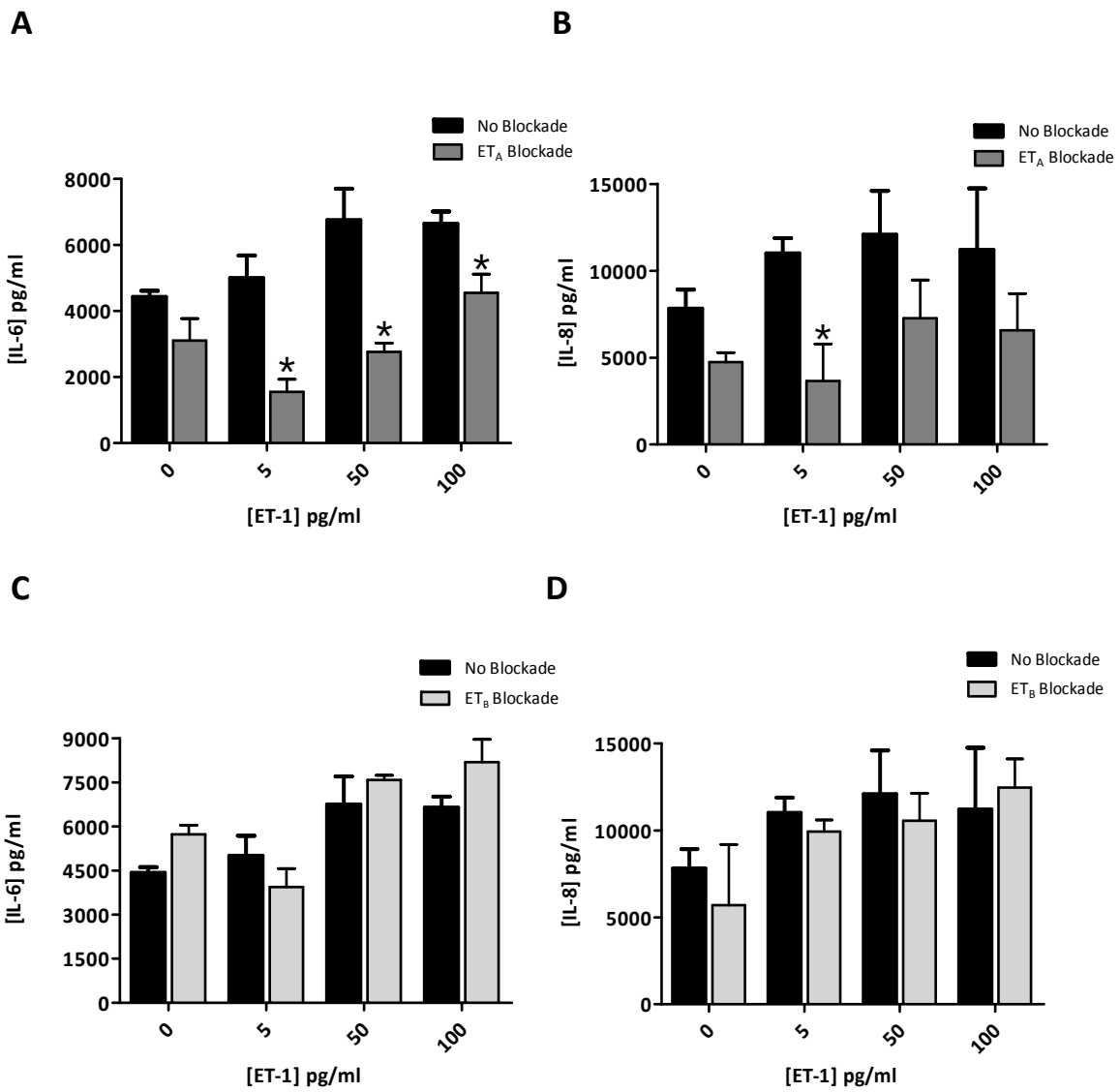

Figure 6.10 Selective ET receptor antagonism effects on ET-1 induced podocyte cytokine production

A-D Cytokine content in podocyte supernatant assessed by ELISA. Podocytes upregulate IL-6 and IL-8 production in response to ET-1 stimulation. This effect is reduced by (A&C) selective ET_A antagonism, whereas (B&D) selective ET_BR antagonism confers no change. Data analysed by 2-way ANOVA and Bonferroni post-tests (n=3) * $p < 0.05$ Symbols displayed above bars represent significance compared to no blockade.

6.11 ET receptor antagonism influences ET-1 induced podocyte structural changes

The following assays were performed in order to determine whether ET-1 induced cytoskeletal aberrations are ET_AR and/or ET_BR mediated.

6.11.1 ET_A receptor antagonism prevents ET-1 mediated human podocyte cytoskeletal rearrangements

As previously shown, human podocytes exposed to increasing concentrations of ET-1 demonstrate actin fibre disorganisation and contraction, with peripheral redistribution (Fig 6.11 A-D). Upon exposure to a selective ET_AR antagonist however, the cells do not undergo these cytoskeletal changes in response to ET-1 (Fig 6.11 E-H).

6.11.2 ET_B receptor antagonism prevents ET-1 induced F-Actin reorganisation

Contrarily, treatment of podocytes with an ET_B receptor antagonist in addition to increasing concentrations of ET-1 results in cytoskeletal abberations. Exposure of podocytes to ET_BR antagonist alone does not alter the cells structure and F-actin organisation, confirming that these are ET-1 effects mediated via the ET_AR (Fig 6.11 I-L).

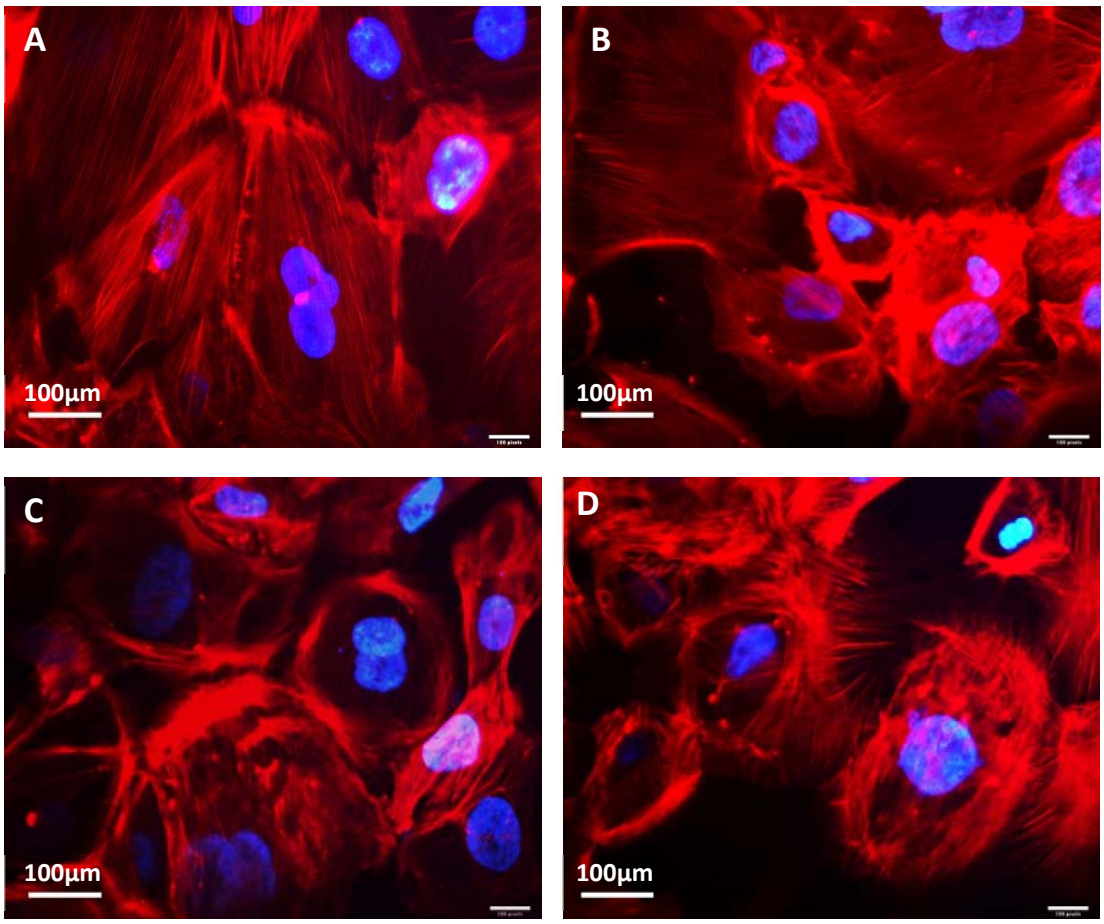

Fig 6.11 Selective ET receptor antagonism effects on ET-1 induced cytoskeletal changes

A-D Photomicrographs (x600) of human podocytes IF stained for F-actin with rhodamine-conjugated phalloidin. (A) Untreated cells with no receptor blocker demonstrate linear trans-cytoplasmic staining. Exogenous ET-1 induces cytoskeletal disruptions at (B) 10 pg/ml, (C) 100 pg/ml (D) 1000 pg/ml. Representative images of n=3.

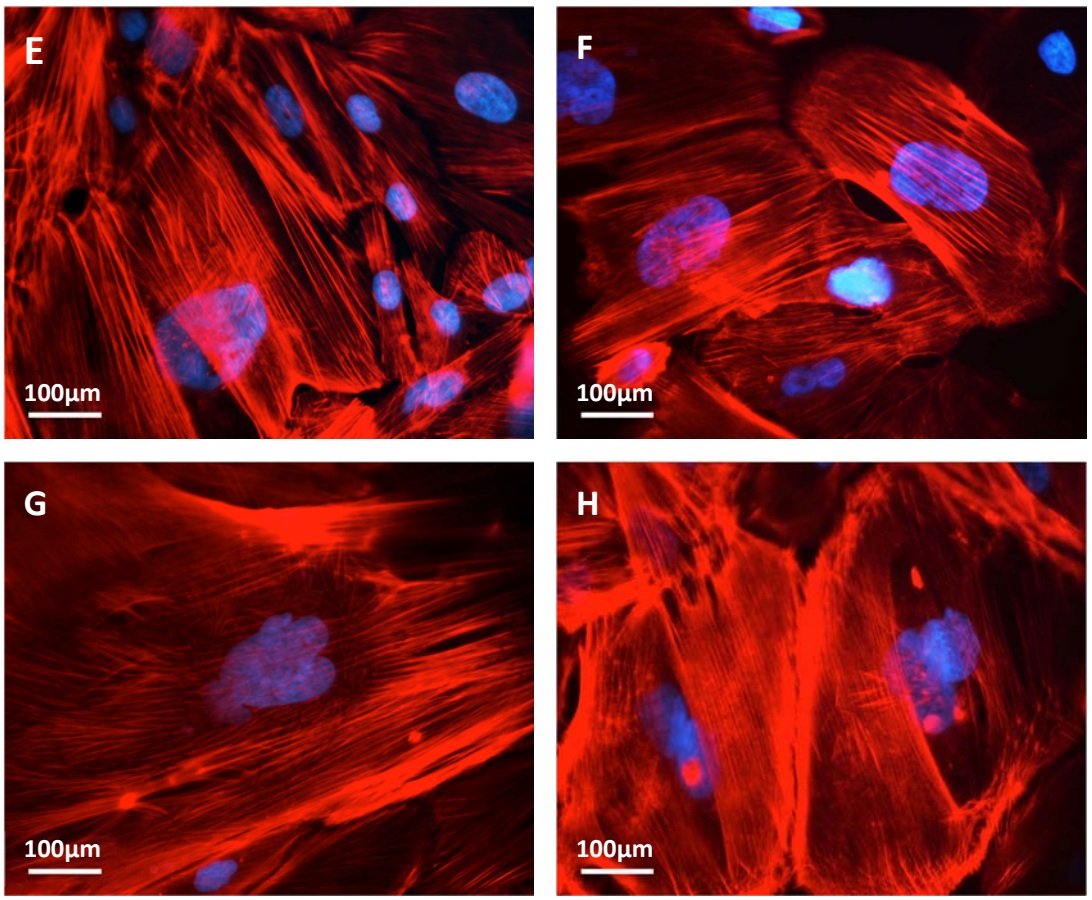

Fig 6.11 Cont. Selective ET receptor antagonism effects on ET-1 induced cytoskeletal changes

E-H Photomicrographs (x600) of human podocytes IF stained for F-actin with rhodamine-conjugated phalloidin. (E) BQ123 alone does not alter F-actin organisation. Selective ET_A receptor antagonism prevents cytoskeletal disruptions elicited by ET-1 at (F) 10 pg/ml, (G) 100 pg/ml (H) 1000 pg/ml (n=3).

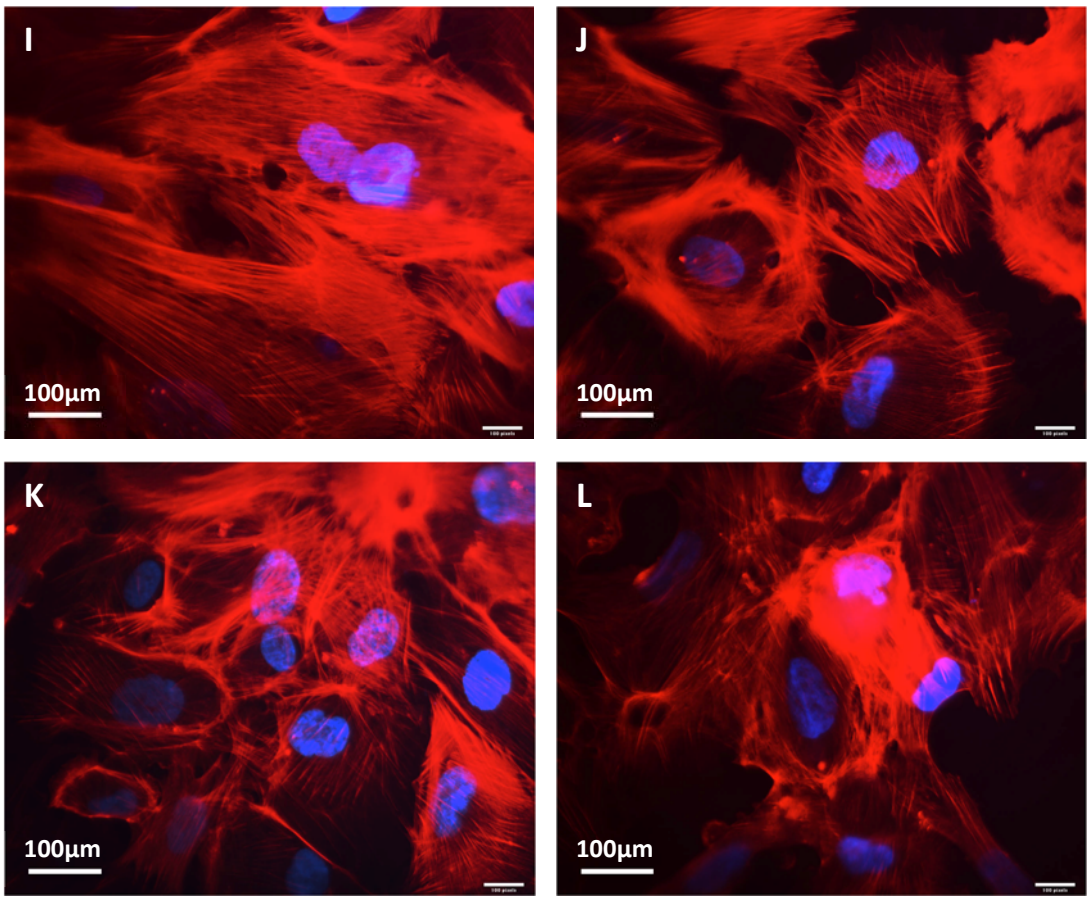

Fig 6.11 Cont. Selective ET receptor antagonism effects on ET-1 induced cytoskeletal changes

I-L Photomicrographs (x600) of human podocytes IF stained for F-actin with rhodamine-conjugated phalloidin. (I) ET_B receptor antagonist alone does not alter F-actin organisation. ET-1 induces cytoskeletal disruptions with selective ET_B receptor antagonist at (J) 10 pg/ml, (K) 100 pg/ml (L) 1000 pg/ml (n=3).

6.12 ET receptor antagonism affects ET-1 induced podocyte dedifferentiation

The following assays were performed in order to determine whether ET-1 induced dedifferentiation of podocytes is ET_AR and/or ET_BR mediated using selective antagonists BQ123 and BQ788 respectively.

6.12.1 ET_AR antagonism prevents ET-1 mediated human podocyte nephrin loss

As previously shown, human podocytes exposed to increasing concentrations of ET-1 demonstrate a trend towards nephrin mRNA down-regulation, with statistically significant effects at 1000 pg/ml ($p < 0.05$). Upon exposure to the selective ET_AR antagonist, ET-1 induced nephrin loss is prevented (Fig 6.12 A &B).

6.12.2 ET_BR antagonism does not affect ET-1 induced nephrin loss

Treatment of podocytes with a selective ET_BR antagonist, however, does not affect ET-1 induced nephrin down-regulation, and a significant down-regulation of nephrin upon ET-1 treatment at 1000pg/ml ($p<0.05$) can still be observed. These results implicate the ET_A receptor as the mediator of ET-1 induced podocyte de-differentiation.

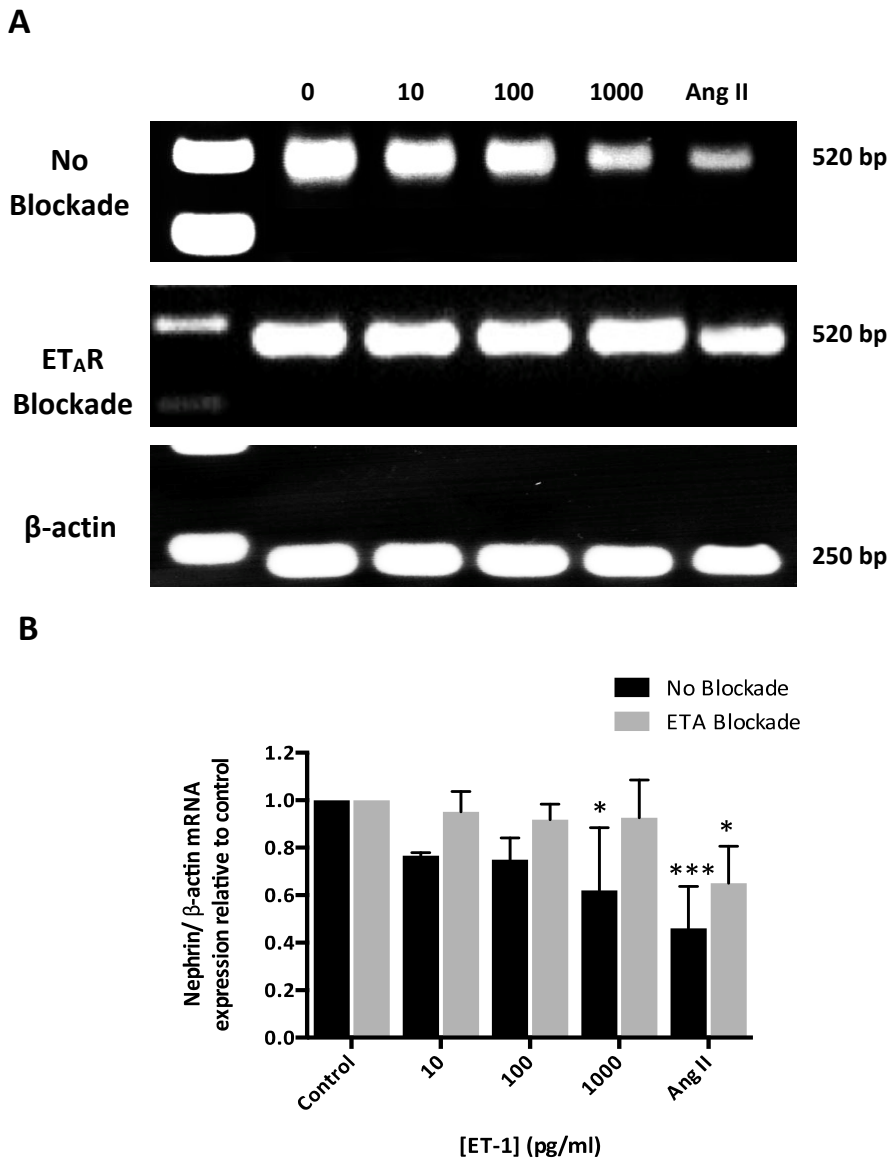

Figure 6.12 Selective ET receptor antagonism effects on ET-1 induced nephrin loss

A&B Gel images and semi quantitative band analysis of nephrin mRNA expression. RT-PCR of (A) *NPHS1* gene encoding nephrin. (B) Mean band intensity of mRNA relative to β-actin, expressed as a ratio of the untreated control. Nephrin mRNA levels are reduced in response to ET-1 stimulation. Loss of nephrin expression is more profound with increasing concentration. BQ123 prevents ET-1 induced nephrin loss. Data are mean ± SD, analysed by 2-way ANOVA followed by Tukey post hoc test (n=3). Symbols displayed above bars represent significance compared to control * $p<0.05$, *** $p<0.005$.

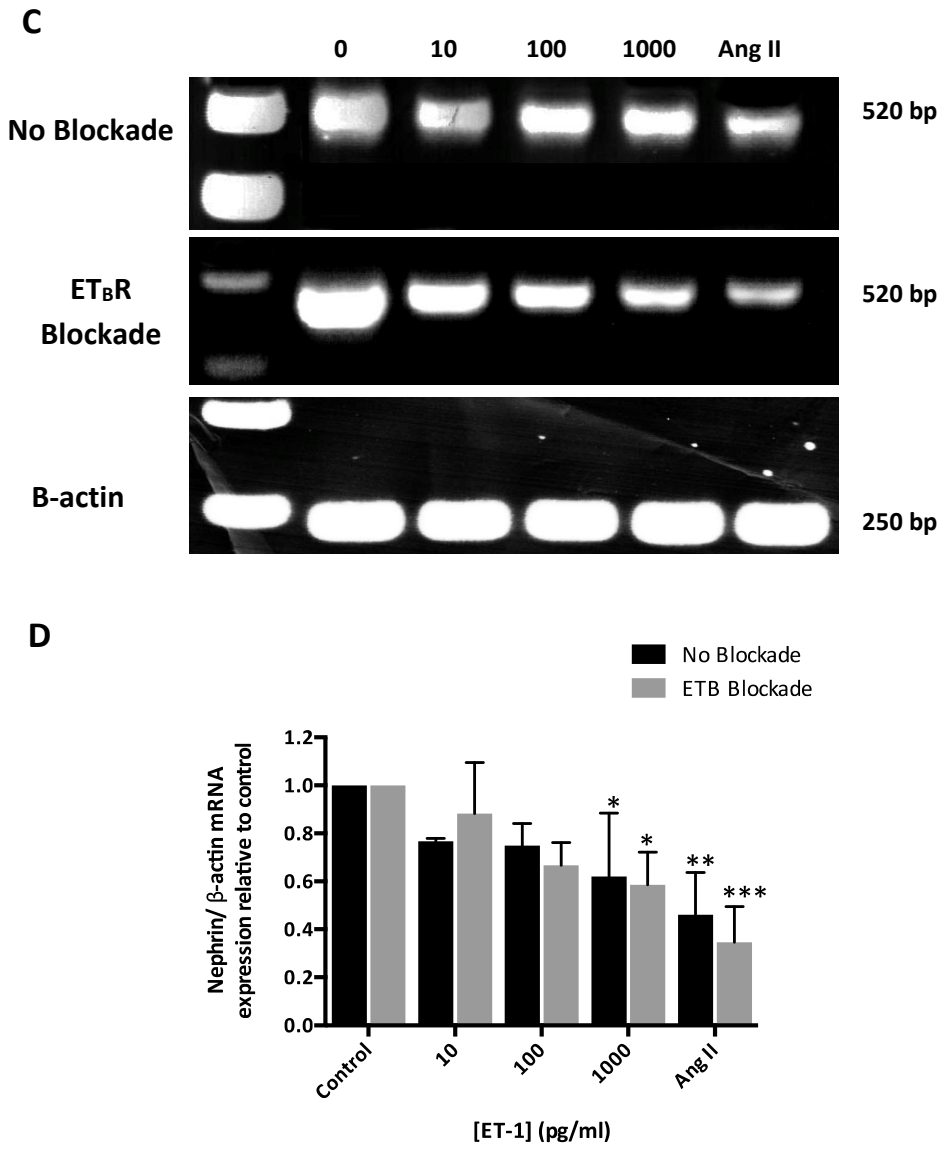

Figure 6.12 cont. Selective ET receptor antagonism effects on ET-1 induced nephrin loss

C&D Gel images and semi quantitative band analysis of nephrin mRNA expression. RT-PCR of (C) *NPHS1* gene encoding nephrin. (D) Mean band intensity of mRNA relative to β-actin, expressed as a ratio of the untreated control. Nephrin mRNA levels are reduced in response to ET-1 stimulation. Nephrin loss is more profound with increasing concentration. Addition of BQ788 results in a similar ET-1 induced nephrin loss. Data are mean ± SD, analysed by 2-way ANOVA followed by Tukey post hoc test (n=3). Symbols represent significance compared to control. * $p<0.05$, ** $p<0.01$, *** $p<0.005$,

6.12.13 Summary

- Human immortalised podocyte cells[287] propagate under growth permissive conditions at 33°C in a typical cobblestone monolayer. Thermoswitching to 37°C results in arrest of growth and maturation.
- Cells were characterised by expression of podocyte specific markers nephrin, podocin and synaptopodin using IF, WB and RT-PCR for protein and gene expression.
- Human podocytes poses a functional ET system. They express both ET_A and ET_B receptor subtypes.
- Exposure of podocytes to exogenous ET-1 results in a dose dependant ET-1 uptake over 12h followed by production of ET-1 over 48.
- ET-1 treatment also up-regulates expression of pro-inflammatory cytokines IL-6 and IL-8 in a dose dependant fashion.
- Cells undergo dedifferentiation or effacement in response to ET-1, as demonstrated by nephrin and podocin loss, and aberrations of the actin cytoskeleton.
- In all cases, the deleterious effects of ET-1 are by ameliorated by blockade of the ET_AR using a selective ET_AR antagonist BQ123, with blockade of the ET_BR conferring no alteration in ET-1 action.

6.13 Effect of ET-1 and selective ET receptor antagonism on human podocytes

Multiple lines of evidence demonstrate the presence of an ET system in podocytes. Much of this evidence is derived from rodent models and human primary tissue. In the final chapter the effects of exogenous ET-1 administration *in vitro* in human immortalised podocytes were investigated. Where ET-1 effects were observed, the mechanism was investigated using selective ETR antagonists. Conditionally immortalised human podocyte cells [287] were confirmed as mature, differentiated cells by morphology under LM, and by the gene and protein expression of the podocyte specific SD proteins podocin and nephrin and actin associated protein synaptopodin.

6.13.1 Human podocytes possess a functional ET system

While there is no direct evidence in the literature of the presence of ET_BR on human podocytes, ET_AR expression has been confirmed by agonist-antagonist studies [272], and rodent podocytes have been shown to express both receptor subtypes [195; 229; 270]. As such we hypothesised that these human podocytes would express the relevant ET receptors. These data demonstrate that human podocytes do poses a functional ET system; these cells express the ET_AR and ET_BR gene and protein, and are sensitive to the effects of exogenous ET-1 administration.

6.13.2 ET-1 induces actin cytoskeleton abberations and ET-1 production in human podocytes

These data demonstrate a reorganization and redistribution of the actin cytoskeleton from a linear, trans-cytoplasmic expression, to a disorganized peripheral distribution when challenged with ET-1. As previously discussed, the complex morphology of the podocyte is created and maintained by its cytoskeleton[367; 368; 369]. Well-regulated actin dynamics are crucial determinants during foot process maturation, junction formation, maintenance of structure, cell motility and detachment. In podocyte disease the physiological course of cytoskeletal adaptation is dysregulated.

In addition to cytoskeleton abberations, these experiments also demonstrate ET-1 protein production in human podocytes when treated with physiological doses of ET-1. Previous studies have demonstrated that, utilising murine podocytes, a number of stimuli can elicit podocyte ET-1 synthesis. Morigi and colleagues[195] have demonstrated actin cytoskeleton abberations and ET-1 synthesis in murine podocytes in response to IgG or an albumin load. ET-1 is primarily regulated at the level of gene transcription. Morigi demonstrates transcriptional up-regulation of the *EDN1* gene product pre-pro ET-1 mRNA, which leads to ET-1 protein synthesis occurred as a result of activation of FAK**,** a key component of the signal transduction pathways triggered by integrins.

Morigi also shows that reorganization of the actin cytoskeletal network results in modulation of the ET-1 gene via Rho kinase-dependent FAK activation of NF-κB and Ap-1 in differentiated podocytes. We can speculate that ETR engagement by ET-1 may signal in a similar fashion (discussed in 6.13.5).

In addition to cytoskeletal abberations and ET-1 production, we also demonstrate a loss or shedding of the SD protein nephrin when challenged with ET-1.

6.13.3 ET-1 induces nephrin down-regulation

Nephrin is commonly used in experimental models as a marker of podocyte injury. There are limited *in vitro* data suggesting that ET-1 may lead to podocyte loss of nephrin, however a study by Collino *et al.* (2008)[272] demonstrates treatment of murine podocytes with exogenous ET-1 leads to reduced cell surface nephrin expression. Similarly, infusion of ET-1 into rats caused nephrin excretion into the urine. [263]

A properly established and maintained podocyte slit diaphragm is a necessary component of the selective permeability barrier. Mutation or deletion of the slit diaphragm trans-membrane protein nephrin results in failure of podocyte foot process morphogenesis and concomitant proteinuria and first implicated nephrin as a component of a signalling complex that directly integrates

podocyte junctional integrity with cytoskeletal dynamics. Down-regulation of nephrin expression unrelated to gene mutations also occurs in podocyte injury, [370; 371] and mutations that are within the cytosolic tail and do not affect protein expression also cause glomerular disease,[372; 373] supporting a role for nephrin in cellular signalling. This is verified by evidence that nephrin serves as a signalling scaffold to recruit other podocyte proteins (including β-Arrestins which mediate internalization of plasma membrane receptors),[191; 374; 375; 376] is phosphorylated by Src-family kinases, [129; 377] and associates with adapters such as Nck to regulate the actin cytoskeleton.

6.13.4 ET-1 induces podocyte pro-inflammatory cytokine production

The literature describes podocytes as cells capable of responding to, and producing pro-inflammatory effectors. Our studies in human podocytes also demonstrate an ET-1 dose dependant stimulation of pro-inflammatory cytokines IL-6 and IL-8.

Podocytes have the potential to contribute actively to recruitment of inflammatory cells and glomerular injury, in addition to self-perpetuated injury, by up-regulating receptors linked to pro-inflammatory cytokine pathways, most commonly associated with inflammatory cells such as macrophages and neutrophils. TLR-2, 4 and 6 receptor expression is found on podocytes in nephritic glomeruli, and *in vitro* studies using immortalized mouse podocytes demonstrate induction of chemokine expression in response to lipid A, the specific TLR-4–binding component of LPS ligand. In addition, the co-stimulatory molecule CD80 is also expressed by podocytes[182].

Podocytes respond to pro-inflammatory cytokine stimuli e.g murine podocytes *in vitro* demonstrate activation by TGF-β [378] and by TNFα in a JNK/p38-dependent pathway [197; 198; 199]. *In vivo,* podocytes are a prominent source of TNF-α in murine anti-GBM nephritis [379] and in human membranous nephritis[380]. *In vitro* pro-inflammatory cytokines including IL-1α, IL-1 β, IL-6, IL-8, TNFα, GM-CSF and others have been reported to be produced by podocytes [366; 381 365].

As noted, both integrin involvement and engagement of the nephrin receptor complex are capable of activating NF-κB resulting in ET-1 up-regulation. Studies also demonstrate an up-regulation of pro-inflammatory cytokines, many of which are NF-κB sensitive genes, detectable in injured podocytes. Here we report ET-1 induced up-regulation of pro-inflammatory cytokines IL-6 and IL-8. It is likely that these cytokines are up-regulated in an NF-κB /Ap-1 dependant fashion in response to ET-1 mediated actin reorganization and nephrin loss.

The effects of ET-1 stimulation of these human podocytes- up-regulation of ET-1 and pro-inflammatory cytokines, down-regulation of nephrin and re-organisation of actin cytoskeleton may be attributed to one the effects of integrin, nephrin and cadherin and potentially TLR activation. These are likely downstream events with the initial ET interaction being with the ET receptors.

6.13.5 Mechanism of ET-1 mediated podocyte effacement

These effects of an initial ET-1 insult to the podocyte i.e. actin cytoskeleton reorganization and concomitant ET-1 production, nephrin down-regulation and pro-inflammatory cytokine production, are likely initiated by a single receptor in the first instance- the ET_A receptor.

6.13.5.1 Selective ET_A, but not ET_B antagonism attenuated cytoskeleton abberations and nephrin loss, and prevented ET-1 induced ET-1 and proinflammatory cytokine production

The role of the ET_AR as the receptor primarily responsible for mediating the pathologic effects of ET-1 in renal diseases has been addressed. Evidence in the literature demonstrates that ET-1 would likely induce F-actin abberations acting via the ET_AR. Further work by Morigi's group [274] investigated the effect of treating murine podocytes with shiga toxin, the agent responsible for post-diarrhoeal haemolytic-uraemic syndrome (HUS). In this study, shiga toxin induced podocyte ET-1 production and subsequent autocrinal disruption of the actin cytoskeleton. In this setting, ET_AR blockade inhibited these effects. Furthermore, Ortmann *et al.* [275] investigated the effects of ET-1 induced actin

fibre disruption in murine podocytes. Using selective ETR antagonists, this group confirmed the ET-1 mediated actin cytoskeleton reorganisation is ET_AR dependant. Our data confirm these effects and demonstrate that pre-treatment of human podocyte cells with BQ123 prevents disruption to the cytoskeleton and ET-1 production, an effect that remains unchanged with BQ788.

These effects were mediated by the ET_A receptor, as selective antagonism with BQ123 inhibited these ET-1 induced effects. Blockade with BQ788, a selective ET_B receptor antagonist did not alter cytokine production.

6.13.6 Putative ET-1 induced podocyte intracellular signalling mechanisms

ET-1 binding to the ET receptors has been extensively studied. In addition to its renal specific effects, it also serves a critical role in a multitude of cancers. The primary mechanism involving engagement of this receptor drives EMT in ovarian tumour cells through β-arrestin signalling [135]. As discussed in reference to macrophage migration and motility, receptor-ligand binding activates canonical G-protein-linked receptor phosphorylation leading to recruitment of the scaffolding protein β-arrestin, receptor desensitisation and internalisation[382; 383] with subsequent intracellular signalling cascades being activated. These pathways that are convergent with those discussed in relation to integrin and nephrin stimulation include MAPK Ras/Raf/MEK/ERK1/2, the PI3K/AKT/IκB/NF-κB, β-catenin the RHO-GEF/CDC42/PAK/JNK and others (Reviewed in [384]).

In ovarian tumour cells, β-arrestin is recruited to ET_AR to form two trimeric complexes. The first is through the interaction with Src leading to epithelial growth factor receptor (EGFR) transactivation and E-cadherin/β-catenin tyrosine phosphorylation. EGFR overexpression and down-regulation of E-cadherin, a key component of intercellular junctions, are both known to disrupt cell–cell interactions and these processes are connected by the caveolae-associated protein caveolin-1 (CAV1).[385] In podocytes, curcumin ameliorates EMT *in vivo* and *in vitro* via regulating caveolin-1[386].

The second is through the physical association with axin and APC to β-catenin and GSK-3β. GSK-3β is then released and inactivated and β-catenin is stabilised. Phosphorylated β-catenin is then degraded in proteasomes by the ubiquitination machinery.

The engagement of β-arrestin in these two signalling complexes concurs to activate β-catenin signalling pathways. Silencing of both β-arrestin-1 and β-arrestin-2 inhibits ET_AR mediated signalling, causing suppression of Src, mitogen-activated protein kinase (MAPK), AKT activation, as well as EGFR transactivation and a complete inhibition of ET-1-induced β-catenin transcriptional activity and cell invasion.

Based on these studies, it is reasonable to hypothesise that ET-1, acting via the ET_AR would induce podocyte effacement by inducing an EMT-like event involving β-arrestin-1. This would subsequently induce nephrin endocytosis and attenuated nephrin signalling, and activate downstream Src, MAPK, AKT and EGFR transactivation, β-arrestin-1/β-catenin activation, increased transcriptional activity including *EDN1* and cell invasion. *EDN1* up-regulation and subsequent ET-1 formation and release would also elicit autocrinal and paracrinal perpetuation of ETR activation (Fig 7.1).

This hypothesis was tested by Buelli *et al.* (2014)[387]. In cultured mouse podocytes, ET-1 induced dedifferentiation and EMT (assessed by synaptopodin and α-smooth muscle actin respectively). ET_AR engagement also promoted podocyte migration, activation and increased β-arrestin-1 expression. Activated ET_AR was reported to recruit β-arrestin-1 to form a trimeric complex with Src leading to EGFR transactivation and P-cadherin/β-catenin phosphorylation. P-cadherin/β-catenin are concentrated in caveolae and the E-cadherin/β-catenin complex in ovarian tumour cells, and is connected by CAV1. It is reasonable to hypothesise that CAV1 may be involved in the P-cadherin/β-catenin complex in podocytes, however this is yet to be investigated. β-catenin phosphorylation promoted gene transcription of Snail, and increased migration was Snail induced as confirmed by knockdown experiments. Silencing of β-arrestin-1

prevented podocyte phenotypic changes and motility and inhibited ET_AR driven signalling. *In vitro* findings were confirmed in ADR nephropathy using sitaxsentan as an ET_AR antagonist. These studies translate to human disease, as increased β-arrestin-1 levels in podocytes retrieved from crescents of patients with proliferative glomerulopathies were also demonstrated.

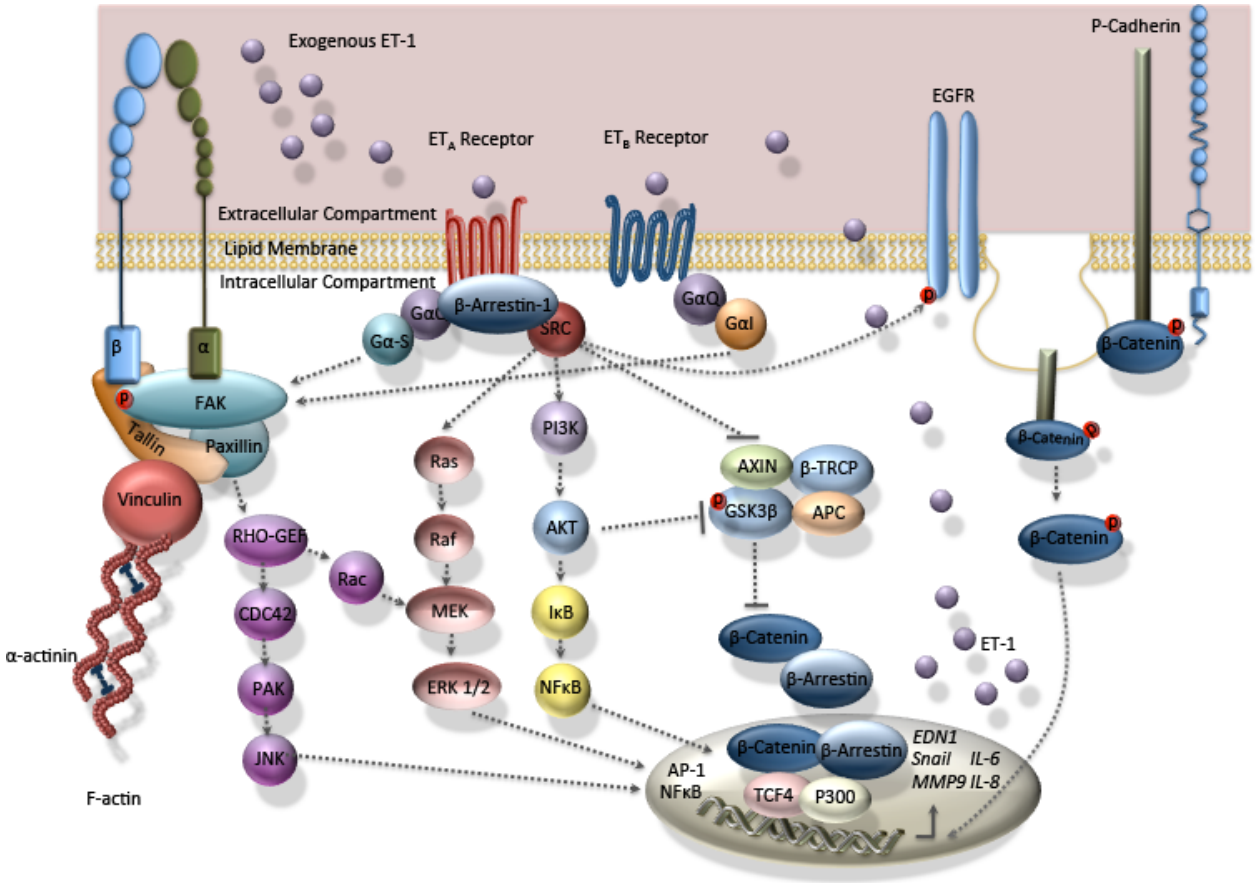

Figure 7.1 ET Receptor mediated podocyte intracellular signalling

ET-1 binding to the ET receptors activates canonical G-protein-linked receptor phosphorylation. Activated ET_AR recruits β-arrestin-1 to form a trimeric complex with Src leading to two pathway mechanisms. The first is through interaction with Src leading EGFR transactivation and P-cadherin/β-catenin tyrosine phosphorylation. The second is through the physical association with AXIN and APC to β-catenin and GSK-3β. GSK-3β is released and inactivated and β-catenin is stabilised. Phosphorylated β-catenin is degraded in proteasomes by ubiquitination. Genes involved in EMT including Snail and MMP-9 are transcriptionally upregulated. ET_AR/ β-arrestin-1/Src complex also initiates other intracellular signalling cascades. ET receptor stimulation activates the MAPKs Ras and Raf with subsequent MEK/ERK1/2 signalling to and NF-κB/AP-1 binding sites. The PI3K/AKT/IκB/NF-κB pathway and the RHO-GEF/CDC42/PAK/JNK pathway leading to NF-κB/AP-1 transcriptional activation occurs.

6.13.7 Limitations and Future work

A body of evidence to demonstrate the mechanism of ET_AR mediated ET-1 induced podocyte effacement exists. The potential intracellular signalling pathways leading to actin remodelling and gene transcription have been discussed. These data are almost exclusively derived from experiments conducted in murine cells, with evidence in a human setting being scarce and ultimately speculative.

Our studies have demonstrated that ET-1 induces podocyte effacement, ET-1 and cytokine production and nephrin down-regulation. Antagonist studies demonstrate that these are ET_AR mediated events. Further studies are required to ascertain whether the intracellular signalling events demonstrated in rodent models are translatable to human disease. The β-arrestin-1/β-catenin complex signal transduction pathway is the most recent example in the literature of ET-1 induced ET_AR mediated podocyte activation. Investigations into this pathway mechanism in human cells would be a necessary next step.

Limitations in these human podocyte studies primarily involved a lack of suitable SD protein antibodies including ZO-1, synaptopodin, podocin and CD2-AP. The actions of ET-1 on these SD proteins may also provide evidence as to the intracellular signalling pathways involved.

When considering experiments performed to determine whether ET-1 would induce ET-1 synthesis in podocytes, several caveats should be noted. ET-1 was added to the wells and ET-1 concentration in the media was measured. After an initial loss of ET-1 in the media at early time-points, ET-1 synthesis then occurred. In order to accurately measure the ET-1 produced, the protein content of the wells were measured. The ET-1 concentration was then normalised to protein content. The limitations of this approach are threefold 1) the cytotoxicity of ET-1 on podocytes was not assessed. If ET-1 is cytotoxic at the doses used, podocyte loss would occur. Ultimately, less protein would be retrieved from the well, skewing the ET-1 data 2) Similarly, the proliferative actions of ET-1 were not assessed. An increase in podocyte number and

therefore protein would equally skew the data. 3) The results state that ET-1 is 'produced' over a specified time and dose. Whether this is true ET-1 production, or release of pre-stored ET-1 is not yet known. To attempt to delineate this, ET-1 mRNA was assessed using qPCR. These experiments were performed but were a technical failure and as such these should be repeated.

As the glomerular endothelial cells (GEnC) and GBM are structurally relevant components of the glomerular filter, and have been shown to play a role in protein handling and barrier functions, further *in vitro* studies to investigate conditionally immortalised human glomerular endothelial cell [388] responses to ET-1 may also be relevant.

Chapter 7
Discussion

7.1 Summary and Concluding Remarks

The present study provides evidence to support our initial hypotheses. Continued studies both *in vitro* and *in vivo* will strengthen the body of evidence to promote the ET system as a potential target. Therapeutic ET_AR antagonism in proteinuric renal diseases may improve disease prognosis.

ET-1 has known inflammatory properties and ET-1 production in a number of cell types is an autocrine and paracrine event. This ET-1 production is likely mediated via stimulation of the ET_AR, with the ET_BR serving to clear ET-1. ET_AR mediated ET-1 production and subsequent ET-1 induced pro-inflammatory cytokine and chemokine gene transcription is likely reduced with sitaxsentan, limiting the ability of glomerular cells to recruit resident interstitial Mϕ and blood derived monocytes.

Taken together, in consideration of the literature and the data surrounding ET-1 effects in renal and inflammatory cells, *in vivo* studies and human clinical evidence, a model of the renal ET-1 system has emerged (Fig 7.1). In podocytes, ET-1 induces alterations in the actin cytoskeleton, foot process effacement and loss of slit diaphragm proteins such as nephrin. This podocyte damage likely contributes to the development of proteinuria, a marker of renal disease progression and a cause of further podocyte effacement. Podocytes also produce ET-1, which then acts in an autocrine and paracrine fashion to cause further podocyte effacement and ET-1 production. It also serves to activate other renal cell types, including mesangial cells, to release pro-inflammatory and pro-fibrotic cytokines, stimulate proliferation and increase production of matrix proteins leading to sclerosis. ET-1 is also chemo-attractant to resident interstitial Mϕs, which infiltrate the glomerulus where they further contribute to renal inflammation. A regulatory feedback mechanism of ET-1 clearance by Mϕ, and increased phagocytosis may then occur. Contrarily, if these recruited macrophages are then classically activated, their ET_BR mediated clearance capacity may be compromised. ET receptor antagonists have been studied in the context of renal diseases whereby blood pressure and proteinuria have been common endpoint measures. Although ETR antagonists show a deal of promise

in the treatment of GN, further studies are required to strengthen this evidence as relatively few pre-clinical studies in GN have been performed. Use of these antagonists in other models of GN would be informative, allowing for the expedition of these classes of drugs into clinical trials. Such models may include any proteinuric disease i.e type 2 diabetic nephropathy (T2DN), models of obstruction such as unilateral ureteric obstruction (UUO), Thy1 nephritis and IgA nephropathy. Taking in to consideration the research presented in this thesis, and previous pre-clinical studies, endothelin receptor antagonists undoubtedly make very attractive candidates for clinical trial. Continued research and funding are absolutely necessary to tackle the ever-increasing global health burden of chronic kidney disease.

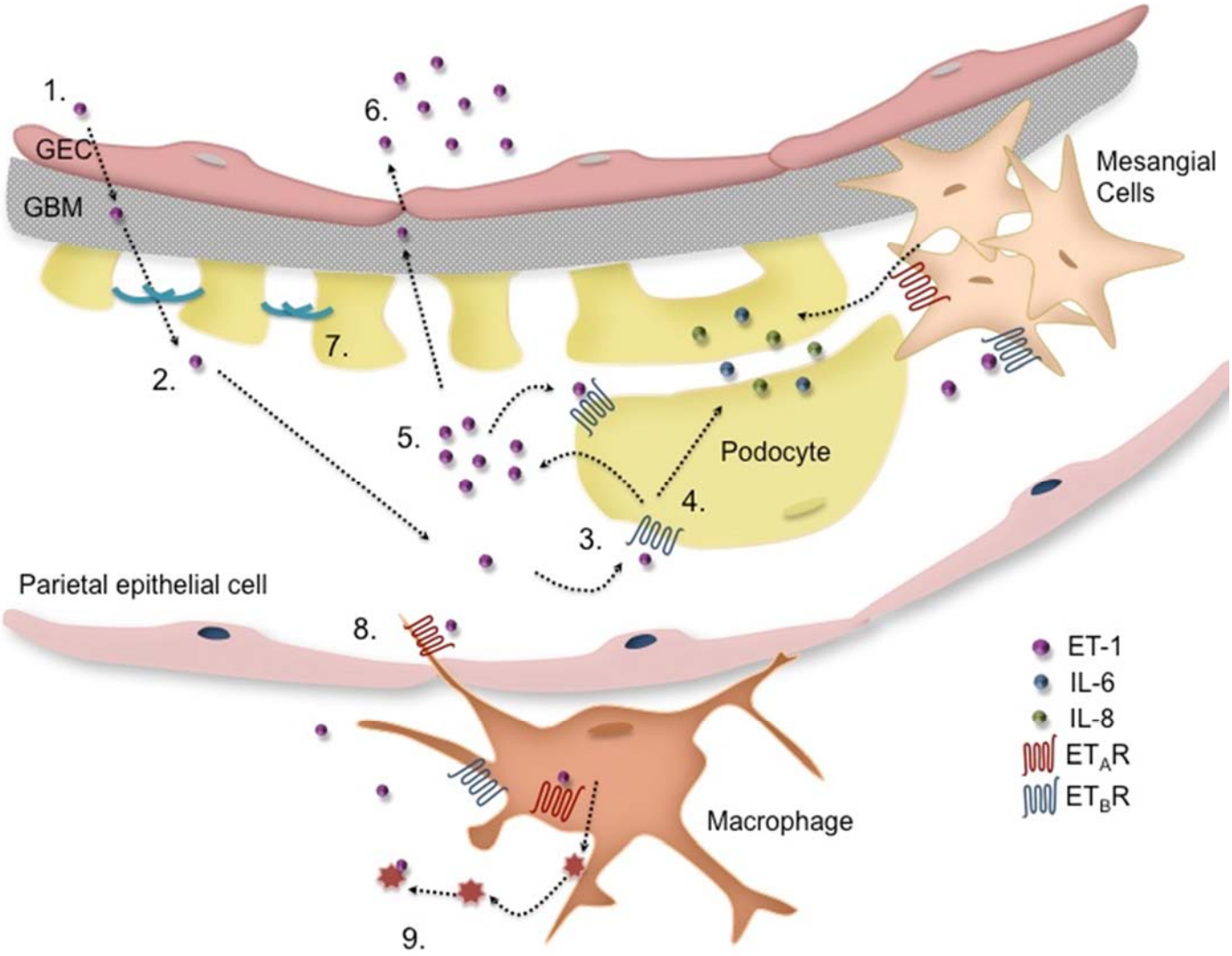

Figure 7.1 Effects of ET-1 on glomerular cells

1. ET-1 is released ablumenally from the glomerular endothelium **2.** ET-1 moves through the GBM to interact with podocytes **3.** ET-1 engages the ET_AR on the plasma membrane of podocytes **4.** ET-1 activates podocyte ET-1 and cytokine production. **5.** ET-1 acts in an autocrine and paracrine fashion and **6.** moves back into the bloodstream where it may interact with blood monocytes or neutrophils **7.** ET-1 also induces down-regulation of podocyte SD proteins including nephrin and disruption of the actin cytoskeleton **8.** In addition to its effects on podocytes, ET-1 also engages interstitial macrophages inducing migration likely via the ET_B receptor towards an ET-1 gradient where it may clear ET-1 **9.** ET_B receptor engagement may also induce macrophage release of proteolytic enzymes so that the cells may degrade ECM components allowing them to migrate. These enzymes are also likely capable of degrading ET-1.

Chapter 8
References

8.1 References

1. Remuzzi, G., Ruggenenti, P. & Benigni, A. (1997). Understanding the nature of renal disease progression. *Kidney Int* **51**, 2-15.
2. Levey, A. S., Coresh, J., Balk, E., Kausz, A. T., Levin, A., Steffes, M. W., Hogg, R. J., Perrone, R. D., Lau, J. & Eknoyan, G. (2003). National Kidney Foundation practice guidelines for chronic kidney disease: evaluation, classification, and stratification. *Ann Intern Med* **139**, 137-47.
3. Brenner, B. M. (1985). Nephron adaptation to renal injury or ablation. *Am J Physiol* **249**, F324-37.
4. Ezzati, M., Lopez, A. D., Rodgers, A., Vander Hoorn, S. & Murray, C. J. L. Selected major risk factors and global and regional burden of disease. *The Lancet* **360**, 1347-1360.
5. Murray, C. J. L., Lauer, J. A., Hutubessy, R. C. W., Niessen, L., Tomijima, N., Rodgers, A., Lawes, C. M. M. & Evans, D. B. Effectiveness and costs of interventions to lower systolic blood pressure and cholesterol: a global and regional analysis on reduction of cardiovascular-disease risk. *The Lancet* **361**, 717-725.
6. Age-specific relevance of usual blood pressure to vascular mortality: a meta-analysis of individual data for one million adults in 61 prospective studies. *The Lancet* **360**, 1903-1913.
7. Knott, C., Mindell, J. (2011). Health, social care and lifestyles: Chapter 3 - Hypertension - Health Survey for England (Centre, H. a. S. C. I., ed.), Vol. 1.
8. Rao, A., Casula, A., Castledine, C. (2013). *UK Renal Registry 17th Annual Report: Chapter 2 UK Renal Replacement Therapy Prevalence in 2013: National and Centre-specific Analyses*.
9. Kerr, M., Bray, B., Medcalf, J., O'Donoghue, D. J. & Matthews, B. (2012). Estimating the financial cost of chronic kidney disease to the NHS in England. *Nephrology Dialysis Transplantation* **27**, iii73-iii80.
10. Hill, N., Fatoba, ST., Oke, JL., Hirst, JA., O'Callaghan, CA., Lasserson, DS., Hobbs, R. (2016). Global prevalence of chronic kidney disease-A systematic review and meta-analysis. *PLoS One* **10**.
11. Atkins, R. C. (2005). The epidemiology of chronic kidney disease. *Kidney Int Suppl*, S14-8.
12. Bell, S., Fletcher, E. H., Brady, I., Looker, H. C., Levin, D., Joss, N., Traynor, J. P., Metcalfe, W., Conway, B., Livingstone, S., Leese, G., Philip, S., Wild, S., Halbesma, N., Sattar, N., Lindsay, R. S., McKnight, J., Pearson, D. & Colhoun, H. M. (2015). End-stage renal disease and survival in people with diabetes: a national database linkage study. *Qjm* **108**, 127-34.
13. Brosnahan, G. & Fraer, M. (2010). Chronic kidney disease: whom to screen and how to treat, part 1: definition, epidemiology, and laboratory testing. *South Med J* **103**, 140-6.
14. Molitch, M. E., DeFronzo, R. A., Franz, M. J., Keane, W. F., Mogensen, C. E., Parving, H. H. & Steffes, M. W. (2004). Nephropathy in diabetes. *Diabetes Care* **27 Suppl 1**, S79-83.
15. Jha, V., Garcia-Garcia, G., Iseki, K., Li, Z., Naicker, S., Plattner, B., Saran, R., Wang, A. Y.-M. & Yang, C.-W. Chronic kidney disease: global dimension and perspectives. *The Lancet* **382**, 260-272.
16. Grams, M. E. & Coresh, J. (2013). Assessing risk in chronic kidney disease: a methodological review. *Nature Reviews Nephrology* **9**, 18-25.

17. Buck, K. & Feehally, J. (1997). Diabetes and renal failure in Indo-Asians in the UK--a paradigm for the study of disease susceptibility. *Nephrol Dial Transplant* **12**, 1555-7.
18. Raleigh, V. S. (1997). Diabetes and hypertension in Britain's ethnic minorities: implications for the future of renal services. *BMJ* **314**, 209-13.
19. Lopez-Novoa, J. M., Rodriguez-Pena, A. B., Ortiz, A., Martinez-Salgado, C. & Lopez Hernandez, F. J. (2011). Etiopathology of chronic tubular, glomerular and renovascular nephropathies: clinical implications. *J Transl Med* **9**, 13.
20. Remuzzi, G., Benigni, A. & Remuzzi, A. (2006). Mechanisms of progression and regression of renal lesions of chronic nephropathies and diabetes. *J Clin Invest* **116**, 288-96.
21. Go, A. S., Chertow, G. M., Fan, D., McCulloch, C. E. & Hsu, C.-y. (2004). Chronic Kidney Disease and the Risks of Death, Cardiovascular Events, and Hospitalization. *New England Journal of Medicine* **351**, 1296-1305.
22. Brenner, B. M., Cooper, M. E., de Zeeuw, D., Keane, W. F., Mitch, W. E., Parving, H. H., Remuzzi, G., Snapinn, S. M., Zhang, Z. & Shahinfar, S. (2001). Effects of losartan on renal and cardiovascular outcomes in patients with type 2 diabetes and nephropathy. *N Engl J Med* **345**, 861-9.
23. Jafar, T. H., Stark, P. C., Schmid, C. H., Landa, M., Maschio, G., de Jong, P. E., de Zeeuw, D., Shahinfar, S., Toto, R. & Levey, A. S. (2003). Progression of chronic kidney disease: the role of blood pressure control, proteinuria, and angiotensin-converting enzyme inhibition: a patient-level meta-analysis. *Ann Intern Med* **139**, 244-52.
24. Dahlof, B., Devereux, R., de Faire, U., Fyhrquist, F., Hedner, T., Ibsen, H., Julius, S., Kjeldsen, S., Kristianson, K., Lederballe-Pedersen, O., Lindholm, L. H., Nieminen, M. S., Omvik, P., Oparil, S. & Wedel, H. (1997). The Losartan Intervention For Endpoint reduction (LIFE) in Hypertension study: rationale, design, and methods. The LIFE Study Group. *Am J Hypertens* **10**, 705-13.
25. Xie, X., Liu, Y., Perkovic, V., Li, X., Ninomiya, T., Hou, W., Zhao, N., Liu, L., Lv, J., Zhang, H. & Wang, H. (2016). Renin-Angiotensin System Inhibitors and Kidney and Cardiovascular Outcomes in Patients With CKD: A Bayesian Network Meta-analysis of Randomized Clinical Trials. *Am J Kidney Dis* **67**, 728-41.
26. Bywaters, E. G. & Beall, D. (1941). Crush Injuries with Impairment of Renal Function. *Br Med J* **1**, 427-32.
27. Brenner, B., Hostetter, T. & Humes, H. (1978). Glomerular permselectivity: barrier function based on discrimination of molecular size and charge. *American Journal of Physiology-Renal Physiology* **234**, F455-F460.
28. Endlich, K., Kriz, W. & Witzgall, R. (2001). Update in podocyte biology. *Curr Opin Nephrol Hypertens* **10**, 331-40.
29. http://webs.ashlandctc.org/mflath/keyurinaryobjectives.htm.
30. https://o.quizlet.com/m4sDQO2iB8Lasv2uz3uDwA_m.jpg.
31. Zollinger, H. U. & Mihatsch, M. J. (1978). Glomerulonephrosis and Glomerulosclerosis. In *Renal Pathology in Biopsy*, pp. 380-406. Springer.
32. Weening, J. J., D'agati, V., Schwartz, M. M., Seshan, S. V., Alpers, C. E., Appel, G. B., Balow, J. E., Bruijn, J. A., Cook, T. & Ferrario, F. (2004). The classification of glomerulonephritis in systemic lupus erythematosus revisited. *Kidney international* **65**, 521-530.
33. Dixon, F. J. (1968). The pathogenesis of glomerulonephritis. *The American journal of medicine* **44**, 493-498.
34. Papper, S. (1977). Asymptomatic proteinuria. Clinical significance. *Postgrad Med* **62**, 125-30.

35. Grossfeld, G. D., Wolf, J. S., Jr., Litwan, M. S., Hricak, H., Shuler, C. L., Agerter, D. C. & Carroll, P. R. (2001). Asymptomatic microscopic hematuria in adults: summary of the AUA best practice policy recommendations. *Am Fam Physician* **63**, 1145-54.
36. Liebeskind, D. S. (2014). Nephrotic syndrome. *Handb Clin Neurol* **119**, 405-15.
37. Khanna, R. (2011). Clinical presentation & management of glomerular diseases: hematuria, nephritic & nephrotic syndrome. *Mo Med* **108**, 33-6.
38. Couser, W. G. (1988). Rapidly progressive glomerulonephritis: classification, pathogenetic mechanisms, and therapy. *Am J Kidney Dis* **11**, 449-64.
39. Turnbull, P. R. (1973). Aetiology of acute glomerulonephritis. *Br Med J* **2**, 666.
40. Abdullah, A., Khanam, A., Biswas, S., Niloy, A., Shahin, M., Murshed, K. & Sultana, T. (2008). Medical causes and histological pattern of glomerulonephritis. *Mymensingh Med J* **17**, 38-41.
41. Couser, W. G. (1993). Pathogenesis of glomerulonephritis. *Kidney Int Suppl* **42**, S19-26.
42. Puri, T. S. & Quigg, R. J. (2007). The many effects of complement C3- and C5-binding proteins in renal injury. *Semin Nephrol* **27**, 321-37.
43. Kurts, C., Heymann, F., Lukacs-Kornek, V., Boor, P. & Floege, J. (2007). Role of T cells and dendritic cells in glomerular immunopathology. *Semin Immunopathol* **29**, 317-35.
44. Tipping, P. G. & Kitching, A. R. (2005). Glomerulonephritis, Th1 and Th2: what's new? *Clin Exp Immunol* **142**, 207-15.
45. Chadban, S. J. & Atkins, R. C. (2005). Glomerulonephritis. *Lancet* **365**, 1797-806.
46. Nangaku, M. & Couser, W. G. (2005). Mechanisms of immune-deposit formation and the mediation of immune renal injury. *Clin Exp Nephrol* **9**, 183-91.
47. Mathieson, P. W. (2007). Glomerulonephritis. *Semin Immunopathol* **29**, 315-6.
48. Holdsworth, S. R., Kitching, A. R. & Tipping, P. G. (1999). Th1 and Th2 T helper cell subsets affect patterns of injury and outcomes in glomerulonephritis. *Kidney international* **55**, 1198-1216.
49. Couser, W. G. & Salant, D. J. (1980). In situ immune complex formation and glomerular injury. *Kidney Int* **17**, 1-13.
50. Tipping, P. & Kitching, A. (2005). Glomerulonephritis, Th1 and Th2: what's new? *Clinical & Experimental Immunology* **142**, 207-215.
51. Cohen, S. L., Fisher, C., Mowbray, J. F., Hopp, A. & Burton-Kee, J. (1979). Circulating and deposited immune complexes in renal disease and their clinical correlation. *J Clin Pathol* **32**, 1135-9.
52. Mannik, M. (1985). Deposition of Circulating Immune Complexes in Glomeruli. In *Chronic Renal Disease*, pp. 29-38. Springer.
53. Kitching, A. R., Tipping, P. G. & Holdsworth, S. R. (1999). IL-12 directs severe renal injury, crescent formation and Th1 responses in murine glomerulonephritis. *European journal of immunology* **29**, 1-10.
54. Kitching, A. R., Holdsworth, S. R. & Tipping, P. G. (1999). IFN-γ mediates crescent formation and cell-mediated immune injury in murine glomerulonephritis. *Journal of the American Society of Nephrology* **10**, 752-759.
55. Tipping, P. G. & Holdsworth, S. R. (2006). T cells in crescentic glomerulonephritis. *Journal of the American Society of Nephrology* **17**, 1253-1263.
56. Danoff, T. M. (1998). Chemokines in interstitial injury. *Kidney international* **53**, 1807-1808.
57. Brady, H. R. (1994). Leukocyte adhesion molecules and kidney diseases. *Kidney international* **45**.

58. Johnson, R. J., Couser, W. G., Chi, E. Y., Adler, S. & Klebanoff, S. J. (1987). New mechanism for glomerular injury. Myeloperoxidase-hydrogen peroxide-halide system. *J Clin Invest* **79**, 1379-87.
59. Johnson, R. J., Klebanoff, S. J., Ochi, R. F., Adler, S., Baker, P., Sparks, L. & Couser, W. G. (1987). Participation of the myeloperoxidase-H2O2-halide system in immune complex nephritis. *Kidney Int* **32**, 342-9.
60. Johnson, R. J., Alpers, C., Pritzl, P., Schulze, M., Baker, P., Pruchno, C. & Couser, W. (1988). Platelets mediate neutrophil-dependent immune complex nephritis in the rat. *Journal of Clinical Investigation* **82**, 1225.
61. Johnson, R., Couser, W. G., Alpers, C. E., Vissers, M., Schulze, M. & Klebanoff, S. J. (1988). The human neutrophil serine proteinases, elastase and cathepsin G, can mediate glomerular injury in vivo. *The Journal of experimental medicine* **168**, 1169-1174.
62. Nathan, C. F., Murray, H. W., Wiebe, M. E. & Rubin, B. Y. (1983). Identification of interferon-gamma as the lymphokine that activates human macrophage oxidative metabolism and antimicrobial activity. *J Exp Med* **158**, 670-89.
63. Stein, M., Keshav, S., Harris, N. & Gordon, S. (1992). Interleukin 4 potently enhances murine macrophage mannose receptor activity: a marker of alternative immunologic macrophage activation. *J Exp Med* **176**, 287-92.
64. Mills, C. D., Kincaid, K., Alt, J. M., Heilman, M. J. & Hill, A. M. (2000). M-1/M-2 macrophages and the Th1/Th2 paradigm. *J Immunol* **164**, 6166-73.
65. Gordon, S. (2003). Alternative activation of macrophages. *Nat Rev Immunol* **3**, 23-35.
66. Nathan, C. (1991). Mechanisms and modulation of macrophage activation. *Behring Inst Mitt*, 200-7.
67. Ulevitch, R. J. & Tobias, P. S. (1995). Receptor-dependent mechanisms of cell stimulation by bacterial endotoxin. *Annu Rev Immunol* **13**, 437-57.
68. Mogensen, T. H. (2009). Pathogen recognition and inflammatory signaling in innate immune defenses. *Clin Microbiol Rev* **22**, 240-73, Table of Contents.
69. Mosser, D. M. (2003). The many faces of macrophage activation. *J Leukoc Biol* **73**, 209-12.
70. Arnold, C. E., Whyte, C. S., Gordon, P., Barker, R. N., Rees, A. J. & Wilson, H. M. (2014). A critical role for suppressor of cytokine signalling 3 in promoting M1 macrophage activation and function in vitro and in vivo. *Immunology* **141**, 96-110.
71. MacMicking, J., Xie, Q. W. & Nathan, C. (1997). Nitric oxide and macrophage function. *Annu Rev Immunol* **15**, 323-50.
72. Iyer, S. S., Ghaffari, A. A. & Cheng, G. (2010). Lipopolysaccharide-mediated IL-10 transcriptional regulation requires sequential induction of type I IFNs and IL-27 in macrophages. *J Immunol* **185**, 6599-607.
73. Goerdt, S. & Orfanos, C. E. (1999). Other functions, other genes: alternative activation of antigen-presenting cells. *Immunity* **10**, 137-42.
74. Rutschman, R., Lang, R., Hesse, M., Ihle, J. N., Wynn, T. A. & Murray, P. J. (2001). Cutting edge: Stat6-dependent substrate depletion regulates nitric oxide production. *J Immunol* **166**, 2173-7.
75. Gratchev, A., Guillot, P., Hakiy, N., Politz, O., Orfanos, C. E., Schledzewski, K. & Goerdt, S. (2001). Alternatively activated macrophages differentially express fibronectin and its splice variants and the extracellular matrix protein betaIG-H3. *Scand J Immunol* **53**, 386-92.
76. Song, E., Ouyang, N., Horbelt, M., Antus, B., Wang, M. & Exton, M. S. (2000). Influence of alternatively and classically activated macrophages on fibrogenic activities of human fibroblasts. *Cell Immunol* **204**, 19-28.

77. Hesse, M., Modolell, M., La Flamme, A. C., Schito, M., Fuentes, J. M., Cheever, A. W., Pearce, E. J. & Wynn, T. A. (2001). Differential regulation of nitric oxide synthase-2 and arginase-1 by type 1/type 2 cytokines in vivo: granulomatous pathology is shaped by the pattern of L-arginine metabolism. *J Immunol* **167**, 6533-44.
78. Kodelja, V., Muller, C., Politz, O., Hakij, N., Orfanos, C. E. & Goerdt, S. (1998). Alternative macrophage activation-associated CC-chemokine-1, a novel structural homologue of macrophage inflammatory protein-1 alpha with a Th2-associated expression pattern. *J Immunol* **160**, 1411-8.
79. Raes, G., De Baetselier, P., Noel, W., Beschin, A., Brombacher, F. & Hassanzadeh Gh, G. (2002). Differential expression of FIZZ1 and Ym1 in alternatively versus classically activated macrophages. *J Leukoc Biol* **71**, 597-602.
80. Martinez, F. O., Helming, L., Milde, R., Varin, A., Melgert, B. N., Draijer, C., Thomas, B., Fabbri, M., Crawshaw, A., Ho, L. P., Ten Hacken, N. H., Cobos Jimenez, V., Kootstra, N. A., Hamann, J., Greaves, D. R., Locati, M., Mantovani, A. & Gordon, S. (2013). Genetic programs expressed in resting and IL-4 alternatively activated mouse and human macrophages: similarities and differences. *Blood* **121**, e57-69.
81. Anderson, C. F. & Mosser, D. M. (2002). A novel phenotype for an activated macrophage: the type 2 activated macrophage. *J Leukoc Biol* **72**, 101-6.
82. Sutterwala, F. S., Noel, G. J., Clynes, R. & Mosser, D. M. (1997). Selective Suppression of Interleukin-12 Induction after Macrophage Receptor Ligation. *The Journal of Experimental Medicine* **185**, 1977-1985.
83. Anderson, C. F. & Mosser, D. M. (2002). Cutting edge: biasing immune responses by directing antigen to macrophage Fc gamma receptors. *J Immunol* **168**, 3697-701.
84. Mantovani, A., Sica, A., Sozzani, S., Allavena, P., Vecchi, A. & Locati, M. (2004). The chemokine system in diverse forms of macrophage activation and polarization. *Trends Immunol* **25**, 677-86.
85. Roszer, T. (2015). Understanding the Mysterious M2 Macrophage through Activation Markers and Effector Mechanisms. *Mediators Inflamm* **2015**, 816460.
86. Duluc, D., Delneste, Y., Tan, F., Moles, M. P., Grimaud, L., Lenoir, J., Preisser, L., Anegon, I., Catala, L., Ifrah, N., Descamps, P., Gamelin, E., Gascan, H., Hebbar, M. & Jeannin, P. (2007). Tumor-associated leukemia inhibitory factor and IL-6 skew monocyte differentiation into tumor-associated macrophage-like cells. *Blood* **110**, 4319-30.
87. Qian, B.-Z. & Pollard, J. W. (2010). Macrophage diversity enhances tumor progression and metastasis. *Cell* **141**, 39-51.
88. Martinez, F. O. & Gordon, S. (2014). The M1 and M2 paradigm of macrophage activation: time for reassessment. *F1000Prime Reports* **6**, 13.
89. Foey, A. D. (2015). Macrophage Polarisation: A collaboration of Differentiation, Activation and Pre-Programming? *Journal of Clinical & Cellular Immunology* **2015**.
90. Kliem, V., Johnson, R. J., Alpers, C. E., Yoshimura, A., Couser, W. G., Koch, K. M. & Floege, J. (1996). Mechanisms involved in the pathogenesis of tubulointerstitial fibrosis in 5/6-nephrectomized rats. *Kidney Int* **49**, 666-78.
91. Fujihara, C. K., Malheiros, D. M., Zatz, R. & Noronha, I. L. (1998). Mycophenolate mofetil attenuates renal injury in the rat remnant kidney. *Kidney Int* **54**, 1510-9.
92. Yang, N., Wu, L. L., Nikolic-Paterson, D. J., Ng, Y. Y., Yang, W. C., Mu, W., Gilbert, R. E., Cooper, M. E., Atkins, R. C. & Lan, H. Y. (1998). Local macrophage and

myofibroblast proliferation in progressive renal injury in the rat remnant kidney. *Nephrology Dialysis Transplantation* **13**, 1967-1974.
93. Shimizu, A., Masuda, Y., Kitamura, H., Ishizaki, M., Sugisaki, Y. & Yamanaka, N. (1998). Recovery of damaged glomerular capillary network with endothelial cell apoptosis in experimental proliferative glomerulonephritis. *Nephron* **79**, 206-14.
94. Viale, G., Dell'Orto, P., Braidotti, P. & Coggi, G. (1985). Ultrastructural localization of intracellular immunoglobulins in Epon-embedded human lymph nodes. An immunoelectron microscopic investigation using the immunogold staining (IGS) and the avidin-biotin-peroxidase complex (ABC) methods. *J Histochem Cytochem* **33**, 400-6.
95. Isaka, Y., Akagi, Y., Ando, Y., Tsujie, M. & Imai, E. (1999). Cytokines and glomerulosclerosis. *Nephrol Dial Transplant* **14 Suppl 1**, 30-2.
96. Wiggins, R. C. (2007). The spectrum of podocytopathies: a unifying view of glomerular diseases. *Kidney Int* **71**, 1205-14.
97. Ziyadeh, F. N. & Wolf, G. (2008). Pathogenesis of the podocytopathy and proteinuria in diabetic glomerulopathy. *Curr Diabetes Rev* **4**, 39-45.
98. Kurogi, Y. (2003). Mesangial cell proliferation inhibitors for the treatment of proliferative glomerular disease. *Med Res Rev* **23**, 15-31.
99. Funabiki, K., Horikoshi, S., Tomino, Y., Nagai, Y. & Koide, H. (1990). Immunohistochemical analysis of extracellular components in the glomerular sclerosis of patients with glomerulonephritis. *Clin Nephrol* **34**, 239-46.
100. Massy, Z. A., Guijarro, C., O'Donnell, M. P., Kim, Y., Kashtan, C. E., Egido, J., Kasiske, B. L. & Keane, W. F. (1999). The central role of nuclear factor-kappa B in mesangial cell activation. *Kidney Int Suppl* **71**, S76-9.
101. Johnson, R. J., Iida, H., Alpers, C. E., Majesky, M. W., Schwartz, S. M., Pritzi, P., Gordon, K. & Gown, A. M. (1991). Expression of smooth muscle cell phenotype by rat mesangial cells in immune complex nephritis. Alpha-smooth muscle actin is a marker of mesangial cell proliferation. *J Clin Invest* **87**, 847-58.
102. Alpers, C. E., Hudkins, K. L., Gown, A. M. & Johnson, R. J. (1992). Enhanced expression of "muscle-specific" actin in glomerulonephritis. *Kidney Int* **41**, 1134-42.
103. Strutz, F. & Neilson, E. G. (2003). New insights into mechanisms of fibrosis in immune renal injury. *Springer Semin Immunopathol* **24**, 459-76.
104. Morel-Maroger Striker, L., Killen, P. D., Chi, E. & Striker, G. E. (1984). The composition of glomerulosclerosis. I. Studies in focal sclerosis, crescentic glomerulonephritis, and membranoproliferative glomerulonephritis. *Lab Invest* **51**, 181-92.
105. Stokes, M. B., Holler, S., Cui, Y., Hudkins, K. L., Eitner, F., Fogo, A. & Alpers, C. E. (2000). Expression of decorin, biglycan, and collagen type I in human renal fibrosing disease. *Kidney Int* **57**, 487-98.
106. Couser, W. G. & Johnson, R. J. (1994). Mechanisms of progressive renal disease in glomerulonephritis. *Am J Kidney Dis* **23**, 193-8.
107. Floege, J., Johnson, R. J. & Couser, W. G. (1992). Mesangial cells in the pathogenesis of progressive glomerular disease in animal models. *Clin Investig* **70**, 857-64.
108. Makino, H., Kashihara, N., Sugiyama, H., Sekikawa, T. & Ota, Z. (1996). Role of apoptosis in the progression of glomerulosclerosis. *Contrib Nephrol* **118**, 41-7.
109. Mundel, P. & Kriz, W. (1995). Structure and function of podocytes: an update. *Anat Embryol (Berl)* **192**, 385-97.

110. Kreidberg, J. A., Donovan, M. J., Goldstein, S. L., Rennke, H., Shepherd, K., Jones, R. C. & Jaenisch, R. (1996). Alpha 3 beta 1 integrin has a crucial role in kidney and lung organogenesis. *Development* **122**, 3537-47.
111. Raats, C. J., van den Born, J., Bakker, M. A., Oppers-Walgreen, B., Pisa, B. J., Dijkman, H. B., Assmann, K. J. & Berden, J. H. (2000). Expression of agrin, dystroglycan, and utrophin in normal renal tissue and in experimental glomerulopathies. *Am J Pathol* **156**, 1749-65.
112. Adler, S. & Chen, X. (1992). Anti-Fx1A antibody recognizes a beta 1-integrin on glomerular epithelial cells and inhibits adhesion and growth. *Am J Physiol* **262**, F770-6.
113. Pavenstadt, H., Kriz, W. & Kretzler, M. (2003). Cell biology of the glomerular podocyte. *Physiol Rev* **83**, 253-307.
114. Kaplan, J. M., Kim, S. H., North, K. N., Rennke, H., Correia, L. A., Tong, H. Q., Mathis, B. J., Rodriguez-Perez, J. C., Allen, P. G., Beggs, A. H. & Pollak, M. R. (2000). Mutations in ACTN4, encoding alpha-actinin-4, cause familial focal segmental glomerulosclerosis. *Nat Genet* **24**, 251-6.
115. Mundel, P., Heid, H. W., Mundel, T. M., Kruger, M., Reiser, J. & Kriz, W. (1997). Synaptopodin: an actin-associated protein in telencephalic dendrites and renal podocytes. *J Cell Biol* **139**, 193-204.
116. Greka, A. & Mundel, P. (2012). Cell biology and pathology of podocytes. *Annu Rev Physiol* **74**, 299-323.
117. http://www.pathguy.com/sol/46463.jpg.
118. Ruotsalainen, V., Ljungberg, P., Wartiovaara, J., Lenkkeri, U., Kestila, M., Jalanko, H., Holmberg, C. & Tryggvason, K. (1999). Nephrin is specifically located at the slit diaphragm of glomerular podocytes. *Proc Natl Acad Sci U S A* **96**, 7962-7.
119. Huber, T. B., Kottgen, M., Schilling, B., Walz, G. & Benzing, T. (2001). Interaction with podocin facilitates nephrin signaling. *J Biol Chem* **276**, 41543-6.
120. Roselli, S., Gribouval, O., Boute, N., Sich, M., Benessy, F., Attie, T., Gubler, M. C. & Antignac, C. (2002). Podocin localizes in the kidney to the slit diaphragm area. *Am J Pathol* **160**, 131-9.
121. Huber, T. B., Simons, M., Hartleben, B., Sernetz, L., Schmidts, M., Gundlach, E., Saleem, M. A., Walz, G. & Benzing, T. (2003). Molecular basis of the functional podocin-nephrin complex: mutations in the NPHS2 gene disrupt nephrin targeting to lipid raft microdomains. *Hum Mol Genet* **12**, 3397-405.
122. Huber, T. B., Schermer, B., Muller, R. U., Hohne, M., Bartram, M., Calixto, A., Hagmann, H., Reinhardt, C., Koos, F., Kunzelmann, K., Shirokova, E., Krautwurst, D., Harteneck, C., Simons, M., Pavenstadt, H., Kerjaschki, D., Thiele, C., Walz, G., Chalfie, M. & Benzing, T. (2006). Podocin and MEC-2 bind cholesterol to regulate the activity of associated ion channels. *Proc Natl Acad Sci U S A* **103**, 17079-86.
123. Boute, N., Gribouval, O., Roselli, S., Benessy, F., Lee, H., Fuchshuber, A., Dahan, K., Gubler, M. C., Niaudet, P. & Antignac, C. (2000). NPHS2, encoding the glomerular protein podocin, is mutated in autosomal recessive steroid-resistant nephrotic syndrome. *Nat Genet* **24**, 349-54.
124. Pawson, T. (1995). Protein modules and signalling networks. *Nature* **373**, 573-80.
125. Lehtonen, S. (2008). Connecting the interpodocyte slit diaphragm and actin dynamics: Emerging role for the nephrin signaling complex. *Kidney Int* **73**, 903-5.
126. Benzing, T. (2004). Signaling at the slit diaphragm. *J Am Soc Nephrol* **15**, 1382-91.

127. Li, C., Ruotsalainen, V., Tryggvason, K., Shaw, A. S. & Miner, J. H. (2000). CD2AP is expressed with nephrin in developing podocytes and is found widely in mature kidney and elsewhere. *Am J Physiol Renal Physiol* **279**, F785-92.
128. Shih, N. Y., Li, J., Karpitskii, V., Nguyen, A., Dustin, M. L., Kanagawa, O., Miner, J. H. & Shaw, A. S. (1999). Congenital nephrotic syndrome in mice lacking CD2-associated protein. *Science* **286**, 312-5.
129. Verma, R., Wharram, B., Kovari, I., Kunkel, R., Nihalani, D., Wary, K. K., Wiggins, R. C., Killen, P. & Holzman, L. B. (2003). Fyn binds to and phosphorylates the kidney slit diaphragm component Nephrin. *J Biol Chem* **278**, 20716-23.
130. Ashworth, S., Teng, B., Kaufeld, J., Miller, E., Tossidou, I., Englert, C., Bollig, F., Staggs, L., Roberts, I. S., Park, J. K., Haller, H. & Schiffer, M. (2010). Cofilin-1 inactivation leads to proteinuria--studies in zebrafish, mice and humans. *PLoS One* **5**, e12626.
131. Huber, T. B., Hartleben, B., Kim, J., Schmidts, M., Schermer, B., Keil, A., Egger, L., Lecha, R. L., Borner, C., Pavenstadt, H., Shaw, A. S., Walz, G. & Benzing, T. (2003). Nephrin and CD2AP associate with phosphoinositide 3-OH kinase and stimulate AKT-dependent signaling. *Mol Cell Biol* **23**, 4917-28.
132. Huber, T. B., Kwoh, C., Wu, H., Asanuma, K., Godel, M., Hartleben, B., Blumer, K. J., Miner, J. H., Mundel, P. & Shaw, A. S. (2006). Bigenic mouse models of focal segmental glomerulosclerosis involving pairwise interaction of CD2AP, Fyn, and synaptopodin. *J Clin Invest* **116**, 1337-45.
133. Lehtonen, S., Ryan, J. J., Kudlicka, K., Iino, N., Zhou, H. & Farquhar, M. G. (2005). Cell junction-associated proteins IQGAP1, MAGI-2, CASK, spectrins, and alpha-actinin are components of the nephrin multiprotein complex. *Proc Natl Acad Sci U S A* **102**, 9814-9.
134. Shukla, A. K., Xiao, K. & Lefkowitz, R. J. (2011). Emerging paradigms of beta-arrestin-dependent seven transmembrane receptor signaling. *Trends Biochem Sci* **36**, 457-69.
135. Maguire, J. J., Kuc, R. E., Pell, V. R., Green, A., Brown, M., Kumar, S., Wehrman, T., Quinn, E. & Davenport, A. P. (2012). Comparison of human ETA and ETB receptor signalling via G-protein and beta-arrestin pathways. *Life Sci* **91**, 544-9.
136. Shenoy, S. K. & Lefkowitz, R. J. (2011). β-arrestin-mediated receptor trafficking and signal transduction. *Trends in Pharmacological Sciences* **32**, 521-533.
137. Kerjaschki, D., Sharkey, D. J. & Farquhar, M. G. (1984). Identification and characterization of podocalyxin--the major sialoprotein of the renal glomerular epithelial cell. *J Cell Biol* **98**, 1591-6.
138. Matsui, K., Breitender-Geleff, S., Soleiman, A., Kowalski, H. & Kerjaschki, D. (1999). Podoplanin, a novel 43-kDa membrane protein, controls the shape of podocytes. *Nephrol Dial Transplant* **14 Suppl 1**, 9-11.
139. Moreno, J. A., Sanchez-Nino, M. D., Sanz, A. B., Lassila, M., Holthofer, H., Blanco-Colio, L. M., Egido, J., Ruiz-Ortega, M. & Ortiz, A. (2008). A slit in podocyte death. *Curr Med Chem* **15**, 1645-54.
140. Kang, Y. S., Li, Y., Dai, C., Kiss, L. P., Wu, C. & Liu, Y. (2010). Inhibition of integrin-linked kinase blocks podocyte epithelial-mesenchymal transition and ameliorates proteinuria. *Kidney Int* **78**, 363-73.
141. Vleming, L. J., Bruijn, J. A. & van Es, L. A. (1999). The pathogenesis of progressive renal failure. *Neth J Med* **54**, 114-28.
142. Jaimes, E. A., Galceran, J. M. & Raij, L. (1998). Angiotensin II induces superoxide anion production by mesangial cells. *Kidney Int* **54**, 775-84.
143. Grande, M. T., Perez-Barriocanal, F. & Lopez-Novoa, J. M. (2010). Role of inflammation in tubulo-interstitial damage associated to obstructive nephropathy. *J Inflamm (Lond)* **7**, 19.

144. Eddy, A. A. (2000). Molecular basis of renal fibrosis. *Pediatr Nephrol* **15**, 290-301.
145. Liu, Y. (2006). Renal fibrosis: new insights into the pathogenesis and therapeutics. *Kidney Int* **69**, 213-7.
146. Ruiz-Ortega, M. & Egido, J. (1997). Angiotensin II modulates cell growth-related events and synthesis of matrix proteins in renal interstitial fibroblasts. *Kidney Int* **52**, 1497-510.
147. Desmoulière, A., Geinoz, A., Gabbiani, F. & Gabbiani, G. (1993). Transforming growth factor-beta 1 induces alpha-smooth muscle actin expression in granulation tissue myofibroblasts and in quiescent and growing cultured fibroblasts. *The Journal of Cell Biology* **122**, 103-111.
148. Strutz, F., Muller, G. A. & Neilson, E. G. (1996). Transdifferentiation: a new angle on renal fibrosis. *Exp Nephrol* **4**, 267-70.
149. Zhang, G., Moorhead, P. J. & el Nahas, A. M. (1995). Myofibroblasts and the progression of experimental glomerulonephritis. *Exp Nephrol* **3**, 308-18.
150. Gharaee-Kermani, M., Wiggins, R., Wolber, F., Goyal, M. & Phan, S. H. (1996). Fibronectin is the major fibroblast chemoattractant in rabbit anti-glomerular basement membrane disease. *Am J Pathol* **148**, 961-7.
151. Eddy, A. A. (1994). Experimental insights into the tubulointerstitial disease accompanying primary glomerular lesions. *J Am Soc Nephrol* **5**, 1273-87.
152. Van Vliet, A., Baelde, H. J., Vleming, L. J., de Heer, E. & Bruijn, J. A. (2001). Distribution of fibronectin isoforms in human renal disease. *J Pathol* **193**, 256-62.
153. Wells, A. F., Larsson, E., Tengblad, A., Fellstrom, B., Tufveson, G., Klareskog, L. & Laurent, T. C. (1990). The localization of hyaluronan in normal and rejected human kidneys. *Transplantation* **50**, 240-3.
154. Beck-Schimmer, B., Oertli, B., Pasch, T. & Wuthrich, R. P. (1998). Hyaluronan induces monocyte chemoattractant protein-1 expression in renal tubular epithelial cells. *J Am Soc Nephrol* **9**, 2283-90.
155. Crawford, S. E., Stellmach, V., Murphy-Ullrich, J. E., Ribeiro, S. M., Lawler, J., Hynes, R. O., Boivin, G. P. & Bouck, N. (1998). Thrombospondin-1 is a major activator of TGF-beta1 in vivo. *Cell* **93**, 1159-70.
156. Hugo, C., Shankland, S. J., Pichler, R. H., Couser, W. G. & Johnson, R. J. (1998). Thrombospondin 1 precedes and predicts the development of tubulointerstitial fibrosis in glomerular disease in the rat. *Kidney Int* **53**, 302-11.
157. Diamond, J. R., Levinson, M., Kreisberg, R. & Ricardo, S. D. (1997). Increased expression of decorin in experimental hydronephrosis. *Kidney Int* **51**, 1133-9.
158. Schaefer, L., Hausser, H., Altenburger, M., Ugorcakova, J., August, C., Fisher, L. W., Schaefer, R. M. & Kresse, H. (1998). Decorin, biglycan and their endocytosis receptor in rat renal cortex. *Kidney Int* **54**, 1529-41.
159. Gonzalez-Avila, G., Vadillo-Ortega, F. & Perez-Tamayo, R. (1988). Experimental diffuse interstitial renal fibrosis. A biochemical approach. *Lab Invest* **59**, 245-52.
160. Eddy, A. A. & Fogo, A. B. (2006). Plasminogen Activator Inhibitor-1 in Chronic Kidney Disease: Evidence and Mechanisms of Action. *Journal of the American Society of Nephrology* **17**, 2999-3012.
161. Hultstrom, M., Leh, S., Skogstrand, T. & Iversen, B. M. (2008). Upregulation of tissue inhibitor of metalloproteases-1 (TIMP-1) and procollagen-N-peptidase in hypertension-induced renal damage. *Nephrol Dial Transplant* **23**, 896-903.
162. Kim, H., Oda, T., Lopez-Guisa, J., Wing, D., Edwards, D. R., Soloway, P. D. & Eddy, A. A. (2001). TIMP-1 deficiency does not attenuate interstitial fibrosis in obstructive nephropathy. *J Am Soc Nephrol* **12**, 736-48.

163. Sanchez-Nino, M. D., Benito-Martin, A., Goncalves, S., Sanz, A. B., Ucero, A. C., Izquierdo, M. C., Ramos, A. M., Berzal, S., Selgas, R., Ruiz-Ortega, M., Egido, J. & Ortiz, A. (2010). TNF superfamily: a growing saga of kidney injury modulators. *Mediators Inflamm* **2010**.
164. Singer, A. J. & Clark, R. A. (1999). Cutaneous wound healing. *N Engl J Med* **341**, 738-46.
165. Eddy, A. (2001). Role of cellular infiltrates in response to proteinuria. *Am J Kidney Dis* **37**, S25-9.
166. Nishida, M., Fujinaka, H., Matsusaka, T., Price, J., Kon, V., Fogo, A. B., Davidson, J. M., Linton, M. F., Fazio, S., Homma, T., Yoshida, H. & Ichikawa, I. (2002). Absence of angiotensin II type 1 receptor in bone marrow-derived cells is detrimental in the evolution of renal fibrosis. *J Clin Invest* **110**, 1859-68.
167. Van Goor, H., Ding, G., Kees-Folts, D., Grond, J., Schreiner, G. F. & Diamond, J. R. (1994). Macrophages and renal disease. *Lab Invest* **71**, 456-64.
168. Campbell, R., Sangalli, F., Perticucci, E., Aros, C., Viscarra, C., Perna, A., Remuzzi, A., Bertocchi, F., Fagiani, L., Remuzzi, G. & Ruggenenti, P. (2003). Effects of combined ACE inhibitor and angiotensin II antagonist treatment in human chronic nephropathies. *Kidney Int* **63**, 1094-103.
169. Lopez-Novoa, J. M., Martinez-Salgado, C., Rodriguez-Pena, A. B. & Lopez-Hernandez, F. J. (2010). Common pathophysiological mechanisms of chronic kidney disease: therapeutic perspectives. *Pharmacol Ther* **128**, 61-81.
170. Chen, H. C., Chen, C. A., Guh, J. Y., Chang, J. M., Shin, S. J. & Lai, Y. H. (2000). Altering expression of alpha3beta1 integrin on podocytes of human and rats with diabetes. *Life Sci* **67**, 2345-53.
171. Regoli, M. & Bendayan, M. (1997). Alterations in the expression of the alpha 3 beta 1 integrin in certain membrane domains of the glomerular epithelial cells (podocytes) in diabetes mellitus. *Diabetologia* **40**, 15-22.
172. Asano, T., Niimura, F., Pastan, I., Fogo, A. B., Ichikawa, I. & Matsusaka, T. (2005). Permanent genetic tagging of podocytes: fate of injured podocytes in a mouse model of glomerular sclerosis. *J Am Soc Nephrol* **16**, 2257-62.
173. Pagtalunan, M. E., Miller, P. L., Jumping-Eagle, S., Nelson, R. G., Myers, B. D., Rennke, H. G., Coplon, N. S., Sun, L. & Meyer, T. W. (1997). Podocyte loss and progressive glomerular injury in type II diabetes. *J Clin Invest* **99**, 342-8.
174. Lemley, K. V., Lafayette, R. A., Safai, M., Derby, G., Blouch, K., Squarer, A. & Myers, B. D. (2002). Podocytopenia and disease severity in IgA nephropathy. *Kidney Int* **61**, 1475-85.
175. Mathieson, P. W. (2012). The podocyte as a target for therapies--new and old. *Nat Rev Nephrol* **8**, 52-6.
176. Mundel, P. & Shankland, S. J. (2002). Podocyte biology and response to injury. *Journal of the American Society of Nephrology* **13**, 3005-3015.
177. Kriz, W., Gretz, N. & Lemley, K. V. (1998). Progression of glomerular diseases: is the podocyte the culprit? *Kidney Int* **54**, 687-97.
178. Shankland, S. J. (2006). The podocyte's response to injury: role in proteinuria and glomerulosclerosis. *Kidney Int* **69**, 2131-47.
179. Barisoni, L. & Mundel, P. (2003). Podocyte biology and the emerging understanding of podocyte diseases. *Am J Nephrol* **23**, 353-60.
180. Couser, W. G. & Nangaku, M. (2006). Cellular and molecular biology of membranous nephropathy. *J Nephrol* **19**, 699-705.
181. Kerjaschki, D. & Neale, T. J. (1996). Molecular mechanisms of glomerular injury in rat experimental membranous nephropathy (Heymann nephritis). *Journal of the American Society of Nephrology* **7**, 2518-2526.

182. Banas, M. C., Banas, B., Hudkins, K. L., Wietecha, T. A., Iyoda, M., Bock, E., Hauser, P., Pippin, J. W., Shankland, S. J., Smith, K. D., Stoelcker, B., Liu, G., Gröne, H.-J., Krämer, B. K. & Alpers, C. E. (2008). TLR4 Links Podocytes with the Innate Immune System to Mediate Glomerular Injury. *Journal of the American Society of Nephrology* **19**, 704-713.
183. Inokuchi, S., Shirato, I., Kobayashi, N., Koide, H., Tomino, Y. & Sakai, T. (1996). Re-evaluation of foot process effacement in acute puromycin aminonucleoside nephrosis. *Kidney Int* **50**, 1278-87.
184. Sanwal, V., Pandya, M., Bhaskaran, M., Franki, N., Reddy, K., Ding, G., Kapasi, A., Valderrama, E. & Singhal, P. C. (2001). Puromycin aminonucleoside induces glomerular epithelial cell apoptosis. *Exp Mol Pathol* **70**, 54-64.
185. Remuzzi, G. & Bertani, T. (1998). Pathophysiology of progressive nephropathies. *N Engl J Med* **339**, 1448-56.
186. Morioka, Y., Koike, H., Ikezumi, Y., Ito, Y., Oyanagi, A., Gejyo, F., Shimizu, F. & Kawachi, H. (2001). Podocyte injuries exacerbate mesangial proliferative glomerulonephritis. *Kidney Int* **60**, 2192-204.
187. Sawai, K., Mori, K., Mukoyama, M., Sugawara, A., Suganami, T., Koshikawa, M., Yahata, K., Makino, H., Nagae, T., Fujinaga, Y., Yokoi, H., Yoshioka, T., Yoshimoto, A., Tanaka, I. & Nakao, K. (2003). Angiogenic protein Cyr61 is expressed by podocytes in anti-Thy-1 glomerulonephritis. *J Am Soc Nephrol* **14**, 1154-63.
188. Kestila, M., Lenkkeri, U., Mannikko, M., Lamerdin, J., McCready, P., Putaala, H., Ruotsalainen, V., Morita, T., Nissinen, M., Herva, R., Kashtan, C. E., Peltonen, L., Holmberg, C., Olsen, A. & Tryggvason, K. (1998). Positionally cloned gene for a novel glomerular protein--nephrin--is mutated in congenital nephrotic syndrome. *Mol Cell* **1**, 575-82.
189. Li, C., Ruotsalainen, V., Tryggvason, K., Shaw, A. S. & Miner, J. H. (2000). CD2AP is expressed with nephrin in developing podocytes and is found widely in mature kidney and elsewhere. *American Journal of Physiology-Renal Physiology* **279**, F785-F792.
190. Kim, J. M., Wu, H., Green, G., Winkler, C. A., Kopp, J. B., Miner, J. H., Unanue, E. R. & Shaw, A. S. (2003). CD2-associated protein haploinsufficiency is linked to glomerular disease susceptibility. *Science* **300**, 1298-1300.
191. Shih, N.-Y., Li, J., Karpitskii, V., Nguyen, A., Dustin, M. L., Kanagawa, O., Miner, J. H. & Shaw, A. S. (1999). Congenital nephrotic syndrome in mice lacking CD2-associated protein. *Science* **286**, 312-315.
192. Davies, D. J., Messina, A., Thumwood, C. M. & Ryan, G. B. (1985). Glomerular podocytic injury in protein overload proteinuria. *Pathology* **17**, 412-9.
193. Eyre, J., Ioannou, K., Grubb, B. D., Saleem, M. A., Mathieson, P. W., Brunskill, N. J., Christensen, E. I. & Topham, P. S. (2007). Statin-sensitive endocytosis of albumin by glomerular podocytes. *Am J Physiol Renal Physiol* **292**, F674-81.
194. Yoshida, S., Nagase, M., Shibata, S. & Fujita, T. (2008). Podocyte injury induced by albumin overload in vivo and in vitro: involvement of TGF-beta and p38 MAPK. *Nephron Exp Nephrol* **108**, e57-68.
195. Morigi, M., Buelli, S., Angioletti, S., Zanchi, C., Longaretti, L., Zoja, C., Galbusera, M., Gastoldi, S., Mundel, P., Remuzzi, G. & Benigni, A. (2005). In response to protein load podocytes reorganize cytoskeleton and modulate endothelin-1 gene: implication for permselective dysfunction of chronic nephropathies. *Am J Pathol* **166**, 1309-20.
196. Yee, J., Kuncio, G. S. & Neilson, E. G. (1991). Tubulointerstitial injury following glomerulonephritis. *Semin Nephrol* **11**, 361-6.

197. Schiffer, M., Schiffer, L. E., Gupta, A., Shaw, A. S., Roberts, I. S., Mundel, P. & Bottinger, E. P. (2002). Inhibitory Smads and TGF-beta signaling in glomerular cells. *J Am Soc Nephrol* **13**, 2657-66.
198. Takano, Y., Yamauchi, K., Hayakawa, K., Hiramatsu, N., Kasai, A., Okamura, M., Yokouchi, M., Shitamura, A., Yao, J. & Kitamura, M. (2007). Transcriptional suppression of nephrin in podocytes by macrophages: roles of inflammatory cytokines and involvement of the PI3K/Akt pathway. *FEBS Lett* **581**, 421-6.
199. Ikezumi, Y., Suzuki, T., Karasawa, T., Kawachi, H., Nikolic-Paterson, D. J. & Uchiyama, M. (2008). Activated macrophages down-regulate podocyte nephrin and podocin expression via stress-activated protein kinases. *Biochem Biophys Res Commun* **376**, 706-11.
200. Durvasula, R. V., Petermann, A. T., Hiromura, K., Blonski, M., Pippin, J., Mundel, P., Pichler, R., Griffin, S., Couser, W. G. & Shankland, S. J. (2004). Activation of a local tissue angiotensin system in podocytes by mechanical strain. *Kidney Int* **65**, 30-9.
201. Endlich, N., Kress, K. R., Reiser, J., Uttenweiler, D., Kriz, W., Mundel, P. & Endlich, K. (2001). Podocytes respond to mechanical stress in vitro. *J Am Soc Nephrol* **12**, 413-22.
202. Gloy, J., Henger, A., Fischer, K. G., Nitschke, R., Mundel, P., Bleich, M., Schollmeyer, P., Greger, R. & Pavenstadt, H. (1997). Angiotensin II depolarizes podocytes in the intact glomerulus of the Rat. *J Clin Invest* **99**, 2772-81.
203. Sharma, R., Lovell, H. B., Wiegmann, T. B. & Savin, V. J. (1992). Vasoactive substances induce cytoskeletal changes in cultured rat glomerular epithelial cells. *J Am Soc Nephrol* **3**, 1131-8.
204. Ding, G., Reddy, K., Kapasi, A. A., Franki, N., Gibbons, N., Kasinath, B. S. & Singhal, P. C. (2002). Angiotensin II induces apoptosis in rat glomerular epithelial cells. *American Journal of Physiology - Renal Physiology* **283**, F173-F180.
205. Macconi, D., Abbate, M., Morigi, M., Angioletti, S., Mister, M., Buelli, S., Bonomelli, M., Mundel, P., Endlich, K., Remuzzi, A. & Remuzzi, G. (2006). Permselective dysfunction of podocyte-podocyte contact upon angiotensin II unravels the molecular target for renoprotective intervention. *Am J Pathol* **168**, 1073-85.
206. Chen, S., Kasama, Y., Lee, J. S., Jim, B., Marin, M. & Ziyadeh, F. N. (2004). Podocyte-derived vascular endothelial growth factor mediates the stimulation of alpha3(IV) collagen production by transforming growth factor-beta1 in mouse podocytes. *Diabetes* **53**, 2939-49.
207. Kang, Y. S., Park, Y. G., Kim, B. K., Han, S. Y., Jee, Y. H., Han, K. H., Lee, M. H., Song, H. K., Cha, D. R., Kang, S. W. & Han, D. S. (2006). Angiotensin II stimulates the synthesis of vascular endothelial growth factor through the p38 mitogen activated protein kinase pathway in cultured mouse podocytes. *J Mol Endocrinol* **36**, 377-88.
208. Yanagisawa, M., Kurihara, H., Kimura, S., Tomobe, Y., Kobayashi, M., Mitsui, Y., Yazaki, Y., Goto, K. & Masaki, T. (1988). A novel potent vasoconstrictor peptide produced by vascular endothelial cells. *Nature* **332**, 411-5.
209. Inoue, A., Yanagisawa, M., Kimura, S., Kasuya, Y., Miyauchi, T., Goto, K. & Masaki, T. (1989). The human endothelin family: three structurally and pharmacologically distinct isopeptides predicted by three separate genes. *Proc Natl Acad Sci U S A* **86**, 2863-7.
210. Arinami, T., Ishikawa, M., Inoue, A., Yanagisawa, M., Masaki, T., Yoshida, M. C. & Hamaguchi, H. (1991). Chromosomal assignments of the human endothelin family genes: the endothelin-1 gene (EDN1) to 6p23-p24, the endothelin-2 gene (EDN2) to 1p34, and the endothelin-3 gene (EDN3) to 20q13.2-q13.3. *Am J Hum Genet* **48**, 990-6.

211. Haynes, W. G. & Webb, D. J. (1994). Contribution of endogenous generation of endothelin-1 to basal vascular tone. *Lancet* **344**, 852-4.
212. Wesson, D. E., Simoni, J. & Green, D. F. (1998). Reduced extracellular pH increases endothelin-1 secretion by human renal microvascular endothelial cells. *J Clin Invest* **101**, 578-83.
213. Attina, T., Camidge, R., Newby, D. E. & Webb, D. J. (2005). Endothelin antagonism in pulmonary hypertension, heart failure, and beyond. *Heart* **91**, 825-31.
214. Eid, H., de Bold, M. L., Chen, J. H. & de Bold, A. J. (1994). Epicardial mesothelial cells synthesize and release endothelin. *J Cardiovasc Pharmacol* **24**, 715-20.
215. Yoshimoto, S., Ishizaki, Y., Sasaki, T. & Murota, S. (1991). Effect of carbon dioxide and oxygen on endothelin production by cultured porcine cerebral endothelial cells. *Stroke* **22**, 378-83.
216. Sakurai, T., Yanagisawa, M. & Masaki, T. (1992). Molecular characterization of endothelin receptors. *Trends Pharmacol Sci* **13**, 103-8.
217. Arai, H., Hori, S., Aramori, I., Ohkubo, H. & Nakanishi, S. (1990). Cloning and expression of a cDNA encoding an endothelin receptor. *Nature* **348**, 730-2.
218. de Nucci, G., Thomas, R., D'Orleans-Juste, P., Antunes, E., Walder, C., Warner, T. D. & Vane, J. R. (1988). Pressor effects of circulating endothelin are limited by its removal in the pulmonary circulation and by the release of prostacyclin and endothelium-derived relaxing factor. *Proc Natl Acad Sci U S A* **85**, 9797-800.
219. Dupuis, J., Stewart, D. J., Cernacek, P. & Gosselin, G. (1996). Human pulmonary circulation is an important site for both clearance and production of endothelin-1. *Circulation* **94**, 1578-84.
220. Fukuroda, T., Fujikawa, T., Ozaki, S., Ishikawa, K., Yano, M. & Nishikibe, M. (1994). Clearance of circulating endothelin-1 by ETB receptors in rats. *Biochem Biophys Res Commun* **199**, 1461-5.
221. Serneri, G. G., Modesti, P. A., Cecioni, I., Biagini, D., Migliorini, A., Costoli, A., Colella, A., Naldoni, A. & Paoletti, P. (1995). Plasma endothelin and renal endothelin are two distinct systems involved in volume homeostasis. *American Journal of Physiology - Heart and Circulatory Physiology* **268**, H1829-H1837.
222. Yanagisawa, M., Kurihara, H., Kimura, S., Goto, K. & Masaki, T. (1988). A novel peptide vasoconstrictor, endothelin, is produced by vascular endothelium and modulates smooth muscle Ca2+ channels. *J Hypertens Suppl* **6**, S188-91.
223. King, A. J., Brenner, B. M. & Anderson, S. (1989). Endothelin: a potent renal and systemic vasoconstrictor peptide. *Am J Physiol* **256**, F1051-8.
224. Munger, K. A., Sugiura, M., Inagami, T., Takahashi, K. & Bath, K. F. (1989). Mechanisms of endothelin-induced natriuresis in the rat. *Clin Res* **37**, 497a.
225. Cunningham, M. E., Huribal, M., Bala, R. J. & McMillen, M. A. (1997). Endothelin-1 and endothelin-4 stimulate monocyte production of cytokines. *Crit Care Med* **25**, 958-64.
226. Kohan, D. E. & Fiedorek, F. T., Jr. (1991). Endothelin synthesis by rat inner medullary collecting duct cells. *J Am Soc Nephrol* **2**, 150-5.
227. Ehrenreich, H., Anderson, R. W., Fox, C. H., Rieckmann, P., Hoffman, G. S., Travis, W. D., Coligan, J. E., Kehrl, J. H. & Fauci, A. S. (1990). Endothelins, peptides with potent vasoactive properties, are produced by human macrophages. *J Exp Med* **172**, 1741-8.
228. Kohan, D. E. & Fiedorek, F. T. (1991). Endothelin synthesis by rat inner medullary collecting duct cells. *Journal of the American Society of Nephrology* **2**, 150-5.
229. Kuc, R. & Davenport, A. P. (2004). Comparison of endothelin-A and endothelin-B receptor distribution visualized by radioligand binding versus

immunocytochemical localization using subtype selective antisera. *J Cardiovasc Pharmacol* **44 Suppl 1**, S224-6.
230. Lanese, D. M. & Conger, J. D. (1993). Effects of endothelin receptor antagonist on cyclosporine-induced vasoconstriction in isolated rat renal arterioles. *J Clin Invest* **91**, 2144-9.
231. Fukuda, K., Yanagida, T., Okuda, S., Tamaki, K., Ando, T. & Fujishima, M. (1996). Role of endothelin as a mitogen in experimental glomerulonephritis in rats. *Kidney Int* **49**, 1320-9.
232. Harris, P. J., Zhuo, J., Mendelsohn, F. A. & Skinner, S. L. (1991). Haemodynamic and renal tubular effects of low doses of endothelin in anaesthetized rats. *J Physiol* **433**, 25-39.
233. Humbert, M. & Ghofrani, H.-A. (2015). The molecular targets of approved treatments for pulmonary arterial hypertension. *Thorax*, thoraxjnl-2015-207170.
234. Giaid, A., Yanagisawa, M., Langleben, D., Michel, R. P., Levy, R., Shennib, H., Kimura, S., Masaki, T., Duguid, W. P. & Stewart, D. J. (1993). Expression of endothelin-1 in the lungs of patients with pulmonary hypertension. *New England Journal of Medicine* **328**, 1732-1739.
235. Cacoub, P., Dorent, R., Nataf, P., Carayon, A., Riquet, M., Noe, E., Piette, J. C., Godeau, P. & Gandjbakhch, I. (1997). Endothelin-1 in the lungs of patients with pulmonary hypertension. *Cardiovascular research* **33**, 196-200.
236. Dupuis, J., Cernacek, P., Tardif, J.-C., Stewart, D. J., Gosselin, G., Dyrda, I., Bonan, R. & Crépeau, J. (1998). Reduced pulmonary clearance of endothelin-1 in pulmonary hypertension. *American heart journal* **135**, 614-620.
237. Marques, J. S., Martins, S. R., Calisto, C., Gonçalves, S., Almeida, A. G., de Sousa, J. C., Pinto, F. J. & Diogo, A. N. (2013). An exploratory panel of biomarkers for risk prediction in pulmonary hypertension: emerging role of CT-proET-1. *The Journal of Heart and Lung Transplantation* **32**, 1214-1221.
238. Montani, D., Souza, R., Binkert, C., Fischli, W., Simonneau, G., Clozel, M. & Humbert, M. (2007). Endothelin-1/endothelin-3 ratio: a potential prognostic factor of pulmonary arterial hypertension. *CHEST Journal* **131**, 101-108.
239. Rubens, C., Ewert, R., Halank, M., Wensel, R., Orzechowski, H.-D., Schultheiss, H.-P. & Hoeffken, G. (2001). Big endothelin-1 and endothelin-1 plasma levels are correlated with the severity of primary pulmonary hypertension. *CHEST Journal* **120**, 1562-1569.
240. Frasch, H. F., Marshall, C. & Marshall, B. E. (1999). Endothelin-1 is elevated in monocrotaline pulmonary hypertension. *American Journal of Physiology-Lung Cellular and Molecular Physiology* **276**, L304-L310.
241. Stelzner, T., O'brien, R., Yanagisawa, M., Sakurai, T., Sato, K., Webb, S., Zamora, M., McMurtry, I. & Fisher, J. (1992). Increased lung endothelin-1 production in rats with idiopathic pulmonary hypertension. *American Journal of Physiology-Lung Cellular and Molecular Physiology* **262**, L614-L620.
242. Miyauchi, T., Yorikane, R., Sakai, S., Sakurai, T., Okada, M., Nishikibe, M., Yano, M., Yamaguchi, I., Sugishita, Y. & Goto, K. (1993). Contribution of endogenous endothelin-1 to the progression of cardiopulmonary alterations in rats with monocrotaline-induced pulmonary hypertension. *Circulation research* **73**, 887-897.
243. Krum, H., Viskoper, R. J., Lacourciere, Y., Budde, M. & Charlon, V. (1998). The effect of an endothelin-receptor antagonist, bosentan, on blood pressure in patients with essential hypertension. Bosentan Hypertension Investigators. *N Engl J Med* **338**, 784-90.

244. Nakov, R., Pfarr, E., Eberle, S. & Investigators, H. (2002). Darusentan: an effective endothelinA receptor antagonist for treatment of hypertension. *Am J Hypertens* **15**, 583-9.
245. Haynes, W. G., Ferro, C. J., O'Kane, K. P., Somerville, D., Lomax, C. C. & Webb, D. J. (1996). Systemic endothelin receptor blockade decreases peripheral vascular resistance and blood pressure in humans. *Circulation* **93**, 1860-70.
246. Ihara, M., Ishikawa, K., Fukuroda, T., Saeki, T., Funabashi, K., Fukami, T., Suda, H. & Yano, M. (1992). In vitro biological profile of a highly potent novel endothelin (ET) antagonist BQ-123 selective for the ETA receptor. *J Cardiovasc Pharmacol* **20 Suppl 12**, S11-4.
247. Ihara, M., Yamanaka, R., Ohwaki, K., Ozaki, S., Fukami, T., Ishikawa, K., Towers, P. & Yano, M. (1995). [3H]BQ-123, a highly specific and reversible radioligand for the endothelin ETA receptor subtype. *Eur J Pharmacol* **274**, 1-6.
248. Leslie, S. J. & Webb, D. J. (2001). Endothelin ligands and their experimental effects within the human circulation. In *Endothelin and its Inhibitors* (Warner, T. D., ed.). Springer, Berlin Heidelberg.
249. Pollock, D. M. (2000). Renal endothelin in hypertension. *Curr Opin Nephrol Hypertens* **9**, 157-64.
250. Remuzzi, G., Perico, N. & Benigni, A. (2002). New therapeutics that antagonize endothelin: promises and frustrations. *Nature Reviews Drug Discovery* **1**, 986-1001.
251. Ohta, K., Hirata, Y., Shichiri, M., Kanno, K., Emori, T., Tomita, K. & Marumo, F. (1991). Urinary excretion of endothelin-1 in normal subjects and patients with renal disease. *Kidney Int* **39**, 307-11.
252. Goddard, J., Johnston, N. R., Hand, M. F., Cumming, A. D., Rabelink, T. J., Rankin, A. J. & Webb, D. J. (2004). Endothelin-A receptor antagonism reduces blood pressure and increases renal blood flow in hypertensive patients with chronic renal failure: a comparison of selective and combined endothelin receptor blockade. *Circulation* **109**, 1186-93.
253. Benigni, A., Zoja, C., Corna, D., Orisio, S., Longaretti, L., Bertani, T. & Remuzzi, G. (1993). A specific endothelin subtype A receptor antagonist protects against injury in renal disease progression. *Kidney Int* **44**, 440-4.
254. Schiffrin, E. L. (2005). Vascular endothelin in hypertension. *Vascul Pharmacol* **43**, 19-29.
255. Opocensky, M., Kramer, H. J., Backer, A., Vernerova, Z., Eis, V., Cervenka, L., Certikova Chabova, V., Tesar, V. & Vaneckova, I. (2006). Late-onset endothelin-A receptor blockade reduces podocyte injury in homozygous Ren-2 rats despite severe hypertension. *Hypertension* **48**, 965-71.
256. Nagase, M., Shibata, S., Yoshida, S., Nagase, T., Gotoda, T. & Fujita, T. (2006). Podocyte injury underlies the glomerulopathy of Dahl salt-hypertensive rats and is reversed by aldosterone blocker. *Hypertension* **47**, 1084-93.
257. Boffa, J. J., Tharaux, P. L., Dussaule, J. C. & Chatziantoniou, C. (2001). Regression of renal vascular fibrosis by endothelin receptor antagonism. *Hypertension* **37**, 490-6.
258. Benigni, A., Colosio, V., Brena, C., Bruzzi, I., Bertani, T. & Remuzzi, G. (1998). Unselective inhibition of endothelin receptors reduces renal dysfunction in experimental diabetes. *Diabetes* **47**, 450-6.
259. Hocher, B., Schwarz, A., Reinbacher, D., Jacobi, J., Lun, A., Priem, F., Bauer, C., Neumayer, H. H. & Raschack, M. (2001). Effects of endothelin receptor antagonists on the progression of diabetic nephropathy. *Nephron* **87**, 161-9.
260. Gagliardini, E., Corna, D., Zoja, C., Sangalli, F., Carrara, F., Rossi, M., Conti, S., Rottoli, D., Longaretti, L., Remuzzi, A., Remuzzi, G. & Benigni, A. (2009). Unlike

each drug alone, lisinopril if combined with avosentan promotes regression of renal lesions in experimental diabetes. *Am J Physiol Renal Physiol* **297**, F1448-56.
261. Watson, A. M., Li, J., Schumacher, C., de Gasparo, M., Feng, B., Thomas, M. C., Allen, T. J., Cooper, M. E. & Jandeleit-Dahm, K. A. (2010). The endothelin receptor antagonist avosentan ameliorates nephropathy and atherosclerosis in diabetic apolipoprotein E knockout mice. *Diabetologia* **53**, 192-203.
262. Zoja, C., Cattaneo, S., Fiordaliso, F., Lionetti, V., Zambelli, V., Salio, M., Corna, D., Pagani, C., Rottoli, D., Bisighini, C., Remuzzi, G. & Benigni, A. (2011). Distinct cardiac and renal effects of ETA receptor antagonist and ACE inhibitor in experimental type 2 diabetes. *Am J Physiol Renal Physiol* **301**, F1114-23.
263. Saleh, M. A., Boesen, E. I., Pollock, J. S., Savin, V. J. & Pollock, D. M. (2010). Endothelin-1 increases glomerular permeability and inflammation independent of blood pressure in the rat. *Hypertension* **56**, 942-9.
264. Sasser, J. M., Sullivan, J. C., Hobbs, J. L., Yamamoto, T., Pollock, D. M., Carmines, P. K. & Pollock, J. S. (2007). Endothelin A receptor blockade reduces diabetic renal injury via an anti-inflammatory mechanism. *J Am Soc Nephrol* **18**, 143-54.
265. Gomez-Garre, D., Largo, R., Liu, X. H., Gutierrez, S., Lopez-Armada, M. J., Palacios, I. & Egido, J. (1996). An orally active ETA/ETB receptor antagonist ameliorates proteinuria and glomerular lesions in rats with proliferative nephritis. *Kidney Int* **50**, 962-72.
266. Benigni, A., Corna, D., Maffi, R., Benedetti, G., Zoja, C. & Remuzzi, G. (1998). Renoprotective effect of contemporary blocking of angiotensin II and endothelin-1 in rats with membranous nephropathy. *Kidney Int* **54**, 353-9.
267. Amann, K., Simonaviciene, A., Medwedewa, T., Koch, A., Orth, S., Gross, M. L., Haas, C., Kuhlmann, A., Linz, W., Scholkens, B. & Ritz, E. (2001). Blood pressure-independent additive effects of pharmacologic blockade of the renin-angiotensin and endothelin systems on progression in a low-renin model of renal damage. *J Am Soc Nephrol* **12**, 2572-84.
268. Dhaun, N., Lilitkarntakul, P., MacIntyre, I. M., Muilwijk, E., Johnston, N. R., Kluth, D. C., Webb, D. J. & Goddard, J. (2009). Urinary endothelin-1 in chronic kidney disease and as a marker of disease activity in lupus nephritis. *American Journal of Physiology - Renal Physiology* **296**, F1477-F1483.
269. Dhaun, N., MacIntyre, I. M., Kerr, D., Melville, V., Johnston, N. R., Haughie, S., Goddard, J. & Webb, D. J. (2011). Selective endothelin-A receptor antagonism reduces proteinuria, blood pressure, and arterial stiffness in chronic proteinuric kidney disease. *Hypertension* **57**, 772-9.
270. Yamamoto, T., Hirohama, T. & Uemura, H. (2002). Endothelin B Receptor-like Immunoreactivity in Podocytes of the Rat Kidney. *Archives of Histology and Cytology* **65**, 245-250.
271. Spath, M., Pavenstadt, H., Muller, C., Petersen, J., Wanner, C. & Schollmeyer, P. (1995). Regulation of phosphoinositide hydrolysis and cytosolic free calcium induced by endothelin in human glomerular epithelial cells. *Nephrol Dial Transplant* **10**, 1299-304.
272. Collino, F., Bussolati, B., Gerbaudo, E., Marozio, L., Pelissetto, S., Benedetto, C. & Camussi, G. (2008). Preeclamptic sera induce nephrin shedding from podocytes through endothelin-1 release by endothelial glomerular cells. *Am J Physiol Renal Physiol* **294**, F1185-94.
273. Rebibou, J. M., He, C. J., Delarue, F., Peraldi, M. N., Adida, C., Rondeau, E. & Sraer, J. D. (1992). Functional endothelin 1 receptors on human glomerular podocytes and mesangial cells. *Nephrol Dial Transplant* **7**, 288-92.

274. Morigi, M., Buelli, S., Zanchi, C., Longaretti, L., Macconi, D., Benigni, A., Moioli, D., Remuzzi, G. & Zoja, C. (2006). Shigatoxin-induced endothelin-1 expression in cultured podocytes autocrinally mediates actin remodeling. *Am J Pathol* **169**, 1965-75.
275. Ortmann, J., Amann, K., Brandes, R. P., Kretzler, M., Munter, K., Parekh, N., Traupe, T., Lange, M., Lattmann, T. & Barton, M. (2004). Role of podocytes for reversal of glomerulosclerosis and proteinuria in the aging kidney after endothelin inhibition. *Hypertension* **44**, 974-81.
276. Sakurai-Yamashita, Y., Yamashita, K., Yoshida, A., Obana, M., Takada, K., Shibaguchi, H., Shigematsu, K., Niwa, M. & Taniyama, K. (1997). Rat peritoneal macrophages express endothelin ETB but not endothelin ETA receptors. *European Journal of Pharmacology* **338**, 199-203.
277. Martin-Nizard, F., Houssaini, H. S., Lestavel-Delattre, S., Duriez, P. & Fruchart, J. C. (1991). Modified low density lipoproteins activate human macrophages to secrete immunoreactive endothelin. *FEBS Lett* **293**, 127-30.
278. Ehrenreich, H., Anderson, R. W., Fox, C. H., Rieckmann, P., Hoffman, G. S., Travis, W. D., Coligan, J. E., Kehrl, J. H. & Fauci, A. S. (1990). Endothelins, peptides with potent vasoactive properties, are produced by human macrophages. *The Journal of Experimental Medicine* **172**, 1741-1748.
279. Wahl, J. R., Goetsch, N. J., Young, H. J., Van Maanen, R. J., Johnson, J. D., Pea, A. S. & Brittingham, A. (2005). Murine macrophages produce endothelin-1 after microbial stimulation. *Exp Biol Med (Maywood)* **230**, 652-8.
280. Achmad, T. H. & Rao, G. S. (1992). Chemotaxis of human blood monocytes toward endothelin-1 and the influence of calcium channel blockers. *Biochem Biophys Res Commun* **189**, 994-1000.
281. Millul, V., Lagente, V., Gillardeaux, O., Boichot, E., Dugas, B., Mencia-Huerta, J. M., Bereziat, G., Braquet, P. & Masliah, J. (1991). Activation of guinea pig alveolar macrophages by endothelin-1. *J Cardiovasc Pharmacol* **17 Suppl 7**, S233-5.
282. Ruetten, H. & Thiemermann, C. (1997). Endothelin-1 stimulates the biosynthesis of tumour necrosis factor in macrophages: ET-receptors, signal transduction and inhibition by dexamethasone. *J Physiol Pharmacol* **48**, 675-88.
283. Kohno, M., Yokokawa, K., Mandal, A. K., Horio, T., Yasunari, K. & Takeda, T. (1995). Cardiac natriuretic peptides inhibit cyclosporine-induced production of endothelin in cultured rat mesangial cells. *Metabolism* **44**, 404-9.
284. Bakris, G. L. & Re, R. N. (1993). Endothelin modulates angiotensin II-induced mitogenesis of human mesangial cells. *Am J Physiol* **264**, F937-42.
285. Nitta, K., Uchida, K., Kimata, N., Kawashima, A., Yumura, W. & Nihei, H. (1995). Endothelin-1 mediates erythropoietin-stimulated glomerular endothelial cell-dependent proliferation of mesangial cells. *Eur J Pharmacol* **293**, 491-4.
286. Zoja, C., Morigi, M., Figliuzzi, M., Bruzzi, I., Oldroyd, S., Benigni, A., Ronco, P. & Remuzzi, G. (1995). Proximal tubular cell synthesis and secretion of endothelin-1 on challenge with albumin and other proteins. *American journal of kidney diseases : the official journal of the National Kidney Foundation* **26**, 934-941.
287. Saleem, M. A., O'Hare, M. J., Reiser, J., Coward, R. J., Inward, C. D., Farren, T., Xing, C. Y., Ni, L., Mathieson, P. W. & Mundel, P. (2002). A conditionally immortalized human podocyte cell line demonstrating nephrin and podocin expression. *J Am Soc Nephrol* **13**, 630-8.
288. Gantner, F., Kupferschmidt, R., Schudt, C., Wendel, A. & Hatzelmann, A. (1997). In vitro differentiation of human monocytes to macrophages: change of PDE profile and its relationship to suppression of tumour necrosis factor-alpha release by PDE inhibitors. *Br J Pharmacol* **121**, 221-31.

289. Morton, J. J. & Webb, D. J. (1985). Measurement of plasma angiotensin II. *Clin Sci (Lond)* **68**, 483-4.
290. Rolinski, B., Sadri, I., Bogner, J. & Goebel, F. D. (1994). Determination of endothelin-1 immunoreactivity in plasma, cerebrospinal fluid and urine. *Res Exp Med (Berl)* **194**, 9-24.
291. European Medicines Agency: Thelin INN: Sitaxsentan Sodium http://www.ema.europa.eu/docs/en_GB/document_library/EPAR_-_Scientific_Discussion/human/000679/WC500037904.pdf.
292. Solomon, D. H., Gardella, J. W., Fanger, H., Dethier, F. M. & Ferrebee, J. W. (1949). Nephrotoxic nephritis in rats: evidence for the glomerular origin of the kidney antigen. *The Journal of experimental medicine* **90**, 267-272.
293. Masugi, M. (1976). Über die experimentelle Glomerulonephritis durch das spezifische Antinierenserum: Ein Beitrag zur Pathogenese der diffusen Glomerulonephritis. *Beiträge zur Pathologie* **158**, 117-126.
294. Churc, J., Grishman, E. & Mautner, W. (1960). Nephrotoxic serum nephritis in the rat: Electron and light microscopic studies. *The American journal of pathology* **37**, 729.
295. Okabayashi, A., Kondo, Y. & Shigematsu, H. (1976). Cellular and histopathologic consequences of immunologically induced experimental glomerulonephritis. In *Glomerulonephritis*, pp. 1-43. Springer.
296. Unanue, E. R. & Dixon, F. J. (1965). Experimental glomerulonephritis V. Studies on the interaction of nephrotoxic antibodies with tissues of the rat. *The Journal of experimental medicine* **121**, 697-714.
297. Kühn, K., Ryan, G., Hein, S. J., Galaske, R. & Karnovsky, M. (1977). An ultrastructural study of the mechanisms of proteinuria in rat nephrotoxic nephritis. *Laboratory investigation; a journal of technical methods and pathology* **36**, 375-387.
298. Schreiner, G. F., Cotran, R. S., Pardo, V. & Unanue, E. (1978). A mononuclear cell component in experimental immunological glomerulonephritis. *The Journal of experimental medicine* **147**, 369-384.
299. Kanno, K., Okumura, F., Toriumi, W., Ishiyama, N., Nishiyama, S. & Naito, K. (1998). Nephrotoxic serum-induced nephritis in Wistar-Kyoto rats: a model to evaluate antinephritic agents. *Jpn J Pharmacol* **77**, 129-35.
300. Börner, U. & Szaz, G. (1979). A specific fully enzymatic method for creatinine reference values in serum. *Journal of Clinical Chemistry* **17**, 679-882.
301. Matsuzawa, T., Hayashi, Y., Nomura, M., Unno, T., Igarashi, T., Furuya, T., Sekita, K., Ono, A., Kurokawa, Y. & Hayashi, Y. (1997). A survey of the values of clinical chemistry parameters obtained for a common rat blood sample in ninety-eight Japanese laboratories. *J Toxicol Sci* **22**, 25-44.
302. Duffield, J. S., Forbes, S. J., Constandinou, C. M., Clay, S., Partolina, M., Vuthoori, S., Wu, S., Lang, R. & Iredale, J. P. (2005). Selective depletion of macrophages reveals distinct, opposing roles during liver injury and repair. *Journal of Clinical Investigation* **115**, 56-65.
303. Guo, S., Wietecha, T. A., Hudkins, K. L., Kida, Y., Spencer, M. W., Pichaiwong, W., Kojima, I., Duffield, J. S. & Alpers, C. E. Macrophages are essential contributors to kidney injury in murine cryoglobulinemic membranoproliferative glomerulonephritis. *Kidney International* **80**, 946-958.
304. Bardelmeijer, H. A., Buckle, T., Ouwehand, M., Beijnen, J. H., Schellens, J. H. & van Tellingen, O. (2003). Cannulation of the jugular vein in mice: a method for serial withdrawal of blood samples. *Lab Anim* **37**, 181-7.

305. Kurowski, S. Z., Slavik, K. J. & Szilagyi, J. E. (1991). A method for maintaining and protecting chronic arterial and venous catheters in conscious rats. *J Pharmacol Methods* **26**, 249-56.
306. Parasuraman, S., Raveendran, R. & Kesavan, R. (2010). Blood sample collection in small laboratory animals. *J Pharmacol Pharmacother* **1**, 87-93.
307. Cochrane, C. G., Unanue, E. R. & Dixon, F. J. (1965). A role of polymorphonuclear leukocytes and complement in nephrotoxic nephritis. *The Journal of experimental medicine* **122**, 99-116.
308. Hawkins, D. & Cochrane, C. G. (1968). Glomerular basement membrane damage in immunological glomerulonephritis. *Immunology* **14**, 665.
309. Henson, P. M. (1972). Pathologic mechanisms in neutrophil-mediated injury. *The American journal of pathology* **68**, 593.
310. Ehrich, W., Forman, C. & Seifer, J. (1952). Diffuse glomerular nephritis and lipid nephrosis; correlation of clinical, morphological, and experimental observations. *AMA archives of pathology* **54**, 463.
311. Murer, L., Zacchello, G., Basso, G., Scarpa, A., Montini, G., Chiozza, M. L. & Zacchello, F. (1994). Immunohistochemical distribution of endothelin in biopsies of pediatric nephrotic syndrome. *Am J Nephrol* **14**, 157-61.
312. Roccatello, D., Mosso, R., Ferro, M., Polloni, R., De Filippi, P. G., Quattrocchio, G., Bancale, E., Cesano, G., Sena, L. M. & Piccoli, G. (1994). Urinary endothelin in glomerulonephritis patients with normal renal function. *Clin Nephrol* **41**, 323-30.
313. Nakamura, T., Ebihara, I., Fukui, M., Osada, S., Tomino, Y., Masaki, T., Goto, K., Furuichi, Y. & Koide, H. (1995). Modulation of glomerular endothelin and endothelin receptor gene expression in aminonucleoside-induced nephrosis. *J Am Soc Nephrol* **5**, 1585-90.
314. Lehrke, I., Waldherr, R., Ritz, E. & Wagner, J. (2001). Renal endothelin-1 and endothelin receptor type B expression in glomerular diseases with proteinuria. *J Am Soc Nephrol* **12**, 2321-9.
315. Hocher, B., Thone-Reineke, C., Rohmeiss, P., Schmager, F., Slowinski, T., Burst, V., Siegmund, F., Quertermous, T., Bauer, C., Neumayer, H. H., Schleuning, W. D. & Theuring, F. (1997). Endothelin-1 transgenic mice develop glomerulosclerosis, interstitial fibrosis, and renal cysts but not hypertension. *J Clin Invest* **99**, 1380-9.
316. Hocher, B., Schwarz, A., Fagan, K. A., Thone-Reineke, C., El-Hag, K., Kusserow, H., Elitok, S., Bauer, C., Neumayer, H. H., Rodman, D. M. & Theuring, F. (2000). Pulmonary fibrosis and chronic lung inflammation in ET-1 transgenic mice. *Am J Respir Cell Mol Biol* **23**, 19-26.
317. Boesen, E. I., Krishnan, K. R., Pollock, J. S. & Pollock, D. M. (2011). ETA activation mediates angiotensin II-induced infiltration of renal cortical T cells. *J Am Soc Nephrol* **22**, 2187-92.
318. Amiri, F., Paradis, P., Reudelhuber, T. L. & Schiffrin, E. L. (2008). Vascular inflammation in absence of blood pressure elevation in transgenic murine model overexpressing endothelin-1 in endothelial cells. *J Hypertens* **26**, 1102-9.
319. Fogo, A. B. (2003). Animal models of FSGS: lessons for pathogenesis and treatment. *Semin Nephrol* **23**, 161-71.
320. Wang, Y. P., Tay, Y. C. & Harris, D. C. (2000). Progressive adriamycin nephropathy in mice: sequence of histologic and immunohistochemical events. *Kidney Int* **58**, 1797-804.
321. Damoiseaux, J., Döpp, E., Calame, W., Chao, D., MacPherson, G. & Dijkstra, C. (1994). Rat macrophage lysosomal membrane antigen recognized by monoclonal antibody ED1. *Immunology* **83**, 140.

322. Beelen, R., Eestermans, I., Dopp, E. & Dijkstra, C. (1987). *Transplantation Proceedings*.
323. Damoiseaux, J., Döpp, E. & Dijkstra, C. (1991). Cellular binding mechanism on rat macrophages for sialylated glycoconjugates, inhibited by the monoclonal antibody ED3. *Journal of leukocyte biology* **49**, 434-441.
324. Dijkstra, C., Döpp, E., Joling, P. & Kraal, G. (1985). The heterogeneity of mononuclear phagocytes in lymphoid organs: distinct macrophage subpopulations in rat recognized by monoclonal antibodies ED1, ED2 and ED3. In *Microenvironments in the Lymphoid System*, pp. 409-419. Springer.
325. Dijkstra, C. D., Döpp, E. A., Joling, P. & Kraal, G. (1985). The heterogeneity of mononuclear phagocytes in lymphoid organs: distinct macrophage subpopulations in the rat recognized by monoclonal antibodies ED1, ED2 and ED3. *Immunology* **54**, 589-599.
326. Bacon, C. R., Cary, N. R. & Davenport, A. P. (1996). Endothelin peptide and receptors in human atherosclerotic coronary artery and aorta. *Circ Res* **79**, 794-801.
327. Chai, S. P., Chang, Y. N. & Fong, J. C. (2009). Endothelin-1 stimulates interleukin-6 secretion from 3T3-L1 adipocytes. *Biochim Biophys Acta* **1790**, 213-8.
328. Yoshimura, T., Yuhki, N., Moore, S. K., Appella, E., Lerman, M. I. & Leonard, E. J. (1989). Human monocyte chemoattractant protein-1 (MCP-1). Full-length cDNA cloning, expression in mitogen-stimulated blood mononuclear leukocytes, and sequence similarity to mouse competence gene JE. *FEBS Lett* **244**, 487-93.
329. Leonard, E. J. & Yoshimura, T. (1990). Human monocyte chemoattractant protein-1 (MCP-1). *Immunol Today* **11**, 97-101.
330. Jiang, Y., Beller, D. I., Frendl, G. & Graves, D. T. (1992). Monocyte chemoattractant protein-1 regulates adhesion molecule expression and cytokine production in human monocytes. *J Immunol* **148**, 2423-8.
331. Zahuczky, G., Kristóf, E., Majai, G. & Fésüs, L. (2011). Differentiation and glucocorticoid regulated apopto-phagocytic gene expression patterns in human macrophages. Role of Mertk in enhanced phagocytosis. *PLoS One* **6**, e21349.
332. Steinman, R. M., Mellman, I. S., Muller, W. A. & Cohn, Z. A. (1983). Endocytosis and the recycling of plasma membrane. *J Cell Biol* **96**, 1-27.
333. Rutz, M., Metzger, J., Gellert, T., Luppa, P., Lipford, G. B., Wagner, H. & Bauer, S. (2004). Toll-like receptor 9 binds single-stranded CpG-DNA in a sequence- and pH-dependent manner. *Eur J Immunol* **34**, 2541-50.
334. Hart, O. M., Athie-Morales, V., O'Connor, G. M. & Gardiner, C. M. (2005). TLR7/8-mediated activation of human NK cells results in accessory cell-dependent IFN-gamma production. *J Immunol* **175**, 1636-42.
335. Shintani, T. & Klionsky, D. J. (2004). Autophagy in health and disease: a double-edged sword. *Science* **306**, 990-5.
336. de Almeida, M. C., Silva, A. C., Barral, A. & Barral Netto, M. (2000). A simple method for human peripheral blood monocyte isolation. *Mem Inst Oswaldo Cruz* **95**, 221-3.
337. Wilson, S. H., Simari, R. D. & Lerman, A. (2001). The Effect of Endothelin-1 on Nuclear Factor Kappa B in Macrophages. *Biochemical and Biophysical Research Communications* **286**, 968-972.
338. Juergens, U. R., Racke, K., Uen, S., Haag, S., Lamyel, F., Stober, M., Gillissen, A., Novak, N. & Vetter, H. (2008). Inflammatory responses after endothelin B (ETB) receptor activation in human monocytes: new evidence for beneficial anti-inflammatory potency of ETB-receptor antagonism. *Pulm Pharmacol Ther* **21**, 533-9.

339. Speciale, L., Roda, K., Saresella, M., Taramelli, D. & Ferrante, P. (1998). Different endothelins stimulate cytokine production by peritoneal macrophages and microglial cell line. *Immunology* **93**, 109-14.
340. Spirig, R., Potapova, I., Shaw-Boden, J., Tsui, J., Rieben, R. & Shaw, S. G. (2009). TLR2 and TLR4 agonists induce production of the vasoactive peptide endothelin-1 by human dendritic cells. *Mol Immunol* **46**, 3178-82.
341. Kluth, D. C. (2007). Pro-resolution properties of macrophages in renal injury. *Kidney Int* **72**, 234-6.
342. Elferink, J. G. & de Koster, B. M. (1996). Modulation of human neutrophil chemotaxis by the endothelin-B receptor agonist sarafotoxin S6c. *Chem Biol Interact* **101**, 165-74.
343. Bremnes, T., Paasche, J. D., Mehlum, A., Sandberg, C., Bremnes, B. & Attramadal, H. (2000). Regulation and intracellular trafficking pathways of the endothelin receptors. *Journal of Biological Chemistry* **275**, 17596-17604.
344. Verollet, C., Charriere, G. M., Labrousse, A., Cougoule, C., Le Cabec, V. & Maridonneau-Parini, I. (2011). Extracellular proteolysis in macrophage migration: losing grip for a breakthrough. *Eur J Immunol* **41**, 2805-13.
345. Gottlieb, T. A., Ivanov, I. E., Adesnik, M. & Sabatini, D. D. (1993). Actin microfilaments play a critical role in endocytosis at the apical but not the basolateral surface of polarized epithelial cells. *J Cell Biol* **120**, 695-710.
346. Durrbach, A., Collins, K., Matsudaira, P., Louvard, D. & Coudrier, E. (1996). Brush border myosin-I truncated in the motor domain impairs the distribution and the function of endocytic compartments in an hepatoma cell line. *Proc Natl Acad Sci U S A* **93**, 7053-8.
347. Geli, M. I. & Riezman, H. (1996). Role of Type I Myosins in Receptor-Mediated Endocytosis in Yeast. *Science* **272**, 533-535.
348. Matteoni, R. & Kreis, T. E. (1987). Translocation and clustering of endosomes and lysosomes depends on microtubules. *J Cell Biol* **105**, 1253-65.
349. Gruenberg, J., Griffiths, G. & Howell, K. E. (1989). Characterization of the early endosome and putative endocytic carrier vesicles in vivo and with an assay of vesicle fusion in vitro. *The Journal of Cell Biology* **108**, 1301-1316.
350. Kelly, R. B. (1990). Microtubules, membrane traffic, and cell organization. *Cell* **61**, 5-7.
351. Whyte, C. S., Bishop, E. T., Rückerl, D., Gaspar-Pereira, S., Barker, R. N., Allen, J. E., Rees, A. J. & Wilson, H. M. (2011). Suppressor of cytokine signaling (SOCS)1 is a key determinant of differential macrophage activation and function. *Journal of Leukocyte Biology* **90**, 845-854.
352. Valberg, P. A., Brain, J. D. & Kane, D. (1981). Effects of colchicine or cytochalasin B on pulmonary macrophage endocytosis in vivo. *J Appl Physiol Respir Environ Exerc Physiol* **50**, 621-9.
353. Lippincott-Schwartz, J., Yuan, L., Tipper, C., Amherdt, M., Orci, L. & Klausner, R. D. (1991). Brefeldin A's effects on endosomes, lysosomes, and the TGN suggest a general mechanism for regulating organelle structure and membrane traffic. *Cell* **67**, 601-616.
354. Por, E. D., Bierbower, S. M., Berg, K. A., Gomez, R., Akopian, A. N., Wetsel, W. C. & Jeske, N. A. (2012). β-Arrestin-2 Desensitizes the Transient Receptor Potential Vanilloid 1 (TRPV1) Channel. *Journal of Biological Chemistry* **287**, 37552-37563.
355. Machnik, A., Dahlmann, A., Kopp, C., Goss, J., Wagner, H., van Rooijen, N., Eckardt, K. U., Muller, D. N., Park, J. K., Luft, F. C., Kerjaschki, D. & Titze, J. (2010). Mononuclear phagocyte system depletion blocks interstitial tonicity-responsive enhancer binding protein/vascular endothelial growth factor C expression and induces salt-sensitive hypertension in rats. *Hypertension* **55**, 755-61.

356. Crowley, S. D., Song, Y. S., Sprung, G., Griffiths, R., Sparks, M., Yan, M., Burchette, J. L., Howell, D. N., Lin, E. E., Okeiyi, B., Stegbauer, J., Yang, Y., Tharaux, P. L. & Ruiz, P. (2010). A role for angiotensin II type 1 receptors on bone marrow-derived cells in the pathogenesis of angiotensin II-dependent hypertension. *Hypertension* **55**, 99-108.
357. Blank, U., Essig, M., Scandiuzzi, L., Benhamou, M. & Kanamaru, Y. (2007). Mast cells and inflammatory kidney disease. *Immunol Rev* **217**, 79-95.
358. Machnik, A., Neuhofer, W., Jantsch, J., Dahlmann, A., Tammela, T., Machura, K., Park, J. K., Beck, F. X., Muller, D. N., Derer, W., Goss, J., Ziomber, A., Dietsch, P., Wagner, H., van Rooijen, N., Kurtz, A., Hilgers, K. F., Alitalo, K., Eckardt, K. U., Luft, F. C., Kerjaschki, D. & Titze, J. (2009). Macrophages regulate salt-dependent volume and blood pressure by a vascular endothelial growth factor-C-dependent buffering mechanism. *Nat Med* **15**, 545-52.
359. Machnik, A., Dahlmann, A., Kopp, C., Goss, J., Wagner, H., van Rooijen, N., Eckardt, K.-U., Müller, D. N., Park, J.-K., Luft, F. C., Kerjaschki, D. & Titze, J. (2010). Mononuclear Phagocyte System Depletion Blocks Interstitial Tonicity-Responsive Enhancer Binding Protein/Vascular Endothelial Growth Factor C Expression and Induces Salt-Sensitive Hypertension in Rats. *Hypertension* **55**, 755-761.
360. Schmaderer, C., Eißler, R., Seibel, S., van Rooijen, N. & Baumann, M. (2010). Blood Pressure Control: A Facelift for Macrophages? *Hypertension* **56**, e23.
361. Clausen, B. E., Burkhardt, C., Reith, W., Renkawitz, R. & Forster, I. (1999). Conditional gene targeting in macrophages and granulocytes using LysMcre mice. *Transgenic Res* **8**, 265-77.
362. Kedzierski, R. M., Grayburn, P. A., Kisanuki, Y. Y., Williams, C. S., Hammer, R. E., Richardson, J. A., Schneider, M. D. & Yanagisawa, M. (2003). Cardiomyocyte-specific endothelin A receptor knockout mice have normal cardiac function and an unaltered hypertrophic response to angiotensin II and isoproterenol. *Mol Cell Biol* **23**, 8226-32.
363. Ge, Y., Bagnall, A., Stricklett, P. K., Strait, K., Webb, D. J., Kotelevtsev, Y. & Kohan, D. E. (2006). Collecting duct-specific knockout of the endothelin B receptor causes hypertension and sodium retention. *Am J Physiol Renal Physiol* **291**, F1274-80.
364. Dhaun, N., Goddard, J. & Webb, D. J. (2006). The endothelin system and its antagonism in chronic kidney disease. *J Am Soc Nephrol* **17**, 943-55.
365. Niemir, Z. I., Stein, H., Dworacki, G., Mundel, P., Koehl, N., Koch, B., Autschbach, F., Andrassy, K., Ritz, E., Waldherr, R. & Otto, H. F. (1997). Podocytes are the major source of IL-1 alpha and IL-1 beta in human glomerulonephritides. *Kidney Int* **52**, 393-403.
366. Greiber, S., Muller, B., Daemisch, P. & Pavenstadt, H. (2002). Reactive oxygen species alter gene expression in podocytes: induction of granulocyte macrophage-colony-stimulating factor. *J Am Soc Nephrol* **13**, 86-95.
367. Andrews, P. M. (1981). Investigations of cytoplasmic contractile and cytoskeletal elements in the kidney glomerulus. *Kidney Int* **20**, 549-62.
368. Cortes, P., Mendez, M., Riser, B. L., Guerin, C. J., Rodriguez-Barbero, A., Hassett, C. & Yee, J. (2000). F-actin fiber distribution in glomerular cells: structural and functional implications. *Kidney Int* **58**, 2452-61.
369. Kobayashi, N. & Mundel, P. (1998). A role of microtubules during the formation of cell processes in neuronal and non-neuronal cells. *Cell Tissue Res* **291**, 163-74.
370. Doublier, S., Ruotsalainen, V., Salvidio, G., Lupia, E., Biancone, L., Conaldi, P. G., Reponen, P., Tryggvason, K. & Camussi, G. (2001). Nephrin redistribution on

podocytes is a potential mechanism for proteinuria in patients with primary acquired nephrotic syndrome. *The American journal of pathology* **158**, 1723-1731.
371. Saran, A. M., Yuan, H., Takeuchi, E., McLaughlin, M. & Salant, D. J. (2003). Complement mediates nephrin redistribution and actin dissociation in experimental membranous nephropathy1. *Kidney international* **64**, 2072-2078.
372. Lenkkeri, U., Männikkö, M., McCready, P., Lamerdin, J., Gribouval, O., Niaudet, P., Antignac, C., Kashtan, C. E., Holmberg, C. & Olsen, A. (1999). Structure of the gene for congenital nephrotic syndrome of the Finnish type (NPHS1) and characterization of mutations. *The American Journal of Human Genetics* **64**, 51-61.
373. Koziell, A., Grech, V., Hussain, S., Lee, G., Lenkkeri, U., Tryggvason, K. & Scambler, P. (2002). Genotype/phenotype correlations of NPHS1 and NPHS2 mutations in nephrotic syndrome advocate a functional inter-relationship in glomerular filtration. *Human Molecular Genetics* **11**, 379-388.
374. Boute, N., Gribouval, O., Roselli, S., Benessy, F., Lee, H., Fuchshuber, A., Dahan, K., Gubler, M.-C., Niaudet, P. & Antignac, C. (2000). NPHS2, encoding the glomerular protein podocin, is mutated in autosomal recessive steroid-resistant nephrotic syndrome. *Nature genetics* **24**, 349-354.
375. Lehtonen, S., Ryan, J. J., Kudlicka, K., Iino, N., Zhou, H. & Farquhar, M. G. (2005). Cell junction-associated proteins IQGAP1, MAGI-2, CASK, spectrins, and α-actinin are components of the nephrin multiprotein complex. *Proceedings of the National Academy of Sciences of the United States of America* **102**, 9814-9819.
376. Quack, I., Rump, L. C., Gerke, P., Walther, I., Vinke, T., Vonend, O., Grunwald, T. & Sellin, L. (2006). β-Arrestin2 mediates nephrin endocytosis and impairs slit diaphragm integrity. *Proceedings of the National Academy of Sciences* **103**, 14110-14115.
377. Lahdenperä, J., Kilpeläinen, P., Liu, X. L., Pikkarainen, T., Reponen, P., Ruotsalainen, V. & Tryggvason, K. (2003). Clustering-induced tyrosine phosphorylation of nephrin by Src family kinases1. *Kidney international* **64**, 404-413.
378. Lai, K. N., Leung, J. C., Chan, L. Y., Saleem, M. A., Mathieson, P. W., Tam, K. Y., Xiao, J., Lai, F. M. & Tang, S. C. (2009). Podocyte injury induced by mesangial-derived cytokines in IgA nephropathy. *Nephrol Dial Transplant* **24**, 62-72.
379. Timoshanko, J. R., Sedgwick, J. D., Holdsworth, S. R. & Tipping, P. G. (2003). Intrinsic Renal Cells Are the Major Source of Tumor Necrosis Factor Contributing to Renal Injury in Murine Crescentic Glomerulonephritis. *Journal of the American Society of Nephrology* **14**, 1785-1793.
380. Neale, T. J., Ruger, B. M., Macaulay, H., Dunbar, P. R., Hasan, Q., Bourke, A., Murray-McIntosh, R. P. & Kitching, A. R. (1995). Tumor necrosis factor-alpha is expressed by glomerular visceral epithelial cells in human membranous nephropathy. *Am J Pathol* **146**, 1444-54.
381. Xing, C. Y., Saleem, M. A., Coward, R. J., Ni, L., Witherden, I. R. & Mathieson, P. W. (2006). Direct effects of dexamethasone on human podocytes. *Kidney Int* **70**, 1038-45.
382. Dai, X. & Galligan, J. J. (2006). Differential trafficking and desensitization of human ETA and ETB receptors expressed in HEK 293 cells. *Experimental Biology and Medicine* **231**, 746-751.
383. Drake, M. T., Shenoy, S. K. & Lefkowitz, R. J. (2006). Trafficking of G protein–coupled receptors. *Circulation research* **99**, 570-582.
384. Rosano, L., Spinella, F. & Bagnato, A. (2013). Endothelin 1 in cancer: biological implications and therapeutic opportunities. *Nat Rev Cancer* **13**, 637-651.

385. Croager, E. (2004). CAV1 connection. *Nat Rev Cancer* **4**, 90-91.
386. Sun, L.-n., Chen, Z.-x., Liu, X.-c., Liu, H.-y., Guan, G.-j. & Liu, G. (2014). Curcumin ameliorates epithelial-to-mesenchymal transition of podocytes in vivo and in vitro via regulating caveolin-1. *Biomedicine & Pharmacotherapy* **68**, 1079-1088.
387. Buelli, S., Rosano, L., Gagliardini, E., Corna, D., Longaretti, L., Pezzotta, A., Perico, L., Conti, S., Rizzo, P., Novelli, R., Morigi, M., Zoja, C., Remuzzi, G., Bagnato, A. & Benigni, A. (2014). beta-arrestin-1 drives endothelin-1-mediated podocyte activation and sustains renal injury. *J Am Soc Nephrol* **25**, 523-33.
388. Satchell, S. C., Tasman, C. H., Singh, A., Ni, L., Geelen, J., von Ruhland, C. J., O'Hare, M. J., Saleem, M. A., van den Heuvel, L. P. & Mathieson, P. W. (2006). Conditionally immortalized human glomerular endothelial cells expressing fenestrations in response to VEGF. *Kidney Int* **69**, 1633-40.